



ΠΑΝΕΠΙΣΤΗΜΙΟ ΔΥΤΙΚΗΣ ΑΤΤΙΚΗΣ
ΣΧΟΛΗ ΜΗΧΑΝΙΚΩΝ
ΤΜΗΜΑ ΗΛΕΚΤΡΟΛΟΓΩΝ ΚΑΙ ΗΛΕΚΤΡΟΝΙΚΩΝ ΜΗΧΑΝΙΚΩΝ
ΠΡΟΓΡΑΜΜΑ ΔΙΔΑΚΤΟΡΙΚΩΝ ΣΠΟΥΔΩΝ

ΔΙΔΑΚΤΟΡΙΚΗ ΔΙΑΤΡΙΒΗ

**Αυτόματη παρακολούθηση της βιοποικιλότητας με τη χρήση
ασύρματων δικτύων και οπτικών / οπτικοακουστικών αισθητήρων**

Ηρακλής Ηλίας Ρηγάκης

ΑΙΓΑΛΕΩ

Ιανουάριος 2023



UNIVERSITY OF WEST ATTICA

**SCHOOL OF ENGINEERING
DEPARTMENT OF ELECTRICAL AND ELECTRONICS ENGINEERING**

PROGRAM OF DOCTORAL STUDIES

PhD THESIS

**Automatic monitoring of insect fauna at global scales using wireless
networks and opto-acoustic sensors**

Iraklis Ilias Rigakis

ATHENS-EGALEO

January 2023

ΔΙΔΑΚΤΟΡΙΚΗ ΔΙΑΤΡΙΒΗ

Automatic monitoring of insect fauna at global scales using wireless networks and opto-acoustic sensors

Ηρακλής Ηλίας Ρηγάκης

ΕΠΙΒΛΕΠΩΝ ΚΑΘΗΓΗΤΗΣ: **Νικόλαος Αλέξανδρος-Τάτλας**, Αναπληρωτής Καθηγητής
Τμήμα Ηλεκτρολόγων & Ηλεκτρονικών Μηχ., ΠαΔΑ.

ΤΡΙΜΕΛΗΣ ΕΠΙΤΡΟΠΗ ΠΑΡΑΚΟΛΟΥΘΗΣΗΣ:

Νικόλαος Αλέξανδρος-Τάτλας, Αναπληρωτής Καθηγητής, Τμ. ΗΗΜ, ΠαΔΑ
Στέλιος Ποτηράκης, Καθηγητής, Τμ. ΗΗΜ, ΠαΔΑ
Ηλίας Ποταμίτης, Καθηγητής, Τμ. ΜΤΑ, ΕΛΜΕΠΑ

ΕΠΤΑΜΕΛΗΣ ΕΞΕΤΑΣΤΙΚΗ ΕΠΙΤΡΟΠΗ

Νικόλαος-Αλέξανδρος Τάτλας,
Αναπληρωτής Καθηγητής ΠαΔΑ

Στυλιανός Ποτηράκης,
Καθηγητής ΠαΔΑ

Ηλίας Ποταμίτης,
Καθηγητής ΕΛΜΕΠΑ

Χαράλαμπος Πατρικάκης,
Καθηγητής ΠαΔΑ

Σωτηρία Γαλατά,
Επίκουρη Καθηγήτρια ΠαΔΑ

Μανόλης Αντωνιδάκης,
Καθηγητής ΕΛΜΕΠΑ

Ανδρέας Φλώρος,
Καθηγητής Ιονίου Πανεπιστημίου

Ημερομηνία εξέτασης 25/1/2023

PhD THESIS

Automatic monitoring of insect fauna at global scales using wireless networks and opto-acoustic sensors

Iraklis Ilias Rigakis

SUPERVISOR: Nikolaos-Alexander Tatlas, Associate Professor UniWA

THREE-MEMBER ADVISORY COMMITTEE:

Nikolaos-Alexander Tatlas, Associate Professor UniWA

Stylios Potirakis, Professor UniWA

Ilyas Potamitis, Professor HMU

SEVEN-MEMBER EXAMINATION COMMITTEE

**Nicolaos-Alexandros Tatlas,
Associate Professor UniWA**

**Stelios Potirakis,
Professor UniWA**

**Ilyas Potamitis,
Professor ELMEPA**

**Charalambos Patrikakis,
Professor UniWA**

**Sotiria Galata,
Assistant Professor UniWA**

**Manolis Antonidakis,
Professor ELMEPA**

**Andreas Floros,
Professor Ionion University**

Examination Date 25/01/2023

Copyright © Με επιφύλαξη παντός δικαιώματος. All rights reserved.

ΠΑΝΕΠΙΣΤΗΜΙΟ ΔΥΤΙΚΗΣ ΑΤΤΙΚΗΣ και Ηρακλής Ρηγάκης,

Ιανουάριος 2023

Η παρούσα διδακτορική διατριβή καλύπτεται από τους όρους της άδειας χρήσης Creative Commons «Αναφορά Δημιουργού Μη Εμπορική Χρήση Όχι Παράγωγα Έργα 4.0 Διεθνές» (CC BY-NC-ND 4.0). Συνεπώς, το έργο είναι ελεύθερο για διανομή (αναπαραγωγή, διανομή και παρουσίαση του έργου στο κοινό), υπό τις ακόλουθες προϋποθέσεις:

α. Αναφορά δημιουργού: Ο χρήστης θα πρέπει να κάνει αναφορά στο έργο με τον τρόπο που έχει οριστεί από το δημιουργό ή τον χορηγούντα την άδεια.

β. Μη εμπορική χρήση: Ο χρήστης δεν μπορεί να χρησιμοποιήσει το έργο αυτό για εμπορικούς σκοπούς.

γ. Όχι Παράγωγα Έργα: Ο Χρήστης δεν μπορεί να αλλοιώσει, να τροποποιήσει ή να δημιουργήσει νέο υλικό που να αξιοποιεί το συγκεκριμένο έργο (πάνω από το έργο αυτό).

Απαγορεύεται η αντιγραφή, αποθήκευση και διανομή της παρούσας εργασίας, εξ ολοκλήρου ή τμήματος αυτής, για εμπορικό σκοπό. Επιτρέπεται η ανατύπωση, αποθήκευση και διανομή για σκοπό μη κερδοσκοπικό, εκπαιδευτικής ή ερευνητικής φύσης, υπό την προϋπόθεση να αναφέρεται η πηγή προέλευσης και να διατηρείται το παρόν μήνυμα. Ερωτήματα που αφορούν τη χρήση της εργασίας για κερδοσκοπικό σκοπό πρέπει να απευθύνονται προς τους συγγραφείς.

Οι απόψεις και τα συμπεράσματα που περιέχονται σε αυτό το έγγραφο εκφράζουν τον/την συγγραφέα του και δεν πρέπει να ερμηνευθεί ότι αντιπροσωπεύουν τις θέσεις του επιβλέποντος, της επιτροπής εξέτασης ή τις επίσημες θέσεις του Τμήματος και του Ιδρύματος.

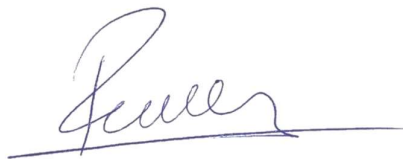
ΔΗΛΩΣΗ ΣΥΓΓΡΑΦΕΑ ΔΙΔΑΚΤΟΡΙΚΗΣ ΔΙΑΤΡΙΒΗΣ

Ο/η κάτωθι υπογεγραμμένος Ηρακλής Ρηγάκης του Ηλία, υποψήφιος/α διδάκτορας του Τμήματος Ηλεκτρολόγων και Ηλεκτρονικών Μηχανικών της Σχολής Μηχανικών του Πανεπιστημίου Δυτικής Αττικής, δηλώνω ότι:

«Είμαι συγγραφέας και δικαιούχος των πνευματικών δικαιωμάτων επί της διατριβής και δεν προσβάλω τα πνευματικά δικαιώματα τρίτων. Για τη συγγραφή της διδακτορικής μου διατριβής δεν χρησιμοποίησα ολόκληρο ή μέρος έργου άλλου δημιουργού ή τις ιδέες και αντιλήψεις άλλου δημιουργού χωρίς να γίνεται αναφορά στην πηγή προέλευσης (βιβλίο, άρθρο από εφημερίδα ή περιοδικό, ιστοσελίδα κ.λπ.). Επίσης, βεβαιώνω ότι αυτή η εργασία έχει συγγραφεί από μένα αποκλειστικά και αποτελεί προϊόν πνευματικής ιδιοκτησίας τόσο δικής μου, όσο και του Ιδρύματος.

Παράβαση της ανωτέρω ακαδημαϊκής μου ευθύνης αποτελεί ουσιώδη λόγο για την ανάκληση του πτυχίου μου».

Ο Δηλών



ΠΕΡΙΛΗΨΗ

Η παρούσα διατριβή εισάγει νέα τεχνολογικά εργαλεία στην εντομολογία και στην τεχνολογία της γεωπονίας που βοηθούν στην παρατήρηση, τον εντοπισμό και την αναγνώριση είδους των εντόμων. Προτείνονται νέες συσκευές και υλικό λογισμικού που ανιχνεύει και καταγράφει την παρουσία των εντόμων, τεχνικές επεξεργασίας δεδομένων και αλγόριθμους μηχανικής μάθησης που αναγνωρίζουν το είδος. Γιατί όμως υπάρχει η ανάγκη ώστε να εντοπιστούν και να ταξινομηθούν τα ταπεινά και μερικές φορές απαρατήρητα έντομα;

Ορισμένα είδη εντόμων (τα λεπιδόπτερα για παράδειγμα) θεωρούνται κατάλληλοι δείκτες για τη βιοποικιλότητα που σήμερα μειώνεται παγκοσμίως με άγνωστο ρυθμό. Όλα τα έντομα διαδραματίζουν ζωτικό ρόλο καθώς αποτελούν διακριτούς κρίκους στη βιολογική εξάρτηση των ειδών και αποτελούν πηγές τροφής για τα σπονδυλωτά. Ως εκ τούτου, δεν είναι μόνο σημαντικά, αλλά και κρίσιμης σημασίας. Ωστόσο, πολλά από αυτά μπορούν να φτάσουν σε υψηλές, επιζήμιες πυκνότητες και να βλάψουν σοβαρά τις καλλιέργειες στην γεωργία (αρκετές μύγες όπως η μύγα της Μεσογείου, ο δάκος, η *bactrocera dorsalis*) και τα ξυλοφάγα έντομα. Κάποια άλλα, όπως τα κουνούπια και ορισμένες σκνίπες, αποτελούν σοβαρή απειλή για την υγιεινή, καθιστώντας τα κουνούπια το πιο θανατηφόρο ζώο στον πλανήτη. Ωστόσο, αν έπρεπε να δώσουμε ένα επιχείρημα για τη σημασία των εντόμων για τον άνθρωπο, θα περιγράφαμε αυτή την προτεραιότητα με μια μόνο φράση «επηρεάζουν την παραγωγή τροφίμων».

Μια μεγάλη πρόκληση που αντιμετωπίζει ο 21ος αιώνας είναι η βιώσιμη παραγωγή τροφίμων για τον αυξανόμενο ανθρώπινο πληθυσμό. Ο παγκόσμιος πληθυσμός προβλέπεται να φτάσει τα 10,4 δισεκατομμύρια άτομα στη δεκαετία του 2080. Τα τεχνολογικά μέσα και η αυξανόμενη διαθεσιμότητα νέων αισθητήρων και ηλεκτρονικών συσκευών και η συλλογή «μεγάλων δεδομένων» στοχεύουν στη βελτίωση της βιωσιμότητας των συστημάτων παραγωγής τροφίμων. Υπάρχει επείγουσα ανάγκη να μετριάσουν οι απώλειες των καλλιεργειών λόγω των εντόμων, αποφεύγοντας παράλληλα περιττούς ψεκασμούς που έχει αποδειχθεί ότι επηρεάζουν αρνητικά την ανθρώπινη υγεία.

Οι γεωπόνοι ανέκαθεν χρησιμοποιούσαν παγίδες (συνήθως μπουκάλια ή κουβάδες) για να παγιδεύουν και να μετρούν τα έντομα ως μέσο αξιολόγησης της κατάστασης προσβολής. Με τον καιρό είχαν αναπτύξει τα λεγόμενα «πρωτόκολλα απόφασης» που έπρεπε να ακολουθήσουν ως εμπειρικό κανόνα για το τι πρέπει να κάνουν παρουσία συγκεκριμένης πυκνότητας εντόμων σε αγροτικές περιοχές και δάση. Στην πράξη, οι αναφορές από παγίδες παρακολούθησης δεν γίνονται δεκτές στα τυφλά αλλά χρησιμεύουν ως υποστηρικτικά στοιχεία. Οι πιστοποιημένοι κρατικοί εντομολόγοι προσαρμόζουν τον κανόνα στις ιδιαιτερότητες διαφορετικών γεωγραφικών περιοχών

της χώρας και ενσωματώνουν διαφορετικές πηγές πληροφοριών πριν χορηγήσουν άδεια για ψεκασμούς μεγάλης κλίμακας. Οι αναφορές που προέρχονται από την ανθρώπινη παρακολούθηση παγίδων γίνονται δεκτές με διαφορετικό βαθμό εμπιστοσύνης. Η κύρια δυσκολία αυτής της διαδικασίας είναι ότι ένας μεγάλος αριθμός παγίδων πρέπει να τοποθετηθεί στρατηγικά σε αγροκτήματα, μερικές φορές σε απομακρυσμένες τοποθεσίες και πολλοί άνθρωποι θα πρέπει να τοποθετούν, να συντηρούν και να επιθεωρούν τις παγίδες κάθε 5 ημέρες από το τέλος της Άνοιξης μέχρι το τέλος Φθινοπώρου. Οι επόπτες των καλλιεργειών πρέπει να διακρίνουν το έντομο-στόχο του συλλεγόμενου πλήθους των νεκρών εντόμων και ακόμη να εξαγάγουν και να παραδώσουν έντομα (πχ δάκους) στις αρχές για επαλήθευση. Αυτή η διαδικασία είναι περίπλοκη, περιλαμβάνει μεγάλο αριθμό ανθρώπων που δεν έχουν πάντα τα προσόντα για να φέρουν εις πέρας την εργασία, αλλά το πιο σημαντικό, μπορούν εύκολα να παρακαμφθούν. Ως εκ τούτου, συχνά αναφέρεται μεγάλη οικονομική ζημία λόγω των εντόμων-προσβολέων και αυτό συνήθως αποδίδεται από τους ειδικούς εντομολόγους όχι στην αναποτελεσματικότητα του πρωτοκόλλου παρακολούθησης αλλά στην ευκαιριακή εφαρμογή του που συχνά οδηγεί σε μια εικασία για το πότε και από πού (χωρικές συντεταγμένες) να ξεκινήσει η διαδικασία αντιμετώπισης.

Από διαχειριστική άποψη, υπάρχει επείγουσα ανάγκη να αυξηθεί η ροή πληροφοριών αναπτυγμένες σε μεγάλες περιοχές για μεγάλη χρονική διάρκεια από τις εντομολογικές παγίδες, κατευθείαν σε μια κεντρική υπηρεσία παρακολούθησης, καθώς και να οπτικοποιηθεί και να συνοψιστεί αυτή η ροή με στατιστικά αξιόπιστα αποτελέσματα. **Για το σκοπό αυτό, η παρούσα διατριβή αναπτύσσει τεχνολογίες για τη βελτίωση, την επέκταση και την αυτοματοποίηση της παρακολούθησης σε μεγάλη κλίμακα των εντόμων οικονομικής και υγειονομικής σημασίας.**

Η ανάπτυξη αυτής της τεχνολογίας απαιτεί γνώσεις από διάφορους τομείς της επιστήμης όπως: ηλεκτρονικά χαμηλής κατανάλωσης, οπτο-ηλεκτρονική, επιστήμη δεδομένων, τεχνητή νοημοσύνη και εντομολογία.

Αναπτύσσουμε νέους απλούς και πολυφασματικούς αισθητήρες (υλικό και λογισμικό μικροεπεξεργαστή) για να καταγράψουμε το φτερούγισμα των ιπτάμενων εντόμων. Η συχνότητα των φτερών και οι αρμονικές της συνδέονται με την ταυτότητα του είδους όπως η φωνή ενός ανθρώπου. Περιγράφουμε νέες τεχνικές οπτικής ανίχνευσης στις οποίες το φως που ανακλάται από τα φτερά ενός ιπτάμενου εντόμου και οι παραλλαγές της σκιάς του καταγράφονται από έναν αισθητήρα που εξάγει μια εγγραφή σε αρχείο ήχου. Κατασκευάζουμε νέους μετρητές μελισσών που είναι προσαρτημένοι σε κυψέλες και μετρούν την κίνηση των εισερχόμενων/εξερχομένων μελισσών.

Στη συνέχεια, αναπτύξαμε έναν νέο τύπο αισθητήρα που τοποθετείται σε δέντρα και καταγράφει τα έντομα που μεταβολίζουν ή κινούνται μέσα στο δέντρο και στέλνει ασύρματα ηχογραφήσεις δόνησης (αρχεία ήχου .mp3) σε έναν απομακρυσμένο διακομιστή.

Τέλος, εισάγουμε την ηλεκτρονική παγίδα funnel (e-funnel) αυτόματης παρακολούθησης για όλα τα είδη λεπιδόπτερον με γνωστή φερομόνη. Οι e-funnels φέρουν έναν οπτικό μετρητή που μετρά τις συλλήψεις λεπιδοπτέρων και σχηματίζουν δικό τους δίκτυο με χρήση της ασύρματης τεχνολογίας μεγάλης εμβέλειας LoRa. Το LoRa gateway συλλέγει και αναφέρει τα αποτελέσματα συλλογής μετρήσεων εντόμων, τοποθεσιών GPS, χρονικών σημάνσεων και θερμοκρασίας σε έναν διακομιστή νέφους.

ΘΕΜΑΤΙΚΗ ΠΕΡΙΟΧΗ: Ασύρματα δίκτυα ακουστικών αισθητήρων, ηλεκτρονικά χαμηλής ισχύος, IoT

ΛΕΞΕΙΣ ΚΛΕΙΔΙΑ: Πολύ χαμηλής ισχύος οπτικοί αισθητήρες, αυτόματη αναγνώριση εντόμων, κατηγοριοποίηση εντόμων, ασύρματες επικοινωνίες, οπτικοί καταγραφείς φτερουγίσματος εντόμων, πιεζοηλεκτρικοί αισθητήρες

ABSTRACT

This thesis introduces novel technological tools related to insects from various angles: hardware platforms that detect and register insect's presence, data processing techniques and machine learning classification algorithms that identify the species. But why there is such necessity to detect and classify the humble and sometimes, unnoticed insects?

Some insect species (moths and butterflies for example) are considered suitable indicators for biodiversity that is currently declining globally at an unknown and unmeasured rate. All insects play a vital role as they are discrete links in the biological dependence of species and are food sources for vertebrates. Therefore, they are not only important, but they are also crucial. However, many of them can reach high, damaging densities and severely impair plant processes in agricultural (several flies like the medfly, dacus, *bactrocera dorsalis*) and forest (e.g., wood boring insects) ecosystems. Some other like mosquitoes and biting midges pose a serious hygienic threat making the mosquitoes the deadliest animal on the planet. However, If we would prioritize the significance of insects to humans, we would describe this priority with a single phrase 'they impact food production'.

A grand challenge facing the 21st century is the sustainable production of food for the growing human population. The world population is projected to reach 10.4 billion people sometime in the 2080s. Technological means with the increasing availability of new sensors and electronic components and the associated collection of 'big data' aim at improving the sustainability of food production systems. The urgent necessity is to moderate crop losses due to insects while avoiding unnecessary spraying that has been deemed to impact human health in a negative way.

Agronomists had always deployed traps (usually bottles or buckets) to trap and count pests as a means to assess the infestation situation. With time they had developed the so called 'decision protocols' to follow as a rule of thumb of what to do in the presence of a specific density of pests in agricultural fields and forests. In practice, reports from monitoring traps are not accepted blindly but serve as supportive evidence. Certified state entomologists adapt the rule to the particularities of different geographical parts of the country and integrate diverge sources of information before granting permission for large-scale spraying. Reports coming out of manual monitoring of traps are accepted with a varying degree of trust. The main difficulty of this procedure is that a large number of traps must be strategically placed in orchards, sometimes on distant and remote locations and numerous people should place, maintain and inspect the traps on a 5-day basis from the end of spring till the end of fall. The pest-managers must discern the pest in the mass of collected maze of dead insects and even extract and deliver the pest to authorities for verification.

This procedure is complicated, it involves a large number of people that are not always qualified to carry the task but, most importantly, can be easily bypassed by practitioners. Therefore, large economic loss is often reported because of the pest and this is usually attributed by expert entomologists not to the inefficiency of the monitoring protocol but to its opportunistic application that often leads to an ‘educated guess’ of when and where to start the treatment procedure.

From both a conceptual and management perspective, there is an urgent need to increase the information flow over large areas and through time from the field-traps and in other cases probes, straight to a central monitoring agency, as well as to visualize and summarize this flow in a statistically reliable sense. To this end, this thesis develops technologies to improve, expand and automate global monitoring of insects of economic and hygienic importance.

This study required intensive interdisciplinary collaboration and consultation with specialists and experts from various disparate fields of science such as: low-power electronics, optoelectronics, data science, artificial intelligence, and entomology. Automatic detection of such insects is crucial to the future of crop protection by providing critical information to the appropriate personnel in a timely manner to assess the risk to a crop or a tree and the need for preventative measures.

We develop novel single and multispectral sensors (hardware and microprocessor’s software) to record the wingbeat of flying insects. The wingbeat frequency and its harmonics are associated to species identity like the human voice to an individual. We describe new optical sensing techniques in which the light scattered by the beating wings of a flying insect and its casted shadow variations are recorded by a sensor that outputs a recording. We fabricate novel bee-counters that are attached to beehives and count the traffic of incoming/outgoing bees.

We subsequently developed a new type of sensor that is attached to trees and records the woodboring insects the chew or move inside the tree and wirelessly uploads the vibrational snippets to a remote server.

Finally, we introduce the electronic funnel trap (e-funnel) of automatic monitoring for all the Lepidoptera species with known pheromone. The e-funnels carry an optical counter that counts captures of Lepidopterans and form their own network based on the long range (LoRa) radio technology. The gateway of the network reports collection results of insect counts, GPS locations, timestamps and temperature to a cloud server.

SUBJECT AREA: Wireless sensor networks, low power electronics, IoT.

KEYWORDS: Low power optical sensors, automatic insect detecting, insect classification, wireless communications, optical insect wingbeats recorders, piezoelectric sensors.

Dedicated to my son Ilias.

Acknowledgments

First and foremost, I would like to express my deep and sincere gratitude to Associate Professor Nikolaos-Alexandros Tatlas, for his invaluable assistance throughout my PhD Studies. I would like to thank him for his guidance, the influence in my way of thinking, the knowledge that he transmitted to me over all these years. I was really lucky to meet him and have him as mentor.

I would like also to thank Professor Ilyas Potamitis, who immediately accepted to become a valuable advisor of this Thesis and helped out with any difficulty that occurred. I am also grateful for his insightful comments and recommendations over these years, even before the beginning of my PhD studies.

I would also like to thank Professor Stelios Potirakis for his valuable help in subjects of his specialty and the advice he gave me throughout my thesis.

Special thanks are reserved for all my friends and collaborators for all moments that we shared throughout these years. It was really a pleasure to work with such a great group of people and I am happy to say that except of co-workers they became my friends over the years.

Last but not least, I would like to deeply thank all my friends who supported me over these years and made this journey a lot easier. But most importantly, none of this could have happened without the understanding and support of my family especially my wife Eleni.

LIST OF PUBLICATIONS

During the preparation of this thesis the following publications were published:

- [1] Iraklis I Rigakis, Kiki N Varikou, Antonis E Nikolakakis, Zacharias D Skarakis, Nikolaos A Tatlas, Ilyas G Potamitis, The e-funnel trap: Automatic monitoring of lepidoptera; a case study of tomato leaf miner, *Computers and Electronics in Agriculture* 185, 2021, 106154

- [2] I Rigakis, I Potamitis, NA Tatlas, SM Potirakis, S Ntalampiras, TreeVibes: Modern tools for global monitoring of trees for borers, *Smart Cities* 4 (1), 2021, 271-285

- [3] I Potamitis, I Rigakis, NA Tatlas, On Fresnel-Based Single and Multi Spectral Sensors for Insects' Wingbeat Recording, 2019 20th International Conference on Solid-State Sensors, Actuators and Microsystems & Eurosensors XXXIII (TRANSDUCERS & EUROSENSORS XXXIII)

- [4] Potamitis, I.; Rigakis, I.; Tatlas, N.-A.; Potirakis, S. In-Vivo Vibroacoustic Surveillance of Trees in the Context of the IoT. *Sensors*, 2019, 19, 1366.

- [5] Rigakis, I.; Potamitis, I.; Tatlas, N.-A.; Livadaras, I.; Ntalampiras, S. A Multispectral Backscattered Light Recorder of Insects' Wingbeats. *Electronics* 2019, 8, 277. <https://doi.org/10.3390/electronics8030277>

- [6] I Potamitis, I Rigakis, NA Tatlas, S Kouzoupis, A novel electronic gate that identifies and counts bees based on their RGB backscattered light, *MATEC Web of Conferences* 292, 2019, 01005

Moreover, the following publication was submitted and is under review:

- [7] Iraklis Rigakis, Ilyas Potamitis, Nikolaos A. Tatlas, Giota Psirofonia, Efsevia Tzagaraki, and Eleftherios Alyssandrakis, A Low-cost, low-power, multisensory device and multivariable timeseries prediction for beehive health monitoring, *Sensors MDPI* (submitted 20/12/2022)

TABLE OF CONTENTS

LIST OF FIGURES	27
LIST OF TABLES.....	33
TERMINOLOGY.....	35
ABBREVIATIONS - ARCHIVES - ACRONYMS.....	37
1. INTRODUCTION	39
2. FRESNEL-BASED SINGLE AND MULTI SPECTRAL SENSORS FOR INSECT'S WINGBEAT RECORDING	43
2.1 Introduction	43
2.2 Materials and Methods.....	44
2.3 Results.....	48
2.4 NOVEL NOISE-ROBUST OPTOACOUSTIC SENSORS TO IDENTIFY INSECTS THROUGH WINGBEATS	50
2.4.1 Introduction.....	50
2.4.2 Materials and Methods.....	53
2.4.3 Discussion.....	65
2.5 LARGE APERTURE OPTOELECTRONIC DEVICES TO RECORD AND TIME-STAMP INSECTS' WINGBEATS	68
2.5.1 Introduction.....	68
2.5.2 Materials and Methods.....	69
2.5.3 Experiments	77
2.5.4 Discussion.....	83
3. A MULTISPECTRAL RECORDER OF INSECTS' WINGBEAT	84
3.1 Introduction	84
3.2 Materials and Methods.....	85
3.3 Results.....	90

3.4 Discussion	94
4. A NOVEL ELECTRONIC GATE THAT IDENTIFIES AND COUNTS BEES BASED ON THEIR RGB BACKSCATTERED LIGHT	96
4.1 Introduction	96
4.2 Materials and Methods	97
4.3 Results and Discussion	101
5. IN-VIVO VIBROACOUSTIC SURVEILLANCE OF TREES	106
5.1 Introduction	106
5.2 Materials and Methods	109
5.3 Results	114
5.3.1 In Lab Experiments	118
5.3.2 Tree Inspection in the Field	119
5.3.3 The Deep Learning Database.....	121
5.3.4 Deep-learning as Applied to Spectrograms of Vibro-Acoustic Signals.....	122
5.3.5 Verification Experiments.....	123
5.4 List of Applications	126
5.5 Discussion	127
5.6 Concluding Remarks and Further Steps	129
6. THE E-FUNNEL TRAP	131
6.1 Introduction	131
6.2 Materials & Methods	133
6.2.1 Trap Design & Function	133
6.3 System's Design and Implementation	134
6.4 Network and Gateway Communication	137
6.5 Study Area	137
6.5.1 Data Analysis.....	138

6.6	Results	140
6.6.1	Efficiency of Automatic vs Manual Counting	140
6.6.2	Comparision of e-traps vs Typical Funnel Traps	143
6.6.3	Histograms of Insect Captures vs Time	143
6.7	Discussion	145
7.	CONCLUSIONS – FURTHER RESEARCH	149
7.1	Conclusions	149
7.2	Further Research	152
8.	REFERENCES	155
9.	APPENDIX	169
9.1	On Fresnel-Based Sensors for Insects Wingbeat Recording Schematics	169
9.2	Novel Noise-Robust Optoacoustic Sensors to Identify Insects through Wingbeats Parts List	173
9.3	Multispectral Sensor Parts List & Schematics	175
9.4	Bees Electronic Gate Pictures	181
9.5	TreeVibes Users Guide	182
9.5.1	Introduction.....	182
9.5.2	Assembling Instructions.....	182
9.5.3	Applications	183
9.5.4	Waveguides and drill bits.....	184
9.5.5	Remote vs Manual Operation	185
9.5.6	The communication Modem	186
9.5.7	The Use of SD Card.....	186
9.5.8	Deployment on Trees.....	187
9.5.9	Time-Scheduling of the Device’s Operation.....	189
9.5.10	Frequently Asked Questions	193
9.5.11	Power Sufficiency & Data Consumption	194
9.5.12	Format of the Files	195
9.5.13	Setting The Time Correctly To Different Time-Zones	195
9.5.14	Exambles of Recordings.....	196
9.5.15	TreeVibes Designed Parts	198

9.6 e-Funnel Users Guide..... 202

- 9.6.1 Introduction 202
- 9.6.2 Assembling Instructions 202
- 9.6.3 Connectivity and Insect Counting..... 203
- 9.6.4 Frequently Asked questions..... 212
- 9.6.5 e-Funnel Design Files 214

LIST OF FIGURES

Figure 2-1. Block diagram of the single band recorder.....	44
Figure 2-2. The Fresnel lens	45
Figure 2-3. A prototype of the extinction light sensor.	45
Figure 2-4. Block diagram of the multispectral sensor.	47
Figure 2-5. Prototype of the multispectral sensor.	47
Figure 2-6. Prototype of the multispectral recorder.....	48
Figure 2-7. Wingbeat event	49
Figure 2-8. 3-band Optical wingbeat recording of backscattered light.	49
Figure 2-9. Spectrum of 3-Band recording of backscattered light.....	50
Figure 2-10. Receiver: a linear array of photodiodes	56
Figure 2-11. System diagram of the optoacoustic sensor	56
Figure 2-12. Filters and demodulator	57
Figure 2-13. Power supply.....	57
Figure 2-14. Clock and emitter circuit	58
Figure 2-15. <i>Musca domestica</i> adult insect recorded with an IR light and microphone.	59
Figure 2-16. Single <i>Musca Domestica</i> power spectral density (Infra-Laser-MIC)	59
Figure 2-17. A 2.5mm <i>Drosophila melanogaster</i> with LASER beam.	62
Figure 2-18. Spectrogram of a single adult mosquito <i>Anopheles gambiae</i>	63
Figure 2-19. Spectrogram of a single <i>Apis mellifera</i> worker.	64
Figure 2-20. In-flight recording from the optoacoustic device.	64
Figure 2-21. A close-up view of the electronics board	65
Figure 2-22. An in-flight recording of <i>Apis mellifera</i> flying in the light beam.	66
Figure 2-23. In-flight recording of several <i>B. oleae</i> insects.....	66
Figure 2-24. Optical receiver & transmitter	72
Figure 2-25. Recorder ADC circuit.....	72

Figure 2-26. Demodulator and Filter.....	73
Figure 2-27. Sensor connector & SD Card Connector.....	73
Figure 2-28. Recorder Microprocessor unit.....	74
Figure 2-29. The recorder main unit.....	75
Figure 2-30. The sensor.....	76
Figure 2-31. 2D array of photodiodes sensor and system.....	76
Figure 2-32. 1-2mm <i>Culicoides nubeculosus</i> in flight recording.....	78
Figure 2-33. Mean fundamental and standard deviation vs temperature.	79
Figure 2-34. Welch spectral density vs temperature.	79
Figure 2-35. The system time-stamps insects crossing the sensor.	80
Figure 2-36. Spectrum of an optical recording of a single <i>Ae. Albopictus</i>	81
Figure 2-37. <i>Ae. albopictus</i> , both sexes.....	81
Figure 2-38. Power Spectral Density of <i>C. pipiens molestus</i> wingflap.	82
Figure 2-39. <i>M. domestica</i> tethered.....	83
Figure 3-1. The multispectral sensor.....	85
Figure 3-2. The photodiode is placed at the.....	86
Figure 3-3. Block diagram of the multispectral device.	87
Figure 3-4. Multispectral Timing Diagram.....	87
Figure 3-5. The multispectral recorder prototype.....	88
Figure 3-6. A diagram explaining the recording procedure.	89
Figure 3-7. The ways to use the suggested sensor and its associated recorder.	91
Figure 3-8. The bee <i>Apis mellifera</i>	92
Figure 3-9. The wasp <i>Polistes gallicus</i>	92
Figure 3-10. The fruit fly <i>Zaprionus</i>	93
Figure 3-11. the fruit fly <i>Drosophila suzukii</i>	93
Figure 3-12. The fruit fly <i>Drosophila melanogaster</i>	94
Figure 4-1. Single multispectral cell in the new e-gate.	98

Figure 4-2. Block diagram of the electronic gate for beehives.	98
Figure 4-3. The microcontroller unit.....	99
Figure 4-4. The LEDs unit.....	100
Figure 4-5. The colour sensor unit (1/4).	100
Figure 4-6. The complete system. Left the recorder, right a single e-cell of the gate.....	101
Figure 4-7. Testing the e-gate.	102
Figure 4-8. Backscattered RGB light for four different bees.	102
Figure 4-9. Backscattered RGB for four different wasps.	103
Figure 4-10. Backscattered RGB for the discrimination between bees and wasps.	104
Figure 4-11. Backscattered RGB for four different wasps.	104
Figure 4-12. Backscattered RGB for four different insects	104
Figure 5-1. The concept of acoustic surveillance of trees in forests and urban environments. .	109
Figure 5-2. The vibrations recorder	110
Figure 5-3. Metal waveguide fastened to the input of the accelerometer.	110
Figure 5-4. The recorder prototype.....	112
Figure 5-5. Block diagram of the vibrations recorder.....	112
Figure 5-6. The reporting server manages recordings	113
Figure 5-7. A suspicious tree-trunk.....	115
Figure 5-8. Mulberries positive for <i>X. chinensis</i> (trees chopped and alive larvae found)	116
Figure 5-9. A typical case with no signs of any vibration	117
Figure 5-10. A recording in the presence of strong wind (stormy weather).....	117
Figure 5-11. Heavy rain hitting the trunk. The impulses are due to the raindrops.	117
Figure 5-12. Recordings in the presence of heavy traffic in a rush hour.	118
Figure 5-13. A <i>X. chinensis</i> positive case in a mulberry trunk.....	118
Figure 5-14. The device attached to a palm tree listening for <i>R. ferrugineus</i>	121
Figure 5-15. Automatic verification of borers' infestation in trees in the field data.	124
Figure 5-16. Infestation state of a tree after examining the folder no. 33.	125

Figure 6-1. Funnel trap.....	135
Figure 6-2. The electronics funnel trap.....	135
Figure 6-3. e-Funnel & LoRa Gateway in field.	136
Figure 6-4. System diagram of the functionality of the e-funnel trap.	139
Figure 6-5. Schematic drawing of the optical sensing unit.	139
Figure 6-6. A network of 10 e-funnel traps on the map.	140
Figure 6-7. The map of the field with marks of the traps.	141
Figure 6-8. Mean number (\pm SE) of <i>T. absoluta</i> male adult counts	142
Figure 6-9. Mean number (\pm SE) of <i>T. absoluta</i> male adults.	142
Figure 6-10. Insects per trap per visit ($\log(x + 1)$ transformation).....	142
Figure 6-11. Divergence (counts) of manual counting vs automatic counting.	144
Figure 6-12. Insects per trap per visit ($\log(x + 1)$ transformation).....	144
Figure 6-13. Mean number (\pm SE) of <i>T. absoluta</i> male adults every 3 days.	144
Figure 6-14. Male flight activity of <i>T. absoluta</i> during the day	146
Figure 9-1. Main CPU of recorder.	169
Figure 9-2. Demodulator, filter and gain control.....	170
Figure 9-3. Analog to digital converter.....	170
Figure 9-4. \pm 12V power supply.....	171
Figure 9-5. Battery charger.	171
Figure 9-6. Optical sensor connector.....	172
Figure 9-7. Photodiode transimpedance amplifier.....	172
Figure 9-8. LED driver.....	172
Figure 9-9. Multispectral Microprocessor unit.	176
Figure 9-10. Three-channel ADC.	177
Figure 9-11. Demultiplexer.....	178
Figure 9-12. Photodiode receiver.....	178
Figure 9-13. Three-channel LED driver.....	179

Figure 9-14. LEDs array. Three LEDs per spectral band.	179
Figure 9-15. Sensor LEDs' power supply.	180
Figure 9-16. Indicator LEDs.	180
Figure 9-17. 3D Plastic design of the bee tunnels.	181
Figure 9-18. Counter's placement in the beehive.	181
Figure 9-19. Close up view of bee tunnels.	181
Figure 9-20. Complete tree vibes system.	183
Figure 9-21. Waveguides that can be inserted in the tree trunks or wooden surfaces.	184
Figure 9-22. The back of the device.	185
Figure 9-23. For outdoor operation, the device has a solar panel on its back.	186
Figure 9-24. A <i>X. chinensis</i> positive case in a mulberry trunk.	187
Figure 9-25. Operating in continuous output mode.	188
Figure 9-26. Operating in transmission mode.	188
Figure 9-27. Pop-up window when someone clicks on device's icon on the map in system server.	190
Figure 9-28. System server.	190
Figure 9-29. System server time-table of a specific device.	191
Figure 9-30. Trap update controls how often one needs to see the recordings.	193
Figure 9-31. Mulberry examined in the field was found positive for <i>X. chinensis</i>	196
Figure 9-32. The designed printed circuit board of TreeVibe.	198
Figure 9-33. The designed main plastic enclosure internal view.	198
Figure 9-34. The external view of TreeVibe main plastic enclosure.	199
Figure 9-35. The Top plastic of enclosure (internal view).	199
Figure 9-36. Top plastic of enclosure(external view).	199
Figure 9-37. The plastic protector of TreeVibe interface.	200
Figure 9-38. TreeVibe plastic enclosure parts.	200
Figure 9-39. Assembled PCB (SMT components only).	200

Figure 9-40. Assembled PCB (all components placed).....	201
Figure 9-41. Assembled Device	201
Figure 9-42. (Left) A typical funnel trap. (Right) The optical counter attached to the funnel trap.	203
Figure 9-43. The torus in the picture is the optical counter.	203
Figure 9-44. e-Funnel & LoRa Gateway on trees.....	204
Figure 9-45. A network of 10 e-funnel traps on the map.	208
Figure 9-46. IMEI is a unique number related to the hardware of the e-funnel.	209
Figure 9-47. System server timetable of a specific device.....	210
Figure 9-48. A Pop-up window will appear when someone clicks on device’s icon.....	211
Figure 9-49. The designed Printed circuit board of Funnel (panel)	214
Figure 9-50. e-Funnel plastic enclosure Top Internal View.....	214
Figure 9-51. e-Funnel plastic enclosure Top external View	215
Figure 9-52. e-Funnel plastic enclosure Bottom Internal View.....	215
Figure 9-53. e-Funnel plastic enclosure Bottom External View.....	216
Figure 9-54. e-Funnel Optical parts plastic enclosure internal view	216
Figure 9-55. e-Funnel Optical parts plastic enclosure external view	217
Figure 9-56. Sunlight Blocker	217
Figure 9-57. Prototype e-Funnel Top View.....	218
Figure 9-58. Prototype e-Funnel Bottom View.....	218
Figure 9-59. Prototype of optical parts	219
Figure 9-60. Assembled PCBs	219
Figure 9-61. The production for real experiments.....	220

LIST OF TABLES

Table 1. Mean distance measures of opto-recordings over 10382 segments.....	61
Table 2. Field application using the suggested device in the city of Heraklion-Crete.	119
Table 3. 10-fold cross-validation results for various deep learning models.	123
Table 4. Precision (P), recall (R) and F1 score metrics on a random 20% holdout data for the best performing model.....	124
Table 5. A list of applications directly treated by using the suggested device	127
Table 6. A list of benefits using automatic screening of trees' vibrational records.....	130
Table 7. The recorder parts list.....	173
Table 8. Cost break-down of the multispectral sensor and recorder (Euros).	175
Table 9. Dimensions of provided waveguides	184
Table 10. Time schedule and reporting to the server vs. Power sufficiency and data consumption.	194
Table 11. Time schedule and reporting to the server with respect to power sufficiency and data consumption.	211

TERMINOLOGY

Ξενόγλωσσος όρος	Ελληνικός Όρος
Wingbeat	Φτερούγισμα
Fundamental frequency	Θεμελιώδης συχνότητα
Power Spectral Density	Φασματική πυκνότητα ισχύος
Spectrum	Φάσμα
Interference	Παρεμβολή
Time stamp	Χρονική σήμανση
Pollination	Επικονιασμός
Monocultures	Μονοκαλλιέργειες
Ecosystem	Οικοσύστημα
Borer	Ξυλοφάγο έντομο
Multispectral	Πολυφασματικό
Backscattered light	Ανακλώμενο φως
Optoelectronics sensor	Οπτοηλεκτρονικός αισθητήρας
Threshold	Κατώφλι
Embedded	Ενσωματωμένο

ABBREVIATIONS - ARCHIVES - ACRONYMS

CPU	Central Processing Unit
ADC	Analog to Digital Converter
DAC	Digital to Analog Converter
EMI	Electro Magnetic Interference
FOV	Field Of View
LIDAR	Light Detection And ranging
NIR	Near Infrared
LED	Light Emitting Diode
PDM	Pulse Density Modulation
PSD	Power Spectra Density
OPAMP	Operational Amplifier
LPC	Linear Prediction Coefficient
FET	Field Effect Transistor
TDM	Time Division Modulation
DMA	Direct Memory Access
DOA	Direction Of Arrival
CNN	Convolution Neural Network
DL	Deep Learning
GPS	Global Positioning System
IPM	Integrated Pest Management
EIL	Economic Injury Level

1. INTRODUCTION

Humans often disregard the existence of insects. This is partly to their cryptic nature, and size but also due to the dominant human species. They ignore their biology and the complex ecological roles and treat them all -more or less- as pests, and attempt to control them using insecticides. This is a technologically inclined thesis; therefore, we need to say few things for the interested reader about the crucial role of insects.

Insects are invertebrates and the largest group and most diverse group of animals; they include more than a million described species and represent more than half of all known living organisms and have an inherent high reproductive capacity.

They are important for humans, wildlife and the environment in many positive ways, namely:

1. The **pollination of plants** is an essential process for reproducing a range of flowers, trees and food crops. Of the approximately 300 commercial crops about 84% are insect pollinated. Insects are responsible for 80–85% of all pollinated commercial hectares, with fruits, vegetables, oilseeds, legumes and fodder, representing approximately one-third of global food production, mostly pollinated honeybees [1]. The value of *A. mellifera* for crop pollination in North America, is €13.82(\$14.8 billion) annually.
2. **breaking down and decomposing organic matter**, which involves turning dead animals and waste into healthy, fertile soil. Without insects, there would be pending health issues and poor quality of soil that would, in turn, result into poor quality of crops [2]
3. **providing animals with food**. Birds, fish cultivation and many terrestrial vertebrates feed on insects, and these, in turn, have their unique place in the chain of food-dependence. The ecosystems would be disturbed to the point of collapse in the absence of insects.
4. **providing humans with food**. Insects as a food source capable of providing nutrients with potential benefits to human health and is an upcoming trend in Europe as their production does not produce the increased greenhouse gas emissions that animal farming does. Estimates of numbers of edible insect species consumed globally range from 1,000 to 2,000 [3]. Insects are nutrient-efficient and packed full of protein, vitamins and minerals and become flour, burgers, fitness-bars and snacks.

5. **Provide humans with useful products.** Honey, wax and pollen produced by certain bees and silk produced by silkworms are distinct examples.

Overspraying with pesticides, habitat loss due to expansion of agricultural land, and climate change are threatening insect populations worldwide. In 2019, it was reported that 40% of all insect species are declining globally and that a third of them are endangered [4]. In [5] the first-ever comprehensive assessment of the extinction risk of all Orthoptera species native to Europe the International Union for Conservation of Nature (IUCN) lists 343 endangered insect species and a United Nations assessment in 2019 found that half a million insect species are under threat of extinction, some in the coming decades. The arguments presented so far aim to document the fact that insects should not be treated as pests because their role is of grave importance to wellbeing of all animals including the human species and we are currently heading to a sharp and uncontrolled decline of insect fauna.

However, some insects are of grave importance to humans but in a negative way. Some insects damage crops by feeding on sap, leaves, fruits, or wood. Some other species are parasitic to trees such as woodborers and contribute significantly to the environmental deterioration of agricultural trees and forestry. The problem worsens as we are experiencing an unprecedented extent of lifestyle changes due to technology advances, availability of fossil fuels and global trade. Due to these reasons the climate changes and facilitates the establishment of pest populations outside their native ranges (i.e., introduction of invasive species), in places that are not biologically adapted to regulate their multiplication [6][7]. Invasive species are widely recognized as among the greatest threats to biodiversity and ecosystem stability worldwide, and they impose serious economic and social costs.

Some other pests, may vector diseases like certain mosquito species (that are considered the deadliest animals on earth) and biting midges. They spread diseases such as malaria, dengue virus, Zika and West Nile virus, which can lead to disabling and potentially deadly effects (such as encephalitis, meningitis, and microcephaly) [8].

While agricultural and forest pests can inflict serious economic damages at the same time, the world population is expected to reach 9.7 billion in 2050 and could peak at nearly 11 billion around 2100 [9]. Due to increasing rates of human population, the total global food demand is expected to increase by 35% to 56% between 2010 and 2050 [10]. Therefore, there is a pressing need to augment food production in a sustainable way for the growing human population. One of the solutions often suggested is investing in technology to increase yields by decreasing quantitative and qualitative crop losses due to pests [11]. To

reduce crop losses due to pests one needs to balance the fact of the losses with the cost of the treatment and the technological means required as well as the ecological impact due to the treatment. Integrated pest management (IPM) is about making better decisions on how to suppress pest populations below the economic injury level (EIL). The suppression of pests needs to take into account human health and the least possible disruption of the environment due to insecticides while keeping the cost of intervention low compared to the EIL. The efficacy of modern pest monitoring relies on information about localizing in space and time the detection and evolution of pest populations. Monitoring traps are commonly used to sample insect fauna to make informative assumptions on the actual pest load of large areas to reach decisions on treatment or actions. A timely prediction of the occurrence of the onset of an infestation and the location of its concentration can define the decisions on an insecticide application program. If the problem is controlled at its initial stage, then it inflicts a loss below the EIL. Simultaneously, the uniform, unnecessary sprayings that are usually applied by farmers in fear of pest losses are mitigated.

Regarding wood- and phloem-boring insects, these are anticipated to cause the largest economic impacts by annually inducing nearly \$1.7 billion in local government expenditures and approximately \$830 million in lost residential property values just in the US [7]. Based on the economic figures above of the significant impact of pests to agriculture and forestry of several countries, it is evident that one needs to mitigate the damage of goods due to forest and agricultural pests. The first step in providing a treatment is to know where and when there is an infestation problem due to pests (i.e., detection and localization) and estimate its seriousness mainly by estimating the density of the infestation (i.e., designation of an infested area and sampled insect counts as a proxy for pest density in the field). Moreover, insects are indicators of environmental change and pollution, which can help to show us when it's time to act.

The growing recognition that insect populations effect serious economic losses and simultaneously the fact that useful insects may be in decline has given rise to a renewed call for insect population monitoring by scientists, and a desire to automate the monitoring process with novel technological means. The automatic biodiversity monitoring of flying insects' fauna using optical sensors such as Lidars, infrared emitting devices, vision-cameras and optoelectronic sensors are especially suited for this noble cause since they do not require termination of the monitored insects. This thesis focuses on pests and not on biodiversity monitoring, but the spectral and multispectral wingbeat recorders presented in

this thesis can be embedded in moving platforms such as tractors and drones for biodiversity monitoring.

This thesis presents new technological solution for insect activity data monitoring combined with time, geolocation and environmental data that are wirelessly transmitted to monitoring servers: wingbeat recorders for all flying insects (i.e., for the slow wingbeat of moths and butterflies that flap their wings <50 Hz to biting midges that beat their wings at around 1 kHz). It suggests smart insect traps that count and wirelessly report their captured insects (a.k.a e-traps) for several agricultural pests (lepidoptera and moths). We also introduce novel probes that are attached to trees and record the internal vibrations of the tree originating from wood boring insects, compress the audio recording and transmit it to remote servers. Finally, we introduce counting gates for beehives that count the incoming and outgoing bees. All these new devices are novel and are described in detail in the following chapters.

The thesis performed numerous experiments on insects. Please note, that there are regulatory ethical frameworks governing animal experimentation and animal welfare. While most countries have ethical standards regarding the use of animals for scientific purposes, experiments involving insects are not included in these standards. Although termination of insects is not preferred for biodiversity monitoring it is certainly not a prerequisite for agricultural pests. Biodiversity monitoring should refrain from killing a large number of insects to assess the situation of insect fauna composition and abundance. Our research did not involve endangered insect species and mainly focused to serious pests (i.e., various xylophagus insects such as *Xylotrechus chinensis*, and *Rhynchophorus ferrugineus*), flies like *Ceratitis capitata* and *Bactrocera oleae*, and lepidoptera as *Helicoverpa armigera*, *Plodia interpunctella*, and *Tuta absoluta*). Best practices involved termination in ethanol or freezing.

2. FRESNEL-BASED SINGLE AND MULTI SPECTRAL SENSORS FOR INSECT'S WINGBEAT RECORDING

2.1 Introduction

The simplest method to monitor the population of insects is by using insect traps. There is a current trend to automate the reporting procedure of sampled insect fauna [12][13]. One way is to embed optoelectronic sensors in typical traps that sense the fall or the wingbeat of the pest and, depending on the situation, count insects, discern sex and species of captured insects, report daily results, wirelessly, to remote servers [14][15][16]. In this work, we present stand-alone optoelectronic devices that shape their probe volume (PV) through Fresnel lenses. The devices are designed in a way that are detachable from their base and its size is reconfigurable so that it can take different forms depending on the e-trap in which we are interested in embedding it.

When an insect is hit by the light of an infrared emitter, there are two types of optical parameters that can originate from its main body and wing-beating: (a) The so-called extinguished light (or extinction radiation) which is the light variation due to the shadow cast on the receiver by the wings of the insects and (b) the back-scattered or reflected light by the wings and main body.

The first recorder shown in this work is based on extinction light solely (i.e. on the casted shadow). We find it very practical and robust against optical and electromagnetic interference.

The second recorder is based on scattered light and is multiband. It aims at the microstructural and melanisation features of the wing and body of the species. The information contained in the samples of these recordings will provide complementary information on the difficult task of discerning morphologically similar insects whose wingbeat spectrum may overlap significantly in the frequency domain.

Even the slightest morphological differences (i.e. size, shape, and mass of the wings) as well as stiffness and kinetic properties of the muscle system controlling flight will be reflected on the wingbeat spectrum. Therefore, during automatic classification one must not only take into account the fundamental frequency, that is the frequency that the insect beats its wings, but also the harmonics produced by the movement of the wings. The harmonics produced are related to the size and shape of the wings. The slightest difference among species results into an acoustic imprint. Insects of the same species (e.g. *Apis mellifera*) will have differences in the spectrum of their in-flight wingbeat, as they are

unrepeatable biological organisms. These differences have an imprint on the fundamental frequency which is characteristic for each species and drifts slightly around a central value but also on the distribution of harmonics [17]. The spectrum of individuals of the same species do not have the almost absolute repetitiveness of a note of a musical instrument. However, their spectrum follows a consistent, recognizable pattern and the differences in the spectrum of the same species (inter- species spectral variability) are smaller compared to other insects of different species whose wings have different shape, size and wingbeat frequency (intra- species spectral variability). As reported in [18] for the case of bumblebees, flying insects hold a rather constant wingbeat frequency, in a given temperature, regardless of the speed and flight pattern they hold.

2.2 Materials and Methods

Regardless of the light mode that is tracked, the main body of the bee and its beating wings flying in the field of view (FOV) partially intercept and modulate the flow of light. Therefore, the sensors presented in this work, can efficiently detect walking and wing-beating insects (e.g. bees, wasps, fruit flies).

The first optoelectronic sensor based on extinction light is composed of a light emitter opposite to a light receiver, whereas the backscatter sensor has the emitter and receiver on the same side.

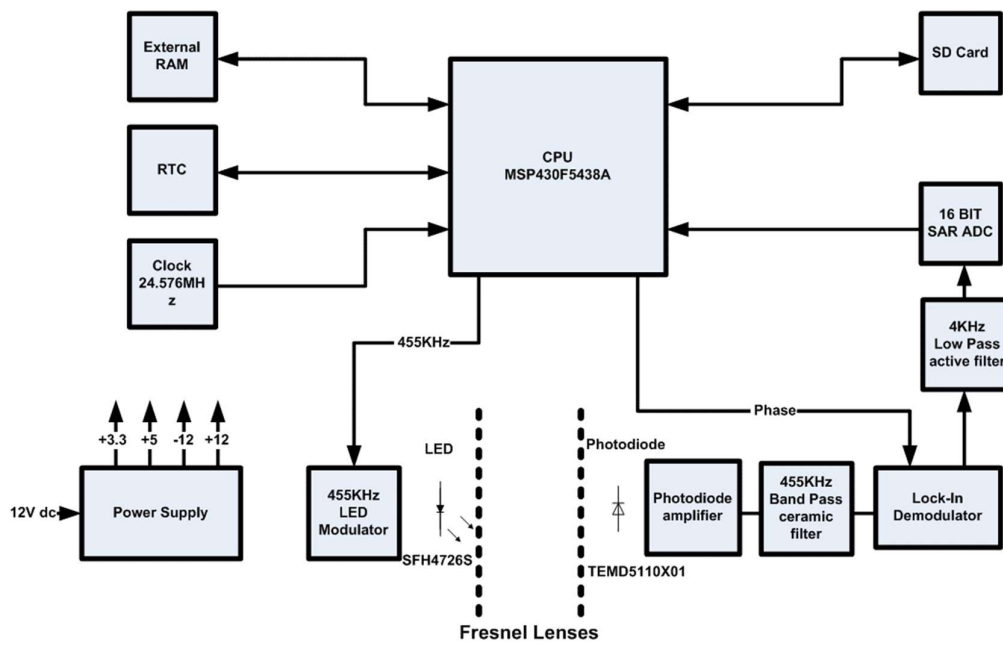


Figure 2-1. Block diagram of the single band recorder.

The characteristic of this sensor type is its immunity towards light and electromagnetic interference (EMI). This is achieved by modulating the emitted light at high frequencies (i.e. at 455 kHz), rejecting the low frequency spectrum and demodulating back the received signal. This procedure allows the functioning of the system in laboratories where EMI is almost always present and in the sunlight. Being immune to physical light is important as we do not wish to detect something outside its FOV (e.g. from insects flying over the FOV and modulating the sun light). Due to this capability it does not rely on shading to avoid light interferences, but this comes to a cost of more complicated construction.



Figure 2-2. The Fresnel lens



Figure 2-3. A prototype of the extinction light sensor.

A brief description follows: The CPU MSP430F5438A controls all processing stages. We use external SPI RAM 128KB for the cyclic buffer. The main clock of the system is an oscillator at 24.576MHz. This frequency divided by 54 produces the 455 kHz for LED modulator. The photodiode's amplifier amplifies the received signal and drives the 455 kHz ceramic band pass filter. This filter rejects the environment optical interference. The lock-in demodulator receives the output of band pass filter and produces a line level signal for ADC. The Microcontroller reads continuously the ADC and saves the data in a cyclic buffer at the external RAM.

In LIDAR applications is reported that near-infrared wavelengths (NIR), e.g. 808 nm, are affected by melanisation and that different spectral bands carry complementary information on the insect's main body and wings coloration [19][20]. We pursue this direction by developing a device (see. Figure 2-4) that examines the possibility of extracting a different kind of information than the casted shadow, based on backscattered light recordings of wingbeat events under different spectral bands. In this task, we use three different LEDs (one in the visible frequency range (450-700nm), one at 810 nm and one at 940 nm) as seen in Figure 2-5 & Figure 2-6.

To this end, for the multiband task we use 3 different LEDs (one in the visible frequency range (450-700nm), one at 810 nm and one at 940 nm). We want to see if the multiple LEDs can capture different degrees of melanisation and coloration of insects and to quantify precisely their size. We will investigate the complementarity of different spectral bands in extracting relevant information on the identity of the insect. We suggest an innovative type of sensor construction based on Fresnel lenses and capable of taking simultaneous recordings of all spectral bands hitting an insect (multichannel recording). The system is controlled from an STM32L4R7 ARM CPU of ST. The LED drivers produces the sequentially current pulses of each LED. The photodiode receives the reflected signal from insect, focused by a Fresnel lens (Fresnel Technologies Inc. Part number: 3*). This signal is amplified from the transimpedance photodiode amplified OPA380. The output of amplified contains multiplexed information from the three wavelengths. 20.8microseconds from each led. The demultiplexer receives this multiplexed signal and outputs three different audio signals, one for each wavelength. The multichannel sigma-delta ADC converter AD7768-4 receives the audio signal and sends the digital words to the CPU using the PDM interface.

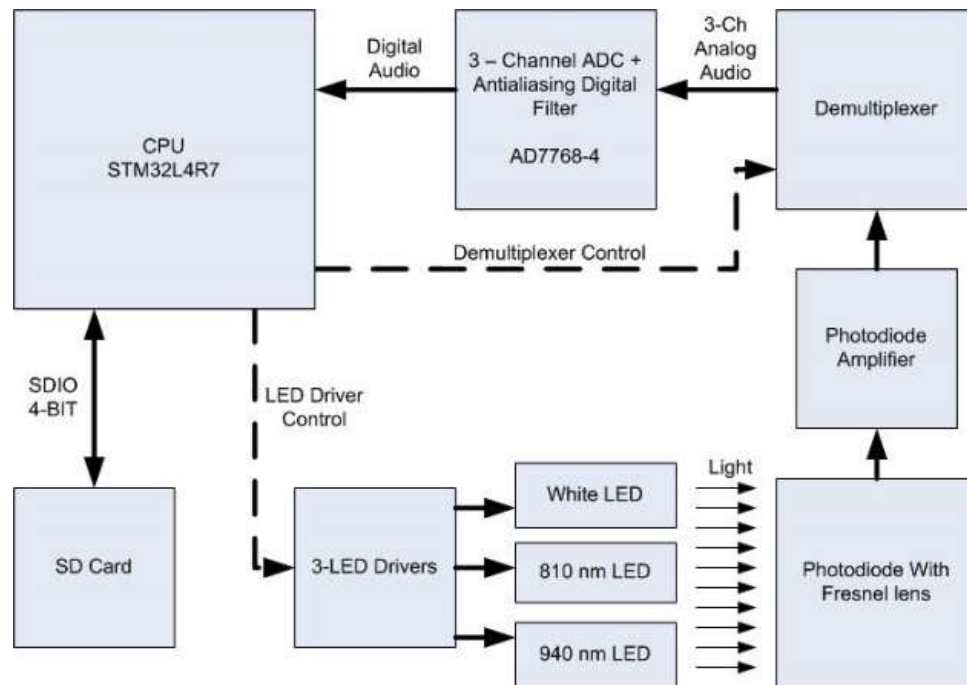


Figure 2-4. Block diagram of the multispectral sensor.



Figure 2-5. Prototype of the multispectral sensor.

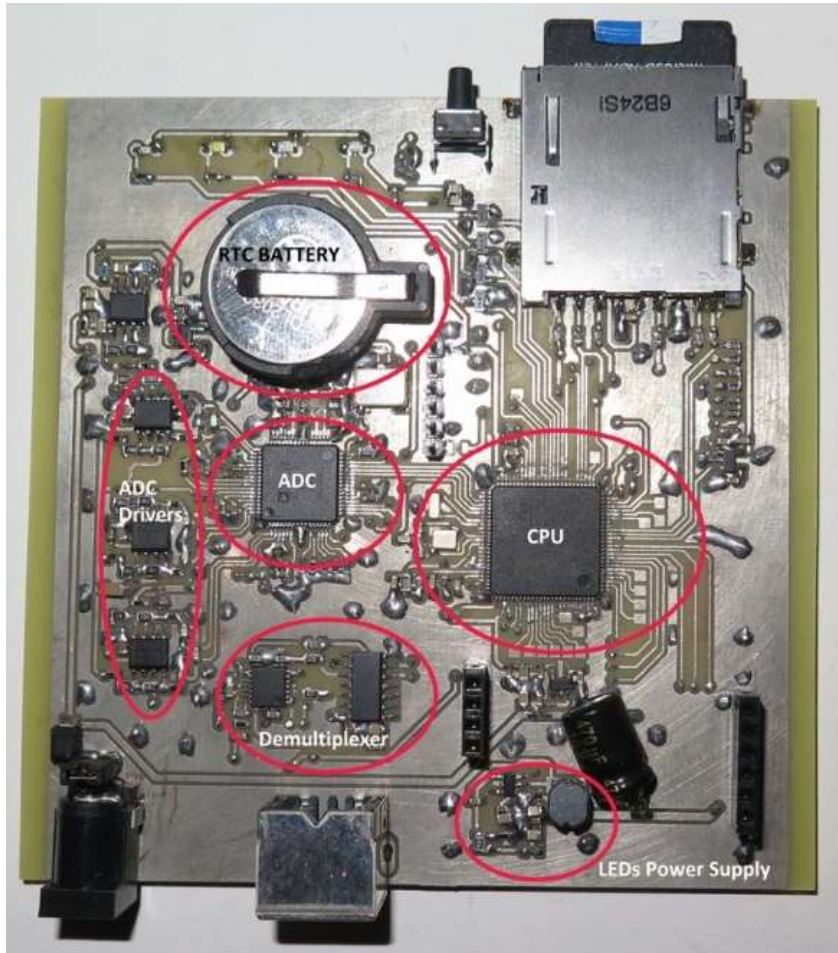
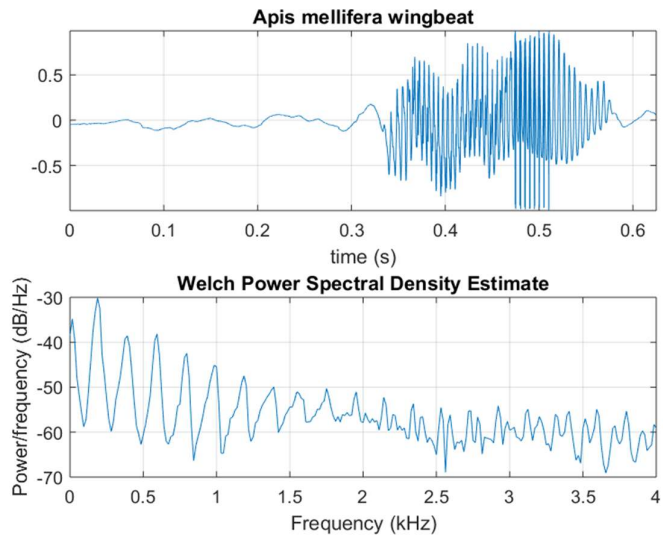


Figure 2-6. Prototype of the multispectral recorder.

2.3 Results

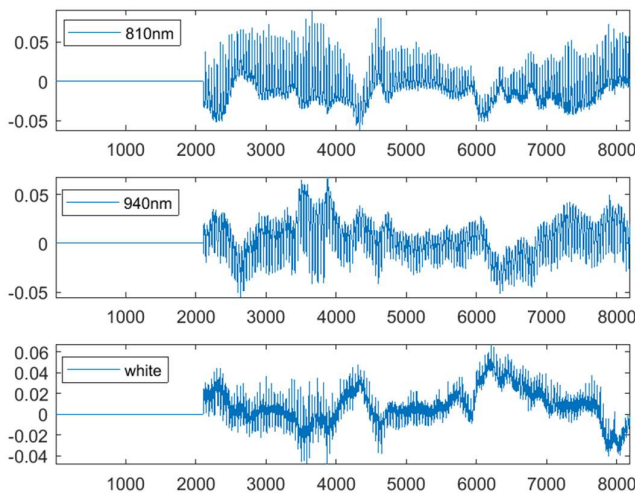
It takes a flying bee or a wasp 200-300 ms to cross the FOV of the Fresnel in a direct quick flight but can reach 625 ms in slower types of flying patterns and even more in rare cases. The light fluctuation is recorded by the sensor as it crosses the light path from emitter to receiver and subsequently analyzed (see Figure 2-7 top for a typical case of an in-flight recording). Fourier transform can reveal how the energy of the recorded signal is distributed on its constituent frequencies (see Figure 2-7 bottom the Welch periodogram).



(Top) A typical wingbeat event of *Apis mellifera* recorded as the insect crossed the extinction light, Fresnel-based optical sensor (31 oC). (bottom) Magnitude spectral density. The fundamental frequency of *Apis mellifera* typically drifts between 190 and 240 Hz.

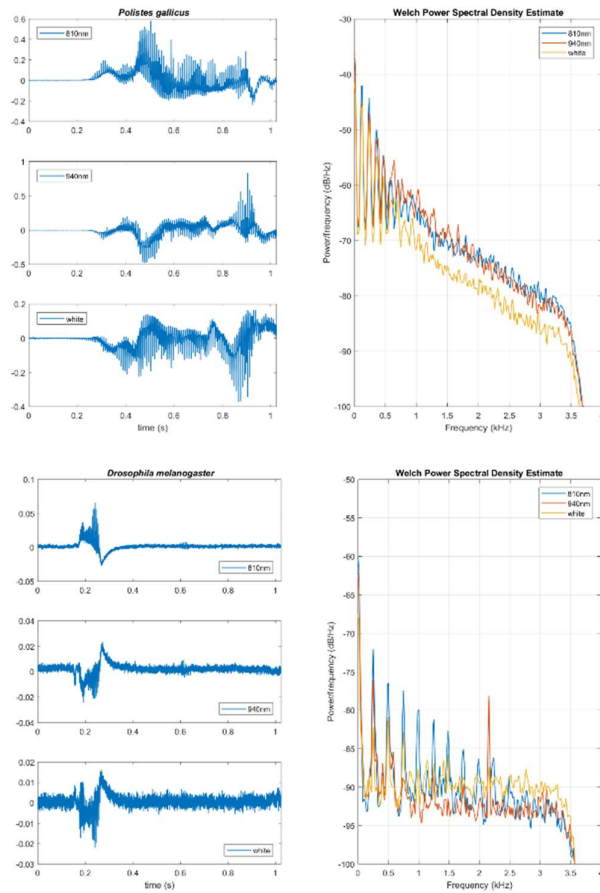
Figure 2-7. Wingbeat event

A multispectral recording is shown in Figure 2-8 for a bee and in this figure can see various recordings of the wingbeat of insects. The frequencies and the harmonics coincide for the different bands as expected but the ratio of light at different bands is not the same.



From a bee's wings and main body using three different spectral bands (810 nm, 940 nm, white). Time domain signal at 8 kHz sampling rate. Recordings are treated as audio and the amplitude in y-axis is normalized between [-1, 1].

Figure 2-8. 3-band Optical wingbeat recording of backscattered light.



From the wings and main body using three different spectral bands (810 nm, 940 nm, white). (left) Time domain signal at 8 kHz sampling rate and (right) Welch Power Spectral Density. The wingbeat of (top) the wasp *Polistes gallicus*, (bottom) the fruit fly *Drosophila melanogaster*.

Figure 2-9. Spectrum of 3-Band recording of backscattered light.

In Figure 2-9 we show on the left the consistency of the wingbeat spectrum measured on a specific native wasp *Polistes gallicus* and a smaller insect namely, the fruit fly *Drosophila melanogaster*. One can see this by observing the coincidence of the peaks regarding the harmonics. Contrary on the right, one can see the grave differences between the f_0 and f_1 . In Figure 2-9 right, the difference between the wasp and the fruit fly is obvious as confirmed by the spectral peaks in the PSD that are quite different for these different insects.

2.4 NOVEL NOISE-ROBUST OPTOACOUSTIC SENSORS TO IDENTIFY INSECTS THROUGH WINGBEATS

2.4.1 Introduction

In this chapter, novel high-precision and noise-robust optoacoustic sensors that can record the wingbeats of insects are presented. Certain insects, e.g., fruit flies of the *Tephritidae* family, have a great impact on international marketing and world trade of agricultural products because they can infest a wide range of commercial and native fruits

and vegetables [23]. We offer a small sample of referenced figures, mainly to present the serious impact of these pests on economies, which may not be well known in other research areas:

- a) The olive fruit fly *Bactrocera oleae* (Gmelin) (Diptera: Tephritidae) is the world's most serious insect pest of olive fruit. It inhabits the Mediterranean area, Africa, the Middle East and North America. If left untreated it is held responsible for losses of 80% of oil value and up to 100% of table cultivars and actually effects economic damage of hundreds of millions dollars per year [24][25].
- b) *Ceratitis capitata* (Wiedemann) (Diptera: Tephritidae) causes extensive damage to a wide range of fruit crops. It is native to the Mediterranean area but has spread invasively to many parts of the world, including Australia, Asia and America [26].
- c) West Nile virus, malaria, certain forms of encephalitis and other infectious diseases that annually prove lethal to humans are transmitted by a number of mosquito species, such as *Aedes albopictus*, *Aedes aegypti*, *Culex pipiens*, *Anopheles gambiae* and many others.

Insect traps of various shapes are commonly used to determine the nature, density and location of such pests; they are currently inspected manually [27]. Manual inspection is tedious and unreliable and prevents large-scale spatial and temporal deployment. A sensor that could reliably analyze the sound spectrum of a flying insect entering a trap would allow the recognition of the species and thus radically change the way monitoring is carried out.

The acoustical properties of the flight activities of economically and socially important insects have drawn much attention even prior to the wide acceptance of microphones. The research literature is rich in studies of the acoustical properties of various insects, their relationships to temperature, their flight habits and their communication [28]. However, a device based on microphones functioning in the field is exposed to an uncontrolled number of audio sources that will be recorded by the microphones regardless of the trap configuration [29]. Because the number of audio sources, and possibly also their spectral content, is unknown and time-varying, their practical use in the field for reliable counting and recognition of flying insect identity is limited. The present work reviews and builds on optoelectronics applied to this specific task; it does not address camera vision solutions.

Efforts to study insect wing motion can be traced back to 1939 [30]. Chadwick refers to acoustic and optical methods applied to the study of insect wing-flaps that are based on techniques that date back to 1827. He describes a stroboscope approach in which the cyclic motion of the wings appears still when a light source is synchronous with the motion to be

observed, and therefore the frequency of the wing-beat can be derived. The use of the wing-beat frequency to classify insect species was explicitly stated for the case of *Drosophila pseudoobscura* in [31]. In the early works of Sotovalta in [32] and his contemporaries referenced, one can also see attempts to establish a clear connection between wing-beat frequency and perceived frequency using all technical means of the time and even subjective acoustical observations.

In 1955, Richards discovered by chance that insects flying between the sun and photoelectric cells produce fluctuations in the light intensity received that can be converted to audio [33]. Repeating the experiment with insects in a transparent box, he reported that wing fluttering is imprinted in electrical fluctuations due to the wings' partial occlusion of the light path between an emitter and a receiver. Both Chadwick and Richards make an implicit claim that different species have different wing-beat characteristics and that the optical sensing of their wing-beat can possibly lead to insect classification. Subsequently, the notion that the perceived wingbeat tone could potentially be used as a taxonomic characteristic appears in many publications, e.g., Sawedal [34]. The work of Richards inspired a generation of researchers to use different photosensors to detect fluctuations in light intensity caused by reflections of flying insects [35]. By that time, it was clearly suggested that automatic instrumentation and various types of photosensors could be used to discriminate among flying insects by analyzing not only the fundamental frequency associated with the wing-flap but also the harmonics produced by this action [36][37]. Various configurations of opto-electronic systems have been developed to study different insects [38][39][40][41]. An unseen connection between lasers, bees and explosives can be found in [42]. Despite these efforts, until 2006, all publications were constrained to laboratory experiments, probably because the electronics of the time and the diversity of disciplines involved made it difficult to develop a stand-alone prototype that could be employed in the field to monitor insects of economic importance. Although not a widely known contribution, Kirsch [43] introduced a beta-system approaching a device that could recognize flying insects in the field. In [44], the authors presented a stand-alone device that would count and transmit counts of *Bactrocera Dorsalis* from the field. This system, however, used an optical system that had the basic functionality of on-off, i.e., photo-interruptions due to the passages of insects that were counted. It did not involve spectral analysis of recordings and therefore could not discern insect species. Keogh E. and his team revived the idea of optically sensing insects and gathered recordings from optical sensors [45]. The same team made a part of the database available and organized an open

competition for classification algorithms to crowdsource the answer to an important question: the extent to which recordings of optically sensed wing-beats generally lasting between 50 and 100 ms allow separation of species. This step is important because past results indicated medium scores, probably because the electronics of the time were not sufficiently advanced and the authors performing the classification experiments were not dedicated data scientists but wanted to show a proof of concept. The outcome of this large experiment [22][46] was that optoelectronic recordings combined with advanced signal-classification techniques could indeed return highly accurate recognition results for several species in flight. Despite these efforts, at the time of writing, to the best knowledge of the authors, there was no definitive demonstration of a device that classifies insects and operated in the field using optoelectronic principles. The first actual prototype trap that integrated all these components and was functional was presented in [47], where the widely adopted McPhail type trap [27] was modified to be electronic. In the present work, we describe a more advanced optoacoustic device that can monitor the wingbeats of any insect species. Certain butterflies and Lepidoptera flap their wings with frequencies of a few hertz, but the vast majority of insects flap their wings at frequencies between 100 and 1000 Hz. Our sensors are based on photodiodes that can operate at much higher frequencies and therefore can perfectly resolve the fundamental and overtones of wing-flapping.

Controlled experiments on insects of great economic and social importance, namely, the devastating pest for olive trees, *B. oleae*, a mosquito vector of malaria, *A. gambiae*, and *Apis mellifera* (the western honey bee) were carried out in this part of the work.

The sensors described here are noise immune to the interference commonly found both in the lab and in the field because they perform modulation/demodulation of light at high frequencies. They can work unobtrusively either in the dark or in sunlight, and we will demonstrate that their accuracy in analyzing the spectrum of a wingbeat recording matches that of the microphone. The simultaneous recording of insect sounds using optical devices and microphones and their comparison is currently absent from the research literature.

2.4.2 Materials and Methods

We describe in detail the construction of an optoelectronic sensor that is able to record the elusive motion of a wingbeat. The sensor must be able to operate in illumination conditions ranging from bright light to total darkness. The energy of the wingbeat signal is very small; therefore, the smallest interference can mask the useful signal. The construction of our

sensor is virtually immune to interference from electric devices, power supplies and lamps typically found in laboratories where insectaries typically exist. This immunity is achieved by employing appropriate modulation to the emitting light while the demodulation at the receiver end is performed at high frequencies. We also study different light sources (infrared and laser), and we demonstrate that they perform almost equally with a slight objective advantage to laser sources. We also experimentally demonstrate that the analytic accuracy of the spectrum of the optoelectronic sensors matches that of microphones; this is the first such report in the literature.

2.4.2.1 Recording Devices

In view of practical applications in the field, there are clear advantages to using optoelectronics instead of microphones for recording insects' wing-flaps:

- a) the optoelectronic device records an event only when the path from the emitter of some form of light (e.g., infrared, laser) to the receiver (e.g., phototransistor, photodiode, photoresistor) is interrupted, whereas a microphone picks up sound from all-directions,
- b) optoelectronic devices return a very high signal-to-noise ratio, whereas microphones record all sound sources (e.g., mechanical sounds, birds, cicadas, weather effects), and therefore, the recordings can become very noisy,
- c) microphones, although they can be protected in several ways against weather conditions, are more vulnerable to open field conditions.

A block diagram of our optoelectronic device designed to record the very low-level signals of a wing-flap is shown in Figure 2-11. Amplitude modulation is intended to shift the low frequencies of the wingbeat to high frequencies and suppress interference due to electronic light appliances in the lab. These appliances produce strong optical interference at multiples of the main power supply frequency; other sources of electrical/electronic interference (mainly LED lighting) are possible as well. Wing-beating motion modulates the amplitude of light scattered from an insect and the frequency of the modulation provides information that can be used to categorize its species. We have developed two versions of the optoelectronic device; the emitter is either a laser or an infrared light source.

The receiver (Figure 2-10) is an array of photodiodes connected to a low-noise operational amplifier (OPAMP). The OPAMP is selected to have large bandwidth (54 MHz), a quick response time (640 V/ μ s), low noise levels (6.6 nV/ \sqrt Hz) and a small input bias current of 0.6 pA. We did not use phototransistors because their response times of 10 μ s are slow

compared to those of photodiodes (response time 40 ns). The output of the OPAMP drives a switched capacitor band-pass filter (Figure 2-12). This 8th-order filter (based on IC1 in Figure 2-12) has a 60 kHz center frequency and a 10 kHz bandwidth and therefore rejects the signals from conventional light sources by at least 60 dB, allowing only the signal from the emitter after amplitude modulation by insect wingbeats. The insect wingbeat causes a modulation in amplitude of the light beam from the emitter to the receiver; the signal is demodulated through a precision rectifier (IC2 in Figure 2-12).

The output of IC2 drives a low-pass switched capacitor filter (IC4 in Figure 2-12) with a 3 kHz cut-off frequency that cuts off the carrier at 60 kHz; IC5 is a filter-buffer to eliminate any clock feed from the switched capacitor filters. The power supply (Figure 2-13) has input voltage varying from 3.3 VDC to 5 VDC and three output voltages: +8 V, -8 V and 3.3 V. The input voltage can be a 3.7 V lithium battery, the USB voltage of any PC or a single 220 VAC to 5 VDC power supply. Figure 2-14 shows the microcontroller circuit; it emits light pulses at 60 kHz frequency instead of continuously and the receiver, composed of an array of photodiodes and filters, demodulates the signal back to acoustic frequencies. This circuit produces the 3 MHz clock to the band-pass switched capacitor filter, the 150 kHz clock to the low-pass switched capacitor filter and the pulses for the laser and led infrared emitters. The laser emitter has a beam splitter that opens the laser beam as a thin sheet, directing beams to terminate on the array of photodiodes. The infrared light is diffused and no splitter is used. The details of all elements are included in Appendix.

Figure 2-10 to Figure 2-13 and the Appendix provide all necessary details needed to build the optoacoustic sensor. With the exception of [35] from 1979, to the best of our knowledge, there is no publicly available description of an optical sensor that can record movements of insects at the scale of a wing-beat.

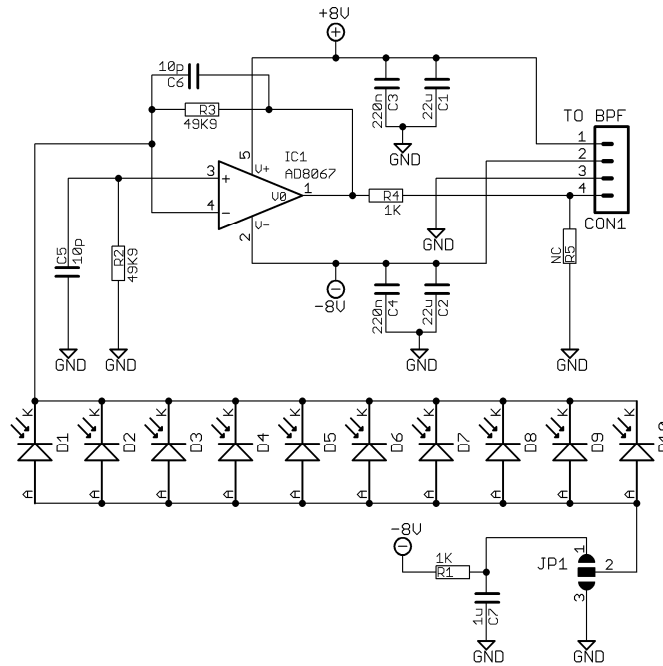


Figure 2-10. Receiver: a linear array of photodiodes

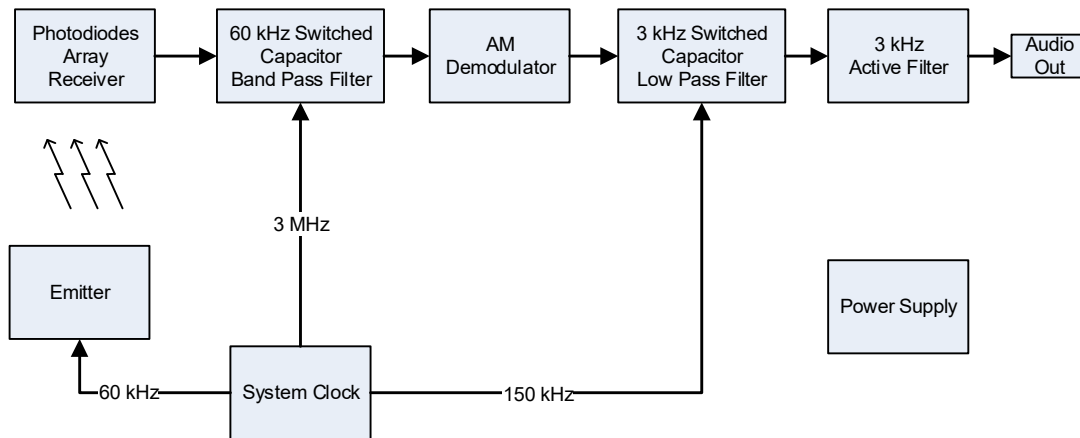


Figure 2-11. System diagram of the optoacoustic sensor

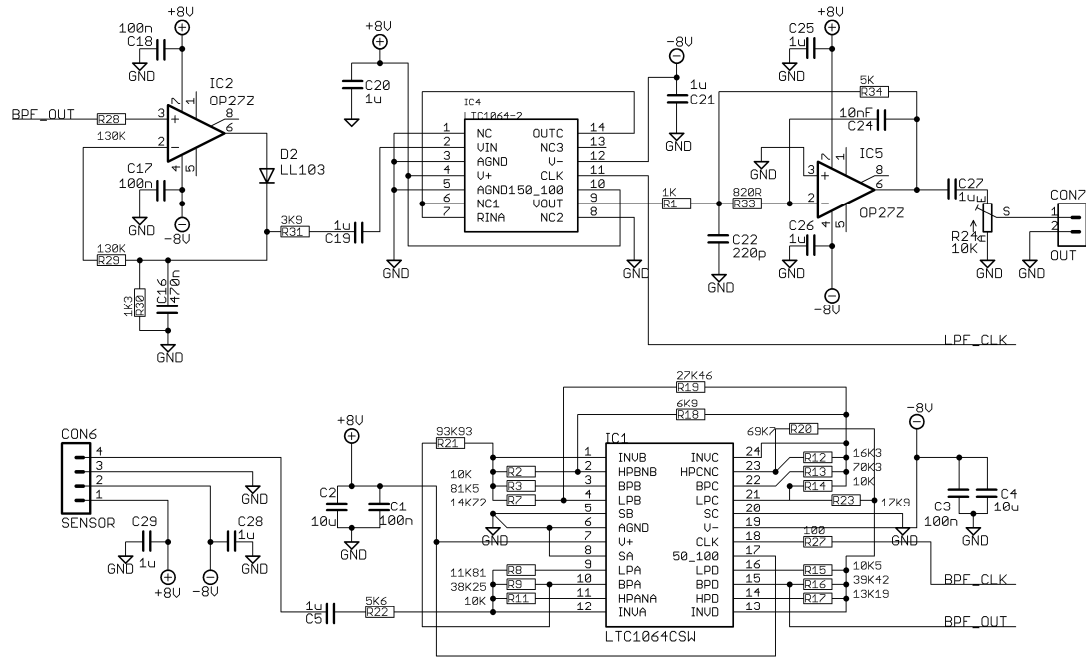


Figure 2-12. Filters and demodulator

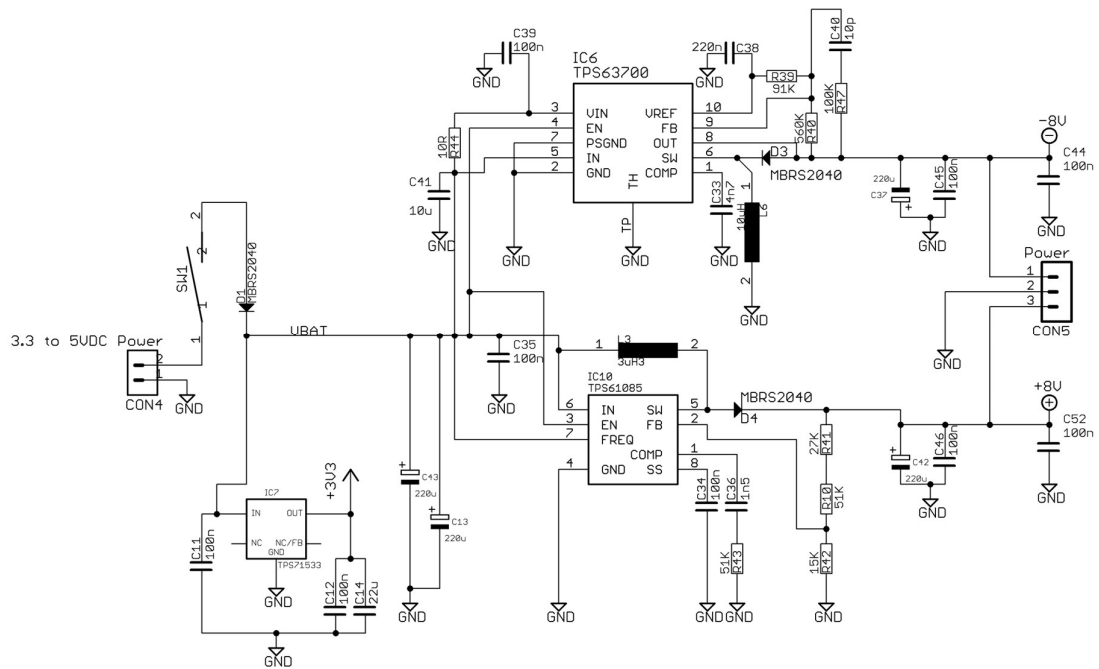


Figure 2-13. Power supply

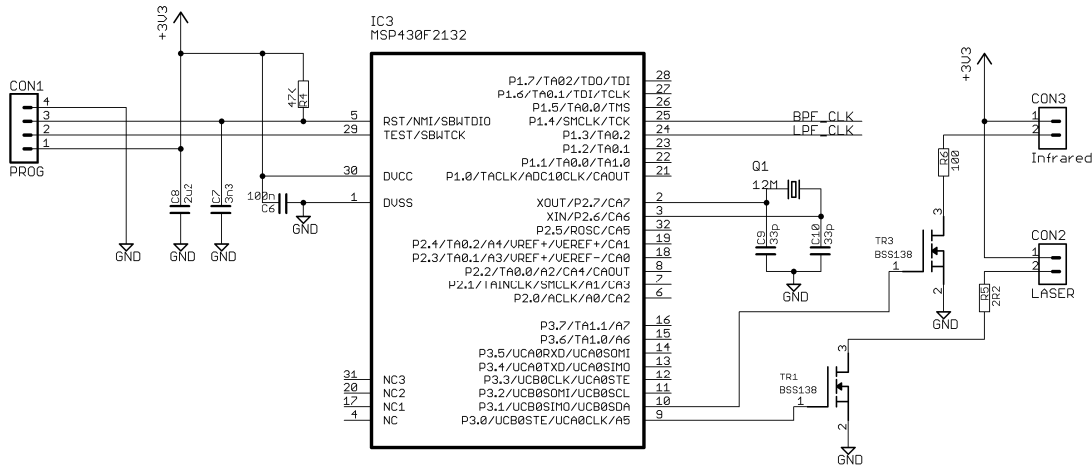


Figure 2-14. Clock and emitter circuit

2.4.2.2 The equivalence of optical and microphone acoustics

The waveforms generated by the flight sounds of *Musca domestica* (the common fly) were recorded and analyzed simultaneously using the optoelectronic devices and a small-aperture microphone (UMIK-1 omnidirectional measurement microphone), and we compared these two different modalities. To avoid subjectiveness regarding the produces that provide the best results, we took measurements of each light source (laser and infrared) while simultaneously recording the wing-flap with a microphone. Therefore, we always had the two different modalities recording the same event. We kept the microphone recording as a reference, and we measured the difference between the optoelectronic recording and the microphone signal. The distances between the receiver and the emitter and the insect were fixed for both experiments. The optoelectronic apparatus and the microphone both sensed the wing movements but are actually two modalities functioning on different principles. The optical one is based on interrupting the light between emitter and receiver. The wings are semi-transparent membranes that are usually strengthened by a number of longitudinal veins. Cross-connections between veins form closed ‘cells’ in the membrane. The wing shape, the patterns on it and the complex movement affect the waveform of light intensity recorded by the photodiode. The microphone is indifferent to transparency issues and body movements. The shape of the wing and the rhythm that is vibrated play the key role in setting the air molecules in vibration during the complete wing stroke. The optical and sound recording modalities are based on completely different principles. Yet, the resulting waveforms are almost identical, as shown in Figure 2-15 and Figure 2-16. In Figure 2-15, we have recorded the same adult fly using an infrared optoelectronic device simultaneously with a microphone. We present all phases recorded side by side using both modalities, and

we see the striking resemblance in the spectrograms. Both recordings are rich in harmonics; the fundamental frequency often drifts slightly. Both the fundamental and the harmonics up to 2 kHz are clearly resolved. The microphone was able to resolve harmonics above 2 kHz, but this also depends on the relative position of the microphone with respect to the insect. In this case, the microphone was placed 1-2 cm away from the insect, whereas the distance from the light emitter to the receiver was 11 cm, and the insect was placed approximately in the middle.

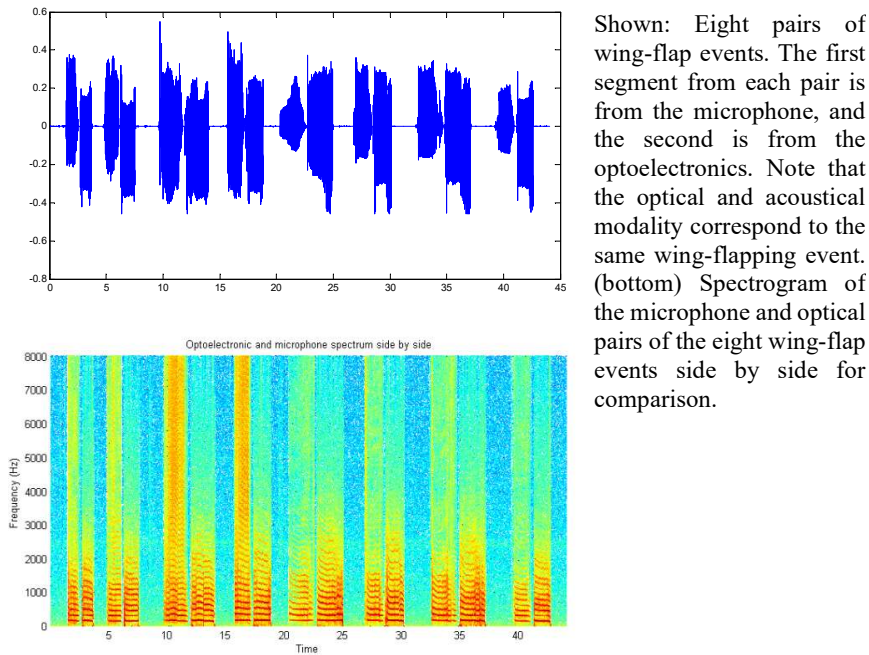


Figure 2-15. *Musca domestica* adult insect recorded with an IR light and microphone.

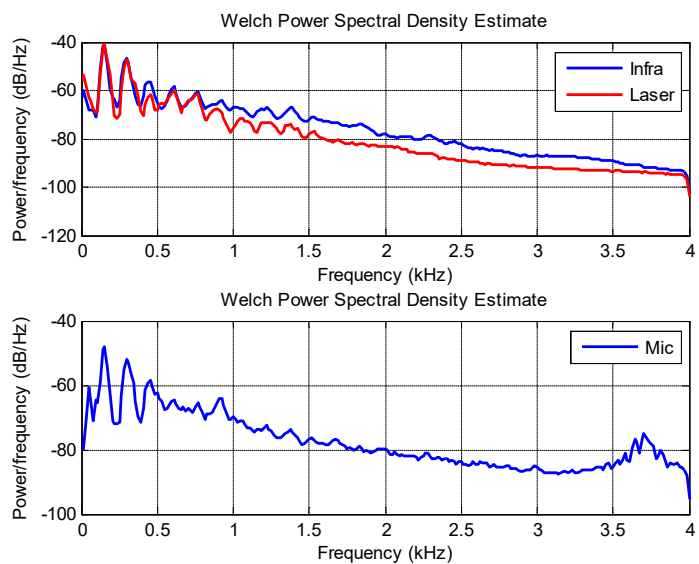


Figure 2-16. Single *Musca Domestica* power spectral density (Infra-Laser-MIC)

Figure 2-16 is also enlightening in terms of the relationship of the infrared and laser optoelectronic device with respect to the microphone recordings. All recordings are almost identical, with the laser having a slightly sharper analysis of the spectrum, as shown by the objective distance measures (see following paragraph). All insect measurements in this work were carried out in a controlled laboratory environment of 25o Celsius and 55% humidity.

2.4.2.3 Distance Measures

Listening to the recording of either the laser or infrared version of the optoacoustic device sounds quite similar to the microphone recording to the point of being difficult to discriminate. The microphone sounds slightly more ‘natural’ to a human listener. Because most reported work is based on audio recordings and much less on optoacoustic recordings (see [48][49] and the references therein) and the audio reflects our everyday experience, we take the microphone as a measure of “naturalness” and we compare the optoacoustic devices to the microphone. To determine objectively which emitter is closer to the microphone recordings, we calculated several distance measures [50]. The corpus we used to compare is composed of 32 wing-flapping events totaling approximately 3 minutes of recordings with the silences between events removed. These events were recorded with the laser, the infrared and the microphone.

We applied a normalization that we found to work better than normalizing with the maximum value:

$$s_i / \sqrt{\sum_{i=1}^N s_i^2}, i = 1, \dots, 512 \quad \text{Equation 1}$$

Normalization is applied to match the level of each optical modality with the microphone level. After normalization, both signals to be compared possess the same energy (i.e., the laser and microphone pair first, and then the infrared and microphone pair).

We derived the Log spectral distance defined in (2) between two data chunks of 256 samples each, and we averaged over 10382 frames that corresponded to the recorded data.

$$D_{LS} = \sqrt{\sum_i^M \left(10 \log_{10} \frac{P_o(i)}{P_a(i)} \right)^2} / M \quad \text{Equation 2}$$

where P_o and P_a are the power spectra of the optical and audio data and M is the number of spectral bins.

The Itakura distance between autoregressive parameters is defined in (3), where x is the observed linear prediction coefficient (LPC) $[-1 \ a_1 \ a_2 \ \dots \ a_p]$ and y is the corresponding LPC for the reference signal (the microphone recording):

$$D_I = \log \left(\frac{xRx^T}{yRy^T} \right) \quad \text{Equation 3}$$

The Itakura-Saito distance is defined as in (4):

$$D_{IS} = \sqrt{\sum_i^M \left(\frac{P_o(i)}{P_a(i)} - \log_{10} \frac{P_o(i)}{P_a(i)} - 1 \right)} \quad \text{Equation 4}$$

Note that the smaller the distance is, the closer is an observed recording to a reference recording, and a perfect match results in 0 distance. All distance measures agree, giving a small benefit to the laser emitter compared to the infrared emitter (see Table 1). The small differences between the optical modalities and the microphone are consistent with Figure 2-16. Informal listening experiments do not demonstrate a perceptible difference between the laser and the infrared emitter. We use as a result that the laser emitter is closer by a small margin to the microphone signal compared with the infra-red emitter.

Table 1. Mean distance measures of opto-recordings over 10382 segments.

Distance Measure	Laser	Infrared
Log spectral distances	1.21	1.33
Itakura distances between AR coefficients	0.57	0.62
Itakura-Saito distance	0.82	0.99
*The reference signal is the microphone recording.		

One should note that the goal of the optoacoustic devices in the context of our future work on electronic insect traps is not listening naturalness but classification accuracy.

2.4.2.4 A case study of very small insects

In Figure 2-17, we attempt to study the practical limits of the device in analyzing the wing-flap of insects. Therefore, we have chosen a *Drosophila melanogaster* insect. *D. melanogaster* is a very small insect; the specimen we used was 2.5 mm long, and the major axis of its wings was 2 mm. One can see in Figure 2-17 (top) that the signal-to-noise ratio in this case was not as high as in other recordings. However, wing-flap events are resolved even for this very small insect and the recording is clearly audible.

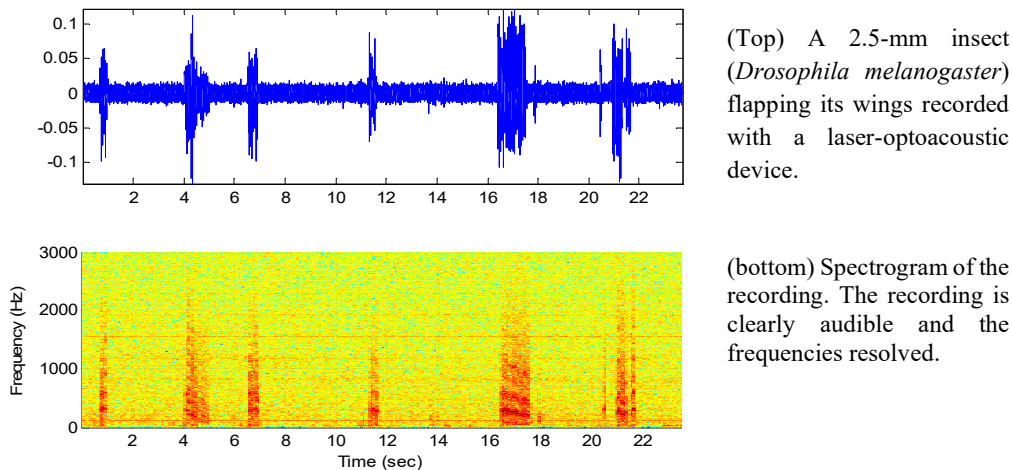


Figure 2-17. A 2.5mm *Drosophila melanogaster* with LASER beam.

2.4.2.5 Analyzing insects of social and economic importance

The objective of the spectrograms in Figure 2-17 to Figure 2-19 is to study the waveforms generated by flight sounds of different insects and see how they develop a frequency signature of the wing-beat so that we can determine whether different insect species can be identified by their opto-acoustical properties. The spectrogram of a potentially dangerous mosquito species is shown in Figure 2-18, and an irritated bee is wing-flapping constantly for 37 seconds in Figure 2-19. The sounds of insects in general are considered to be fingerprints of the species and can be used for insect recognition [41][42]. *A. gambiae* is a mosquito species in the genus *Anopheles* and is one of the most important vectors of malaria. Although many insect traps are available in the market, there is no device known to the authors that can recognize the species of the insects. We envision that the sensors described here can be embedded in normal traps and can subsequently count and transmit data regarding the species captured. These counts are invaluable as inputs to mosquito-borne epidemic models that currently receive their input data from manual counting of

dispersed traps. In Figure 2-18, we show the recording of a male *A. gambiae*. One notes the high frequency of wing flapping compared to the much larger bees in Figure 2-19. One should also note how the different fundamental frequencies of the wing flap, the difference in the shape of the wings and the different beating habits result in a unique frequency signature for each species.

2.4.2.6 In flight recordings

Figure 2-20 illustrates a different experiment in which insects were enclosed in a plexiglass box containing the powered-on sensor (see Figure 2-21 for a close view of the electronics board) to record in-flight wing-flapping (in contrast to a specimen held manually in front of the sensor). In-flight wing-flapping is a procedure in which an insect flies freely as in nature and crosses the beam of the emitter. If we observe the insects in slow motion, the flying insects gradually partially overlap the light beam. As an insect moves totally inside the beam the light variation measured by the sensor starts from the noise level, achieves a peak and then returns to the noise level, producing the quasi-periodic recordings of Figure 2-22 and Figure 2-23 .

In Figure 2-22, 150 ms of flight is recorded for *Apis mellifera* (a large insect compared to a fruit fly), and in Figure 2-23, 50-100 ms of flight is recorded for *B. oleae* fruit flies. In [35][36], it is demonstrated in other datasets that this duration provides data sufficient for accurate discrimination of species. Moreover, we spent time observing the entrance angles of the arrivals of various insects crossing the emitter-receiver path and their corresponding spectrograms.

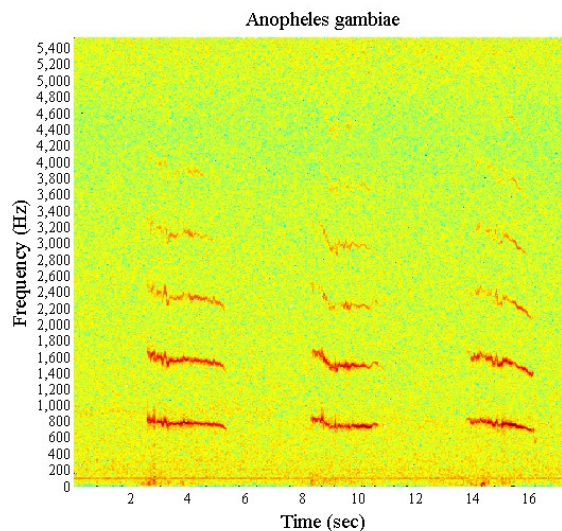


Figure 2-18. Spectrogram of a single adult mosquito *Anopheles gambiae* (Recorded with a laser optoacoustic device)

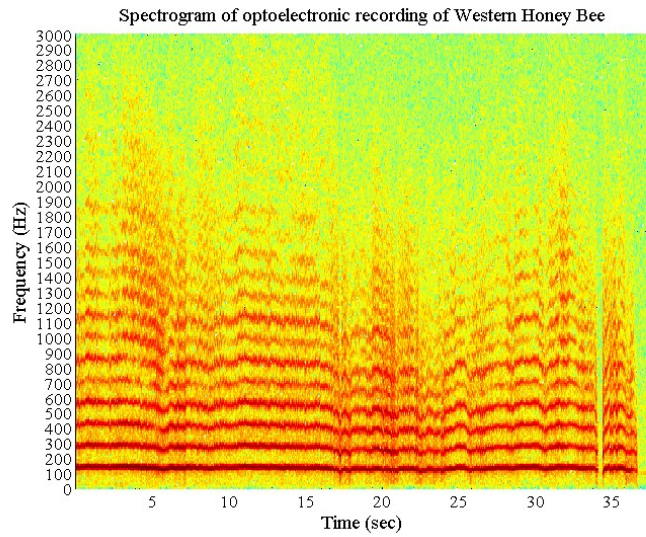


Figure 2-19. Spectrogram of a single *Apis mellifera* worker. (recorded with a laser optoacoustic device). Note how the fundamental frequency of 140 Hz is clearly resolved, as are the harmonics



Figure 2-20. In-flight recording from the optoacoustic device.
a) The laser emitter and the beam splitter attached to the emitter,
b) small aperture gun microphone,
c) array of photodiodes. The cross-lock tweezer in the middle holds insects by their legs

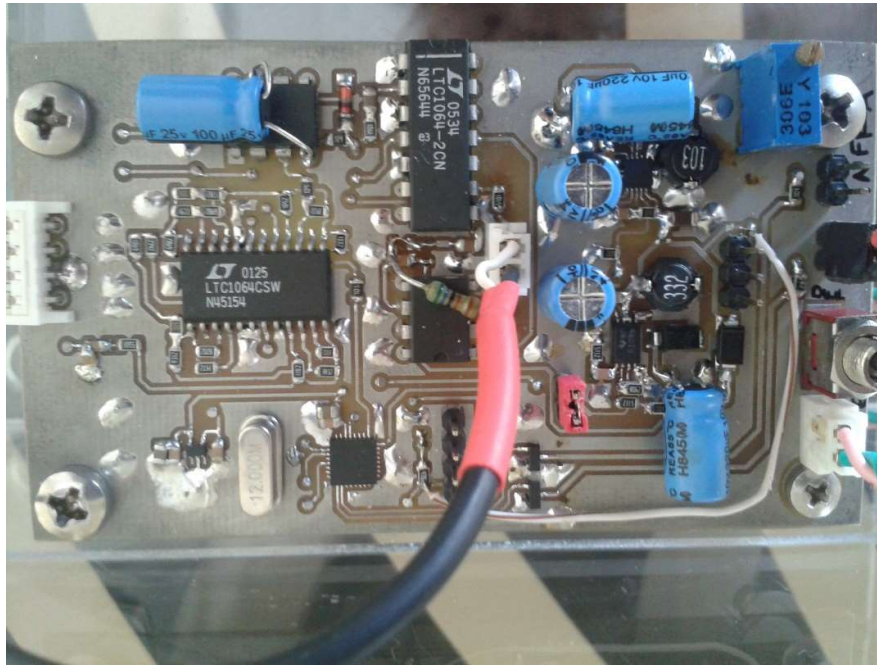


Figure 2-21. A close-up view of the electronics board

A small sample of our observations is gathered in Figure 2-23, in which six different freely flying *B. oleae* insects are recorded. Their spectra and spectrograms provide similar results, with small variations expected from biological organisms. This implies a significant attribute of the sensors: the spectra they provide are invariant to the entrance angle of the flying insect.

2.4.3 Discussion

We have constructed an opto-electronic sensor that can accurately analyze any insect's wing flapping. Note that most insects beat their wings with frequencies <1 kHz (see [53] for a large collection of wing-beat frequencies). Clearly, the operating frequency of photodiodes that responded perfectly at 60 kHz is far higher than any biological organism can reach with its wings. Therefore, we conclude that optoelectronic devices cannot fail to respond in tracking the wing-beat of any insect. The constructed sensor is indifferent to illumination variations and operates from bright light to total darkness. It is robust against electronic interference because it modulates emitted light to high frequencies and therefore is immune to interference from devices typically encountered in laboratories; therefore it can be useful for in-lab research and in the field. All experiments presented were performed in the laboratory under strong electric lamps that had no effect on the recorded spectrogram.

We did not observe any difference in the spectrogram when we rotated the insect specimens held with a short pointed, self-closing cross lock tweezer. At this point, we note that we also used the simpler sensors presented in [47]. These sensors differ mainly in that they do

not modulate-demodulate at high frequencies. We report that they failed in the context of these specific artificially illuminated conditions because these sensors registered strong interference at the frequency of the power supply as well as its harmonics, mainly from the electric lights of the laboratory and other electronic appliances. This interference totally masked the very low-level signals of a wing-flap.

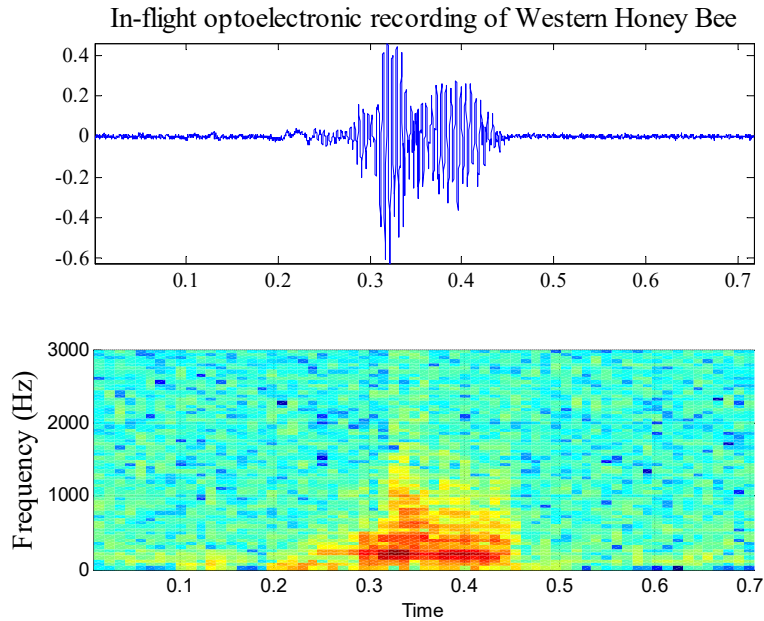


Figure 2-22. An in-flight recording of *Apis mellifera* flying in the light beam. Crossing it and finally leaving the laser beam. (Top) sonogram, (bottom) spectrogram.

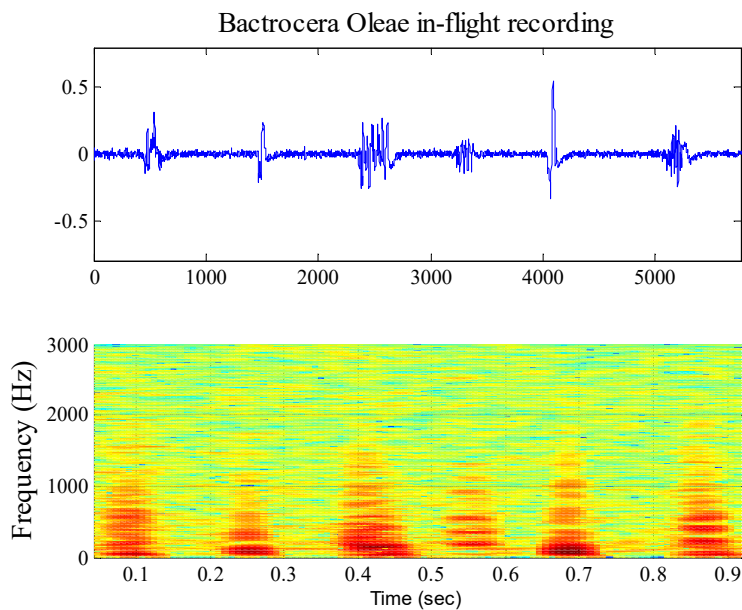


Figure 2-23. In-flight recording of several *B. oleae* insects. They fly in and out of the laser beam. (Top) sonogram, (bottom) spectrogram.

We have demonstrated that the recordings are very close to the quality of a microphone, yet they do not face the problems of a microphone that picks up sounds from every direction. We did not find significant differences in quality between an optoacoustic sensor that employs a laser emitter and a simpler infra-red emitter, though objective distance measures give a small advantage to the laser emitter. We have operated our sensors on insects of economic and social importance, such as fruit flies, mosquitoes, and bees, and found that the sensors clearly resolve their spectra by finding the fundamental frequencies and the manner in which wing-flap energy is distributed in the harmonics.

We believe our sensors are an important contribution to the construction of a reference database of insects' wingbeats because these data can now be collected easily anywhere, even in the insects' own habitats, without interference from competing bird and insect species. Reference collections are constructed because they serve as an invaluable tool for educating new scientists and for saving information about a species before it becomes extinct. Currently, there are collections of sounds but are constrained in the use of microphones. This involves a difficult procedure because the recordings are prone to acoustic interference and an anechoic chamber is required for reliable recordings. We propose that optoacoustic devices can replace microphones for the specific task of recording insects that produce sound by wing-flapping.

We project that our robust sensors pave the way for many innovative applications not yet in the market, such as the following:

- a) Electronic beehives [54] that would count the number of incoming and outgoing bees, guard against invasive species and even assess the health of the entering bee, as the health of an insect has an impact on its flying patterns.
- b) Mosquito traps that will transmit counts per species to alarm for species that are possible carriers of serious diseases and to provide input to statistical vector models that predict the spread of mosquito-borne diseases based on counts of traps at dispersed locations.
- c) Electronic traps that are hung from trees and report the density of captured insects and their species composition to initiate spraying procedures at large scales for a number of fruits.

2.5 LARGE APERTURE OPTOELECTRONIC DEVICES TO RECORD AND TIME-STAMP INSECTS' WINGBEATS

2.5.1 Introduction

Insects affect cultivations that are vital for rural economy, local heritage and environment in both positive and negative ways: insects pollinate a large number of plant species, while certain kinds of insects are considered pests that cause major production and economic losses in agriculture [11]. On top of the hazard list, mosquitoes and biting midges can transmit serious diseases to humans and livestock. Innovative uses of sensors and networks targeting animals are starting to be translated into new ecological knowledge [55]. This work describes in detail a novel device that can be used in both applied and basic research in the context of automatic insect monitoring. In entomology one is often interested to study the flight mechanism and movement patterns of insects [18]. The proposed device can be used to derive the frequency content of wingbeats of a large number of insects on the order of hundreds to thousands. In this study we present a practical setting where the optical sensor is inserted inside insectary cages that enclose many flying adults of the targeted insect to record their wingbeats as they incidentally cross the field of view (FOV) of the sensor. We show how this setting allows to automatically record and analyze big datasets of wingbeats stemming from insects that have large economic and social importance such as fruit flies and mosquitoes. It is a daunting task to run these studies manually, based on direct observation, as insects are hard to manipulate especially on free flight and studies involving a large number of insects are not replicated through time or across sites to great extent because of the manpower requirement. In the context of our work, we make a distinction between optoelectronic sensors and vision cameras as the optoelectronic sensor is always composed of a light emitter opposite to a light receiver. The beating wings of insects flying in the FOV partially intercept and modulate the flow of light. The implications of this technology are discussed in view to embedding it in insect traps to count and classify flying-in insects based on the spectrum of their wingbeat [16]. A historical retrospection of optical methods applied to measuring insect movement is presented in [15] and the references therein. Various configurations of opto-electronic systems have been developed in the past to study the movement of insects [35][38][39][40]. Prior work, reaching back 15-20 years, focused mainly on the sensor. Moreover, the sensors presented at that time were not immune to electronic and light interferences. In this work, the sensor is of high-precision, and immune to optical interferences from natural or electric light. Moreover, a complete system is described in detail where the light fluctuation in the output of the receiver is monitored by a microprocessor and the device is auto-triggered when it senses a

wingbeat. Once triggered the light fluctuation is turned to an audio snippet, time-stamped and internally stored in the SD of the device as a permanent record. As in [15] this work is based on modulating-demodulating high frequency light pulses hitting the beating wings of the insect. However, in this chapter we introduce several novelties in the sensors' construction and offer a complete wingbeat recording system as well. In detail: a) The receiving aperture of the sensor is made large enough to accommodate the full motion of a wingbeat and to allow tracking of fast flying insects such as fruit flies that would otherwise spend little time inside the FOV while crossing the surface of a single diode. Lack of sufficient duration data is translated to poor frequency resolution for fast flying insects. We present two ways of expanding the light receiving surface: First we construct a 2D array of photodiodes and secondly, we make use of a large aperture optical light guide. The latter one, to our point of view, opens new grounds as a deformable, slim sheet of polymer/acrylic light guides will allow tracking of flying insects inside various curved shapes of traps. b) In the new sensor, though the FOV increases by a factor 2-10 compared to a linear 1D array of diodes, a series of improvements in the circuit design result into a lower noise level than in [15]. c) In this study we send pulses at much higher rates (i.e. 455 kHz compared to the 60 kHz in [15]) allowing us to reject a wider range of light interferences.

2.5.2 Materials and Methods

In this section we describe in detail the construction of an optoelectronic sensor and the recorder that is able to record the fragile signature of a wingbeat. The sensor must be able to operate in illumination conditions ranging from darkness to bright light including in the presence of lamps commonly encountered in laboratories. In the following discussion we also include all alternative routes we tried with a view to assist the interested reader to take our implementation further.

2.5.2.1 Recording Devices

In this work we use infrared LEDs of the SFH4356 series at 860nm. They have a sharp raise time 12 ns. We need fast LEDs faster than e.g. TCRT5000 at 950nm with 4 μ s rise and fall time [16] to respond to the frequency of 455 kHz.

Regarding the connectivity of photodiodes we have tried connecting them in row, parallel and combining both ways. In the parallel configuration (see Figure 2-24 left) the change in the power of the spectrogram of the signal is smoother as the insect moves from one

photodiode to the neighboring diode passing over the border and the gap that separates them. In the case of row connectivity or when combining both ways the variability in amplitude is stronger when we move a tethered wingbeating insect parallel to the diodes.

Emitting LEDs are configured as in Figure 2-24 (right), that is, in a combination of row and parallel connection in order to reach an equal current in all LEDs and to a smooth light distribution across the emitting light surface. Regarding photodiodes' amplifier we tried the ICs THS4281, AD8606 και OPA380. We ended up with OPA380 which is a high speed, precision transimpedance amplifier having a large bandwidth of 90 MHz and high slew rate $80\text{V}/\mu\text{s}$ and noise smaller than $10\text{nV}/\sqrt{\text{Hz}}$. This one achieved the best results in reducing the overall noise of the system. As a single-ended input to differential output conversion circuit we used the dual rail-to-rail input and output, single-supply operational amplifier AD8606 that demonstrates low noise ($8\text{nV}/\sqrt{\text{Hz}}$) and small power consumption ($1\text{mA}/\text{channel}$). As an analog to digital converter, we used ADS8863 that has the required analysis of 16-bit, a conversion time 930nS and a power consumption $60\mu\text{W}$ for sampling frequency 10KSPS (see Figure 2-25). As a demodulator we used the lock-in amplifier AD630 functioning as a precision rectifier to extract the envelope of the high frequency content of the photodiodes' output. The envelope follows the wingbeat movement once the insect flies inside the FOV. We have also tried the lock-in amplifier ADA2200 but attained better results with AD630. As a low-pass filter applied to the output of the demodulator (see Figure 2-26) we used the quad FET-input operational amplifier OPA1654 which has a very low noise ($4.5\text{nV}/\sqrt{\text{Hz}}$) and small power consumption ($2\text{mA}/\text{channel}$).

The system is powered by a Li-Ion battery of 3.7V. Since the circuits need a symmetric supply of $\pm 12\text{V}$, we used the inverting DC/DC converter TPS63700 to generate a negative output voltage -12V and TPS61085 for generating $+12\text{V}$. The 3.3V are supplied from the LP2985-33 fixed-output, low-dropout regulator: One for powering the digital circuits and one for the analogue circuits respectively. The charging of the battery is carried out with a BQ24075 integrated Li-Ion linear charger and system power path management device. The recorded wingbeat snippets are stored locally in an SD (see Figure 2-27).

In [15] we designed a rectifier using an operational amplifier while in this work we used AD630 which is designed for this purpose. The frequency of 455kHz was chosen for two reasons: a) The LED lamps often used in internal spaces and laboratories can produce interferences reaching 60kHz and therefore we needed to move higher in modulating frequencies, and b) The carrier frequency is far from the targeted audible bandwidth of insect's wingbeat and it was handful to use a ceramic filter at this frequency. This filter

suppresses by 50 dB the signal amplitude at low frequencies prior to demodulating the high frequency signal back to the acoustic frequencies.

The greatest challenge was to improve signal to noise ratio of the output. We found that noise was due to the fact that the modulation frequency was generated by a microprocessor with not perfectly stable input since the master clock is based on a phase lock loop (PLL). We de-activated the internal PLL of the processor and used an external clock that led to a significant improvement in noise (see Figure 2-28).

Regarding the light receiving configurations we have been experimenting with two types: a 2D arrangement of diodes and alternatively an optical light guide. As an optical light guide we used a common polymer sheet commonly used in edge-lit backlight units of liquid crystal displays of laptop computers (e.g. we used LTN154U2-L03). In a laptop a light source from the bottom of the layer is guided through the light-source towards the 2D surface of the screen. In our configuration we make reverse use of this functionality by directing the light stemming from the array of infrared LEDs acting as an emitter towards the 2D receiving surface. The polymer sheet guides the light at the bottom edge of the sheet. The bottom of the sheet rests on a 1D array of photodiodes and all other edges of the sheet as well its back are covered with another polymer sheet that blocks light from leaking out. The outcome of this setting is to enlarge the receiving surface of the device without increasing its cost thus avoiding to use a large number of photodiodes needed in complicated arrays. Large photodiode arrays have intrinsically large capacitance that prevents the system from achieving high frequency rates. We investigated the cause of the remaining noise: We use an array of 22 photodiodes in parallel configuration. The output of the receiver gives a signal with amplitude 1Vpp. Assuming the insect is placed in front of a diode and its wingbeat generates a light intensity change of the order of 30%, then the change in the output of the receiver will be $(1V / 22) * 0.3 = 13mV$. We need to amplify the output by 100 times and lead it to ADC. Amplification of the 13mV output leads to amplifying the noise from the following 21 diodes and associated circuits. In a similar device with lower number of diodes one will end up with lower noise.

Power consumption totals to 816.7mW from which 678mW are consumed on the analogue part of the device (LEDs 310 mW, demodulator 130 mW, filter 235 mW and digital potentiometer 3mW) and 138.66 mW on the digital part (MCU 18.9 mW, RTC 0.39 mW, ADC 0.33mW, diodes receiver 24.7 mW, SD 33 mW, and system clock 61.34 mW).

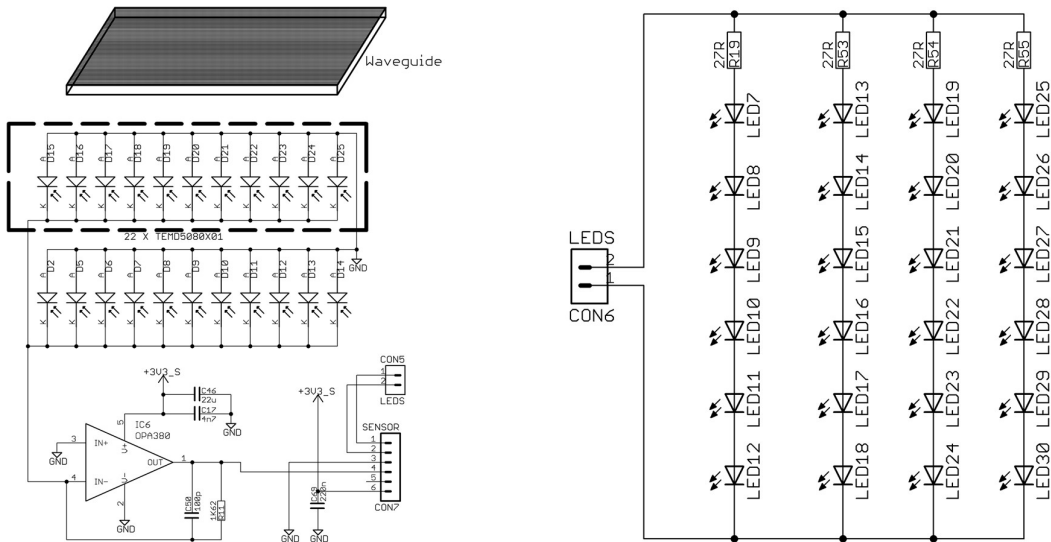


Figure 2-24. Optical receiver & transmitter
 (Left) Optical receiver based either on a light guide or on a 2D array of diodes. (Left-top) an optical light guide attached to a 1D linear array of photodiodes. (Left-bottom) a 2D surface of photodiodes. (Right) The LED array light emitter.

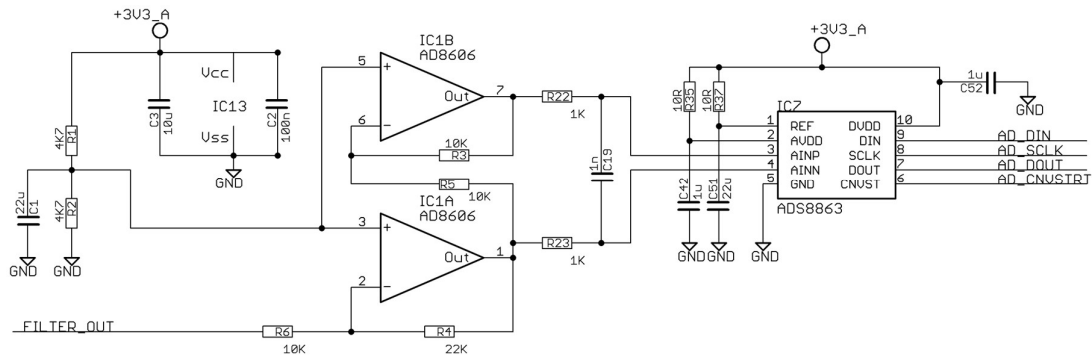


Figure 2-25. Recorder ADC circuit.
 The output of the low-pass filter is passed to the dual OPA AD8606 that converts the single output of the filter to differential in order to allow the ADC to make full use of its 16-bit accuracy.

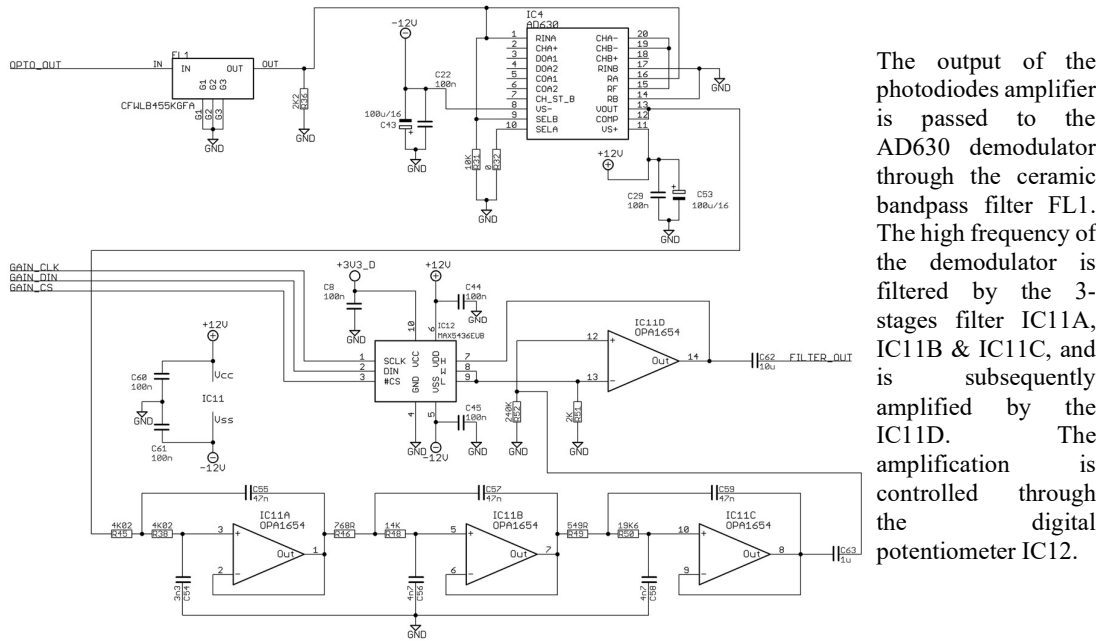


Figure 2-26. Demodulator and Filter.

The output of the photodiodes amplifier is passed to the AD630 demodulator through the ceramic bandpass filter FL1. The high frequency of the demodulator is filtered by the 3-stages filter IC11A, IC11B & IC11C, and is subsequently amplified by the IC11D. The amplification is controlled through the digital potentiometer IC12.

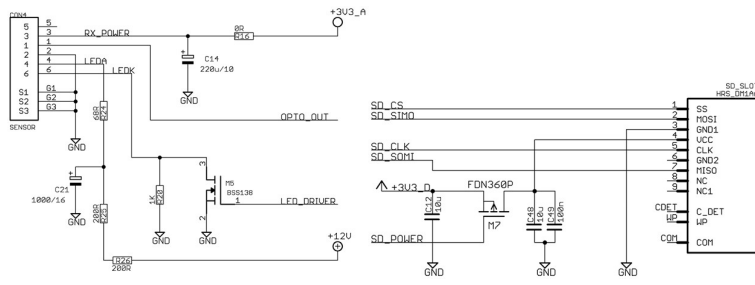


Figure 2-27. Sensor connector & SD Card Connector

(Left) Sensor driver unit: CON4 connects the sensor to the recorder. It passes the output of photodiode's amplifier, the square pulse-series of 455 kHz that drives the LEDs and the 3.3V for powering photodiode's amplifier. (Right) SD interface. The SD_SLOT is the socket to the SD card which is connected to the microcontroller through SPI connection.

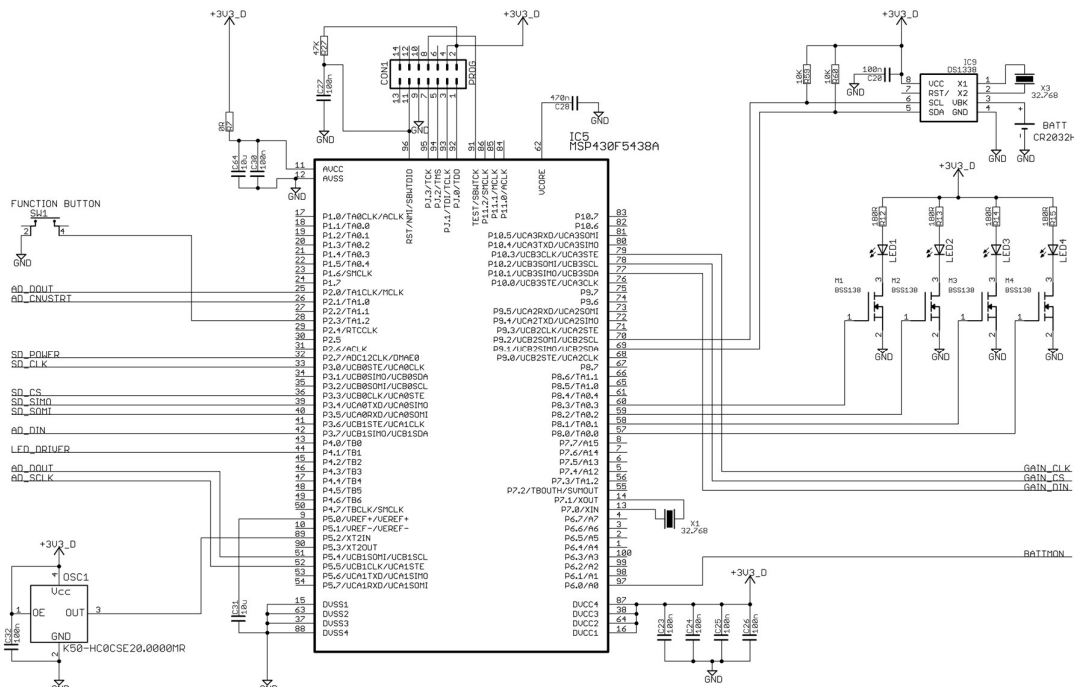


Figure 2-28. Recorder Microprocessor unit.

The microprocessor operates at 3.3V and is synchronized by the 20MHz clock provided by the oscillator OSC1. It controls all functions of the recorder: recording to the SD card, controlling the ADC, the analogue gain before the ADC, the real time clock IC9 that time-stamps detection events, the driving of the LEDs and the user interface through the function button and the status LEDs, named LED1 to LED4.

2.5.2.2 Optical Light Guide vs 2D Array of Diodes

A wide receiving aperture is beneficial compared to a 1D array of diodes because fast flying insects spend more time in front of the receiving surface and therefore, offer more information on the flight process (see Figure 2-29 and Figure 2-30). The 2D has a larger FOV than the configuration presented in [16][15]. As a contrast, in [15] we cover a pyramidal volume with base 3.3mm x 50mm and length 100 mm. In the 2D case of infrared LEDs covers a volume of 70mm x 59mm x 11mm. The light guide is even larger than the 2D diodes' array and has the advantage of not having gaps in the receiving surface except the gaps of the 1D diodes array that receive light from the bottom edge of the light guide. The spectrogram of all insects we examined is slightly smoother in the case of the light guide vs the 2D array. On the other hand the larger light receiving surface makes the system more vulnerable to interferences stemming from electric light. To give an illustrative example: The 2D sensor at 15 cm from a fluorescent lamp did not trigger due to the interference while it was able to detect small object of 1 mm passing its FOV. Even though we use shading for both versions and lower frequencies are suppressed by 50 dB before demodulation the remaining interference can trigger the light guide version if it is very close to a strong electric lamp.

2.5.2.3 Triggering the Recording Process

The embedded microprocessor runs a constantly-looping program which processes data captured by the sensors. The board is programmed in C/C++. The line-level output from the optoelectronic sensor is copied to two circular buffers. The first buffer is used to monitor the signal's root-mean-square (RMS) using a window of 128 samples (16 ms in 8 kHz sampling rate). If the RMS of the window exceeds a pre-defined threshold, we call that an event has occurred, i.e. an insect has crossed the sensor's FOV. This triggers the recording of the signal capturing 5000 samples from the second cyclic buffer coded with 16-bit resolution, at 8 kHz sampling rate. 1000 samples are drawn before and up to the triggering point and 4000 after that point in order to ensure that the onset of a wingbeat event is not lost. Wingbeat events are short in time for fast flying insects such as flies and one cannot afford discarding any useful part of the signal such as the onset. The sampling frequency, window length and triggering threshold are pre-stored in the SD-card of the system and the settings (i.e. sampling frequency, triggering level, and record length in samples) are read once from the SD card during powering-on the device.



Figure 2-29. The recorder main unit



Figure 2-30. The sensor
The light-guide aperture inside a dark box providing shade and sitting on 1D array of diodes



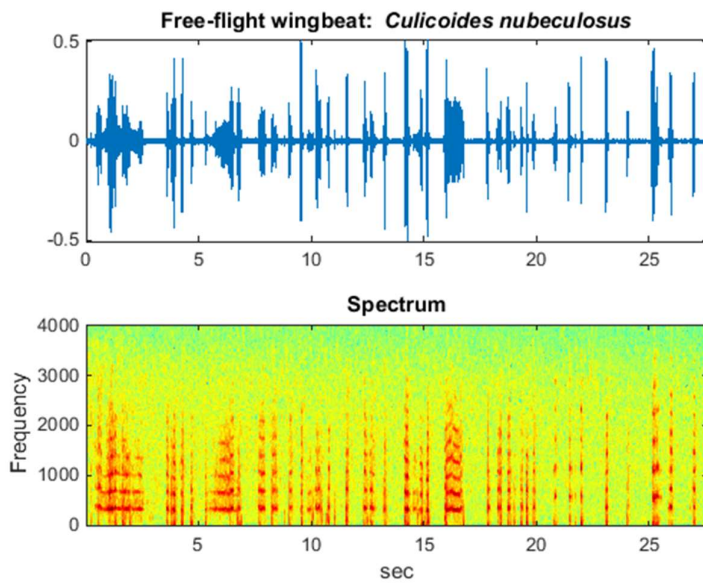
Figure 2-31. 2D array of photodiodes sensor and system
in their final position in an insectary cage.

2.5.3 Experiments

We have identified a series of use case scenarios to demonstrate the utility of the proposed system in research studies as well as its effectiveness in the context of practical applications. Regarding basic research we have chosen to carry out a series of experiments that would be very difficult and impractical to be performed manually. Hereinafter, we make use of the time-stamping possibility to derive daily flight activity of insects and the change of their wingbeat characteristics due to the change of environmental conditions. In such experiments we place a large number of insects of a single species in a cage and the recording of their wingbeat occurs the moment they pass through the rectangle of the sensors on a random basis. The size and shape of the sensor is designed in a way that is possible to pass it through the entrance of a normal insectary cage and record unattended for extended periods of time. With a view to practical application we envision that the sensors described here can be embedded in normal traps and can subsequently detect, count, recognize and eventually transmit data regarding the species captured. Depending on the targeting insect (e.g. mosquitoes) traps would include suction through a ventilator that inflicts one-directional flow of flying insects through the system. These counts are invaluable information to assess the status of an outbreak as well as to epidemic models that currently receive their input data from manual counting of dispersed traps.

2.5.3.1 A Case Study of Very Small Insects

Culicoides is a genus of 1–3 mm long biting midges. Though small to the point of being invisible to the untrained eye, they are vectors of serious diseases to livestock notably of blue tongue fever. In 2006-2008 there have been huge outbreaks of bluetongue virus in Northern Europe that have caused large economic damages on cattle and sheep [56]. We attempt to study the practical limits of the device in analyzing the wing-flap of such insects with a view to develop detectors of their presence. Note that wingbeat recordings of such small insects would be problematic with microphones and the literature on these insects is scarce to non-existent as regards their wingbeat imprint (see [57] for a notable exception on midges). We have enclosed 10 *Culicoides nubeculosus* in a transparent glass jar and placed the jar in between the emitter and receiver of the optical sensor to record their wingbeat. One can see in Figure 2-32 (top) that the signal-to-noise ratio is very high. Wing-flap events are resolved even for this very small insect (Figure 2-32 bottom) and the recordings are clearly audible. One can only admire the flying capabilities of this biological micro-vehicle literary floating on the slightest air stream while beating its wings at a rate of 330 Hz.



(Top) Ten 1-2 mm long midges (*Culicoides nubeculosus*) in flight recorded with a light-guide.

(Bottom) Spectrogram of the recording. The recording is clearly audible and the frequencies resolved. Fundamental measured at 330 Hz.

Figure 2-32. 1-2mm *Culicoides nubeculosus* in flight recording

2.5.3.2 Analyzing Insects of Economic Importance

Fruit flies such as *Bactrocera oleae* (Gmelin) and *Ceratitis capitata* (Wiedemann), *Diptera* of the *Tephritidae* family effect a crop-loss/per year calculated in billions of dollars worldwide [25]. There is always an interest to study insects of economic importance with a view to mitigating their negative impact. In this study we enclosed in a 20x20x20 cm³ insectary cage 220 free flying *B. oleae* adults (see Figure 2-31– right). Depending on the insect density of the cage, one can have recorded wingbeats of the order of hundreds to thousands in just few hours. *B. oleae* is ectothermic and increases its wingbeat frequency along with the rise in temperature. It is interesting to study this effect and we show that our setting is practical for carrying out such studies. We put the cage in a control room with the temperature varying from 15-35 °C and we record the wingbeats of the insects. The temperature is increased 5 °C/day and after one hour of adapting to new temperature we record wingbeat events for the following 24 hours. Daily mortality incidents are replaced with new alive insects so that the total number remains constant through the five days experiment. Note that the sensor samples the true flight space, therefore, is proportional but not exact to the flight activity. In Figure 2-33 we observe an almost linear increase in the wingbeat rate along with frequency. This increase is also confirmed in the Power Spectral Density plots vs frequency Figure 2-34 where we observe a gradual shift of the fundamental frequency along with the harmonics with respect to an increase in temperature. At 15 oC

we observed only 70 flight cases and starting from 35 oC and higher very high mortality rates.

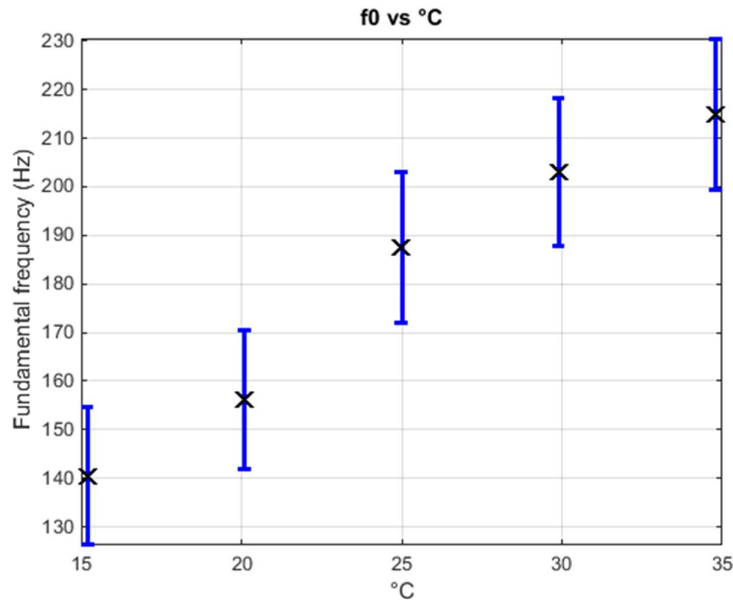


Figure 2-33. Mean fundamental and standard deviation vs temperature. Optical wingbeat recordings of *B.oleae* in flight. The pest is ectothermic.

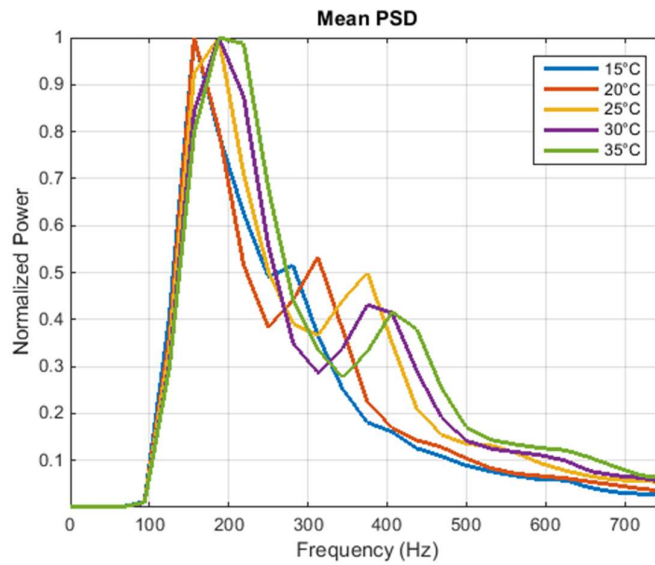
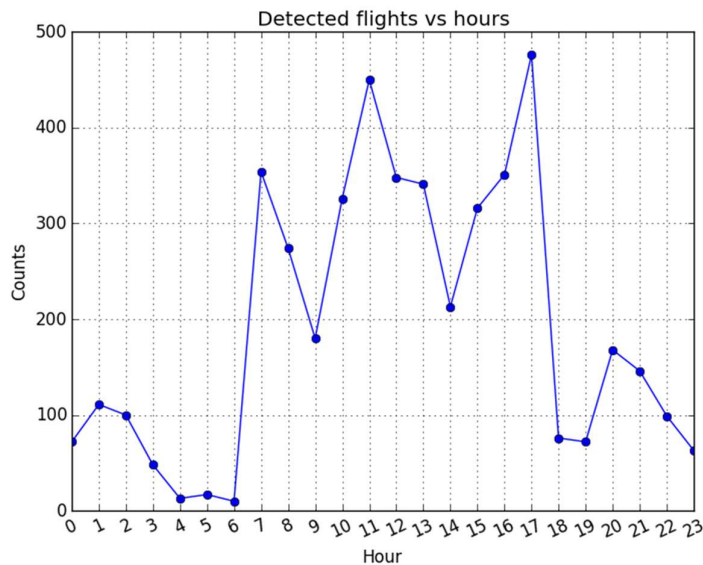


Figure 2-34. Welch spectral density vs temperature. Mean Power spectral density (Welch) vs temperature of optical wingbeat recordings of *B.oleae* in flight. One can clearly discern the frequency shift to higher frequencies as the temperature rises in steps of 5 oC.

2.5.3.3 Analyzing Insects of Epidemiological and Social Importance

Aedes albopictus also known as ‘Tiger mosquito’ is 2 to 10 mm long. It is an aggressive and invasive type of mosquito widely spreading due to its remarkable adaptivity even in cool regions. It is a vector carrier of a series of pathogens and viruses, including West Nile virus, Yellow fever virus, Dengue fever, Chikungunya fever and a suspected competent vector of the Zika virus [58]. We inserted the sensor in an insectary containing 100 adult *Ae. albopictus*. We subsequently derived the daily flying activity pattern of the pest as depicted in Figure 2-34. This information can be embedded in probabilistic detectors as an independent source of information and help classifiers discern among similar species but with differences in their activity patterns [45]. A-priori information on insect activity can also be used to plan application of insecticides as the latter ones are effective if they intercept the mosquito in flight.



The system time-stamps insects crossing the sensor embedded in an insectary. Per hour flight activity in the insectary derived from about 100 insect monitored for 2 days. Cage includes both sexes, under natural lighting conditions at 24 °C, 66% R.H.

Figure 2-35. The system time-stamps insects crossing the sensor.

In Figure 2-36 we analyze the spectrum of a single wingbeat to identify its wingbeat frequency at 620 Hz and clearly resolve its harmonics up to 4 kHz. Subsequently, we take 124 recordings of *Ae. Albopictus* and estimate their fundamental frequency by peak-picking the first harmonic on the spectrum. Then the spectra of the snippets are ordered from lower to higher fundamental and stacked together in Figure 2-37 in order to assess visually interspecies wingbeat variability. One can see that the spectrum is quite consistent thus encouraging the automatic classification of mosquito species. Male *Ae. Albopictus* are smaller and thus they have a higher beating frequency. Frequencies below 100 Hz are due to the main body moving through the FOV of the sensor and is the part of the spectrum that

is typically dropped in classification tasks. Data used in Figure 2-36 & Figure 2-37 are taken in a laboratory under the presence of light interference from two fluorescent lamps at a distance of 1.5 m from the device.

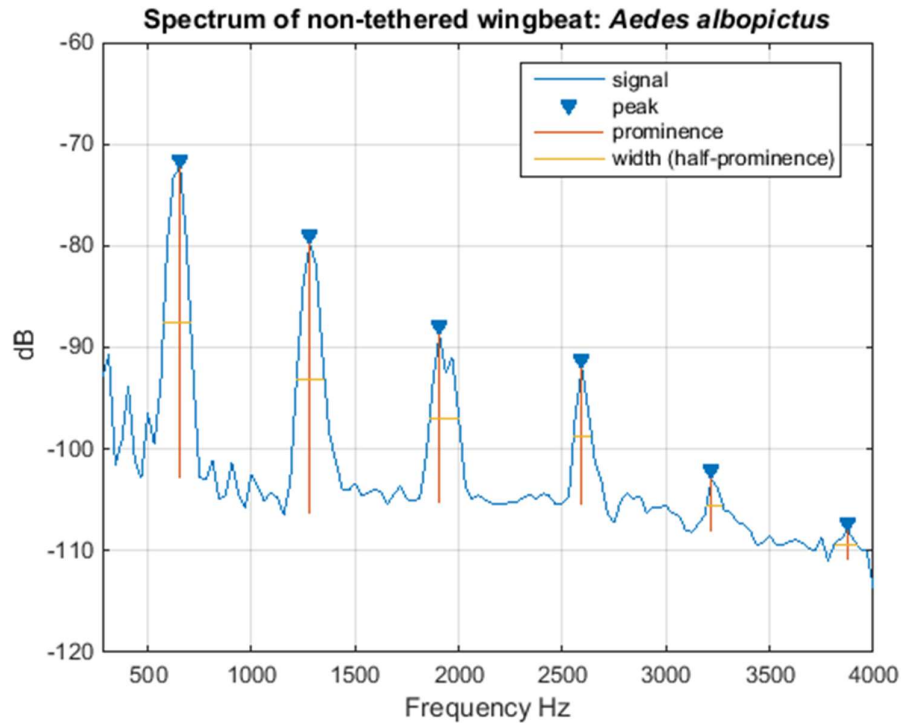


Figure 2-36. Spectrum of an optical recording of a single *Ae. Albopictus*. (Wingbeat in free flight)

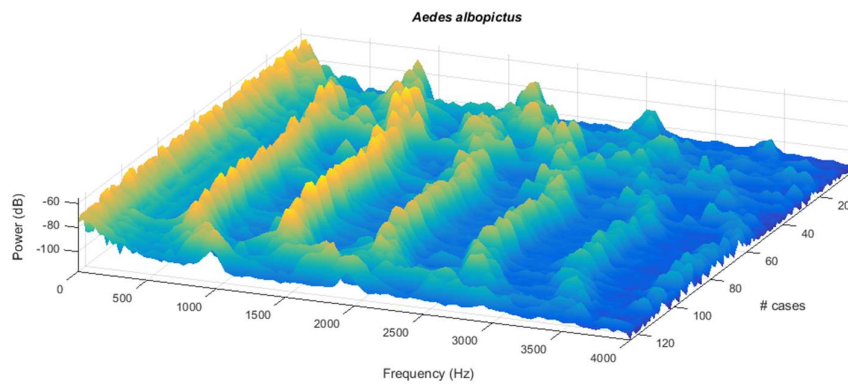
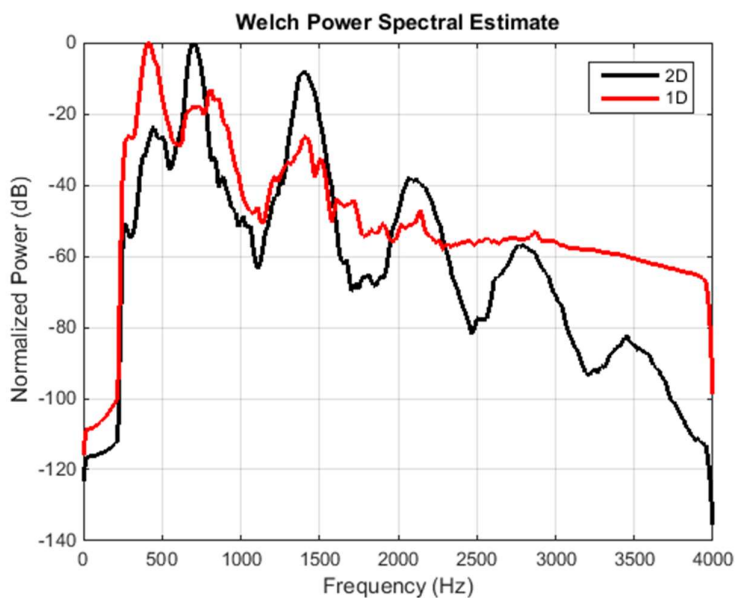


Figure 2-37. *Ae. albopictus*, both sexes

Spectrum of 124 flight cases stacked together and ordered based on the wingbeat frequency from lower to higher values. Optical recordings using the 2D device in the presence of strong lamps at a distance of 1.5 m. Low frequencies below 100 are due to main body movement. The first line is the fundamental frequency (500-750 Hz). The other wave patterns are the harmonics. The fundamental and the higher harmonics are clearly resolved.

2.5.3.4 Comparing 2D vs 1D Photodiode Arrays

In this section we compare the sensor and device reported in [15] with the one presented in this work. First, we experiment with one dimensional arrays (as the one used in [15]) and two dimensional arrays of photodiodes as receivers. We placed 1D and 2D sensors inside the same cage with approximately 100 *Culex pipiens molestus* of both sexes and we take the power spectral density (PSD) of all recordings. We observe a qualitative difference in the spectrum of the signal in favor of the 2D sensors. The 2D resolves better the higher frequencies and we also see that it effects deeper attenuation between the harmonics (see Figure 2-38). The 2D array is made by two 1D arrays connected in parallel. The reception area of 1D photodiodes is smaller than 2D. 2D sensors allow for longer recordings, as the insect spends more time in the field of view and allow better tracking of the full wing movement as the effective aperture of a single diode in a 1D array is around 3.5 mm².



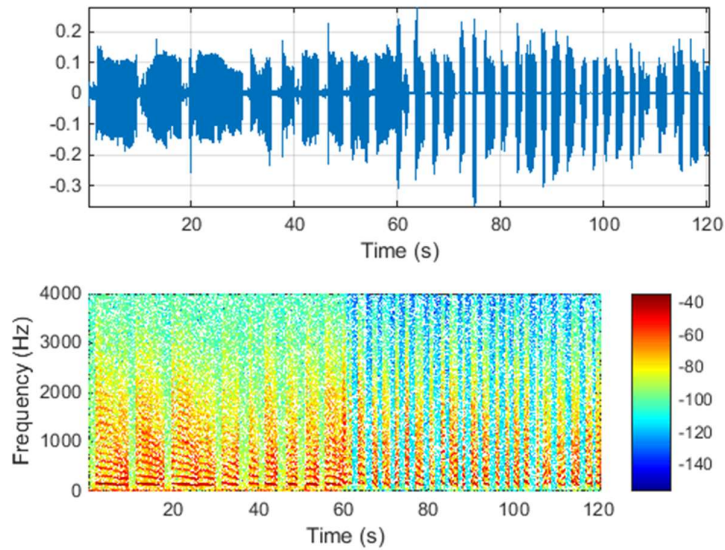
Measured by a 1D and 2D photodiodes arrays inserted in the same cage simultaneously. Both sensors resolve the fundamental frequency and harmonics of the wing-flap. 2D sensors resolve better the frequency content, especially higher harmonics.

Figure 2-38. Power Spectral Density of *C. pipiens molestus* wingflap.

2.5.3.5 Noise Measurements

In Figure 2-39 we compare recordings taken with the device reported in [15] (laser version) and the one presented here. The tethered insect we experiment with is the same for both devices namely: *Musca domestica* better known as the housefly, beating its wings at around 200 Hz. In order to compare the noise level of both devices, the recording taken from each device is amplified so that the recorded wingbeat level is almost equal in both devices. The first 60 seconds are recorded with one dimensional photodiodes array and the recorder in

[15]. The subsequent 60 seconds are with a 2D sensor and the device presented in this work. One can see clearly that the noise level is much lower (at -115 dB) compared to -85 dB of the device in [15].



First 60 sec recorded with [5] and the following 60 sec with the new device. (Top) sonogram. (Bottom) Spectrogram. One can note the lower noise output of the proposed device.

Figure 2-39. *M. domestica* tethered.

2.5.4 Discussion

We have constructed a novel system that automatically detects the event of a wingbeat and triggers a recording procedure for flying insects smaller than 1.5 mm. The recording is stored locally in an SD card and in our settings is 625 ms long while the time-stamp is passed to the filename.

Since most insects beat their wings with frequencies <1 kHz and the operating frequency of photodiodes is designed to receive light pulses at 455 kHz -that is far higher than any biological organism can reach with its wings- we conclude that it can track the wingbeat of any insect starting from low frequency Lepidoptera to high frequency midges. The system is immune to physical light. This is important as we do not wish to detect something outside its FOV (e.g. from insects flying over the FOV and modulating the sun light). It is also robust against electronic interference because it modulates emitted light by sending high frequency pulses instead of continuous light, subsequently the low frequencies are suppressed and the modulated by the wingbeat signal is demodulated back in the acoustic range. Therefore, it can be operated in laboratories that use electric light in the breeding and reproduction cycle of insects as well as in the field.

3. A MULTISPECTRAL RECORDER OF INSECTS' WINGBEAT

3.1 Introduction

In order to monitor insects' presence and density to design policies and apply measures, entomologists deploy a high number of traps that are currently checked manually [83]. Our constant goal is to automate the reporting procedure without involving a human in the loop. To this end, we augment typical traps with optoelectronic sensors that, depending on the situation, may count insects, discern sex and species of captured insects and report wirelessly results daily to remote servers and update infestation maps, decision support systems and predictive analytics. To give some lucid examples of how things are already evolving in several application areas we report that:

- a) e-gates applied in the entrance of beehives measure the bee traffic and discern the presence of a drone, a worker and inform for the case of an outgoing queen.
- b) In the case of insect traps that are based on pheromones to attract targeted insects such as grain pitfall for stored-products insects, Picusan traps for the red palm weevil, Lindgren traps etc. [12], an optical counter is incorporated, and accuracy in species identification relies on the effectiveness and specificity of the pheromone attractants.

Cases (a) and (b) are simple in the sense that they count insects that pass through specific constrictions and quantify their size based on the measured optical intensity variation between an emitter and a receiver. For these applications a simple optical counter based on extinction light is recommended. There are other cases however that either there are no widely accepted pheromones that attract both sexes (entomologists are especially interested in female counts) and, therefore, a general food bait is used (i.e. in the case of fruit flies) or sent in the cases of mosquitoes. In such cases we rely on the wingbeat of the incoming insect and the analysis of its frequency content to classify sex and/or species identity [45][84][17] we have demonstrated that a backscattered light signal originating from an insect is better than the extinction light provided by the same wingbeat event. In this work we elaborate on this finding and we expand to a multispectral sensor configuration. The sensor aims to extract complementary information from the microstructural and melanisation features of the wing and coloration of the main body of the species. The information contained in the samples of these recordings will provide complementary information and precise quantification of size on the difficult task of discerning morphologically similar insects whose wingbeat spectrum may overlap significantly in the frequency domain. Note that, although we present a stand-alone device as in [15][85][86], it is designed in a way that is detachable from its base and its size

reconfigurable so that it can take different sizes depending on the e-trap we are interested to embed it.

There other approaches that are based on LIDAR technology to record the wingbeat of insects at large distances [87][19][88]. Our approach is different to this approach in two aspects: a) we are interested in functioning at small scales usually at the entrance of the trap. Therefore, the distance of emitter-receiver and targeted insect is of the order of cm and b) we a-priori constrain ourselves to low-cost passive elements such as LEDs, photodiodes and acrylic lenses and c) all our technical solutions are necessary low-power as we do not have power supply in the field.

Finally, in this chapter we present recordings of different species of insects some of them never reported in the literature.

3.2 Materials and Methods

It has been reported in LIDAR applications that near-infrared wavelengths (NIR), e.g. 808 nm, are affected by melanisation and that different spectral bands carry complementary information on the insect's main body and wings coloration [86][87]. Therefore, we develop a device that examines the possibility of extracting more information that the casted shadow, based on recording a wingbeat under different spectral bands. In this task we use 3 different LEDs (one in the visible frequency range (450-700nm), one at 810 nm and one at 940 nm).



Figure 3-1. The multispectral sensor: The disk in the middle is the Fresnel lens. The three LED's in each plate emit, in turn, visible light 450-700nm, and infrared at 810 nm and 940 nm. All eight LEDs of each spectral band are lit simultaneously and each band switches in turn every 20.8 microseconds. All LED plates have 68.5o with respect to the Fresnel plane;

Note that this configuration is naturally expandable to more wavelengths that are distinct; we are constrained here by the cost of the LEDs, their operational wavelength, and their capability to operate at high frequencies. We illuminate the wingbeating insect from different orientations and we average on a per wavelength basis to achieve a smoother



Figure 3-2. The photodiode is placed at the focal point of the Fresnel lens.

signal. In brief, the main concept of the sensor is as follows: the central processing unit (CPU) turns on the three circular arrays of eight LED's successively, each having the same wavelength. The Fresnel lens focuses the backscattered light stemming from the wingbeating insect onto the photodiode. The photodiode directs its output to the demultiplexer that has three sample-and-hold circuits. The demultiplexer sends its output to a multichannel analog to digital converter (ADC) and the latter back to the CPU, and finally a wav-type recording to the secure digital (SD) card (see also Figure 3-3). In detail, the CPU (ST STM32L4R7) (Figure 9-9) produces the synchronization signals for all system units,

receives the digital words from the analog to a multichannel analog to digital converter (ADC), and stores the signals to a three-channel 16 KHz 24-bit wav in the SD card of the recorder. We place the photodiode (TEMD5080X01, Vishay Intertechnology) at the focal point of the Fresnel lens (Fresnel Technologies Inc, Part number: 3*). The three LED types are white: GW CS8PM1.PM and 810 nm, SFH4780S (both from Osram) and the 940 nm L1I10 (LUMILEDS) and emit for 20.8 μ s. The ADC (Figure 9-10) is based on the AD7768-4 IC (Analog Devices). The ADC receives the three analog outputs of the demultiplexer (Figure 9-11) and converts them to digital words. The output signal from the photodiode is amplified by Texas Instruments OPA380 transimpedance amplifier (Figure 9-12) and then driven to the demultiplexer. It is worth mentioning that the feedback loop in Figure 9-12 ensures the possibility of operating the device in the presence of the sun and allows for considerable power saving in field operation. The demultiplexer (Texas Instruments analog switch TS12A44514 and OPAMP OPA4376 as a Sample & Hold amplifier) separates the photodiode's output to three different signals, one for each band, and drives it to the three-channel ADC. The LED drivers (Figure 9-13) produce consecutive pulses to three LED arrays (Figure 9-14) with constant current controlled by the CPU (see Figure 3-4 for the

timing operations). The CPU also controls the current level of each wavelength. It is based on Infineon, metal-oxide-semiconductor field effect transistor IRF7341, on OPAMPs ADA4805 of Analog Devices and Texas Instruments TS12A44514 analog switches. The multichannel sigma-delta ADC converter AD7768-4 receives the three analog audio signals and sends the digital words to the CPU using the time division multiplexing (TDM) output.

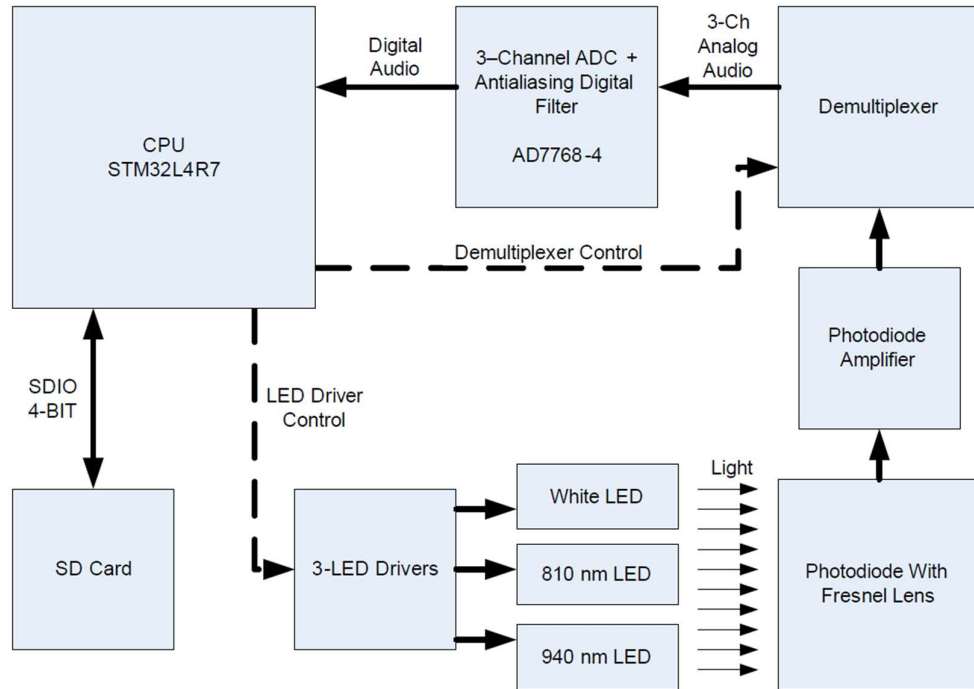
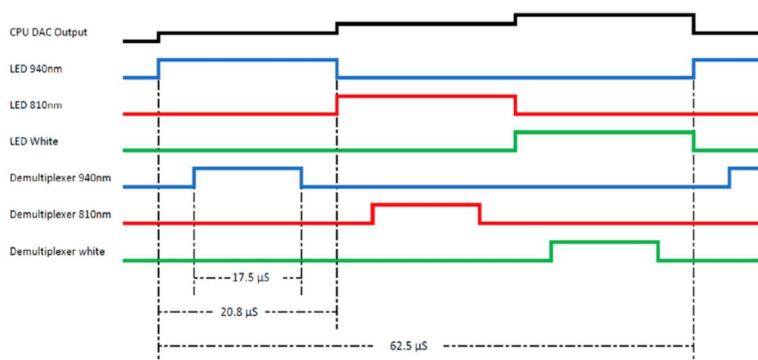


Figure 3-3. Block diagram of the multispectral device. The system is controlled from an STM32L4R7 ARM CPU of ST. The LED drivers produces the sequentially current pulses of each LED.

Powering of the LEDs is carried out through the TPS54302 IC of Texas Instruments (Figure 9-15) and the device state (trigger, SD card, power status) is indicated in the front LEDs of the device (Figure 9-16).



The CPU digital to analog converter (DAC) output defines the current level for each light pulse per spectral band. The signals LED 940 nm, LED 810 nm, and LED White initiate the output of the LED drivers for each spectral band. The signals: demultiplexer 940 nm, demultiplexer 810 nm, and demultiplexer-white initiate the corresponding sample and hold amplifier so that the photodiode is demultiplexed.

Figure 3-4. Multispectral Timing Diagram

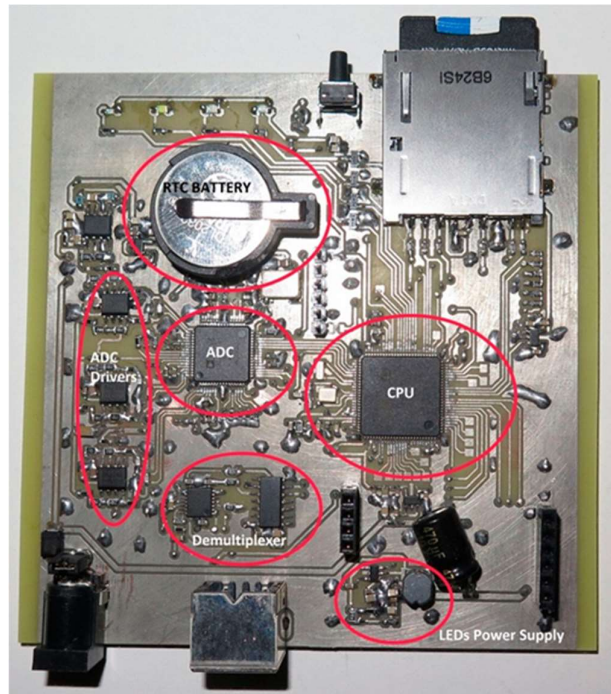


Figure 3-5. The multispectral recorder prototype.
We circle and annotate the main components of the recorder.

Regarding the software, the embedded microprocessor runs a constantly looping program that processes data captured by the sensors. The board is programmed in C/C++. The digital audio output from the optoelectronic sensor is copied to six circular buffers. The first three buffers are used to monitor the backscattered signal's root-mean-square (RMS) using a window of 128 samples (16 ms in 8 kHz sampling rate). The other three circular buffers of 32 kwords (a word equals 32 bit in this processor) each store the recoding of each band. If any of these bands exceeds a common threshold, it triggers the recording process for all bands (see Figure 3-6). The recordings of the signal are coded in 24-bit resolution, at an 8 kHz sampling rate. The first 20% of the samples are drawn before and up to the triggering point and 80% after that point in order to ensure that the onset of a wingbeat event is not lost. Wingbeat events are short in time for fast flying insects and one cannot afford discarding any useful part of the signal such as the onset. The sampling frequency, window length, and triggering threshold are pre-stored in the SD-card of the system and the settings (i.e., sampling frequency, triggering level, and record length in samples) are read once from the SD card during powering-on. The software is written in C language using the IAR Embedded workbench. The programming of the flash memory was carried out using the ST-Link V2 programmer. The code initialization was done using the STM32CubeMX of ST. For programming the peripheral sub-components, such as the SD and ADC, we made

use of the STM32 HAL drivers. The control signals and data transfers were done using the direct memory access (DMA) controller of STM32L4R7.

Regarding the insect specimens, we collected the insect species *Zaprionus* (*Diptera: Drosophilidae*), *Drosophila suzukii* (*Diptera: Drosophilidae*), and *Drosophila melanogaster* (*Diptera: Drosophilidae*) from the area Gouves, Chersonisoss Crete. The insects have been transported to an entomological laboratory to breed and reproduce. Their diet contained sugar, yeast, agar, cornflower, and nipogen. Their breeding conditions had been kept constant at 25 °C, 60% relative humidity following a cycle of 14 h of light and 10 h of darkness. After breeding, the adult insects have been transferred to different cages 50 × 60 cm and the device has been inserted in turn into the cages.

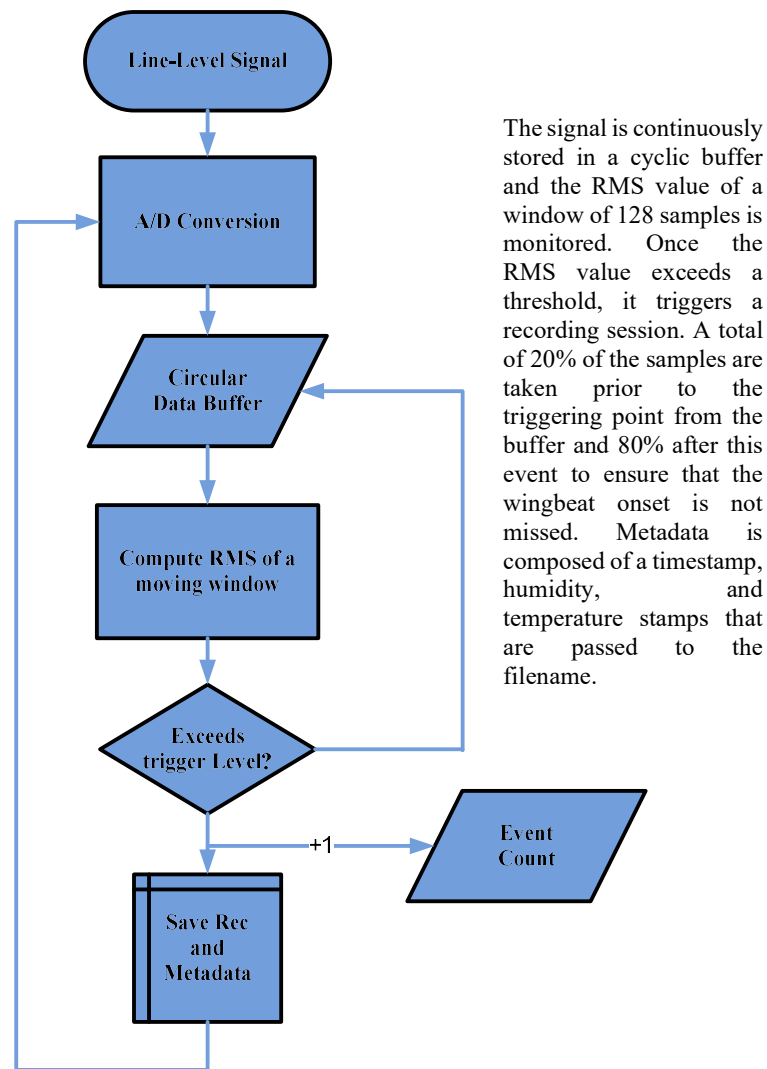


Figure 3-6. A diagram explaining the recording procedure.

3.3 Results

Figure 3-7 demonstrates the various ways we can use the device. One can tether an insect with an inverted tweezer inside the sensor's probe volume, or confine the insect in a Plexiglas box, or insert the sensor in an insectary cage that contains the insects of interest without the Plexiglas box.

Multispectral recordings from various flying insects are presented here using the confinement into a transparent box. The reflected light relates to the refractive index of the wing membrane and the glittering of the insect [19][88][73]. Therefore, the intensity of light in the absence of an insect is theoretically zero and practically equal to the minimum light reflection stemming from the black termination plane. We performed many recording sessions for various insects and the main results of this experiment show that:

- Walking insects are efficiently detected due to the backscattered light from their body.
- We visually confirmed that all wingbeat events observed in the confinement box were registered, and the frequency content of the recording was clearly resolved.
- The wingbeat “signature” of insects in the spectral domain is consistent and repeatable with small interspecies variation.
- The signal to noise ratio is very high (30–35 dB) and the number of harmonics often exceeds 20 (see Figure 3-8, Figure 3-9, Figure 3-10 & Figure 3-11).

One can see that the power spectral density (PSD) of the different spectral bands are not identical (see Figure 3-8, Figure 3-9, Figure 3-10 & Figure 3-11), and this is an encouraging observation as we aim at extracting complementary information. We derive the PSD estimate of the discrete-time signals using Welch's averaged, modified periodogram method using a Hanning window of 512 samples, 50% overlap, and 512 samples Fast Fourier Transform (FFT) at 8 kHz sampling frequency. The spectral peaks, corresponding to the fundamental frequency and their harmonics reside on the same frequencies as expected since they relate to the same insect and wingbeat event. However, the details of the spectral signature, especially at high frequencies, are different for each spectral band.

We can discern morphologically different insects, such as the bee, the wasp, and the fruit flies, as they have very different wingbeating frequencies (*Apis mellifera*: 190 Hz, *Polistes gallicus*: 124 Hz, *Zaprionus*: 220 Hz, *D. sukuzii*: 250 Hz, *D. melanogaster*: 250 Hz) and distribution of power over harmonics. We took all measurements at the same temperature.

The light intensity close to the DC frequencies can quantify the size of the insect. In terms of physical size and in descending order the insects are ranked as follows: *bee* \rightarrow *wasp* \rightarrow *Zaprionus* \rightarrow *D. suzukii* \rightarrow *D. melanogaster*. The PSD plots in Figure 3-8 to Figure 3-11 follow the same ranking. Note that size classification is correct not only for the gross cases of a bee versus fruit flies, but also among fruit flies, paving the way for automatic discrimination of similar fruit flies.

The spectral tilt in the PSD of large insects has a slope, whereas in small insects, it is more flat and we attribute this to their main body contribution.

The current implementation is sensitive to the AC frequency of artificial light and further development is needed to make it noise immune.



By tethering an insect inside the probe volume of the sensor (e.g., by holding its legs with an inverted tweezer), by confining the insect in a transparent cage that is large enough to allow the insect to fly, or by inserting the sensor in an insectary cage containing a free-flying insect. Notice the black termination plane on the right of the Plexiglas (MAXiBLACK, Advanced Coating Products, Acktar Store LTD, Kiryat-Gat, Israel).

Figure 3-7. The ways to use the suggested sensor and its associated recorder.

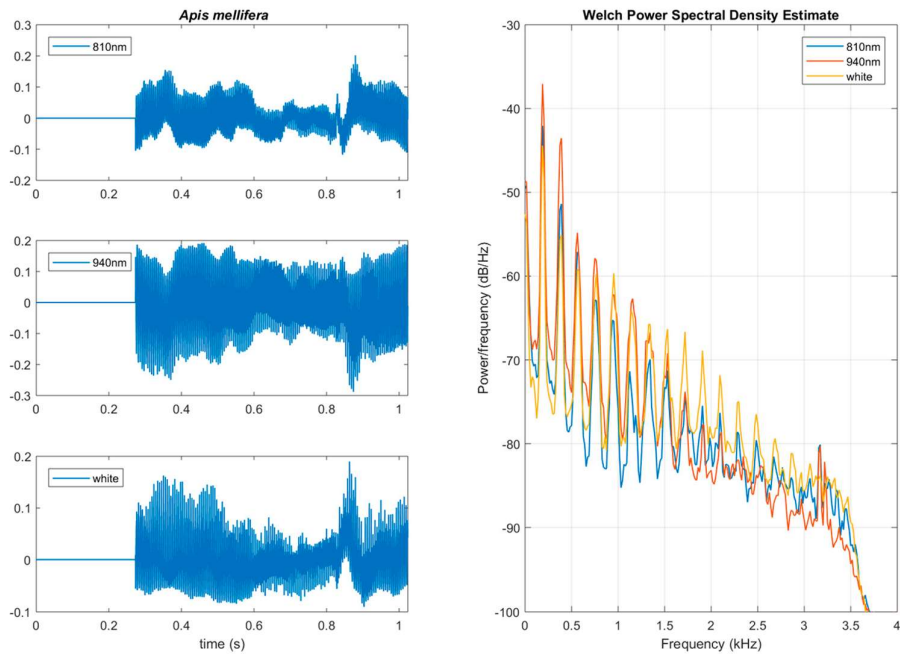


Figure 3-8. The bee *Apis mellifera*

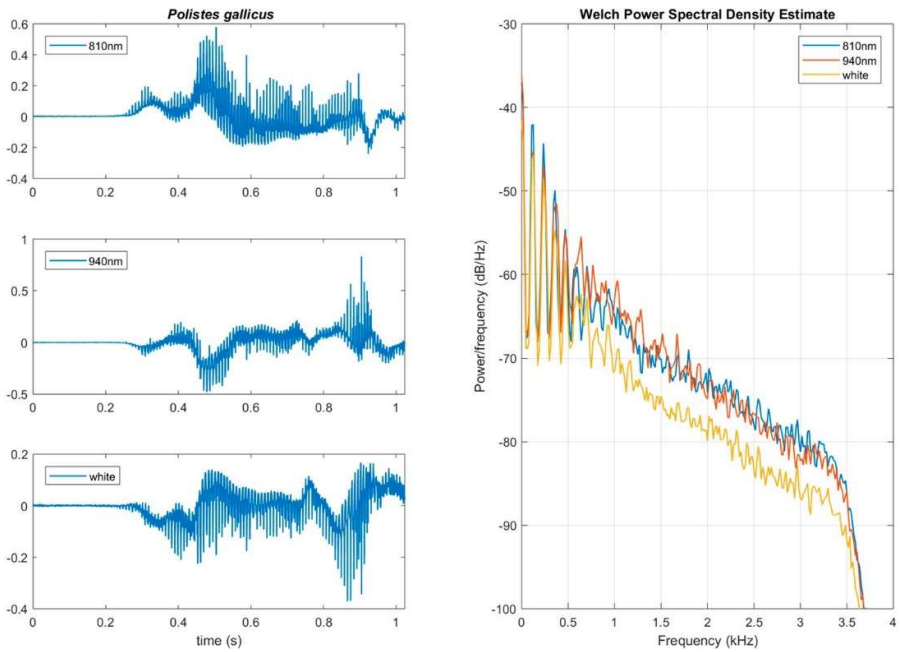


Figure 3-9. The wasp *Polistes gallicus*

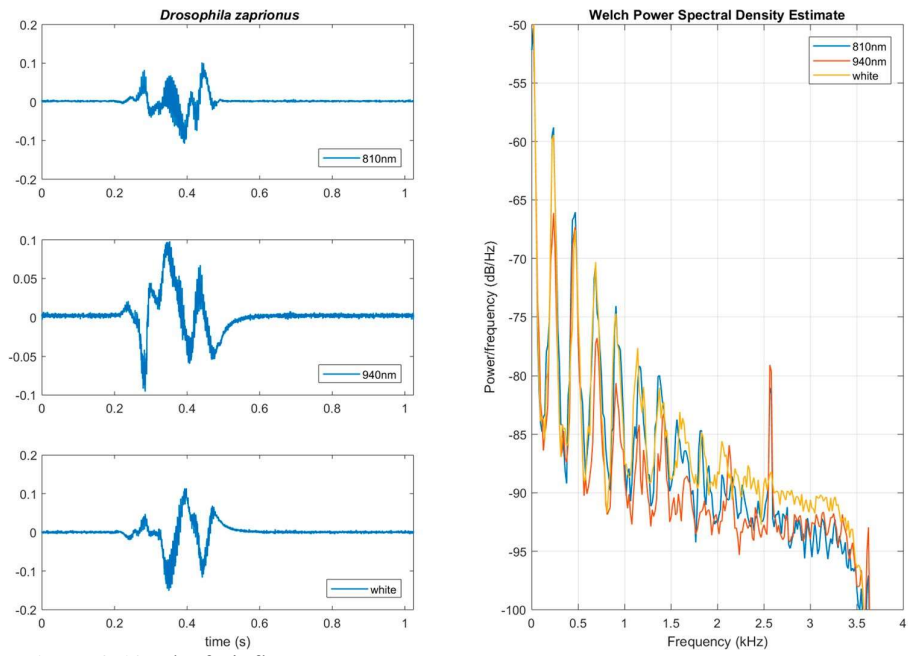


Figure 3-10. The fruit fly *Zaprionus*

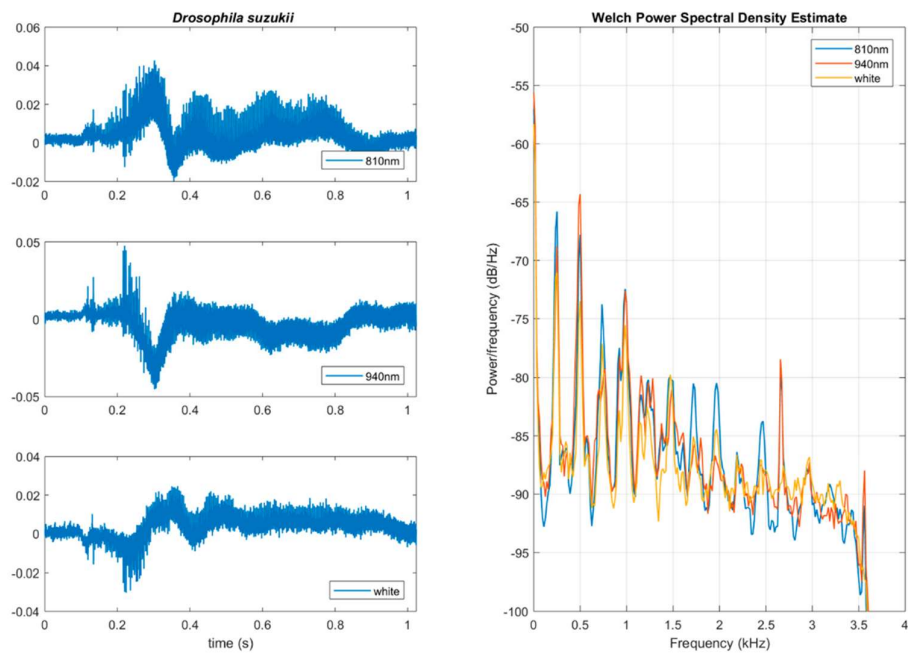


Figure 3-11. the fruit fly *Drosophila suzukii*

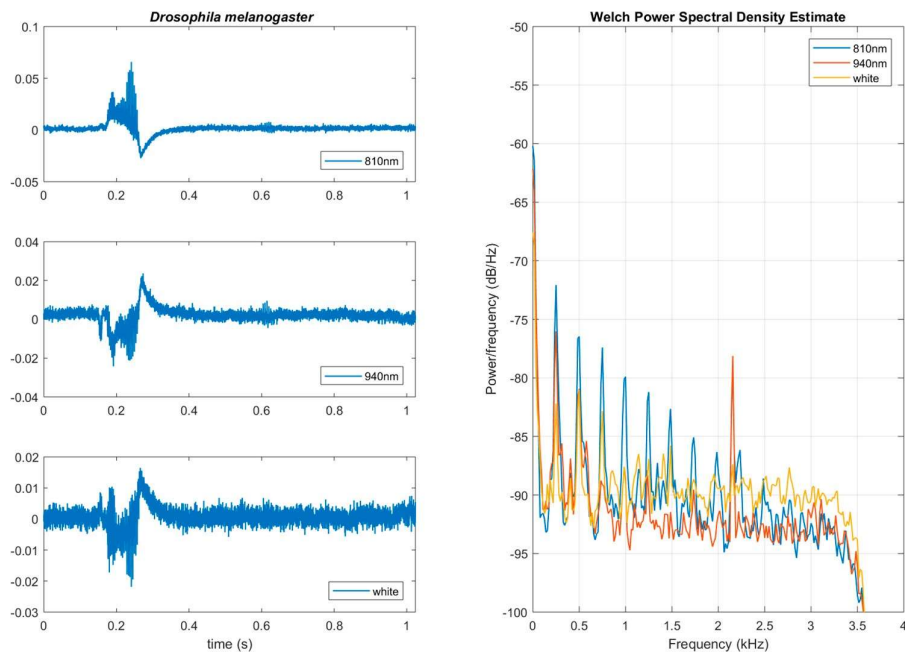


Figure 3-12. The fruit fly *Drosophila melanogaster*

Figures 3-8 to 3-12. Optical wingbeat recording:

Backscattered light wings and main body using three different spectral bands (810 nm, 940 nm, white). Time domain signal at 8 kHz sampling rate for each band on the left column of each sub-figure and the Welch power spectral density on the right column. Recordings are treated as audio and the amplitude in y-axis is normalized between $[-1, 1]$. (Figure 3-8) The bee *Apis mellifera*, (Figure 3-9) the wasp *Polistes gallicus*, (Figure 3-10) the fruit fly *Zaprionus*, (Figure 3-11) the fruit fly *Drosophila sukukii*, and (Figure 3-12) the fruit fly *Drosophila melanogaster*.

3.4 Discussion

Undoubtedly, any sensor type related to the context of our application, such as microphones and vision cameras, have advantages and disadvantages [89][90]. Multispectral imaging has been suggested in a different context to our work in agriculture and entomology [91][92][93]. Optical sensors are the suitable choice for use in electronic insect gates and automatized insect traps working in the field because they record intermittently, i.e., on per event basis, and only if their probe volume (that can be shaped with proper lenses) is interrupted in contrast to the continuous recording of microphones. Microphones receive continuous input from an uncontrolled and unknown number of audio sources in the field and are not generally suitable for field applications. The proposed multispectral sensors do not require the bandwidth of a vision camera and do not face the difficulty of a photograph of a pile of insects that are not easily discernable in detail. Fresnel lenses provide an affordable way to collimate light, and therefore, it is possible to effectively avoid interferences from the sun or diffuse light sources. Using the sensor presented in this work, walking insects (e.g., bees and wasps) were efficiently detected and

their presence was registered in the power of low frequencies around the DC level. The power level of the received light was suitable to rank insects according to their size. The wingbeat event could be easily discerned from a walking event due to the harmonic structure of the power spectral density of the former and the flat spectrum of the latter. The wingbeat “signature” of all insects in the spectral domain was consistent and repeatable [18]. The signal to noise ratio of the backscattered light sensor was at 30–40 dB and often reached 20–30 harmonics. Multispectral signatures look richer than the ones provided by simple one-band sensors but their advantage on classification improvement needs to be clarified and quantified with large-scale experiments (see References [81][82][54] for related work).

Future work will focus on different wavelengths with an aim to discern mosquitoes that have had a blood meal, or are dyed with fluorescent dust or carry a marker gene in the context of the sterile insect technique. The work in Reference [94] demonstrated that is possible to discern with high accuracy whether a mosquito carries a virus load based on NIR spectroscopy. While our current application constraints do not allow us to reach this level of analysis, our ultimate goal is to finally embed this kind of sensor in commercial mosquito traps. With the advance of high rate RGB wavelength demultiplexers [95] and all-optical neural networks [96], we envision that the size of the sensors will become smaller and artificial intelligence tools will be embedded in smart traps that will provide a detailed analysis of incoming insects based on their back-scattered multi-spectral signature. A dispersed network of “e-flowers” like the one depicted in Figure 3-1, when deployed in the field, could unobtrusively sample the insect’s fauna and report on insect densities that can be correlated to pollination studies (e.g., estimate insect counts and distribution of bees) or assess agricultural risks, e.g., due to aphids.

4. A NOVEL ELECTRONIC GATE THAT IDENTIFIES AND COUNTS BEES BASED ON THEIR RGB BACKSCATTERED LIGHT

4.1 Introduction

For the past 25 years, European beekeepers have been reporting weakening bee numbers and colony losses and the situation is worsening. According to the EU Reference Laboratory for honeybee health, some countries in the EU are losing up to a third of their colonies every year [59]. This problem also afflicts North American countries and Asia. At present, the honeybee population in the USA is less than half of what it was in the 1940s [60]. Honeybees are essential in the pollination of many agricultural crops. In [61] it is estimated that in EC the number of beekeepers is 700.000, keeping around 15 million hives and honey production is estimated to be close to 200.000 tons/year. *Apis mellifera* is the only managed honeybee species in Europe providing food, which has been domesticated by beekeepers to produce beekeeping products [62] (honey, pollen, wax). When wild bees do not visit agricultural fields, managed honey beehives are often the only solution for farmers to ensure crop pollination. Indeed, *A. mellifera* remains the most economically valuable pollinator of crop monocultures worldwide [63]. The direct value of honey produced in the EU is estimated about €140 million [64], while the value of insect pollination for European agriculture has been estimated to be around €20 billion per year, €153 billion worldwide [65]. Pollinator declines result in loss of pollination services, that have negative ecological and economic impacts significantly affecting the maintenance of wild plant diversity, wider ecosystem stability with potential knock-on effects on crop production, food security and human welfare. There is clear evidence of recent declines of managed bee colonies, correlated with parallel declines in the plants that rely upon them [66][67]. To help prevent the decline of bee numbers we support the effort of developing IoT sensor applications that can automatically assess the health and threat status of colonies. Forager traffic is related to food availability and demand [68] and therefore, it is an important variable to monitor. Sudden changes in the traffic level indicate a possible threat at the colony level. Forager activity is described in terms of the number of bees entering/exiting the hive over time. The bee counter is a device that fits over the entrance of a beehive [69][70][71][72]. Bees pass through any one of a series of adjacent tunnels. Each tunnel is equipped with light beams, one at the entrance and one at the exit of each tunnel. The direction of the bee's travel is denoted by the order in which these beams are broken. The novelty of this work is that the bee counter we present decomposes the backscattered light stemming from the insect's main body into Red-Green-Blue (RGB)

channels and capture the colour of the incoming insect. Therefore, the novel gate is able to assess forager activity, quantify the size of the insect based on the intensity of the backscattered light and discern insects based on their coloration. When integrated with wireless communication abilities, the system will wirelessly transmit health and threat status results to a cloud server, making data open for running prediction models and risk assessments, issue warnings and make historical analysis. This will allow beekeepers and public authorities to be active participants in colony surveillance programs, overcoming labor costs of manual inspections. As a result, unhealthy or threatened colonies will be remotely detected in time with greater precision and treated accordingly.

4.2 Materials and Methods

The LED emits white light that includes the three basic colors (RGB). The color sensor decomposes backscattered light to individual RGB channels independently. The backscattered RGB color can capture differences in the coloration of insects' main body and wing veins of incoming insects and backscattered light intensity can quantify the size of the incoming insect.

The coloration of the insect can reveal different aspects of insects' characteristics. Two identical insects with differences only in the melanisation of the wings and coloration of the main body will produce different reflected light patterns. The reflected light stemming from insects, relates to the refractive index of the wing membrane and the glittering of the insect [73][19]. Different spectral bands carry complementary information on the insect's main body and wings coloration [74][17].

In Figure 4-1 we see the main components of a single cell that monitors one tunnel of the e-gate. The LEDs and the receiving photodiode are on the same side so that when the light is emitted, it is subsequently backscattered by the main body of the insect and received from the photodiodes of the color sensor in the center. The photodiodes have several filters that decompose the white light of the LEDs into different spectral bands corresponding to the RGB light.

In Figure 4-2 we depict a block diagram of the e-gate with its sub-modules. The communication between the microcontroller (STM32L4R7 ST Microelectronics) and colour sensors (APDS-9250, Broadcom Inc) is carried out through the I2C bus (see Figure 4-3). The I2C bus requires two lines, the serial clock (SCL) and serial data (SDA). In one I2C bus it is possible to connect many devices with different address. In our case, all devices

(colour sensors) have the same address therefore, it is not possible to connect the devices in the same bus. For this reason, we use four I2C switches.

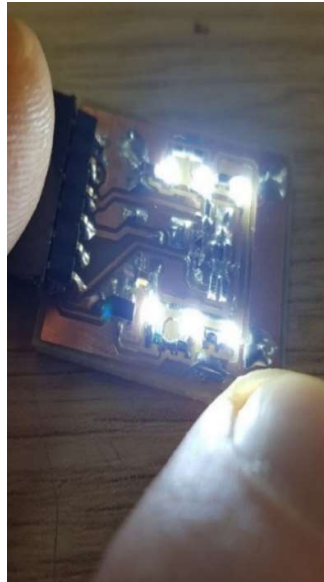
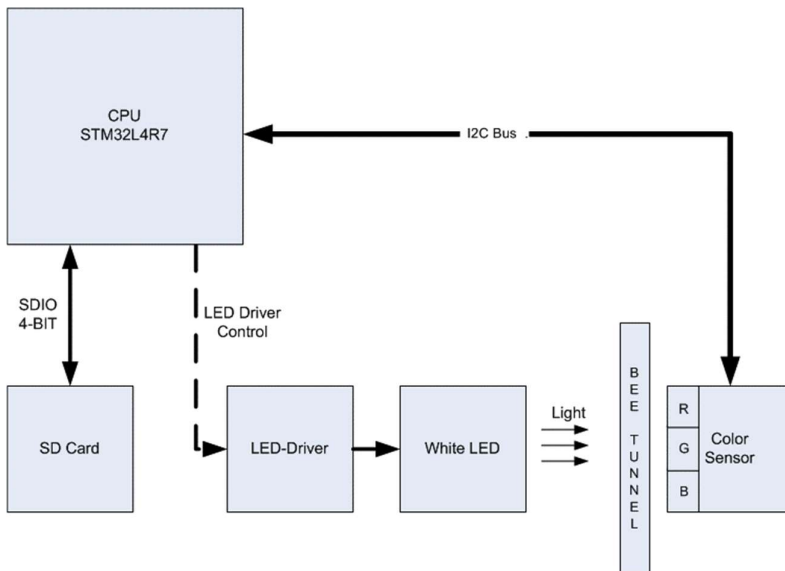


Figure 4-1. Single multispectral cell in the new e-gate. The final gate has thirty-one of them concatenated.



The system is controlled from an STM32L4R7 ARM CPU of ST. The color sensor drivers decompose the white light of the LEDs. All three channels are stored separately in the SD card for further processing.

Figure 4-2. Block diagram of the electronic gate for beehives.

The SDA & SCL from MCU drives four I2C switches. Each I2C switch drives eight APDS-9250 colour sensors.

The light of each gate (see Figure 4-4) is produced by the white LEDs (HSMW-C170-U0000). The thirty-one LEDs of all cells are split to three arrays and are controlled by the CPU through the mosfets Q1, Q2 & Q3 (BSS138). The power is handled by the linear regulator LP2985-33. CPU operates at 100MHz produced by the crystal X2 and multiplied by its internal PLL. See also Figure 4-5 for details on the colour sensor.

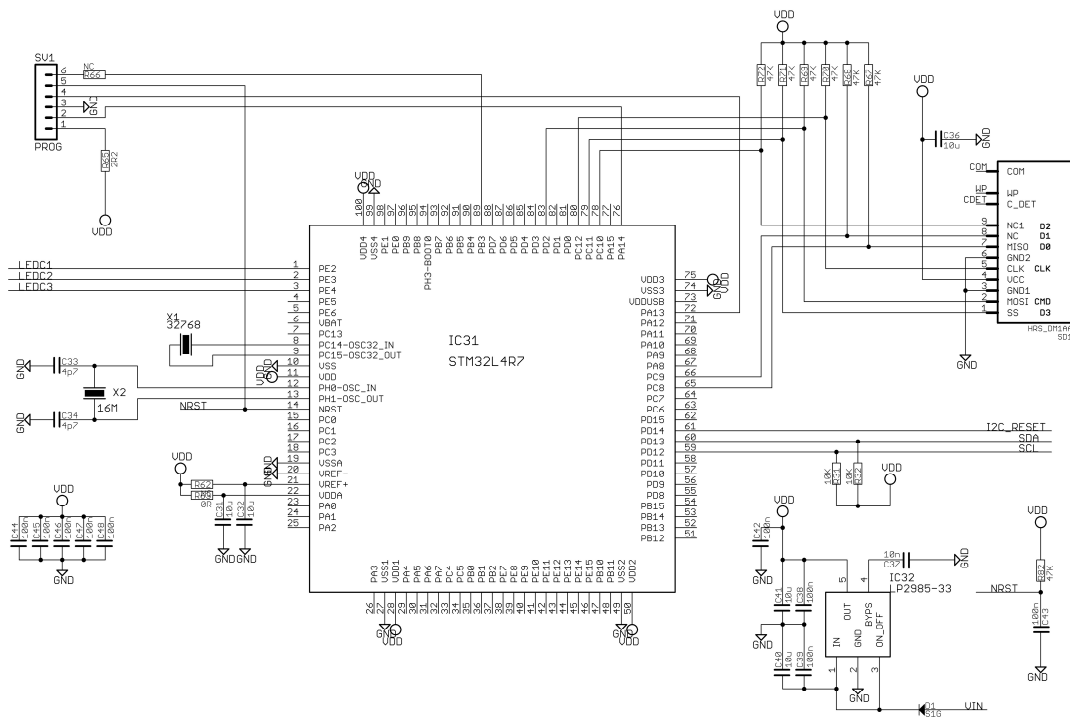
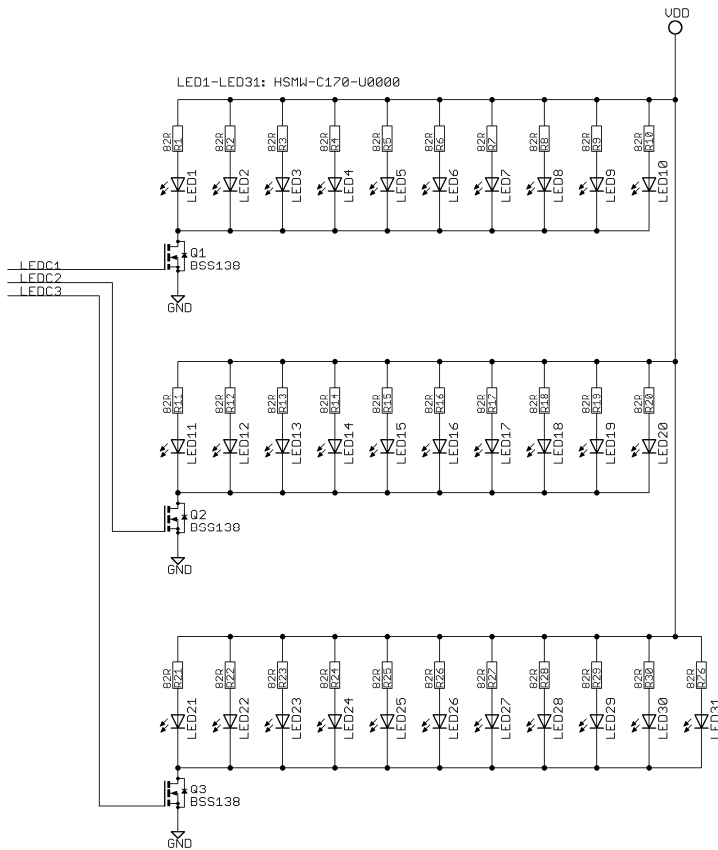


Figure 4-3. The microcontroller unit

This unit is responsible to communicate with the color sensors of all cells constituting the gate, the LEDs, the SD card and the running the classification software. The power is handled by the linear regulator LP2985-33. It operates at 100MHz produced by the crystal X2 and multiplied by its internal PLL. The communication with the colour sensors is carried out through the I2C Bus.



The LEDs unit sends white light, which includes the basic colours, Red-Green-Blue. Each LED (HSMW-C170-U0000) is located next to the colour sensor. The LED sends the basic colours and the colour sensor reads the backscattered reflection from the insect passing the tunnel. The ratio of light intensity of each reflected colour is directly related to the colours of the insect.

Figure 4-4. The LEDs unit.

In Figure 4-6 one can see the recorder and a single channel for better visibility.

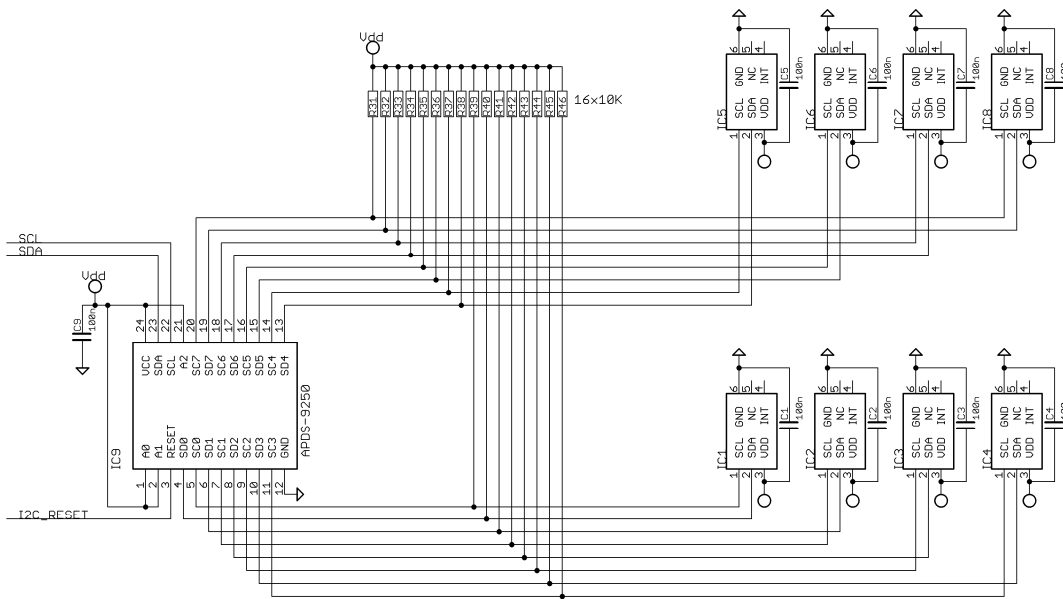


Figure 4-5. The colour sensor unit (1/4).

The colour sensor reads the colours of each insect that will pass through any cell of the 30 composing the e-gate. It is based on the IC APDS-9250 of AVAGO. Internally it has 4 photodiodes with optical filters that decompose light to RGB. It also has an analogue to digital converter (ADC) for each photodiode, and, therefore the design is simplified. The communication with the main processor takes place through the I2C Bus. The colour sensor is located in the upper part of the each cell in the lid next to the LED so that it reads the reflected light. This figure show one from four parts. Each part consists of one to eight I2C switch, and eight colour sensors APDS-9250.

Regarding the software, the embedded microprocessor runs a constantly looping program that processes data captured by the sensors. The board is programmed in C/C++. The data from the colour sensors is copied to sixty-two circular buffers. The first thirty-one buffers are used to monitor the backscattered colour values using a window of 64 samples for each colour. The other thirty-one circular buffers of 256 samples each (256 samples of each colour), store the recoding of each gate. If any of the first thirty-one buffer exceeds a common threshold, it triggers the recording process for the corresponding gate. The recordings of the signal are coded in 16-bit resolution. The first 20% of the samples are drawn before and up to the triggering point and 80% after that point in order to ensure that the data of an event is not lost. The software is written in C language using the IAR Embedded workbench. The programming of the flash memory was carried out using the ST-Link V2 programmer. The code initialization was done using the STM32CubeMX of ST. For programming the peripheral sub-components such as the SD & I2C bus we made use of the STM32 HAL Drivers.

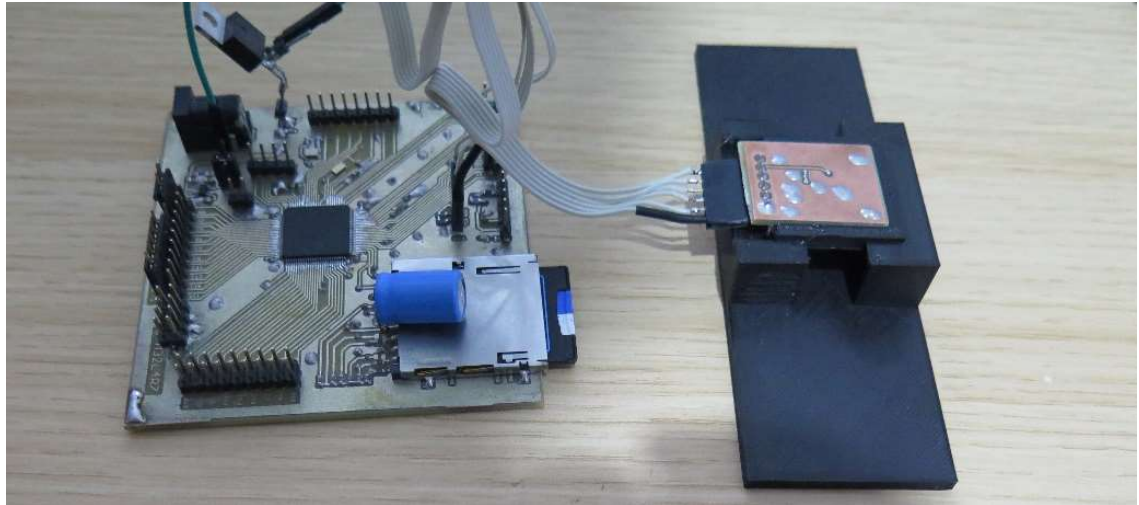


Figure 4-6. The complete system. Left the recorder, right a single e-cell of the gate.

4.3 Results and Discussion

In order to monitor the presence and density of bees and wasps in particular, as well as design policies and apply measures, one augments beehives with sensors so that their health status is assessed remotely [75][76][77][78][79][80]. Forager traffic is closely linked to colony food intake and to pollination, it is particularly useful variable for researchers, beekeepers and growers. Monitoring hive traffic prior to pollination would allow beekeepers to observe hive health and a record of quality control [68]. Hereinafter, we present and examine preliminary results by placing dead bees, wasps, beetles and flies on a

rail and passing the rail through the sensor. A large evaluation plan in vivo will be carried out in the near future but for experimenting with and tuning the system and because of the difficulty of performing experiments with life specimens. Regarding the insect specimens, we collected the insects *A. mellifera* and *P. gallicus* from the area Gouves, Chersonissos Crete, on February 2019. The bees have been found dead around apiaries while wasps have been terminated in situ with acetone and all insects transported to an entomological laboratory.



The gate is first tested with dead specimens of bees, wasps, beetles and various type of flies. The movement process is simulated by placing them in a rail that is passed through the gate to get the backscattered light from the sensor.

Figure 4-7. Testing the e-gate.

All insect specimens (bees, wasps, beetles and flies) are placed on a rail that passes through the sensor. The backscattered light is recorded and stored to the SD card of the recorder (see Figure 4-6). Hereinafter, we present and examine preliminary results that look very promising and lead the way for large in-vivo assessment.

In Figure 4-8 we see four different bees passing through the gate as depicted in Figure 4-7. We observe that the light intensity shape has a repeatable shape among different bees and the ratio between bands holds a consistent pattern.

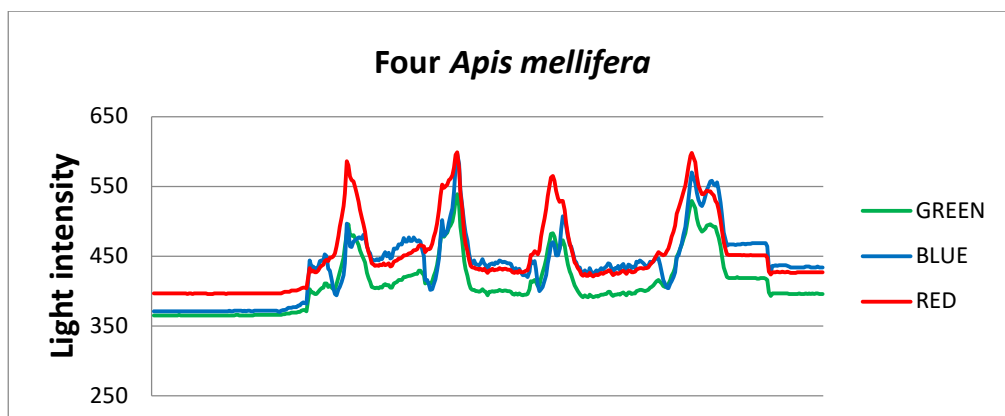


Figure 4-8. Backscattered RGB light for four different bees. Note the consistency of the reflected light pattern among the different cases.

In Figure 4-9 we observe four cases of the wasp *P. gallicus*. One can observe the repeatability of the light intensity pattern regarding wasps as in the case of bees and that the blue colour is lower than the green and this is not the case for the bees. Therefore, the ratio of intensity between colours changes consistently for different insect species. We will pursue this direction and try for different species using different specimens than the ones used in Figure 4-8 and Figure 4-9. In Figure 4-10 the first two peaks correspond to the pattern of the backscattered light stemming from a bee and the subsequent two belong to wasps. Note that, by observing Figure 4-8 and Figure 4-9 we could classify correctly the cases in Figure 4-10. In Figure 4-11 we see the differences between a bee, a wasp and a bumblebee. Moreover in Figure 4-12 the beetle and the black coloured domestic fly have completely different patterns than that of bees and wasps.

The sensor system presented hosts the optoelectronics signal acquisition set-up, which for being multispectral will be optimized to facilitate a reliable registration of the presence of bees and beehive pests, without the possibility of having false alarms due to ambient interferences. The design and set-up is optimized with respect to various technical aspects (data quality, signal-to-noise ratio, etc.)

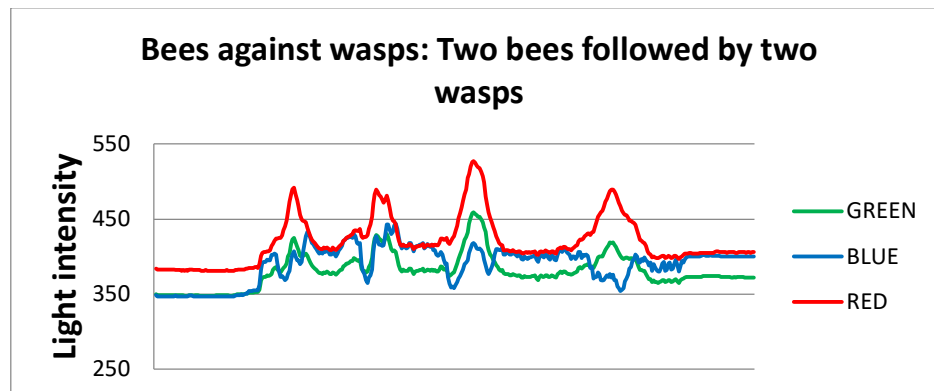


Figure 4-9. Backscattered RGB for four different wasps. Note the consistency of the reflected light pattern among the different cases.

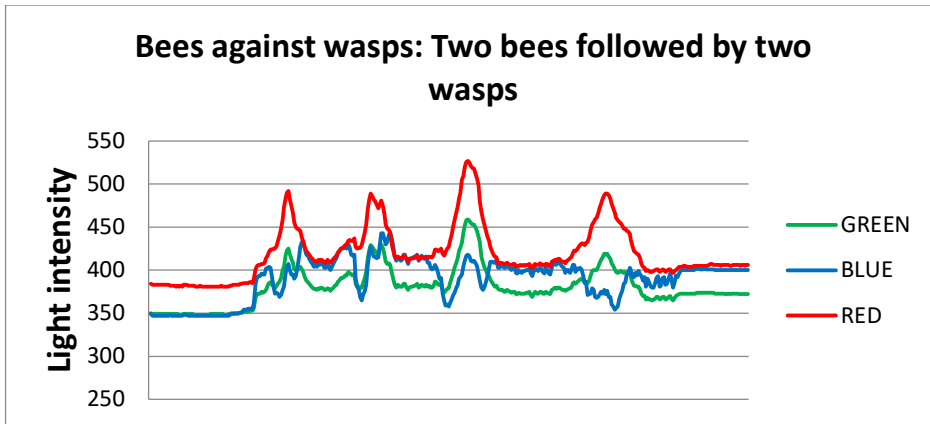


Figure 4-10. Backscattered RGB for the discrimination between bees and wasps. Note the blue light with respect to the other colours for bees and wasps.

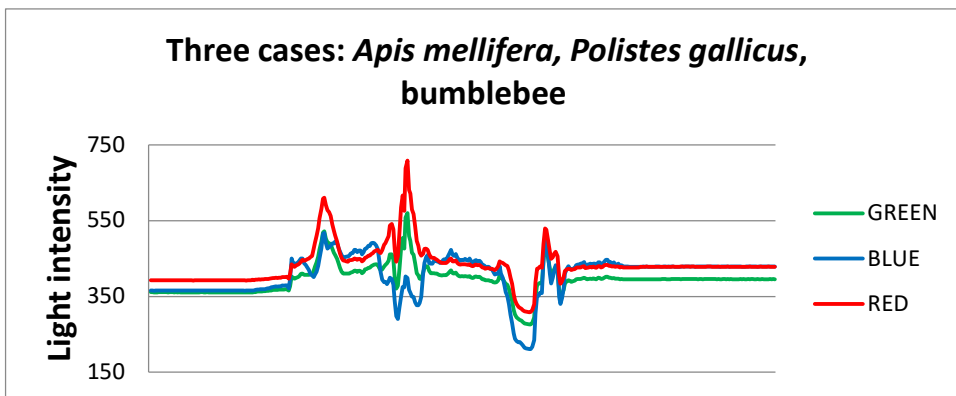


Figure 4-11. Backscattered RGB for four different wasps. Note the consistency of the reflected light pattern among the different cases.

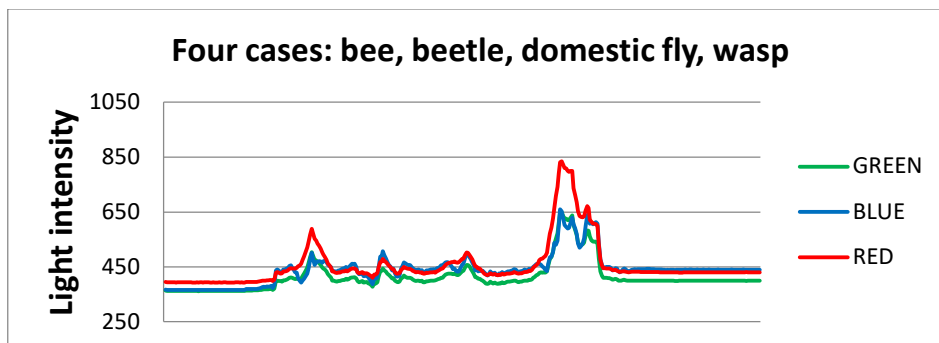


Figure 4-12. Backscattered RGB for four different insects
Namely: a bee, a beetle, black fly and a wasp among the different cases.

Using the sensor presented in this work, walking insects (e.g. bees and wasps) are efficiently detected and their presence is registered in the power of low frequencies around the DC level. The power level of the received light is suitable to rank insects according to their size. Multispectral signatures look richer than the ones provided by simple one-band

Automatic monitoring of insect fauna at global scales using wireless networks and opto-acoustic sensors
sensors but their advantage on classification improvement needs to be clarified and quantified with large-scale experiments (see [81][82][54] for related work).

5. IN-VIVO VIBROACOUSTIC SURVEILLANCE OF TREES

5.1 Introduction

Trees play a vital role in our planet and affect the life cycle of all living creatures. In the special case of urban trees, they provide cultural and aesthetic benefits beyond economic ones. Due to their importance, a range of sensors are currently available for measuring several vital parameters of trees related to health, growth and possible forest damage [97][98]. Yet, the penetration of technology in forest and urban trees management has been slower than in agriculture. Beyond the recording of several parameters that are correlated with tree health such as temperature, humidity, barometric data and precipitation there are several others less known to the generally knowledgeable audience. Dendrometers measure the diameter of trees and cross correlate this parameter with tree growth [99]. Accelerometers attached to the trees can provide long-term data series of tree sway, which is used to infer tree properties such as mass, elasticity, canopy precipitation and interception [100]. Sonic tomography is based on attaching several accelerometers to the trunk to assess the internal decay and cavities in living trees, and by measuring variation in the speed of sound across the trunk to determine patterns of wood integrity [101]. Another apparatus is the resistograph that drives a drilling needle into the wood under constant drive [102]. The drilling resistance is measured at real time as the drill bit passes through the wood layers and reveals the internal decay [103].

Wood-boring insects such as termites, weevils and certain beetles can directly affect the health and growth of specific tree species. There is a wide bibliography on piezoelectric sensors, microphones, accelerometers, laser vibrometry and optical methods [97][104][105] used to detect locomotion and feeding sound of larvae or adult pests inside the tree trunk. One should note that all these methods are currently applied manually. In-situ manual application is the basic difference with our remote approach. The difficulty in detecting wood-boring pests lies in the fact that they breed inside the tree, and therefore, the tree itself becomes the host that provides a physical coverage. These pests inflict detrimental effects on the health of the tree and in many cases, such as *X. chinensis* for mulberries [106] and *R. ferrugineus* (also known as *red palm weevil*) for palms, they attack and kill living trees at high rates [107]. The signs of infestation are usually evident when it is too late for saving the tree and by then the adult pests have escaped from the tree trunk at large numbers to infest other trees.

Global trade and climate change facilitate the establishment of pest populations outside their native ranges. Larvae of invasive species breed in wooden pallets and are

transported through ports, handling facilities or truck roads and, therefore, one after the other, species known to be ‘exotic pests’ appear in Europe [108] and US in places that are not biologically adapted to regulate their multiplication. Since identification of wood-boring larval insects is important for pest risk analysis and management, phytosanitary measures are commonly applied in points of entry such as commercial harbors and airports. Manual inspection of commodities by inserting a piezoelectric probe in the tree trunk to listen for potential internal audio activity due to feeding and locomotion (i.e., passive acoustic detection) is a widely accepted method [109][110][111][112] (listen also to Recording S1 in the Supplementary Materials). This approach has some distinct benefits, for example it is portable, has lower cost than competitive methods, can be operated with batteries, requires minor training and there are commercial products available [113]. It also comes with several practical shortcomings:

- a) Field visits and frequent manual inspection of trees and plants is costly and impractical to scale to large numbers,
- b) The human observer has limited time to inspect a single tree and the larvae could be present but inactive during the inspection time,
- c) When the trees are in urban environments the background noise can be significant and can cover the feeble sounds of wood-boring insects, even if the human observer uses specialized headphones. Moreover, the movement of tree branches or, in the case of palms, of the fibers of the trees due to the wind, produces interference sounds that resemble feeding sounds and can result in false alarms. A false alarm in this case entails a high cost, as the tree must be either treated and re-examined or removed and destroyed.
- d) Manual operation can be inconvenient and stressful, as observers need to perform inspections in very noisy environments (e.g., inside cargo ships, on trees near high traffic), are exposed to weather conditions, often climb on ladders to reach the stems of very tall trees such as palm trees etc.). While being there the user must try not to make noise by himself, by movement of cables, handling of the probe, or even breathing, as the bouncing cables and cable headphones are sensitive to impact and create noise that obstructs the acoustical observation.

A novel accelerometer-based sensor that transmits short vibration clips stemming from an internal part of the tree to a remote server (e.g., 10 s of recording every hour) is presented in this chapter. The server allows the user to have access to the audio recordings in a flexible platform with additional analysis tools for mapping, management and

inventorying. The transmitted clips can be examined manually by hearing and visualization of their spectrogram, or automatically in order to assess the infestation status of the tree. Time scheduling is handled by the server, which communicates remotely with all deployed devices. Therefore, one can schedule recording sessions that would be inconvenient for manual practices (e.g., inspections during the night) and can be taken when background and/or traffic noise is low. Scheduling and automatic reporting can lead to a decision about the infestation state of the tree based on accumulating observations over a larger time span than the usual manual practice e.g., by examining the recordings of a week and accumulating experience before the final decision.

The manual visits are reduced to a single one, as the device is cost-effective and can be placed permanently on the tree (see Figure 5-1). If the observers hear, on time to the feeding sounds of the larva they can apply treatment using systemic insecticides or remove the tree to prevent spread of infestation; the after treatment monitoring cost related to the assessment of the efficacy of the treatment is minimized. The design of the device is low-power and with a small panel attached to its back surface can be power sufficient for many months. In this work, we apply the General Packet Radio Service (GPRS) functionality of the mobile network. Alternatively, the device can apply some basic feature extraction based on the RMS level, counts of impulses, impulses rate and then use the Long Range Wide Area Network (LoRa/WAN) communication protocol. LoRa/WAN can reduce significantly the communication cost and allow the application to be applied at large scales (hundreds to thousands of nodes) in the context of smart cities that already support the Internet of Things (IoT) infrastructure.



Figure 5-1. The concept of acoustic surveillance of trees in forests and urban environments.

Trees are probed for real-time monitoring against wood-boring insects. The device emits recordings of vibrations stemming from inside the tree trunk due to feeding or moving sounds of larvae. The IoT expands the remote monitoring application from a few trees to regional, national or global networks.

This chapter is organized as follows: first the methodology to retrieve the vibration signals and their frequency content is described in the ‘Materials and Methods’ section. Then, we present experimental results based on recordings of different species of insects one of them never reported in the literature. Finally, we discuss the possibilities of different applications of the device on the basis of our experimental results.

5.2 Materials and Methods

The device has 9 X 5 X 4.5cm dimensions and is composed of:

(a) a 16 cm long waveguide, (b) an accelerometer and (c) an electronic board that transforms recorded vibrations into lineout audio signals that are stored, compressed and wirelessly transmitted (see Figure 5-2). The waveguide is just a stainless steel bar, but large nails, bolts and drill bits can serve the same function, that is act as a sound coupler between the wood and the sensor probe.



Figure 5-2. The vibrations recorder
A rugged container for outdoor deployment contains the electronics including GPS and 4G-LTE communication.



Figure 5-3. Metal waveguide fastened to the input of the accelerometer.
The tree trunk is first drilled using a bit matching the size of the probe and the waveguide is subsequently inserted and fastened in the hole.

Drill bits can be conveniently adjusted to a drill bit adapter that, in turn, is fastened onto the accelerometer. Different waveguides apply to different user scenarios e.g., wooden columns, decks, porch tongues, ceilings, roots of plants.

The waveguide is attached to an 805M1-0020 accelerometer (TE Connectivity Ltd), that is based on a stable piezo-ceramic crystal with low power electronics. We chose this accelerometer mainly for its frequency response (i.e., 1–8 kHz) where feeding impulsive sounds lie [104][112] and its sensitivity at 100 mV/g. However, besides these two criteria, we have not optimized the accelerometer selection and other choices may be applicable. The microprocessor carrying out all processing and communication with the submodules is the STM32L476RG (ST Microelectronics). The STM32L476RG device is an ultra-low-power microcontroller based on the high-performance Arm Cortex-M4 32-bit RISC core operating at a frequency of up to 80 MHz. The device carries a GPS and a 4G-LTE SIM7600 (SIMCOM), modem to transmit the recordings and the device's position.

Prior to transmission, the waveforms are compressed using the Opus open source lossy audio coding format (<http://opus-codec.org/>). We show an internal picture of the completed device in Figure 5-4. The system's sub-components are depicted in Figure 5-5. In the version of the device we introduce in this work, the circuit is constantly in sleep mode, wakes up on a predefined time schedule that is configurable through the reporting server and takes a recording before going to sleep again.

A detailed power consumption calculation for a one user-case scenario can be found in the Appendix A.

There is also the possibility to run a constantly looping program that processes data captured by the sensor and records only when triggered by an audio event having power exceeding a threshold. The recording is stored in the SD card, and the time stamp is passed to the filename. All recordings are compressed using the open source Opus compressor prior to sending them over the communication channel. The bit rate is 24 KBPS at a sampling frequency of 8 kHz and effects a compression rate 5 to 1, meaning a wav file of 320 KB is compressed to 63 KB. For 4G-LTE, we use global SIM cards, therefore any tree can be tracked from anywhere in the world.

The board is programmed in C/C++. The output of accelerometer is amplified and filtered. The analog filter output is converted to digital words in 16-bit resolution at 8 kHz sampling rate using the internal ADC of the microcontroller. The sampling frequency, record duration and other initialization parameters are read once from the SD card during powering-on and are configurable through the server. The software is written in C language using the IAR Embedded workbench. The programming of the flash memory was carried out using the ST-Link V2 programmer. The code initialization was done using the STM32CubeMX of ST. For programming the peripheral sub-components such as the SD

Automatic monitoring of insect fauna at global scales using wireless networks and opto-acoustic sensors

and ADC we made use of the STM32 HAL Drivers. The control signals and data transfers were implemented using the DMA controller of STM32L476. The recorded files are compressed using opus encoder and uploaded to a web page using a 4G-LTE module.

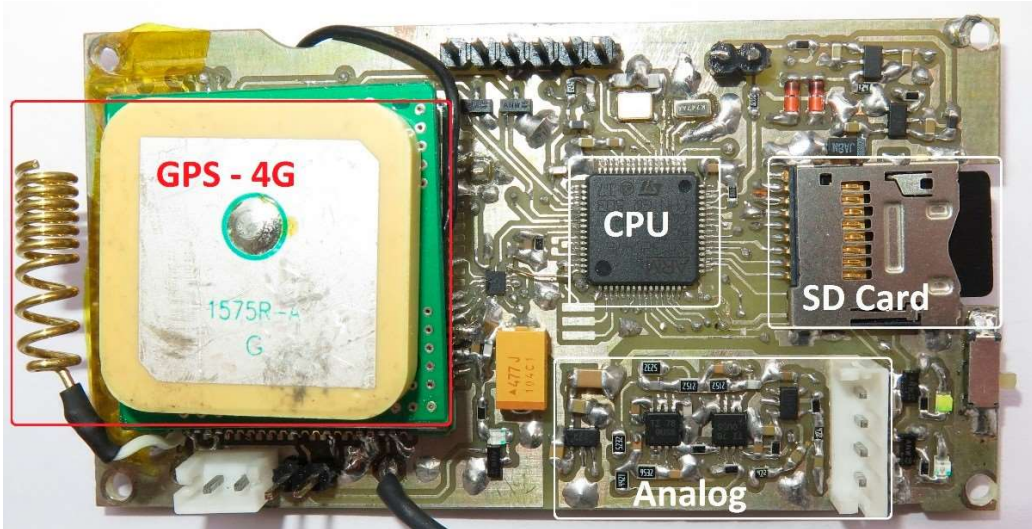


Figure 5-4. The recorder prototype.

We circle and annotate the main components of the recorder. ‘Analogue’ denotes analogue amplification and low pass filtering using the micro-power operational amplifiers OPA313 (Texas Instruments).

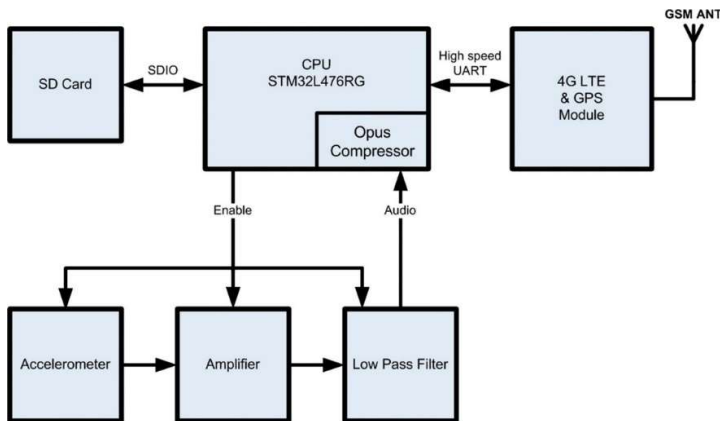


Figure 5-5. Block diagram of the vibrations recorder.

The system is controlled by an STM32L476RG ARM CPU of ST. The 805M1-0020-01 accelerometer picks up the vibrations, that are amplified using the OPA313 and turns them into a line-out signal that is compressed, stored to the SD card and transmitted through the 4G module.

The power consumption depends on user requirements. We provide an example of schedule that records 24 files/day with a duration of 10 s each that are uploaded once per day. The battery capacity is 3000 mAh, the sleep current is 40 uA, and the recording current is 70 mA, the GPS active current: 60 mA and the GSM transmission current (mean value): ~500 mA. The file upload time is 10 s. Therefore:

Automatic monitoring of insect fauna at global scales using wireless networks and opto-acoustic sensors

- Recording current (mean value) = $(10 \text{ s}/3600 \text{ s}) \times 70 \text{ mA} = 194 \text{ uA}$
- File upload current (mean value) = $((24 \text{ files} * 10 \text{ s})/86400 \text{ s}) \times 500 \text{ mA} = 1.38 \text{ mA}$
- GPS current (mean value): $(240 \text{ s}/86400 \text{ s}) \times 60 \text{ mA} = 166 \text{ uA}$
- Total Current: $194 \text{ uA} + 1.38 \text{ mA} + 40 \text{ uA} + 166 \text{ uA} = 1.78 \text{ mA}$
- Final battery duration = $3000 \text{ mAh}/1.78 \text{ mA} = 1685 \text{ h}/24 = 70 \text{ days}$

Note that power sufficiency can be extended to unlimited with the use of a small solar panel matching the back of the device.

The server is described in [12] and manages the data collection and time-stamping, GPS registration and storage process of submitted audio recordings (see Figure 5-6). Moreover, the administrators can manage and customize the data fields and collection process as well as communicating commands to the sensor nodes. The 4G modem of the trap or the gateway in the case of LORA/WAN, once connected to the mobile provider, are capable of having internet connectivity. The trap makes a TCP/IP connection to the webserver of the backend, via a POST request, and uploads the recorded audio files. At this point, the trap inserts its data as parameters for the page that it wants to access. Once the HTTP request reaches the web server, the latter receives the data from the request of the trap (via the appropriate code, written in PHP) and logs the information in the database. The web application consists of two parts: The backend that manages the information and the database in the server and a frontend that visualizes the information at the browser of the user and the interface with the user. The site is based on a web hosting provider running Apache, with PHP 5.5 support. The database is setup using MySQL, which is open source.

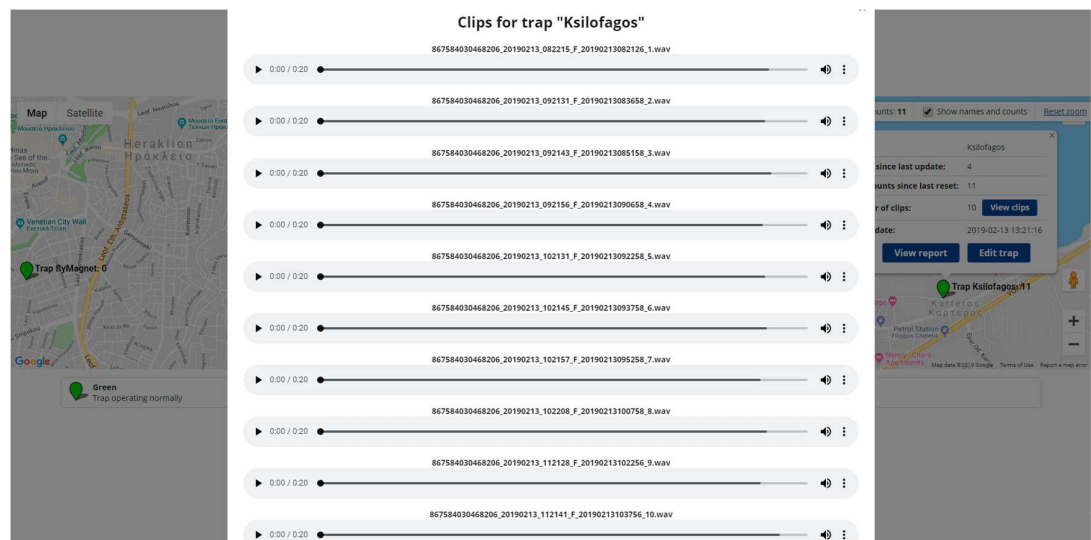


Figure 5-6. The reporting server manages recordings Clips, tracks geospatial data, handles data inventorying and communication with all deployed sensors.

The backend is written in Laravel 5.1 PHP 5.5 and the frontend is written in HTML 5, making use of the Angularjs Javascript and JQuery javascript Framework. The data follow the JSON formalization. The maps are currently provided via the Google Maps API.

5.3 Results

As a means to evaluate performance and in order to confirm a positive prediction of an infestation inside a tree, we need to slice the tree trunks with a chainsaw. This is a laborious process as each tree offers different difficulties during the cutting process (see Figure 5-13). The mulberry is characterized by its solid, hard wood and since the location of the larva or adult insect is unknown, a number of thin slices may be needed whereas palms have a moisty fibrin structure and their juices can corrode the saw in the long run. Healthy trunks have been taken from trees that are not known hosts of the insects investigated, whereas suspicious tree-trunks had marks of exits of adults (see Figure 5-7) and/or sawdust signs. Note that the exit tunnels indicate that the larvae have become adults that escaped from the tree and there is no guarantee that another generation of larvae is breeding inside. However, a new infestation is usually the case.



Exit tunnels of adult *X. chinensis* in a mulberry tree marked with a white rectangle. Although the pests have left the tree through the tunnels they have dug, it is mostly probable that there is another generation of larvae breeding that will lead to the next generation of adult insects.

Figure 5-7. A suspicious tree-trunk

Feeding larva produce impulsive audio events that sound like snaps (i.e., breaking fibers) and appear in the spectrogram of vibration recordings as high-energy, broadband stripes (see Figure 5-8). Activity rates can vary greatly depending on the infestation level, the biological cycle of the pest and the distance from the larva ranging from few hits every ten seconds to hundreds when near to a highly infested area of a trunk. These sounds are visually and acoustically distinctive when not totally masked by another sound. Although background noise can sometimes be audible, it is heavily attenuated as the waveguide attached to the accelerometer is protected inside the wood. In Figure 5-9 to Figure 5-12, we demonstrate several negative cases for the presence of borer taken from trees in an urban environment and the impact of background noise. Visual examination of the spectrogram allows to quickly scan a small to medium number of recordings. A spectrogram is a representation based on the short-time Fourier transform that reveals how the energy of the signal is distributed over frequency with respect to time. The recording is chopped to 512 samples chunks with 50% overlap and a Hamming window is applied to each chunk. Each time-domain chunk is Fourier transformed and the log amplitude of all transformed chunks are stacked together to make the time-frequency representation seen in Figure 5-9 to Figure

5-12. In Figure 5-9, we see a typical example of a case where nothing interesting happens. This is a typical case and the figure of a flat spectrogram allows us to discard this recording immediately from further investigation. Figure 5-10 shows a characteristic recording of the probe inside the tree in the presence of strong wind. In Figure 5-11, we can see the vibrations caused by raindrops in the case of heavy rain. In this tree, the smaller branches have been removed and there are no leaves. Therefore, there is a direct path for the raindrops onto the tree trunk. In Figure 5-12, the probe is inserted in a tree on the pedestrian side of a road in heavy traffic hours.

The advantage of our approach is evident as the observer is not obliged to discern in-situ the infestation state of the tree but can decide in the convenience and silence of the laboratory by examining recordings of several days and picking the most high quality recordings taken e.g., the ones during a silent night in order to base ones decision. Screening of recordings must be applied automatically when the number of recordings reaches the range of thousands of cases. Though we feel this is a route that must be investigated independently from this work, we suggest that can be carried out by counting the peaks exceeding a signal-energy threshold either in the time or frequency domain, or semi-automatically by transmitting only the suspicious recordings (i.e., counts exceeding a threshold) to a human observer for further consideration. The latter approach would also result to considerable power saving. In what follows, we present characteristic results from in-lab experiments with healthy and infested tree trunks followed by field applications.

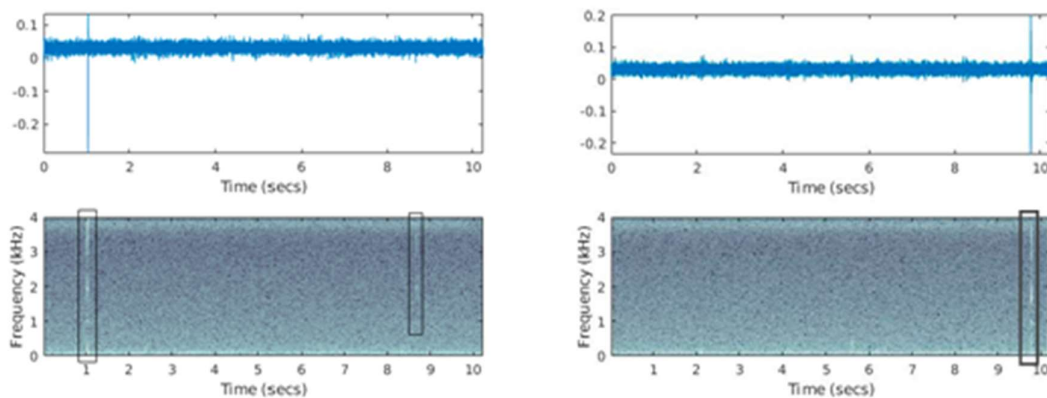


Figure 5-8. Mulberries positive for *X. chinensis* (trees chopped and alive larvae found)

(Top) time domain recording of the vibrations inside a tree trunk acquired using the suggested device, (bottom) Spectrogram of the same recording (i.e., time over frequency representation of the vibroacoustic signal). We mark with rectangles the evidence of audio impulsive sounds from inside the tree shown as white stripes that led into classifying the trunk as infested.

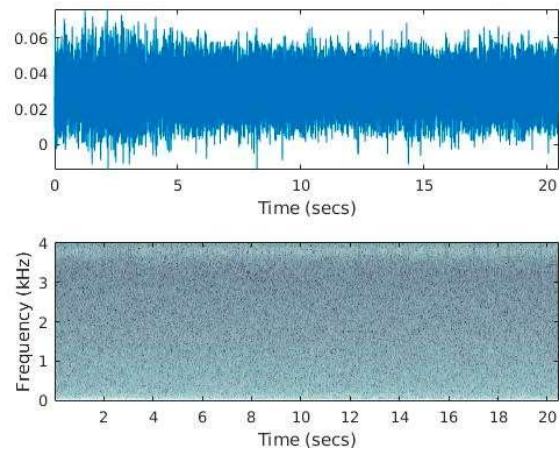


Figure 5-9. A typical case with no signs of any vibration

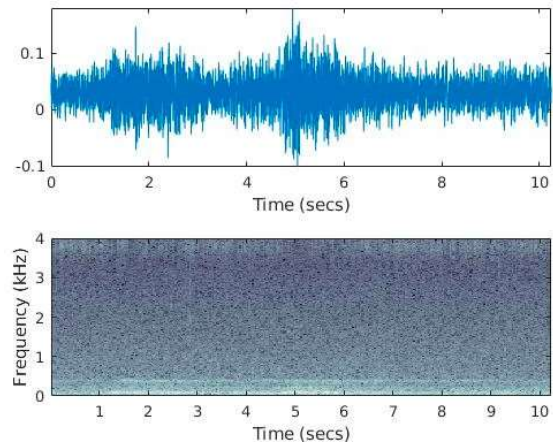


Figure 5-10. A recording in the presence of strong wind (stormy weather)

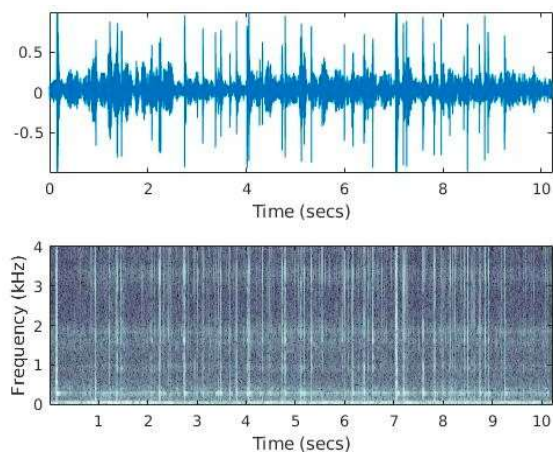


Figure 5-11. Heavy rain hitting the trunk. The impulses are due to the raindrops.

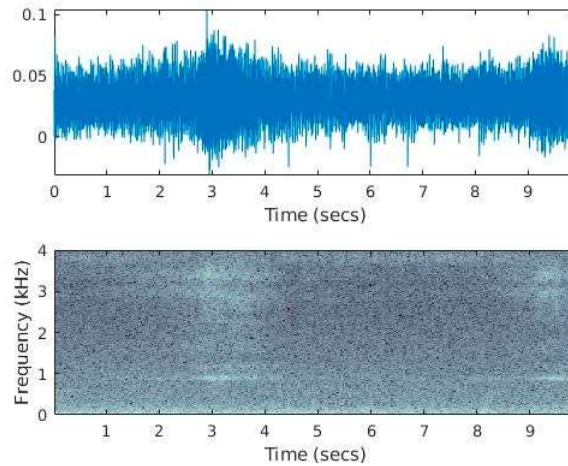


Figure 5-12. Recordings in the presence of heavy traffic in a rush hour.

Figure 5-9 to Figure 5-12. Field-recordings in different mulberries that are negative for the presence of a borer under different environmental conditions.

5.3.1 In Lab Experiments

In Figure 5-13, we show the positioning of the device on a tree trunk. First, we make a hole with a matching drill and we fasten the waveguide tight inside the hole.



Figure 5-13. A *X. chinensis* positive case in a mulberry trunk. (Left) The sensor mounted horizontally in a suspicious trunk in the laboratory, (middle and right) two alive larvae have been found after cutting the suspicious trunk in slices. The larvae tunnels can be seen in the right picture.

The device registered impulsive sounds and the trunk was classified as infested. In Figure 5-13-right we see the first live larva of *X. chinensis* we discovered along with two visible tunnels.

5.3.2 Tree Inspection in the Field

We are mostly interested in the open-field case especially in urban environments as we aim at integrating our approach in the context of smart cities and introducing a new surveillance service: remote vibroacoustic surveillance at large spatial scale of trees for borers. We designed a test involving eleven trees in the city of Heraklion in Crete, Greece. The device pinpointed eight trees to be positive for borers and we acquired special permission from the municipality to cut the mulberries down partially (i.e., removal of branches) or totally. Results are gathered at Table 2.

Table 2. Field application using the suggested device in the city of Heraklion-Crete.

Tree Species	GPS Coordinates	Remote Assessment	Manual Verification
Mulberry	35°19'55.7" N 25°08'03.5" E	Positive	Positive
Mulberry	35°19'56.7" N 25°08'04.5" E	Positive	Positive
Mulberry	35°19'56.4" N 25°08'04.7" E	Positive	Positive
Mulberry	35°19'56.8" N 25°08'05.1" E	Positive	Positive
Mulberry	35°20'05.3" N 25°09'50.1" E	Positive	Positive
Mulberry	35°20'05.4" N 25°09'50.5" E	Positive	Positive
Mulberry	35°20'05.4.8" N 25°09'50.3" E	Positive	Positive
†Palm tree	35°19'37.3" N 25°17'46.3" E	Negative	Negative
±Palm tree	35°18'35.26" N 25°06'45.66" E	Negative	Negative
Palm tree	35°19'46.3" N 25°12'13.5" E	Positive	Positive
Common fig	35°19'09.8" N 25°07' 53.2 E	Negative	Negative

All trees have been partially or totally cut down, sliced and examined. Mulberries and the common fig have been checked for the presence of *X. chinensis* and palm trees for *R. ferrugineus*. †± two cases correctly classified as negative contradicting visual evidence.

It is very difficult to recognize the first signs of *R. ferruginous* presence and only later symptoms are conspicuous. The palm tree at 35°19'37.3" N, 25°17'46.3" E was selected because it had visible signs of damage on the leaves. The device did not register any impulsive signals. The palm has been inspected manually by checking all leaves for exit tunnels and signs of rotten tissue. Two observation windows were opened by removing

four leaves for each window, but no tunnel, larva odor or fungi have been observed. In the case of the palm tree at 35°18'35.26" N, 25°06'45.66" E there was evidence of yellowing of leaves, fall of lower leaves and crown wilting, therefore the tree was a prominent example of infestation. Again, the device and careful manual inspection have been negative. As the palm was in the secured area of a state's institution, we asked about the history of the tree and were informed that half a month earlier the tree had been treated with insecticides on the crown but insecticides had also been injected inside the tree from the crown down. These are notable cases because there were visible signs of degradation but the trees were actually healthy. These cases support the argument that the capability to observe remotely and basing the decision on the infestation status after several days of observing the tree's internal vibrations offers a benefit to visual observations and is useful for after treatment assessment (see Figure 5-14).

Solid wood is easier to check for borers. In the case of mulberries, most cases with background noise due to anthropogenic noise or weather conditions do not result into recordings containing impulsive audio events with the exception of rain. On the other hand, palm trees, due to their fibrin structure can produce easily impulsive events that resemble noises from larvae. In such case, one must avoid making decisions based on recordings that were taken on a windy day and should try to detect pulse trains instead of isolated audio events. Pulse trains are repetitive series of pulses, separated in time and often occur when larvae move or chew. Pulse trains in palms due to wind do not show the systematic nature and compact structure of larvae originating audio events.

In all cases, it was deemed very convenient to listen through the server, one after the other, the trees at different hours and days and switching to listening between adjacent trees in a town square to find out if there is a correlation between detected events indicating that the infestation is spread at least locally. In the case of mulberries, the sensor is placed in the mid-upper part of the trunk, at the base of the main branches joining the trunk. In [106] it was found that this was the most probable location for *X. chinensis*. In the case of palm trees the sensor is placed near the stem or in an open wound as this is the most common entrance point of the red palm weevil. In heavily infested trees the larvae can be anywhere in the tree but for moderate infestations these are the most common locations we find them.



Figure 5-14. The device attached to a palm tree listening for *R. ferrugineus*. The white rectangle is located around the device.

5.3.3 The Deep Learning Database

The device records vibrations from a wooden substrate. It is quite straightforward to acquire recordings in acoustically challenging conditions (i.e., due to background interference) from trees that are not infested by borers. By simply inserting the probe in trees known to be healthy (not necessarily mulberries), one may easily get most of the typical sources of background vibrational interference (traffic, vocalizations, wind etc) while avoiding any vibrational signals due to *X.chinensis*. Although, the correct control is to use non-infested mulberries to gather vibrations due to background noise, externally induced vibrations are propagated mostly through the external part of the device and the substrate, in this case, does not alter the validity of the recordings. It is more complicated, however, to get recordings from infested mulberries, as the ultimate way to verify infestation is to cut down the tree— which is generally illegal in public spaces except for the authorized phytosanitary personnel—and slice it until one finds the larvae.

We gathered the recordings from infested mulberries in two ways: (a) by attaching the device on trees that had serious visual signs of attack and manually verifying the existence of pulse trains from the audio and visual inspection of spectrograms, and (b) from

mulberries that had been cut down with permission by authorities (heavily infested trunks or dead trees).

The database is composed of 33 folders with audio recordings taken from 35 different trees and a corresponding annotation csv file. This corresponds to roughly a folder per tree. The folders contain emitted recordings over a period of 6 months. The recordings are in wav format but are actually decompressed after being received in an ogg format. The sampling frequency is 8 KHz. The first 27 folders are used for training and validation and the last 6 for testing.

The data set of the target insect is composed of 4165 field and 53,676 laboratory recordings mostly at 20 s. Training Folders: Infested (train pulses from borers) 1-6, 11-23, #recs 731. Clean: 7-10, 24-25, 35, #recs 1754. Total training data #recs 2485. Test Folders: #26-#34.

5.3.4 Deep-learning as Applied to Spectrograms of Vibro-Acoustic Signals

Deep learning (DL) architectures have a modular layer composition where the layers close to the input learn to extract low-level features and subsequent layers rely on the previous layer(s) to synthesize patterns of higher abstraction (e.g., starting from edges and textures and ending in objects) [136][137][138]. As it is impractical to listen manually to hundreds of thousands of clips transmitted to a cloud server from a large number of trees, there is need for an automatic process that screens these recordings. Deep learning techniques can provide fast classification (as rule of thumb 5 ms/recording in a single GPU), as they can discern between train pulses originating from borers and events from other external sources of vibrations (as human listeners can). We achieve that by transforming the audio recording to an image through the spectrogram (i.e., the Short-time Fourier Transform is a 2D representation like an image) and feeding the images to a DL model. In the case of the spectrogram the ‘object’ is a spectral blob that corresponds to a vibration source. It is important in our case to not only detect trains of pulses originating from borers but also learn to discern between impulsive events belonging to different sources, which vibrate the tree, although they are located outside it. The operational model calculates the probability of infestation of a tree based on a long history of recordings that can span weeks.

5.3.5 Verification Experiments

We performed 10-fold validation cross-validation on field data to estimate how different convolutional neural networks (CNNs) models are expected to perform in general when used to make predictions on data not used during training. The procedure had a single parameter $k = 10$ referring to the number of groups that a given data corpus was to be split into. Each group, in turn, was held out as a test data set and the remaining groups made the training data set. We fitted a model on the training set and evaluated it on the test set. The accuracy over each fold was measured and the mean score over 10-folds along with the standard deviation is reported in Table 3. We applied a type of data augmentation with rolling of recordings at a random point to randomize the point in time the impulses appeared. In this work, our aim is not to fine-tune the hyper-parameters of the classifiers through grid-search. The images used to feed all CNNs are the spectrogram of the recordings using an FFT size of 256 and 50% overlap, resulting to a 129×1251 matrix.

Table 3. 10-fold cross-validation results for various deep learning models.

CLASSIFIERS (Ranked by Their Parameters Size) †	
ResNet50 (98 MB)	93.68/1.58
Xception (88 MB)	94.16/0.99
DenseNet121 (33 MB)	93.56/1.60
EfficientNetB0 (29 MB)	93.80/1.72
MobileNet (16 MB)	93.84/1.16
† Adam optimizer (learn rate = 0.001, decay = 1×10^{-6})	

Bolded values of Mean accuracy/std.dev indicate they have the highest values in small-memory imprint or convergence- training performance comparisons

We compared a set of state-of-the-art deep learning models to find the best-performing model that is most generalizable, has the least loss, and is the most suitable to be embedded for the task to be performed. In Table 3, we give emphasis on models with small memory imprint (EfficientNetB0, MobileNet) with a view to embedding them in the probes instead of running them on the server level. It can be seen that, among the five models, the EfficientNetB0 and the MobileNet compare favorably to the larger models, while the best scoring Xception had the best convergence and training performance.

To further elaborate on the verification accuracy we use precision, recall and F1 score metrics on a random 20% holdout data for the best performing model (see Figure 5-15 and Table 4). Precision (P) is defined as the number of true positives (Tp) over the number of true positives plus the number of false positives (Fp). Recall (R) is defined as the number of true positives (Tp) over the number of true positives plus the number of false negatives (Fn). These quantities are also related to the (F1) score, which is defined as the harmonic mean of precision and recall.

$$p = \frac{Tp}{Tp+Fp} \quad r = \frac{Tp}{Tp+Fn} \quad F1 = 2 * \frac{P*R}{P+R} \quad \text{Equation 5}$$

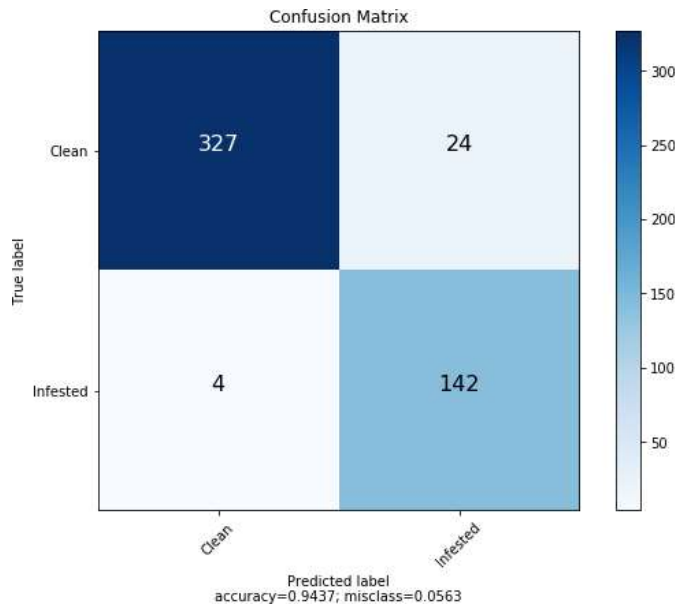


Figure 5-15. Automatic verification of borers’ infestation in trees in the field data. Based on a 20% holdout set. (Left) Confusion matrix of a using an Xception model. (Right) Precision (P), Recall (R) and F1 scores.

Table 4. Precision (P), recall (R) and F1 score metrics on a random 20% holdout data for the best performing model.

	P	R	F1	Support
Clean	0.99	0.93	0.96	351
Infested	0.86	0.97	0.91	146
Accuracy			0.94	497

High precision relates to a low false positive rate (false alarm), and high recall relates to a low false negative rate (miss). High scores for both show that the classifier is returning accurate results (high precision), as well as returning a majority of all positive results (high recall). We did not try to fine-tune classifiers through grid-search and voting schemes of different models as optimization of classifiers is not the focus of this work.

Finally, in Figure 5-16 we demonstrate how automatic assessment on the infestation status of a tree takes place once the CNN is operational: the probed tree provides a folder of snippets spanning a time interval and this folder is directly fed to the trained CNN with spectrograms of vibrations being the input and probability of infestation the output. Probabilities are averaged for all snippets and normalized to unity by dividing with the number of snippets.

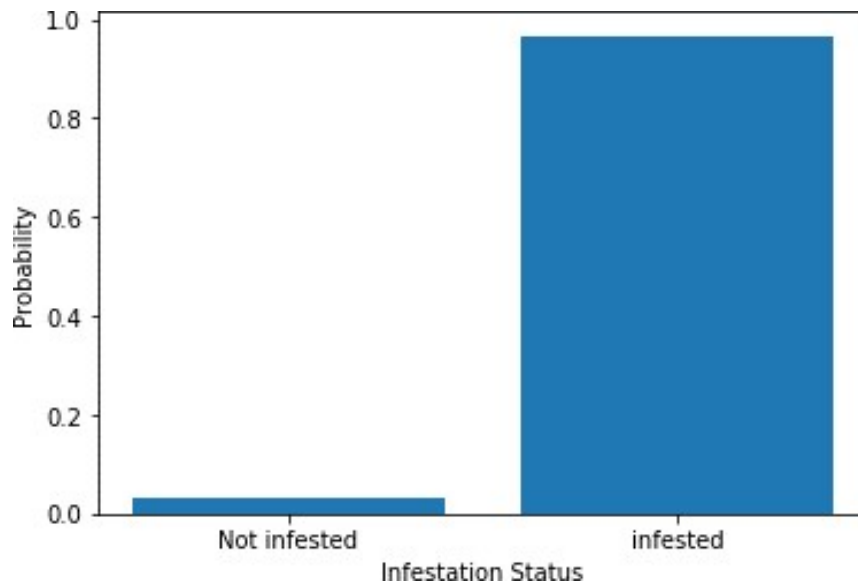


Figure 5-16. Infestation state of a tree after examining the folder no. 33.

The provided database containing 753 recordings spanning several days. The probability is derived by averaging the probabilities of all cases and normalizing to one.

5.4 List of Applications

In Table 5, we gather possible applications that can be carried out by the proposed device. Some of them are originating from different domains:

- a) We envision a widely applied device (i.e., one for each tree for urban environments) and a sample of trees in forests that allows one to listen to the internal audio scene of a tree in view to detect on time the feeding and locomotion sounds of larvae or adult wood-boring pests digging their exit tunnels.
- b) We suggest that the same device but with a small bolt or a drill bit functioning as a waveguide can be an integral part of wooden pallets for the transportation of goods. When the cargo would reach the harbor, the pallets would wirelessly transmit their total internal vibrational history to phytosanitary services located in the harbor to be screened automatically before granting free movement of goods. The goal is to intercept wood-infesting insects breeding in pallets (for this application, manually treated, see [117]).
- c) The suggested device can be used for detection of illegal chopping of trees or unauthorized movement of wooden logs, scented trees etc. The suggested device can be configured to auto-trigger and send an alert e-mail when it receives a shock.
- d) Tree trunks of palm-trees for transplantation remain in the harbor in a quarantine state for some time. Phytosanitary managers usually inspect them. This service is further facilitated, as one needs a non-specialist only to attach the device on the trunks. The trees will be monitored automatically during their quarantine time. This is especially useful as manual inspection is costly, inconvenient and does not scale to large numbers of applied visits. In addition, the observer may happen to inspect an infested tree at a time when a larva is not active.
- e) The device can be inserted in the roots of plants in nurseries to detect larvae feeding on the root system of several plants.
- f) Houses that make extensive use of wood in their construction are popular in the US and in the North of Europe among other places. In the context of smart homes, a device can constantly watch the house in several of its weak spots for the presence of termites and other woodworms. The device alarms the inhabitant by sending an e-mail if the vibration signs originating within the wood persist over time.
- g) Automated monitoring of stored product pests in silos.
- h) When inserted in the ground the device can serve as a spatially localized seismometer that can track the passage of heavy vehicles. Therefore, it can be

deployed at large numbers for border control of vehicles and is very cost-effective and easily deployed compared to cameras.

Table 5. A list of applications directly treated by using the suggested device

#	Applications
1	Detection of wood-boring insects in urban trees and trees of special/historic interest
2	Self-monitored wooden pallets for transportation of goods
3	Detection of illegal chopping of trees or unauthorized movement/theft of wooden logs
4	Inspection of quarantine trees transported for plantation in harbors
5	Insertion of probe to the ground to detect larvae feeding on the root system of several plants
6	Smart home monitoring of wooden houses and structures for termites
7	Detection of stored product pests in silos
8	Heavy vehicles detection and counting, perimeter security, border control

5.5 Discussion

Growing a vibrant urban forest requires maintenance. A very efficient automatic recorder for sensing, registering and wirelessly emitting the acoustic emissions that the larvae produce during eating and feeding inside the trunk of a tree has been designed and developed.

Pathway management and phytosanitary methods are the first line of defense to prevent or reduce the risk that non-native species are inadvertently introduced to new places via association with imported goods. Phytosanitary interception at commodity entry points (e.g., airports, harbors, stations, lorry parks, cargo depots and quarantine facilities) follows [6][118][119][97]. Wooden pallets, wood products, ornamental trees, plants but also cargos of fruits and other agricultural products are typically examined before importation using visual inspection and various technological means [123][127]. Effective interception of potential pests including but not limited to quarantine species already intercepted in the past, is crucial [97]. Though not impossible, it is increasingly difficult to achieve eradication of establishing or established invasive species after initial arrival. Interception is currently based on visual inspection and manual application of several technologies.

This work introduces the novel service of automatic screening of wood-related imports. In short, devices are attached to the trees in storage facilities, the vibrational soundscape of the trees is sampled for the whole quarantine period and clearance is

provided automatically after deep learning models have finished screening the vibrational record of the shipment, otherwise the cargo is returned to the sender. As it does not involve human attendance (one can attach the device and leave), it can be applied to a larger scale than it is currently done. In addition, since it integrates a longer time span of observations than the human service currently applied, it is anticipated that it will be more accurate. However, we need to study further the application of pallets monitoring in practice and the data of this work do not directly address this application.

Another service that currently does not exist is based on transmitting the systematic registration of vibrations to cloud services. The audio data serve as a permanent record of evidence and the process of cross-examination by trained bioacousticians is decentralized in the sense that the trees under investigation, the stored audio records and the human specialists need not be in the same place—pretty much as the way telemedicine is applied.

Due to current manual limitations, only 2% per year of incoming shipments is inspected in US [97]. Therefore, more often than not, invading species are not intercepted at commodity entry-points and—as an example family—*Cerambycidae* beetles are establishing in new locations. Post-border surveillance and containment is easier if the first establishment of the invasive species is detected and localized as early as possible. Forests and parks nearby commodities' entry points are most at risk. If the invasive species attack trees of urban ornamental greenery in public spaces, like in the case of *X. chinensis* for mulberries and *Rhynchoforus ferrugineus (curculionidae)* for palms in Crete, the trees are left untreated until they die without consideration of their aesthetic value [118]. Even in such a case, the automatic screening of vibrational records from trees offers new services and introduces a possible revision of the currently applied protocol. Regarding urban spaces, workers in ornamental greenery assess visually whether the trees already have exit tunnels, discoloration/damage of leaves, signs of rotten tissue and any other visual symptoms of health decline and cut down only the ones that are heavily infested or dead. However, this is too late: visual symptoms appear 1–2 years after the first infestation as regards *cerambycidae/curculionidae*, which means that by the time their traces are visible, the borers have completed several generations inside the tree and have escaped to infest new ones. What we suggest is to remove the trees with positive acoustic records and not to base inspection and assessment on visual records. Even if no other treatment is applied, this procedure is expected to delay the degradation of urban greenery relying on the specific tree species.

Let us give a lucid example on the dilemmas phytosanitary personnel face on a daily basis and how these can be answered with automatic screening of vibrational records. Should we cut down a mulberry without any visible signs of degradation knowing that the city is infested with *X. chinensis* and the *Morus* tree is the primary host? The decision to cut down trees is of grave importance both in terms of financial cost (i.e., removal and secure destruction costs) and in terms of ecological impact. During the experiments of this work, pest specialists would refuse the cutting of trees having no symptoms of degradation. Yet, there have been cases where an examination on the upper-part of the trunk has shown long and vivid pulse trains of vibrations. Again, recordings can serve as evidence and the pulse rate can assess the infestation status (heavy or low). Removing the tree will locally degrade the greenery but the alternative is to remove it dead, 2–3 years later, while escaping adults and their descendants will have infested a large number of healthy trees thus accelerating the degradation on a regional level. On the contrary, removing it a year and a half prior to the visual symptoms will significantly prolong ornamental greenery even if no other treatments are applied.

A different protocol may apply in the cases of trees of economic importance like orchards of stone fruits as heavy infestations lead to fruit drop. In such cases, the usual procedure is the removal and the immediate destruction of all infested trees, as well as those present within a variable radius of the infestation. The decision, however, to characterize a tree as infested is again based on visual signs. As mentioned above, this approach has poor effects because when visual signs are prominent enough to characterize a tree as infested, many generations of adult pests have already escaped. Therefore, removal of trees based on visual assessment of symptoms is not sufficient to stop the invasion to new areas, and to limit the damage where pests are already established. When borers are established, pest control may involve aerial and ground bait pesticide sprays, but their efficiency depends on knowing the time and location of insect infestations as early as possible. The advantage of probing the trees is that they can reveal the problem as early as first-generation larvae and automatically tag their location (the transmitting device carries a GPS).

5.6 Concluding Remarks and Further Steps

To our point of view vibrational sensors attached to trees that have a bidirectional wireless communication with cloud-servers, hold much promise for detecting invasive wood-feeding insects in various novel applications (the new services are gathered in Table 6).

Table 6. A list of benefits using automatic screening of trees' vibrational records.

Automatic interception of infested trees and timber cargos at commodity entry-points
Integration of information from larger time spans (weeks to months)
Replacement of all decisions based on late visual assessment of trees with early vibrational detection
Provision of permanent time-stamped evidence (recordings) interpretable even by non-specialists
Decentralization of the problem of decision making by bringing the knowledge of specialists to remote areas
Delimitation of infestation areas that can reduce use of pesticides and infestation rate by removing infested trees at early stage

Borers can be detected during their larva and adult stage when they move and feed. The algorithms can automatically integrate data from long time spans (daily, weekly, monthly) to infer the infestation state of a tree. The number of nodes applied will increase as the cost of electronics decreases and technology improves when 5G wireless communication is widely adopted. Automatic screening of vibrational data can be carried out at the server allowing the efficient and rapid processing of thousands of recordings allowing novel services to emerge as automatic creation of infestation maps and predictive modelling of invasion and spread. In the era of global trade and climate change, modern tools to monitor remotely trees for borers before they colonize and establish in new habitats can lead to novel services and modernize inspection agencies. This in turn can have a significant reduction on the economic damage caused by pests and spraying costs related to treatments and increase productivity with a lower impact on the environment and human health.

6. THE E-FUNNEL TRAP

6.1 Introduction

A grand challenge facing the 21st century is the sustainable production of food for the growing human population [140]. One of the solutions often suggested is investing in technology to increase yields by decreasing quantitative and qualitative crop losses due to pests [160][11]. Integrated pest management (IPM) is about making better decisions on how to suppress pest populations below the economic injury level (EIL). The suppression of pests needs to take into account human health and the least possible disruption of the environment due to insecticides while keeping the cost of intervention low compared to the EIL [142]. In the era of climate change and intense trade due to globalization, pest monitoring and early detection are key factors of modern pest control and IPM systems [165]. The efficacy of modern pest monitoring relies on information about localizing in space and time the detection and evolution of pest populations. Monitoring traps are commonly used to sample insect fauna in order to make informative assumptions on the actual pest load of large areas to reach decisions on treatment/actions. A timely prediction of the occurrence of the onset of an infestation and the location of its concentration can define the decisions on an insecticide application program. If the problem is controlled at its initial stage then it inflicts a loss below the EIL. Simultaneously, the uniform, unnecessary sprayings that are usually applied by farmers in fear of pest losses are mitigated.

Because of their safety, ease of use, and non-toxicity, traps are a valuable tool in integrated pest management (IPM) programs. Currently, traps need to be visited frequently and checked manually and this imposes a barrier to the extent they can be deployed due to practical and economic reasons.

Lepidoptera species (moths and butterflies), are considered suitable indicators for biodiversity but many of them can reach high, damaging densities and severely impair plant processes in agricultural ecosystems. Specifically, due to species richness of the *Lepidoptera* order [152], the taxon list of a given area provides an extremely detailed view of the environmental conditions of the site; they show a sensitive reaction to the change of abiotic factors [151]. The appearance of high populations of *Margaronia unionalis* Hübner (*Lepidoptera*, *Crambidae*) in olive orchards of Crete (Varikou unpublished data), serious infestations of *Euzophera bigella* (Zeller) (*Lepidoptera*: *Pyralidae*) reported on limbs and trunks of Elounda and Amphipolis [168] as well as extensive infestations of *Tuta absoluta* (Meyrick) (*Lepidoptera*: *Gelechiidae*) on tomato crops have been associated with human

activities affecting the established equilibrium in an agro-ecosystem [147] and climatic changes [141] of the last decade.

Furthermore, a key tool for their effective control is monitoring of their population dynamics which mainly depends on the used sexual attractant. The detection of a great variety of rare or harmful pests of Lepidoptera species of major crops (olive, vines, pear, chestnut, apple etc) such as *Prays oleae* (Bernard) (*Lepidoptera; Yponomeutidae*), *T. absoluta*, *E. bigella*, *Thaumetopoea pityocampa* (Denis & Schiffermüller) (*Lepidoptera: Thaumetopoeidae*), *Lobesia botrana* (Denis & Schiffermüller) (*Lepidoptera: Tortricidae*), *Cydia splendana* (Hobner) (*Lepidoptera: Tortricidae*), depend on the pheromone used [154].

E-traps are common traps enhanced with the capability of reporting wirelessly a key piece of information about their captured content (i.e. counts of Lepidoptera, time of capture, environmental parameters during capture, GPS coordinates). These devices can provide consistent estimates of insects' presence (detection/infestation onset), population dynamics (monitoring) but they are also useful for evaluating insecticide treatment efficacy (post-treatment analysis) and control purposes (population reduction). E-traps offer services that are impractical to deliver manually. They monitor and report insect populations 24 hours a day and thus can determine the precise onset of an infestation. If the user configures the report update on a per hour basis, then the network of traps can infer the dynamics of pest populations. Dense reporting can evaluate the impact of a control treatment (e.g., chemical/biological spraying, release of beneficial entomophagous insects etc.). E-traps time-stamp all captured events, so one can track insects' response to pheromones, their activity related to the circadian rhythm and the optimal time for treatment application.

The reported literature on electronic insect traps that employ optical sensors has come a long way in the past years, but recently a number of attempts in different application areas - using technology based on the same principles- has reached the technological readiness level of (TRL-9). TRL-9 means that the devices are at product level and thoroughly tested in the field. These approaches are either vision based [162][144][146][148][156][155][159][163][164][166][171][173][172] (i.e. traps with cameras) or they use an optical counter combined with selective lures [83][149][150][44][12][47][17][170]. Commercial applications do not appear often in literature so that we cannot assess different approaches like the ones based on capacitive sensors [153]. The principle of optical counters is based on the insect falling through the funnel of the trap and the effectuated interruption of the flow of infrared light from emitter

to receiver. The light fluctuation due to the shadow casted in the receiver by the falling insect is turned to a voltage variation that is finally turned into an insect count. The work reported is based on an optical counter at TRL-9. We are aware of two other applications of the same principle at the same TRL, the BG-Counter [170] that allows to remotely measure the dynamics of mosquito populations and the ZooLog system targeting Lepidoptera, crawling insects and soil living microarthropods [145][116][161][169]. The selectivity of traps relying on optical counters is based on pheromones and not on general food baits and in the case of mosquitoes on CO₂ and suitable scents.

Human monitoring will be replaced by e-traps once the latter reach a high level of reliability and the value of the services, they offer are higher than their cost [157] (as an example on the importance of cost-effectiveness). We elaborate on these issues below.

6.2 Materials & Methods

6.2.1 Trap Design & Function

Common funnel traps are used for the timely detection of a new infestation, for monitoring insects' population size (mainly Lepidoptera) and sometimes for creating a physical barrier (mass trapping). The classic funnel-like trap is made of plastic and comes in many variations but the basic components are three (Figure 6-1-left):

- a) The upper cup functions as an umbrella and prevents water from coming into the trap. It also includes a pheromone dispenser holder. Pests fly around the pheromone dispenser until they are exhausted and they fall through the funnel into the transparent bucket.
- b) The funnel is an inverted plastic cone that makes it easy for the insect to come in while the narrow bottom makes it difficult to escape.
- c) The semi-transparent bucket where the captured insects fall fastens to the funnel. It may contain soapy water or water with detergent. It is used in combination with a species-specific pheromone. It is hanged from a branch using a suspension wire or anchors to a ground support pole.

The aim here is to design an add-on optoelectronic device and not to apply modifications on the original funnel with a potential significant effect on the attractiveness of the trap due to the change of shape or pheromone release. The attractiveness of the typical funnel trap is established and has been used in the field for a long time. The e-funnel (Figure 6-1-right), is a typical plastic funnel trap with an add-on torus (Figure 6-2) that counts

insects as they fall into the trap and a LoRa wireless communication capability to broadcast the sensed data to the gateway. The gateway (Figure 6-3) collectively uploads insect counts, time-stamps of captured insects, GPS coordinates and environmental parameters through the mobile network to cloud services. The communication of the network with the cloud server is bi-directional: trap data are uploaded to the server where they are streamlined, visualized and stored and, vice-versa, the e-traps can be reconfigured by receiving instructions from the server (on-off commands, time scheduling, tuning of thresholds, local time-zone). It is an instance of an internet of things (IoT) application in agriculture. In the context of the IoT, one e-funnel trap is a single node that interacts with other nodes and establishes its own network. The electronics of the e-traps and the LoRa radio protocol are very low power and do not require a solar panel to function. Using their own embedded and rechargeable batteries, they can operate longer than the point in time where the pheromones need replacement (2 months).

The gateway can instantaneously deliver the information of the whole network using a single mobile communication modem (Figure 6-3 for a field installation).

6.3 System's Design and Implementation

Although the principle of an optical counter is simple, its robust, low-power implementation for operating in the field is complex. The main practical obstacles that have been surpassed are:

- A. The double counts problem: insects falling into the bucket sometimes fly inside, and therefore, in the first attempts of this technology, created double counts.
- B. The trap is semi-transparent to ensure attractiveness and the sunrays hit the trap from different angles during the day. Because the counter is optical, special manufacturing care must be taken so that the sun does not interfere with the optical system.
- C. The traps must be power-sufficient to operate at 24/7 for several months with their own batteries, as the use of panels in poles is impractical for large-scale deployment.

The obstacle of double counts has been fully resolved with the embedding of two independent light-beams functioning independently and in parallel: a fall of an insect from top to bottom is counted but not vice versa. The CPU runs a root mean square (RMS) monitoring of the optical intensity of both beams. A valid count is registered only when the first beam is interrupted first and, subsequently, the second as well, whereas the intensity fluctuation must be inside the threshold limits that are related to the size of the insect and

are set in the reporting server using a small set of the targeted insects. The double counter is the key idea that reduced by 90% the false alarms of the initial prototype that used a single light beam.

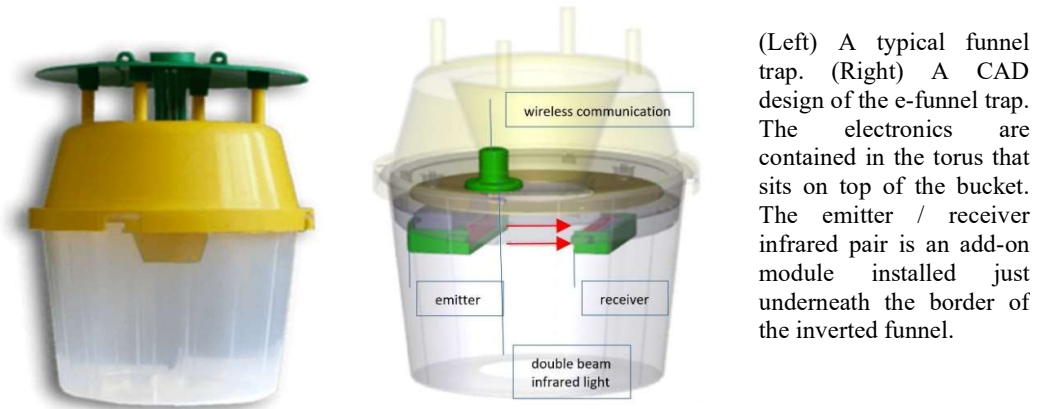


Figure 6-1. Funnel trap

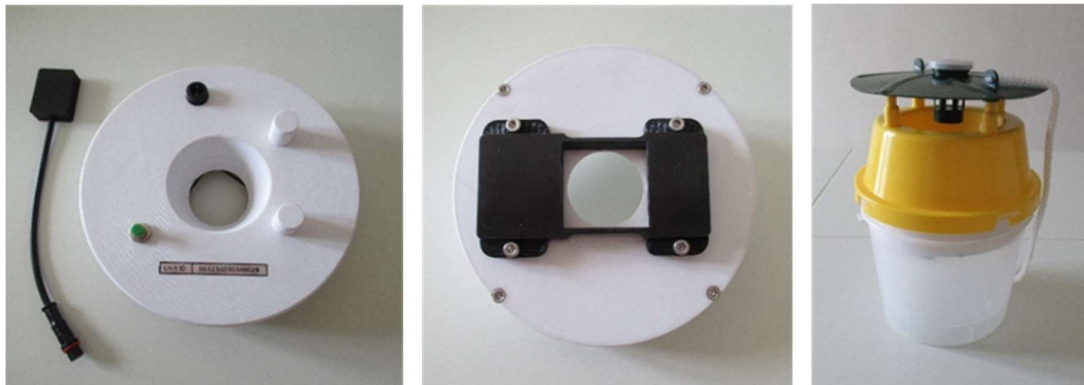


Figure 6-2. The electronics funnel trap

(Left) The torus in the picture is the optical counter. The small black element is the power socket that connects to the USB power-charging cable and the green one is the power up/down push button. The two white blobs are the GSM and the LoRa antennas. (Middle) the optical counter based on an emitter and receiver of infrared light (in black). (Right) The assembled e-funnel trap. (For interpretation of the references to colour in this figure legend, the reader is referred to the web version of this article)

The problem of light interferences has been resolved by installing 8 LEDs in a row for the emitter and the matched 8 photodiodes of the receiver far inside a plastic container that provides shade (the black cup in Figure 6-2–middle). The plastic container that provides shade also allows decreasing the signal intensity -and thus the power consumption- that is required to carry out the task of signal detection. A transparent plexiglas lid is placed in front of the receiving / emitting pair to block insects from infiltrating the optical counter.

The power sufficiency is based on using a synchronized emitter-receiver pair that emits and receives brief pulses of light instead of continuous light. This solution is technologically involved and is analysed in detail in [47][17]. The e-funnel operating in a 24/7 mode and reporting every 2 hours to the gateway consumes 2.08mA (GPS communication included) which means that it lasts four and a half months with the rechargeable batteries of 6800mAh it carries. Therefore, its operation surpasses the time for pheromone displacement that needs to be carried out every 1-2 months.



Figure 6-3. e-Funnel & LoRa Gateway in field.

(Left) Two e-funnels in a tomato field. (Right) The gateway (dim 12x12x11 cm) collects data from all e-funnels (through a LoRa network) and uploads it to the server through the mobile network (3G/4G).

The CPU has all the communication buses and analog parts to control the device (Fig. 4 for a detailed diagram). The LEDs sends 800 nSeconds infrared light pulses, for the top and bottom beams, at 2 kHz frequency. The photodiodes receive the light pulses and drive the photodiode amplifiers. The next signal-processing stage is the sample and hold circuit that samples the output of the amplifiers during the light pulse. The two outputs of sample and hold amplifiers drive two channels of analog to digital converter of CPU. The device has two ways to send data to the hosting cloud server. A GSM module, with LTE CAT-M/NB-IoT capability, to send data using the GSM Network, and a LoRa module to send data to a LoRa gateway. The GSM also has a GPS unit to get the trap coordinates. For reasons of telemetry and validation in the case of a detected event the light fluctuation is stored in the SD card. The recording in wav format can be automatically uploaded to the host when we use the GSM for communication. The software is written in C language using

the IAR Embedded workbench. The programming of the flash memory has been done using the Texas Instruments MSP-FET Flash Emulation Tool.

6.4 Network and Gateway Communication

This work establishes practical and reliable monitoring at large scales involving possibly hundreds of e-traps. At this scale, the LoRa wireless radio communication protocol is effective as all information is gathered at the gateway and a single modem (i.e. a single global SIM card) is used to upload all the information of the network to the server using, this time, the 4G/LTE communication.

Once an e-trap is powered on, it sends a request to the gateway that responds by sending back to the e-trap its attributed ID. After all nodes have been registered, the gateway sends a request of data transfer to all nodes in turn, waits for 1 sec to get a response from each one, and then goes to sleep mode where its power consumption is almost zero. The nodes follow the time schedule from the server and once it is time to report, they transmit their data to the gateway where the data from all nodes are logged until their collective transmission to the server.

Once data are delivered, they become a visualized time-series that can be manipulated in various ways. A common practice is the automatic placement on a map using the GPS coordinates of each trap (Figure 6-6 & Figure 6-7), setting alert thresholds on counts, histograms of counts per hour, visualization of daily activity and logging of all data to cloud services. For our experiments, we have deployed a network of 10 e-traps.

6.5 Study Area

The evaluation trial was conducted in an open-field tomato crop located at the region of Agia, Chania, Crete (Figure 6-6).

The open field crop covered an area of 1ha, planted in early June 2020 with 8000 tomato plants (cv Bobcat) with a distance between rows of 1.70 m and 0.66 m between plants. Tomato plants were drip-irrigated under plastic mulch. No chemical sprays or pesticide treatments were carried out during the whole experiment period of October-November.

The proposed network of automatic traps was also evaluated for its effectiveness as against a network of conventional traps (reference network) in monitoring the tomato leaf

miner *T. absoluta* populations. Each trap was installed at a height of approximately 0.50 m above the ground (the distance between two adjacent trees equipped with a trap was more than 10 m). Pairs of e-funnels and conventional-typical traps were placed in ten replications in the field (e-funnell was followed with typical one). Each trap was loaded with the sex pheromone (Koppert Inc.) which is the commonly used sex attractant for monitoring *T. absoluta* male population in Greece, with water (<10 ml each) and a few drops of liquid soap. The traps were checked twice a week (every Tuesday and Friday, 9.30 AM). After counting the captured moths, the traps were sequentially rotated in a clockwise manner in order to minimize the influence of the trap's position on moth captures. The sex pheromone lures used were renewed every four weeks. Whenever necessary, dirty water in traps was replaced with clean water.

6.5.1 Data Analysis

The evaluation of the monitoring network is based on a) comparing the automatic reports of the 10 e-funnels with manual counting of the e-funnels, b) comparing the manual counting of the e-funnels with manual counting of the 10 typical funnels that have been placed close to the e-funnels (Figure 6-6). Manual counting took place twice per week for a period of 5 weeks (02/10/20-06/11/2020). The evaluation is based on the following (we move along the metrics reported in [83]):

- a) Comparison of counts w.r.t. to time.
- b) Regression analysis between manual and automatic counts to examine the correlation of the two datasets and their statistical difference. The $\log(x+1)$ transformation is applied where x are the counts. We also derive the correlation (R^2) between the two datasets (i.e. automatically reported vs manually verified counts). The calculation of the slope of the regression line allows to see if there is a trend of over- or under-counting and to quantify it.
- c) Box and whisker chart on the divergence of reported vs manually verified insect counts (i.e. calculation of mean, standard deviation and out of bounds counts).
- d) ANOVA tests among all type of counts as well as between manual vs automatic counts and automatic network vs a typical, manually checked network. When significant, means were separated with Tukey (honestly significant difference - HSD test ($\alpha=0.05$)). The analysis was carried out using the statistical package JMP [167]

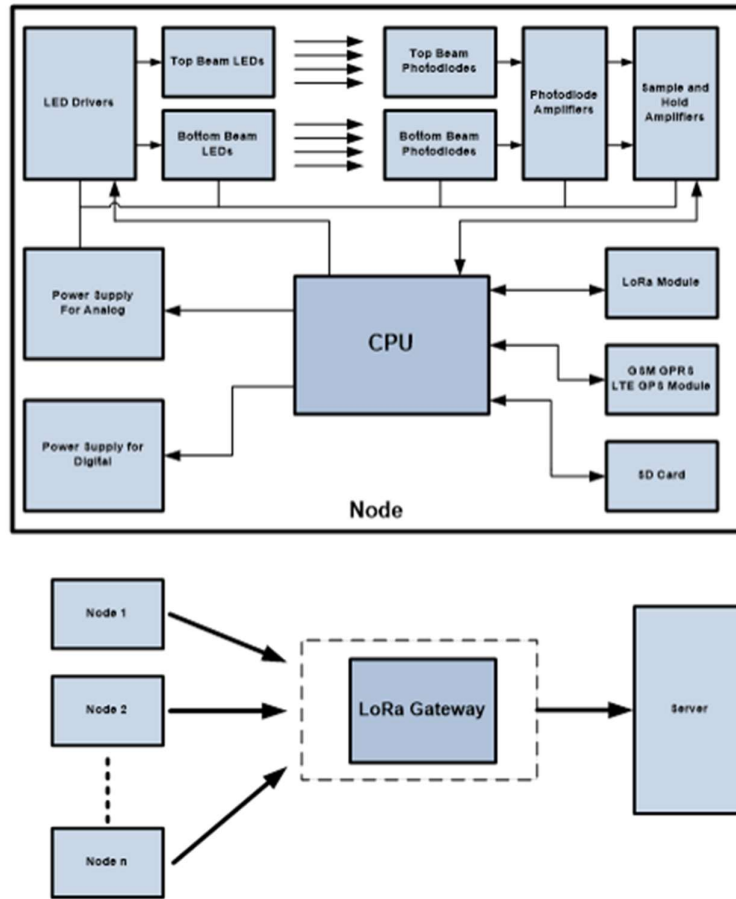


Figure 6-4. System diagram of the functionality of the e-funnel trap.

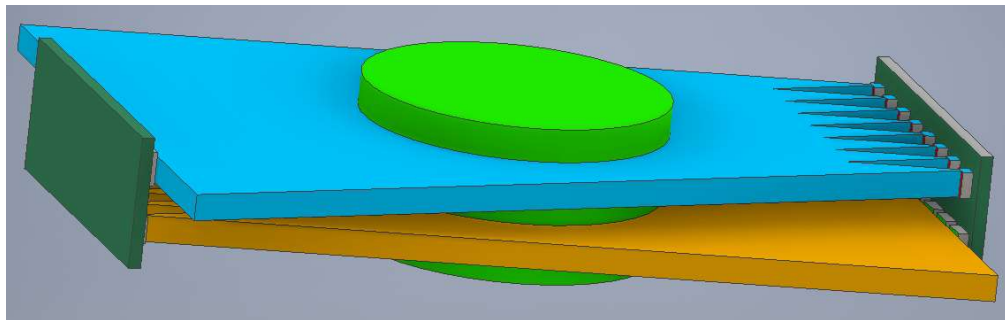


Figure 6-5. Schematic drawing of the optical sensing unit. A double layer, emitter-receiver pair of 8 emitting LEDs and 8 receiving photodiodes per layer. The cylinder denotes the sensing area under the inverted funnel. Note that in this area the light intensity is uniform.

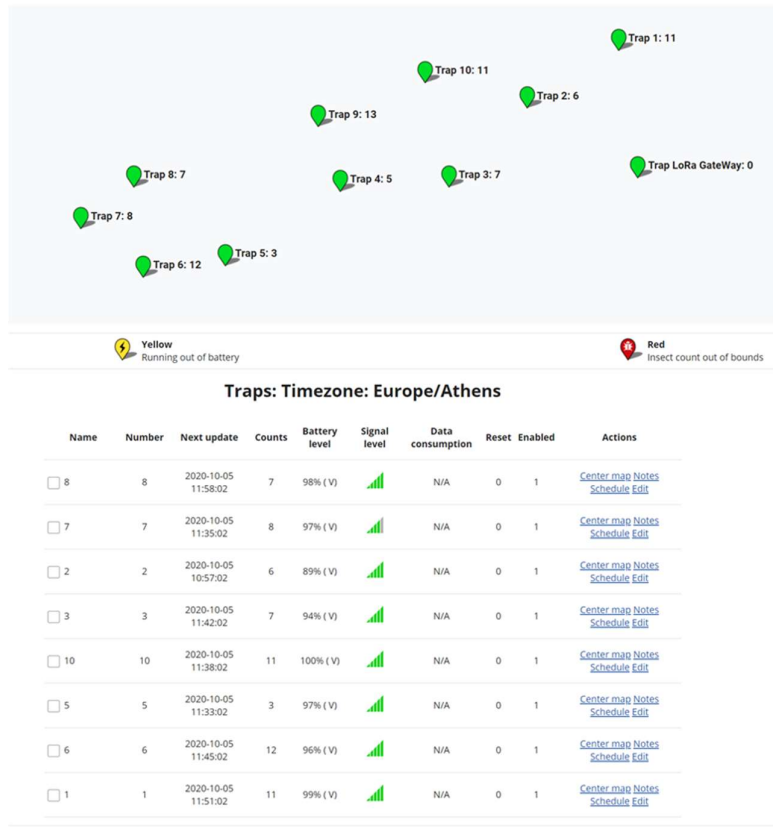


Figure 6-6. A network of 10 e-funnel traps on the map.

The traps and the time-zone appear automatically on the map based on the GPS of each e-funnel. Regarding the columns most labels are self-explanatory. Next Update of the e-funnels corresponds to the time the next measurements will be delivered to the gateway, whereas the Next Update of the Lora Gateway corresponds to the time the measurements will be uploaded to the server. Counts denote the insects counted. Battery level corresponds to the available power. Signal level denotes the quality of the communication link. Data consumption denotes the amount of data uploaded from the gateway to the server.

6.6 Results

6.6.1 Efficiency of Automatic vs Manual Counting

Figure 6-7 allows us to grasp the essence of the experimental results and their trend: in the first measurement (2/10/2020), there is a divergence due to configuring the detection thresholds that has been initially set too high and thus expecting larger insects than *T. absoluta*. After the first measurement, the e-traps are close to the correct values as indicated by the manual counting of the e-traps for the complete reporting period. Initially, the

network of typical funnels caught more insects than the corresponding automated network but this phenomenon faded in time. We proceeded to the quantification of these observations with regression analysis.

We performed ANOVA tests between these three datasets in every observation date to the field that confirms that these distributions do not differ in a statistically significant way except from the observation date of 2/10/20. The mean number of captured male adults of the leaf miner moth at the typical trap was significantly higher compared to that recorded automatically while the manually counted e-trap displayed no difference among them ($F=5.94$, $df=2,27$, $p=0.007$). Instead, significant higher captures were recorded at the e-trap compared to the typical one at the last observation date of the trial ($F=4.12$, $df=2,27$, $p=0.027$) (Figure 6-7). No statistical significance was displayed between manual and automatic counts of funnel traps, as the mean numbers of manually and automatic captured moths were almost equal (11.20 and 11.12 respectively) during the whole period of the trial ($F= 0.002$, $df=1,198$, $p>0.05$, Figure 6-8).

Finally, we performed linear regression analysis between manual and automatic counts, to evaluate the overall correlation between the two sets and the underestimation and overestimation of counts by the optical counter. The high correlation of data reported in Figure 6-9 and the slope that is estimated at 0.96 ($F=240.75$ $df=1,98$, $p<0.0001$) entail that automatic reporting is quite precise and automatic counting does not suffer from systematic gross underestimation nor overestimation of counts. We further report on error analysis to quantify further the extent of over-/underestimation by extracting the histograms of deviations between automatically reported counts and manually verified data. The histogram of the divergence between true and automatically reported counts is zero centered and practically the more usual divergence is between -2 (miss) to +2 (false alarms) counts (Figure 6-10).



(LAT:35.4746284, LON:23.9557972)The green balloons denote the e-funnels and the diamond shapes indicate the typical traps. (For interpretation of the references to colour in this figure legend, the reader is referred to the web version of this article)

Figure 6-7. The map of the field with marks of the traps.

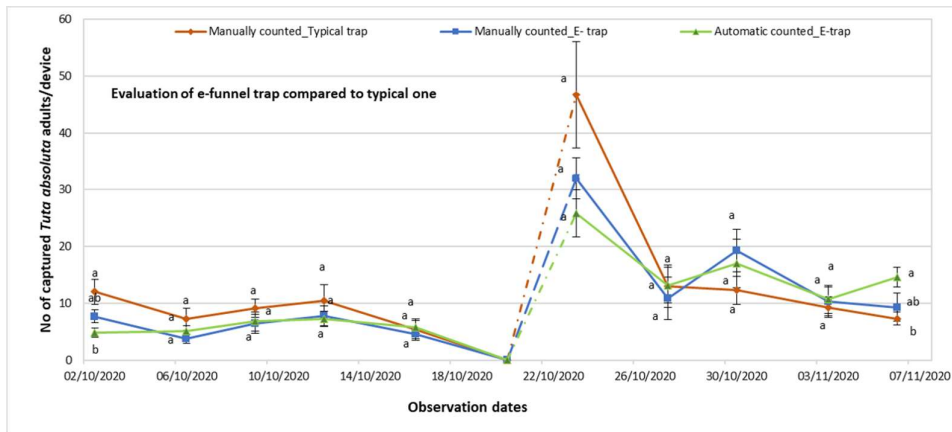


Figure 6-8. Mean number (\pm SE) of *T. absoluta* male adult counts (manual verification of e-traps, automatically reported counts and manual counting of typical funnels for *T. absoluta*) per funnel trap and observation date over a period of 5 weeks. Means of each observation date followed by different letter are significantly different at $P < 0.05$. Counts at 23/10/20 included also counts of the previous date which was missed due to heavy rain (150 mm) during this week period.

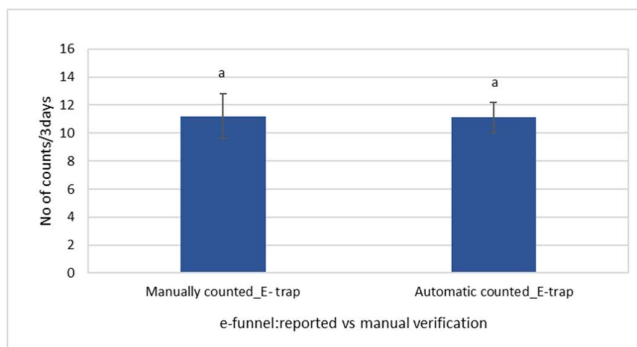


Figure 6-9. Mean number (\pm SE) of *T. absoluta* male adults. Counts every 3 days over a period of 5 weeks (manual verification of e-traps and automatically reported counts of e-funnels for *T. absoluta*). Bars with the same letter are not significantly different at $P < 0.05$.

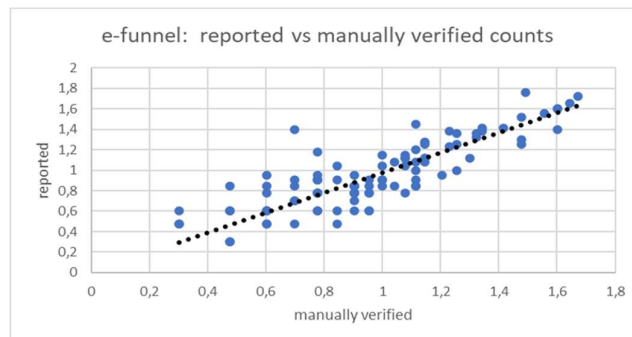


Figure 6-10. Insects per trap per visit ($\log(x + 1)$ transformation). Automatic counting vs. manual counting.

6.6.2 Comparison of e-traps vs Typical Funnel Traps

Besides the network of the e-traps there was a second network of typical traps (Figure 6-6). The funnels of both networks were counted manually at the same visit time (twice per week). The aim of this comparison was to identify any loss of attractiveness due to the optical counter. All 20 funnel traps used in the experiments of this work were identical as well as the pheromones for *T. absoluta*. Figure 6-7 and the calculation of the slope by regression analysis shows an advantage of captures of typical funnels (1334 counts) against the traps bearing and optical counter (1120 counts) which is almost 16% lower. The slope calculated in the regression analysis of Figure 6-11 is 0.91, which is worse than the 0.99 of Figure 6-8 indicating that the typical traps capture more insects compared to the automatic versions of them ($F=73.73$, $df=1,98$, $p<0.0001$).

However, although the records of the typical traps were higher than these of the e-trap, according to ANOVA between these two datasets shown no difference in a statistically significant way; the mean number of automatic reports of the e-funnel trap was 11.12 flies while for the typical trap was 13.34 ($F=1.40$, $df=1,198$, $p>0.05$, Figure 6-11 & Figure 6-12).

6.6.3 Histograms of Insect Captures vs Time

Figure 6-13 is an example of streamlining reported field data and deriving results, a process that would be impractical to be performed manually; our aim was to investigate the response of *T. absoluta* to pheromones by deriving the number of captures during the different hours of the day. The optical counter time-stamped each capture and we pooled together all detection events from all e-traps for the whole reporting period of 5 weeks. We derived that the response of *T. absoluta* to pheromones took place in the morning between 5.30-10 a.m. (Figure 6-13). Note that registered counts occurred after the insects were exhausted and fell inside the trap.

Concerning the time of flying, reported literature is sparse. Studies have shown that the adults of the tomato leaf miner are active during the night and do not move during daytime [139][143]. In the case of the tomato leaf miner, mating and fertilization take place when males are attracted towards females through their pheromone production. Information about pheromone trap deployment and the time of male activity, is valuable for decision making on integrated control strategies against this pest.

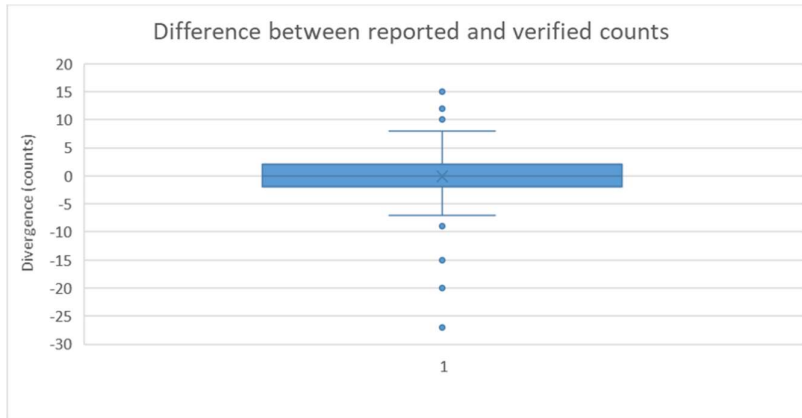


Figure 6-11. Divergence (counts) of manual counting vs automatic counting.

The box and whisker chart are centred at zero, meaning that most of the time there is no difference between reported and verified counts. More than 90% of the values are between $[-2, 2]$ from the true value. Greater differences are rare and most of them occurred during a heavy rain incident.

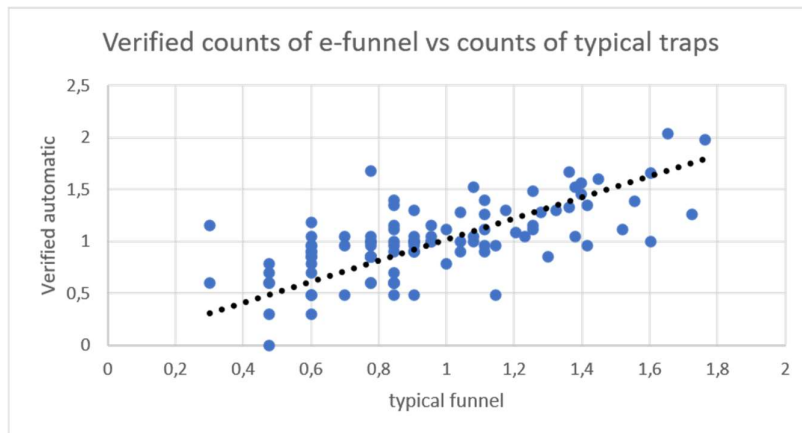


Figure 6-12. Insects per trap per visit ($\log(x + 1)$ transformation).

Automatic network (verified manually) vs typical funnels.

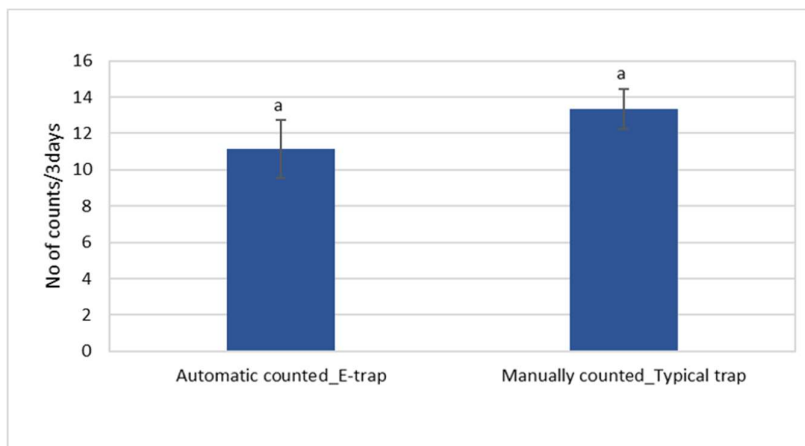


Figure 6-13. Mean number (\pm SE) of *T. absoluta* male adults every 3 days.

Over a period of 5-week counts (automatically reported counts of e-funnels for *T. absoluta* compared to manually counted of the typical funnel trap). Bars with the same letter are not significantly different at $P < 0.05$.

6.7 Discussion

Practical, reliable methods for evaluating targeted insect captures are needed to evaluate the efficacy of crop protection practices, make better decisions on treatment practices, and evaluate the effectiveness of applied treatments. The results presented in this chapter show that there is no statistically significant divergence between automatic and manual counting and this paves the way for the application of automated monitoring at large scales. This is the most important finding of this work as it shows that the errors of the automatic network would not change the decision of a zone manager on the type and timing of a treatment. We found that the automated network captures less insects than a network of identical funnels without optical counter. We attribute this fact to the elongation by 2cm of the tunnel that queues falling insects due to the size of the optical counter. This extra length increases the distance that the insect must cross from the pheromone dispenser to the bucket and some of them go back as they lose touch with the pheromone before being permanently captured or counted. However, this divergence in counts was not statistically significant.

During the test period, the automatic network sustained wind and rain without registering false measurements. However, the operation of automatic counting should be suspended during heavy rain as, in this case, there is the possibility of registering raindrops as valid insect counts (i.e. false alarms). Contrary to common belief, pests are not everywhere and the first step is to place traps where the problem is anticipated so that we reduce the possibility of false alarm. No measure was taken in order to prevent ants or other arthropoda to enter the e-funnels. We occasionally observed the capture of aphids, spiders and moths but at very small numbers compared to the targeted captures. The application of thresholds on the monitored optical intensity as measured in the receiver during the insect fall can reject very small or very big non-targeted insects. If the size of the target insect is comparable to the invasive one then a false alarm will occur, as the optical counter does not discern insect species. In practice, there is a low chance for this event because the attractiveness of the trap relies on the specificity of the pheromones.

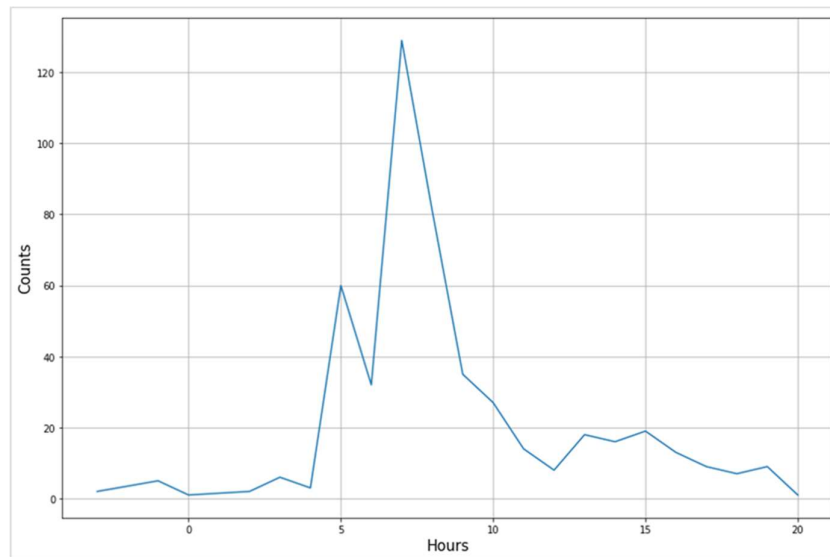


Figure 6-14. Male flight activity of *T. absoluta* during the day (All male captures from all e-funnels pooled together). Daily distribution of insect counts w.r.t hours of a day (local time).

Another advantage of automated insect surveillance is that long-term population and distribution data for insect species of interest can be logged. The logging of adequate historical data can help us to understand the population dynamics of the pest. Along with weather forecasts current data modelling techniques can apply predictive models to estimate statistically meaningful risks of an infestation and its evolution and anticipate future outbreaks. The efficacy of spraying application is significantly increased when it encounters insects during flight and the circadian rhythm as shown in Figure 6-13. In addition, the possibility to monitor the densities in almost real-time allows new directions in decision making.

An important conclusion from this automatically recorded population of *T. absoluta* is that the male flight is restricted to early morning. This has been recently reported only once in [158]; the male activity started with the first light of the day and continued for almost 1h thereafter. We show in this work how the same conclusion can be derived reliably and effortlessly. Additionally, such monitoring of population can show us the ‘hotspots’ within crop areas, where both biotic and abiotic parameters may favor moth population aggregations and probably crop infestation. Spraying application or other control practices can be focused on these plants instead of the whole crop.

We expect automatic monitoring to lead to a reduction of insecticide applications. Currently, manual counting of traps’ captures takes place once per week or once per two weeks due to cost and time restrictions of labour. Zone managers integrate diverse

information in order to reach a decision for initiating a treatment and, in fear of missing an onset or losing control of an evolving infestation, more often than not, overspray. E-traps surpass the labour constraint and, therefore, can be applied to large spatial scales, reporting once per day or even tracking pest dynamics by lowering the reporting schedule to once per hour. Although we have not yet quantified the reduction in spraying, we have confirmed through numerous discussions that producers and zone managers feel more comfortable and reassured when the infestation is monitored closely. Based on the fact that there is no significant statistical difference between automatically reported counts and manually verified ones (in other words, between e-funnel traps and typical ones), we suggest that e-funnels are reliable enough to shift decision making from weekly-based to daily-based. Lower captures in the e-funnel trap can be attributed to the change of microclimate modification of the typical trap. Pheromone-based e-funnel traps for monitoring of indicator species will also be useful in identifying biodiversity ‘hotspots’, and characterizing general changes in biodiversity in response to landscape, climatic, or other environmental changes.

7. CONCLUSIONS – FURTHER RESEARCH

7.1 Conclusions

In this thesis we gather all crucial points regarding the use of optoelectronic and vibration sensors for detecting insects' presence. Optical sensors are the suitable choice for use in electronic insect gates and automatized insect traps working in the field because they record intermittently, i.e. on per event basis, and only if their FOV is interrupted in contrast to the continuous recording of microphones [21]. Microphones receive continuous input from an uncontrolled and unknown number of sources in the field and are not generally suitable for field applications.

The proposed multispectral sensors do not require the bandwidth of a vision camera and do not face the difficulty of a photograph of a pile of insects that are not easily discernable in detail. Non-technical considerations (cost, feasibility for mass production, endurance of materials, etc.) is also in favor of optical solutions. Using the sensors presented in this work, walking insects (e.g. bees and wasps) are efficiently detected and their presence is registered in the power of low frequencies around the DC level. The power level of the received light is suitable to rank insects according to their size. Multispectral signatures look richer than the ones provided by simple one-band sensors but their advantage on classification improvement needs to be clarified and quantified with large-scale experiments.

Optical sensors are a better choice than cameras because they do not require the bandwidth of the latter, nor flashlight and process an insect-presence event at the entrance of the trap/gate the moment it occurs. Therefore, they avoid photographing a pile of insects that are not easily discernable after a while. Fresnel lenses provide an affordable way to collimate light from emitter to receiver and therefore it is possible to avoid effectively interferences from the sun or diffuse light sources.

The wingbeat event can be easily discerned from a walking event due to the harmonic structure of the power spectral density of the former. The signal to noise ratio of both types of optoelectronic sensors (i.e. extinction and backscattered light versions) is very high. Extinction light allows 5-18 harmonics to be resolved depending on the heading of the insect flying through the FOV whereas scattered light reaches 20-30 harmonics. The quality of scattered light is superior to the extinction light, but the final choice of the sensor deployed may depend on the configuration possibilities of the device holding the sensor.

Multispectral signatures look richer than the ones provided by simple one-band sensors but their advantage on classification improvement needs to be clarified and quantified with large scale experiments [22].

The hardware-based boards we constructed demonstrate high precision in analyzing insects' wingbeats. They are immune to external light interference and, therefore, capable of both in-lab and field experimentation. Moreover, we anticipate that once embedded in typical insect traps, the electronic traps will change the manual way insect monitoring is currently performed. The same technique in different configurations can be embedded in traps for different insects, such as mosquitoes (e.g., alerting for species that are possible carriers of the west Nile virus), bees and fruit flies. In the near future, we will report on devices for these separate cases.

We also presented a complete system that can optically detect, count and timestamp objects passing its FOV. It is capable of sensing objects <1 mm and can potentially have different applications such as counting of falling beans, small objects or oscillating parts, etc. We have applied it in the context of entomology to auto-trigger and record the wingbeat of flying or tethered insects under variable illumination conditions including artificial light. We believe it fills a gap on automatic recording units dedicated to insects' wingbeat. This choice of sensors permits effortless acquisition of a large number of wingbeat recordings of insects in flight and the automatic analysis of their spectral content. The practical applications that arise in the context of entomology include optical detectors that can alert for potentially dangerous mosquito species presence in sensitive domestic environments (hospitals, elderly nurseries), traps that report counts and species composition of trapped adults and feed wirelessly these data to epidemiological models that monitor the current situation but also predict future outbreaks based on past count and species distribution.

The e-gate sensor system presented hosts the optoelectronics signal acquisition set-up, which for being multispectral will be optimized to facilitate a reliable registration of the presence of bees and beehive pests, without the possibility of having false alarms due to ambient interferences. The design and set-up is optimized with respect to various technical aspects (data quality, signal-to-noise ratio, etc.)

Optical counters embedded in typical funnel traps are presented and form a network based on the LoRa radio protocol and collectively report insect counts of *T. absoluta* to a cloud server. Reliability of e-funnels are statistically significantly close to the true values (verified manually). We found no statistical difference between numbers reported by the automated network and manual counting. Daily monitoring of insect population dynamics

can improve decision making by reducing the uncertainty in decisions and thus overspraying. Automated insect monitoring will be widely applied as soon as the economic and ecological benefit of its service is quantified and its cost is lower than current manual practices.

We also presented a very efficient automatic recorder for sensing, registering and wirelessly emitting the acoustic emissions that the larvae produce during eating and feeding inside the trunk of a tree. The prototype system was deployed and tested on-site in a real-field setup as well as in the laboratory. It proved to be highly accurate in detecting borers and provided a quick check-up of a large number of mulberry and palm trees with no human intervention which makes it especially suitable for checking out tree trunks in quarantine areas. The device also helps to reduce the cost of treatment and after-treatment analysis of trees using systemic pesticides. After a successful treatment, one should observe a drop of larvae-originated impulsive sounds that must end to a stop in case of a successful treatment. Without an automated procedure, the cost of after treatment monitoring escalates abruptly as the observers need to visit in an iterative mode the same tree to reassess the situation. The novelty of this approach is that the decision can be based on a large time span (e.g., by observing the recordings over a week) and the decision is taken remotely without the need of manual visits. The reason for choosing *X. chinensis* and *R. ferrugineus* was the abundancy of these pests in the island of Crete but the same approach can be applied to different trees and borers around the world by adjusting the length of the waveguide to the targeted trunk e.g., the mountain bark beetle, various longhorn beetles, *Rhynchophorus palmarum* and the *Anoplophora chinensis*.

The proposed solution expands directly to a network of nodes that can cover the trees of a town and which communicate via the low power, LoRa/WAN to a central gateway situated within 1–2 km of the forest plot. This gateway will communicate via satellite or GPRS network to a central server that makes the data available to the end user via a web platform. The LoRa/WAN protocol is optimized for low power consumption and is different to the GPRS we currently use. The first requires that few parameters are transmitted and not complete recordings. The advantage of LoRa is that it can scale to thousands of tree-nodes and fits perfectly in the urban environment. In such case the number of peaks standing out of an energy threshold, the hits rate and the RMS level of the signal can become the communicated data. If one applies two waveguides on a tree then it can record the direction of arrival (DOA) of an audio source. A consistent DOA implies that an audio source is persisting inside the tree whereas random audio events due to tree movement

by exogenous audio sources would map to random DOAs. Three waveguides or more on a single tree would allow the localization (i.e., the x-y-z coordinates) of consistent and persisting audio sources based on mapping time delay of arrival (TDOA) to coordinates. In such a case, the manager could even see the tunnels that the larvae dig in the tree. However, to our point of view, more than one waveguide per tree is not currently practical for large-scale deployment.

Our approach fills a need in literature and practice for more spatial data regarding trees and their infestation status with wood-boring insects. The application of our approach will be facilitated when the 5G network is widely accepted and will acquire a completely new meaning when the coverage of internet reaches planet level.

Borers can be detected during their larva and adult stage when they move and feed. The algorithms can automatically integrate data from long time spans (daily, weekly, monthly) to infer the infestation state of a tree. The number of nodes applied will increase as the cost of electronics decreases and technology improves when 5G wireless communication is widely adopted. Automatic screening of vibrational data can be carried out at the server allowing the efficient and rapid processing of thousands of recordings allowing novel services to emerge as automatic creation of infestation maps and predictive modelling of invasion and spread. In the era of global trade and climate change, modern tools to monitor remotely trees for borers before they colonize and establish in new habitats can lead to novel services and modernize inspection agencies. This in turn can have a significant reduction on the economic damage caused by pests and spraying costs related to treatments and increase productivity with a lower impact on the environment and human health.

7.2 Further Research

Devices like the TreeVibe device and the e-funnel must be self-reliant devices that harvest their own energy so that they are permanently deployed at large numbers in possibly remote areas. When reaching global scales of application, the retrieval and recharging of devices from trees is no longer practical. As a future direction, we intent to employ the latest energy harvesting methods including transformers of vibrations to voltage, thermal, solar and wireless energy harvesting methods. The device will function only when the energy of the supercapacitor is deemed enough to process and transmit data otherwise its low-power electronic board will rest in hibernation mode. Commercially available

hardware such as Arduino and Raspberry pi, though generic, are inadequate to realize this goal, and it is only possible to create an entirely self-powered system by re-engineering the hardware, software of the system for this purpose. We will be taking advantage of advances in ultra-low-power wireless communications, ultra-wideband (UWB) circuit design, new energy aware peer-to-peer networking architectures, and organic semiconductor-based energy harvesting techniques to enable a realization using fully custom hardware and its associated software.

The vibration sensors do not receive signals only from the feeding and locomotion of borers but can also register other sources of vibrations e.g., rain, cars, close bird vocalizations etc. Therefore, a future direction would be the system to have embedded deep learning models in edge devices to cancel all other sources of interference and enhance the useful signal. Deep learning models are currently appearing as a possible solution for source separation and enhancing complex audio and vibrational recordings. Fortunately, the construction of a related, high-quality database that is needed to train the data-demanding, deep learning models is feasible by attaching the sensors to trees that the phytosanitary personnel has examined and classified as healthy versus infested. However, we see prospect in investigating towards the applicability of unsupervised, few-shot deep learning approaches and transformers as applied to signal unmixing and enhancement.

Although the cost is a design parameter rather than a research directive, in the case of automatic monitoring of biodiversity but also agricultural fields, it is a mandatory restriction that must be faced efficiently to ensure that these devices (i.e., an e-funnel and a vibrations detector attached to trees) will be widely adopted by regional stakeholders at large number so that the internet of trees can be created. We will invest time and funds to develop our custom amplifiers which will be attached to high quality piezoelectric ceramics. Note that the accelerometers must have a sensitivity of at least 1000 mV/g to pick up insects' vibrational signals from a radius of 2m and the most common and affordable MEMS are inadequate to meet this restriction.

Finally, we have the vision to establish a regional network of early alert service that is directly expandable to any wood borer. The release of a user-friendly DSS based on holistic population models to help farmers and National Plant Protection Organizations (NPPO) in monitoring and protecting urban greenery, forests, and crop systems; the setting up of Interactive Web Platforms collating surveillance data, updated in real time through smart tools of detection and citizens' records

8. REFERENCES

- [1] Allsopp, M.H., De Lange, W.J. and Veldtman, R., 2008. Valuing insect pollination services with cost of replacement. *PloS one*, 3(9), p.e3128
- [2] Putman, R.J., 1983. *Carrion and dung: the decomposition of animal wastes*. Edward Arnold., London, United Kingdom.
- [3] RAMOS-ELORDUY, J., 2009. Anthro-entomophagy: Cultures, evolution and sustainability. *Entomological Research*, 39(5), pp.271-288.
- [4] Sánchez-Bayo, F. and Wyckhuys, K.A., 2019. Worldwide decline of the entomofauna: A review of its drivers. *Biological conservation*, 232, pp.8-27.
- [5] <https://www.iucnredlist.org/resources/hochkirch2016> (accessed on 14th September 2022)
- [6] Aukema, J.E.; Leung, B.; Kovacs, K.; Chivers, C.; Britton, K.O.; Englin, J.; Frankel, S.J.; Haight, R.G.; Holmes, T.P.; Liebhold, A.M.; et al. Economic Impacts of Non-Native Forest Insects in the Continental United States. *PLoS ONE* **2011**, 6, e24587.
- [7] Pimentel, D.; Zuniga, R.; Morrison, D. Update on the environmental and economic costs associated with alien-invasive species in the United States. *Ecol. Econ.* 2005, 52, 273–288.
- [8] Nosrat C, Altamirano J, Anyamba A, Caldwell JM, Damoah R, Mutuku F, et al. (2021) Impact of recent climate extremes on mosquito-borne disease transmission in Kenya. *PLoS Negl Trop Dis* 15(3): e0009182. <https://doi.org/10.1371/journal.pntd.0009182>
- [9] <https://www.un.org/development/desa/en/news/population/world-population-prospects-2019.html>
- [10] Van Dijk, M., Morley, T., Rau, M.L. & Saghai, Y. (2021). A meta-analysis of projected global food demand and population at risk of hunger for the period 2010–2050. *Nature Food*, 2, 494-501. <https://doi.org/10.1038/s43016-021-00322-9>
- [11] Oerke, E.C., Dehne, H.W., Schonbeck, F., Weber, A., 1994. *Crop Production and Crop Protection: Estimated Losses in Major Food and Cash Crops*. Elsevier Science, Amsterdam, the Netherlands, p. 1994
- [12] Potamitis, P. Eliopoulos, I. Rigakis, Automated Remote Insect Surveillance at a Global Scale and the Internet of Things. *Robotics*, 2017, 6, 19.
- [13] M. Brydegaard , Towards Quantitative Optical Cross Sections in Entomological Laser Radar - Potential of Temporal and Spherical Parameterizations for Identifying Atmospheric Fauna. 2015 *PLoS ONE*. 10, 8, e0135231.

- [14] Potamitis, I. Rigakis. Large Aperture Optoelectronic Devices to Record and Timestamp Insects' Wingbeats, *IEEE Sensors Journal*, Volume: 16, Issue: 15, Aug.1, pp. 6053-6061, 2016.
- [15] Potamitis, I. Rigakis, Novel Noise-Robust Optoacoustic Sensors to Identify Insects Through Wingbeats, *IEEE Sensors Journal*, vol.15, no.8, pp.4621,4631, Aug. 2015.
- [16] Potamitis, I. Rigakis, K. Fysarakis (2015) Insect Biometrics: Optoacoustic Signal Processing and Its Applications to Remote Monitoring of McPhail Type Traps. *PLoS ONE* 10(11): e0140474. doi:10.1371/journal.pone.0140474.
- [17] Potamitis, I. Rigakis, N. Vidakis, M. Petousis, and M. Weber, "Affordable Bimodal Optical Sensors to Spread the Use of Automated Insect Monitoring," *Journal of Sensors*, vol. 2018, Article ID 3949415.
- [18] C. Ellington, (1999). The novel aerodynamics of insect flight: applications to micro-air vehicles. *J. of Experimental Biology*, Dec; 202(Pt 23):3439-48.
- [19] A.Gebru, S. Jansson, R. Ignell, C. Kirkeby, J. Prangma, and M. Brydegaard, Multiband modulation spectroscopy for the determination of sex and species of mosquitoes in flight, 2018, 16, *Journal of Biophotonics*.
- [20] M. Brydegaard, A. Gebru, S. Svanberg (2014) Super resolution laser radar with blinking atmospheric particles—application to interacting flying insects *Progress in Electromagnetics Research* 147: 141–151.
- [21] I. Potamitis, I. Rigakis, N-A. Tatlas, Automated Surveillance of Fruit Flies. *Sensors* 2017, 17, 110.
- [22] I Potamitis, Classifying insects on the fly, *Ecological Informatics*, Volume 21, May 2014, Pages 40-49, ISSN 1574-9541.
- [23] White, I. M., and M. M. Elson-Harris (1992). *Fruit flies of economic importance: their identification and bionomics*. CAB International, Wallingford, United Kingdom.
- [24] Kent, D. Marshall J., (2010). Olive Fruit Fly: Managing an Ancient Pest in Modern Times, *Annual Review of Entomology*, Vol. 55: 151-169.
- [25] Neuenschwander P., Michelakis S., (1981). Olive fruit drop caused by *Dacus oleae* (Gmel.) (Dipt. Tephritidae), *Journal of Applied Entomology*, vol. 91, 1-5, pp. 193-205.
- [26] Szyniszewska AM, Tatem AJ (2014) Global Assessment of Seasonal Potential Distribution of Mediterranean Fruit Fly, *Ceratitis capitata* (Diptera: Tephritidae). *PLoS ONE* 9(11): e111582. doi:10.1371/journal.pone.0111582
- [27] *Plant Health Australia* (2011). *The Australian Handbook for the Identification of Fruit Flies*. Version, 1.0. Plant Health Australia. Canberra, ACT.

- [28] Drosopoulos S. and Claridge M., (2005). *Insect Sounds and Communication: Physiology, Behaviour, Ecology and Evolution*, eds. CRC Press, Boca Raton, FL, 532 pp., ISBN 0-8493-2060-7
- [29] Ganchev T., Potamitis I., (2007). Automatic acoustic identification of singing insects, *Bioacoustics*, Vol. 16, 3.
- [30] Chadwick L., (1939). A simple stroboscopic method for the study of insect flight. *Psyche* 46, 1-8 (<http://www.hindawi.com/journals/psyche/1939/024683/abs/>).
- [31] Reed S, Williams C, Chadwick L., (1942). Frequency of Wing-Beat as a Character for Separating Species Races and Geographic Varieties of *Drosophila*. *Genetics*; 27(3):349-361.
- [32] Sotovalta O., (1952) Flight-tone wing-stroke frequency of insects and the dynamics of insect flight. *Nature*, no. 4338, p. 1057-1058
- [33] Richards I. (1955). Photoelectric cell observations of insects in flight. *Nature* 175:128-129.
- [34] Sawedal L and Hall R (1979). Flight tone as a taxonomic character in Chironomidae (Diptera), *Entomological Scand. Suppl.* 10: 139-143.
- [35] Unwin D., Ellington C., (1979). An optical tachometer for measurement of the wing-beat frequency of free-flying insects, *Journal of experimental biology*, 82, pp. 377-378.
- [36] Moore A., Miller J. R., Bruce E. Tabashnik, Stuart H. Gage (1986). Automated Identification of Flying Insects by Analysis of Wing-beat Frequencies, *Journal of Economic Entomology*, pp. 1703-1706.
- [37] Gotz K. (1987). Course-control, metabolism and wing interference during ultralong tethered flight in *Drosophila Melanogaster*, *Journal of experimental Biology* 128, 35-46.
- [38] Hedwig B. (2000), A highly sensitive opto-electronic system for the measurement of movements, *Journal of Neuroscience Methods*, Volume 100, Issues 1–2, 31, pp. 165-171, ISSN 0165-0270, [http://dx.doi.org/10.1016/S0165-0270\(00\)00255-7](http://dx.doi.org/10.1016/S0165-0270(00)00255-7)
- [39] Engel J. E., Wytenbach R. A. (2001). An optoelectronic sensor for monitoring small movements in insects. *Florida Entomologist*. September; 843: 336-343.
- [40] Moore A., Miller R. H., (2002). Automated identification of optically sensed aphid (Homoptera: Aphidae) wingbeat waveforms. *Annals of the Entomological Society of America* 95(1): 1-8.
- [41] Zhenyu L., Zuji Z., Zuorui S., Qing Y., (2005). Automated Identification of Mosquito (Diptera: Culicidae) Wingbeat Waveform by Artificial Neural Network, Springer US, pp. 483-489.
- [42] Kevin S. Repasky, Joseph A. Shaw, Ryan Scheppele, Christopher Melton, (2005), Optical detection of honeybees by use of wing-beat modulation of scattered laser

- light for locating explosives and land mines, John L. Carsten, and Lee H. Spangler, *Appl. Opt.*, 45: 1839–1843
- [43] Kirsch P, Czokajlo D, McLaughlin J, Moore A, Haynes K, Fadamiro HY. (2006). Automated remote identification and monitoring of moths in flight. 80th Annual Western Orchard Pest and Disease Management Conference
- [44] Joe-Air Jiang, Chwan-Lu Tseng, Fu-Ming Lu, En-Cheng Yang, Zong-Siou Wu, Chia-Pang Chen, Shih-Hsiang Lin, Kuang-Chang Lin, Chih-Sheng Liao, (2008). A GSM-based remote wireless automatic monitoring system for field information: A case study for ecological monitoring of the oriental fruit fly, *Bactrocera dorsalis* (Hendel), *Computers and Electronics in Agriculture*, Volume 62, Issue 2, pp. 243-259, ISSN 0168-1699, <http://dx.doi.org/10.1016/j.compag.2008.01.005>.
- [45] Chen Y., Why A., Batista G., Mafra-Neto A., Keogh E. (2014) Flying Insect Classification with Inexpensive Sensors. *Journal of Insect Behavior*, September 2014, vol. 27, Issue 5, pp 657-677.
- [46] Potamitis I. and Schäfer P., (2014). On classifying insects from their wing-beat: New results,” *Ecology and acoustics: emergent properties from community to landscape*, Paris, France.
- [47] Potamitis, I.; Rigakis, I.; Fysarakis, K. (2014). The Electronic McPhail Trap. *Sensors*, 14, 22285-22299.
- [48] Webb J., Sharp J., Chambers D., Benner J., (1976). Acoustical properties of the flight activities of the Caribbean fruit fly’, *Journal of Experimental Biology*, 64, pp. 761-772.
- [49] Offenhauser W., Kahn M., (1949). The sounds of Disease-Carrying Mosquitoes, *The Journal of the Acoustical society of America*, vol. 21, no. 3, pp. 259-263.
- [50] L. Rabiner and B-H Juang, (1993). *Fundamentals of Speech Recognition*, Section 4.5, Prentice-Hall 1993, ISBN 0-13-015157-2
- [51] Riede, K. (1997). Bioacoustic monitoring of insect communities in a Bornean rainforest canopy. *Canopy Arthropods* (1997): 442-452.
- [52] Riede, K., (1998). Acoustic monitoring of Orthoptera and its potential for conservation. *Journal of Insect Conservation* 2: 217-223.
- [53] David N. Byrne (1988). Relationship between wing loading, wingbeat frequency and body mass in Homopterous insects. *Journal of experimental Biology*. 135, 9-23. The Company of Biologists Limited 1988.
- [54] Roy J, Baerdemaeker J., Saeys W., Ketelaere B, (2014). Optical identification of bumblebee species: Effect of morphology on wingbeat frequency, *Computers and Electronics in Agriculture*, Volume 109, pp. 94-100.
- [55] Porter JH, Nagy E, Kratz TK, Hanson P. (2009). New eyes on the world: advanced sensors for ecology. *BioScience* 59:385-397

- [56] Wilson, Anthony J., and Philip S. Mellor. "Bluetongue in Europe: Past, Present and Future." *Philosophical Trans. of the Royal Society B: Biol. Sciences* 364.1530 (2009): 2669–2681. PMC. Web. 30 Jan. 2016.
- [57] Sotavalta, O. (1953). Recordings of high wing-stroke and thoracic vibration frequency in some midges. *Biol. Bull. Woods H.* 104: 439-444.
- [58] Wong P-SJ, Li M-zI, Chong C-S, Ng L-C, Tan C-H (2013) *Aedes (Stegomyia) albopictus* (Skuse): A Potential Vector of Zika Virus in Singapore. *PLoS Negl Trop Dis* 7(8): e2348. doi:10.1371/journal.pntd.0002348
- [59] A pan-European epidemiological study on honeybee colony losses 2012-2013. European Union Reference Laboratory for honeybee health (EURL), 27st August 2014.
- [60] United States Department of Agriculture- Agricultural Research Service. Colony Collapse Disorder: An Incomplete Puzzle. *Agricultural Research magazine*, July 2012
- [61] European Commission. Communication from the commission to the european parliament and the council on Honeybee Health. Brussels, 06/12/2010.
- [62] VanEngelsdorp D. & Meixner M., 2010. A historical review of managed honeybee populations in Europe and the United States and the factors that may affect them. *Journal of Invertebrate Pathology.* 103: 80–95
- [63] Klein A.M., Vaissiere B.E., Cane J.H., Steffan-Dewenter I., Cunningham S.A., Kremen C. & Tscharntke T., 2007. Importance of pollinators in changing landscapes for world crops. *Proc. R. Society. B.* 274: 303-313.
- [64] Moritz R. F. A., de Miranda J., Fries I., Le Conte Y., Neumann P. & Paxton R. J., 2010. Research Strategies to Improve Honey bee Health in Europe. *Apidologie.* 41: 227-242. 9
- [65] Gallai N., Salles J., Settele J. & Vaissiere B., 2009. Economic valuation of the vulnerability of world agriculture confronted with pollination decline. *Ecological Economics* 68: 810-821.
- [66] Potts S. G., Biesmeijer J. C., Kremen C., Neumann P., Schweiger O. & Kunin W. E., 2010. Global Pollinator Declines: Trends, Impacts and Drivers. *Trends in Ecology and Evolution.* 30: 1-9. 11
- [67] De la Ruá P., Jaffé R., Dall Olio, Munoz I. & Serrano J., 2009. Biodiversity, conservation and current threats to European Honey bees, *Apidologie* 40: 263–284
- [68] W. G. Meikle, N. Holst. Application of continuous monitoring of honeybee colonies. *Apidologie*, Springer Verlag, 2015, 46 (1), pp.10-22.
- [69] Faberge, A.C. (1943) Apparatus for recording the number of bees leaving and entering a hive. *J. Sci. Instr.* 20, 28–311

- [70] Spangler, H.G. (1969) Photoelectrical counting of outgoing and incoming honeybees. *J. Econ. Entomol.* 62, 1183–1184
- [71] Erickson, E.H., Miller, H.H., Sikkema, D.J. (1975) A method of separating and monitoring honey-bee flight activity at the hive entrance. *J. Apic. Res.* 14, 119–125
- [72] Liu, C., Leonard, J., Feddes, J.J. (1990) Automated monitoring of flight activity at a beehive entrance using infrared light sensors. *J. Apic. Res.* 29(1), 20–27
- [73] Gebru, A.; Jansson, S.; Ignell, R.; Kirkeby, C.; Brydegaard, M. Multispectral polarimetric modulation spectroscopy for species and sex determination of malaria disease vectors. In *Proceedings of the 2017 Conference on Lasers and Electro-Optics (CLEO), San Jose, CA, USA, 14–19 May 2017*; pp. 1–2.
- [74] Rigakis, I.; Potamitis, I.; Tatlas, N.-A.; Livadaras, I.; Ntalampiras, S. A Multispectral Backscattered Light Recorder of Insects' Wingbeats. *Electronics* 2019, 8, 277.
- [75] Meitalovs, Jurijs & Histjajevs, A & Stalidzans, Egils. (2009). Automatic Microclimate Controlled Beehive Observation System. 8th International Scientific Conference 'Engineering for Rural Development'. 265-271.
- [76] Joseph A. Shaw, Paul W. Nugent, Jennifer Johnson, Jerry J. Bromenshenk, Colin B. Henderson, and Scott Debnam, "Long-wave infrared imaging for non-invasive beehive population assessment," *Opt. Express* 19, 399-408 (2011)
- [77] Smart, M.; Otto, C.; Cornman, R.; Iwanowicz, D. Using Colony Monitoring Devices to Evaluate the Impacts of Land Use and Nutritional Value of Forage on Honey Bee Health. *Agriculture* 2018, 8, 2.
- [78] Atauri Mezquida, D., Llorente Martínez, J. (2009) Platform for bee-hives monitoring based on sound analysis. A perpetual warehouse for swarm's daily activity. *Span. J. Agric Res* 7(4), 824–828
- [79] Bencsik, M., Bencsik, J., Baxter, M., Lucian, A., Romieu, J., Millet, M. (2011) Identification of the honey bee swarming process by analysing the time course of hive vibrations. *Comput. Electron. Agric.* 76, 44–50.
- [80] Ferrari, S., Silva, M., Guarino, M., Berckmans, D. (2008) Monitoring of swarming sounds in bee hives for early detection of the swarming period. *Comput. Electron. Agric.* 64, 72–77
- [81] Santos, D.A.; Rodrigues, J.J.; Furtado, V.; Saleem, K.; Korotaev, V. Automated electronic approaches for detecting disease vectors mosquitoes through the wing-beat frequency. *J. Clean. Prod.* 2009, 217, 767–775.
- [82] Ouyang, T.H.; Yang, E.C.; Jiang, J.A.; Lin, T.T. Mosquito vector monitoring system based on optical wingbeat classification. *Comput. Electron. Agric.* 2015, 118, 47–55.
- [83] Goldshtein, E.; Cohen, Y.; Hetzroni, A.; Gazit, Y.; Timar, D.; Rosenfeld, L.; Grinshpon, Y.; Hoffman, A.; Mizrach, A. Development of an automatic monitoring

- trap for the Mediterranean fruit fly (*Ceratitidis capitata*) to optimize control applications frequency. *Comput. Electron. Agric.* 2017, 139, 115–125. [to optimize control applications frequency. *Comput. Electron. Agric.* 2017, 139, 115–125.
- [84] Mukundarajan, H.; Hol, F.J.H.; Castillo, E.A.; Newby, C.; Prakash, M. Using mobile phones as acoustic sensors for high-throughput mosquito surveillance. *Elife* 2017, 6, e27854.
- [85] Raman, D.R.; Gerhardt, R.R.; Wilkerson, J.B. Detecting Insect Flight Sounds in the Field: Implications for Acoustical Counting of Mosquitoes. *Agric. Biosyst. Eng. Pub.* 2007, 57, 1481–1485.
- [86] Santos, D.A.A.; Teixeira, L.E.; Alberti, A.M.; Furtado, V.; Rodrigues, J.J.P.C. Sensitivity and Noise Evaluation of an Optoelectronic Sensor for Mosquitoes Monitoring. In *Proceedings of the 2018 3rd International Conference on Smart and Sustainable Technologies (SpliTech)*, Split, Croatia, 26–29 June 2018; pp. 1–5.
- [87] Genoud, A.P.; Basistyy, R.; Williams, G.M.; Thomas, B.P. Optical remote sensing for monitoring flying mosquitoes, gender identification and discussion on species identification. *Appl. Phys. B* 2018, 124, 46.
- [88] Gebru, A.K.; Rohwer, E.G.; Neethling, P.; Brydegaard, M.S. Investigation of atmospheric insect wing-beat frequencies and iridescence features using a multispectral kHz remote detection system. *J. Appl. Remote Sens.* 2014, 8.
- [89] Chen, C.-P.; Chuang, C.-L.; Jiang, J.-A. Ecological Monitoring Using Wireless Sensor Networks—Overview, Challenges, and Opportunities. In *Smart Sensors, Measurement and Instrumentation; Book Section in Advancement in Sensing Technology*; Mukhopadhyay, S.C., Jayasundera, K.P., Eds.; Springer: Berlin/Heidelberg, Germany, 2013; pp. 1–21.
- [90] Prince, P.; Hill, A.; Piña Covarrubias, E.; Doncaster, P.; Snaddon, J.L.; Rogers, A. Deploying Acoustic Detection Algorithms on Low-Cost, Open-Source Acoustic Sensors for Environmental Monitoring. *Sensors* 2019, 19, 553.
- [91] Fennell, J.; Veys, C.; Dingle, J.; Nwezeobi, J.; van Brunschot, S.; Colvin, J.; Grieve, B. A method for real-time classification of insect vectors of mosaic and brown streak disease in cassava plants for future implementation within a low-cost, handheld, in-field multispectral imaging sensor. *Plant Methods* 2018, 14, 82.
- [92] Ma, T.; Kobori, H.; Katayama, N.; Tsuchikawa, S. Non-Destructive Inspection of Insects in Chocolate Using near Infrared Multispectral Imaging. *J. Near Infrared Spectrosc.* 2016, 24, 391–397.
- [93] Vasas, V.; Hanley, D.; Kevan, P.G.; Chittka, L. Multispectral images of flowers reveal the adaptive significance of using long-wavelength-sensitive receptors for edge detection in bees. *J. Compar. Physiol.* 2017, 203, 301–311.
- [94] Fernandes, J.N.; Dos Santos, L.M.; Chouin-Carneiro, T.; Pavan, M.G.; Garcia, G.A.; David, M.R.; Beier, J.C.; Dowell, F.E.; Maciel-de-Freitas, R.; Sikulu-Lord,

- M.T. Rapid, noninvasive detection of Zika virus in *Aedes aegypti* mosquitoes by near-infrared spectroscopy. *Sci. Adv.* 2018, 4, eaat0496.
- [95] Dadabayev, R.; Shabairou, N.; Zalevsky, Z.; Malka, D. A visible light RGB wavelength demultiplexer based on silicon-nitride multicore PCF. *Opt. Laser Technol.* 2019, 111, 411–416.
- [96] Shabairou, N.; Cohen, E.; Wagner, O.; Malka, D.; Zalevsky, Z. Color image identification and reconstruction using artificial neural networks on multimode fiber images: Towards an all-optical design. *Opt. Lett.* 2018, 43, 5603–5606.
- [97] Poland, T.M.; Rassati, D. Improved biosecurity surveillance of non-native forest insects: A review of current methods. *J. Pest Sci.* 2019, 92, 37–49.
- [98] Chen, G.; Meentemeyer, R.K. Remote Sensing of Forest Damage by Diseases and Insects. In *Remote Sensing for Sustainability*; CRC Press: Boca Raton, FL, USA, 2016.
- [99] Drew, D.M.; Downes, G.M. The use of precision dendrometers in research on daily stem size and wood property variation: A review. *Dendrochronologia* 2009, 27, 159–172.
- [100] van Emmerik, T.; Steele-Dunne, S.; Hut, R.; Gentine, P.; Guerin, M.; Oliveira, R.S.; Wagner, J.; Selker, J.; van de Giesen, N. Measuring Tree Properties and Responses Using Low-Cost Accelerometers. *Sensors* 2017, 17, 1098.
- [101] Gilbert, G.S.; Ballesteros, J.O.; Barrios-Rodriguez, C.A.; Bonadies, E.F.; Cedeño-Sánchez, M.L.; Fossatti-Caballero, N.J.; Trejos-Rodríguez, M.M.; Pérez-Suñiga, J.M.; Holub-Young, K.S.; Henn, L.A.; et al. Use of sonic tomography to detect and quantify wood decay in living trees. *Appl. Plant Sci.* 2016, 4, 1600060.
- [102] Goh, C.L.; Rahim, R.A.; Rahiman, M.H.; Talib, M.T.; Tee, Z.C. Sensing Wood Decay in Standing Trees: A Review. *Sens. Actuators A Phys.* 2017, 269, 276–282.
- [103] Johnstone, D.; Moore, G.; Tausz, M.; Nicolas, M. The measurement of wood decay in landscape trees. *Arboric. Urban For.* 2010, 36, 121–127.
- [104] Mankin, R.W.; Hagstrum, D.W.; Smith, M.T.; Roda, A.L.; Kairo, M.T. Perspective and Promise: A Century of Insect Acoustic Detection and Monitoring. *Am. Entomol.* 2011, 57, 30–44.
- [105] Perles, A.; Mercado, R.; Capella, J.V.; Serrano, J.J. Ultra-Low Power Optical Sensor for Xylophagous Insect Detection in Wood. *Sensors* 2016, 16, 1977.
- [106] Sarto i Monteys, V.; Torras i Tutusaus, G. A New Alien Invasive Longhorn Beetle, *Xylotrechus chinensis* (Cerambycidae), Is Infesting Mulberries in Catalonia (Spain). *Insects* 2018, 9, 52.
- [107] Kontodimas, D.C.; Milonas, P.G.; Vassiliou, V.; Thymakis, N.; Economou, D. The occurrence of *Rhynchophorus ferrugineus* in Greece and Cyprus and the risk against the native Greek palm tree *Phoenix theophrasti*. *Entomol. Hell.* 2006, 16, 11–15.

- [108] Leivadara, E.; Leivadaras, I.; Vontas, I.; Trichas, A.; Simoglou, K.; Roditakis, E.; Avtzis, D.N. First record of *Xylotrechus chinensis* (Coleoptera, Cerambycidae) in Greece and in the EPPO region. *Bull. OEPP/EPPO Bull.* 2018, 48, 277–280.
- [109] Mankin, R.W.; Mizrach, A.; Hetzroni, A.; Levsky, S.; Nakache, Y.; Soroker, V. Temporal and spectral features of Sounds of wood-boring Beetle Larvae: Identifiable patterns of Activity enable improved discrimination from background noise. *Fla. Entomol.* 2008, 91, 241–248.
- [110] Fujii, Y.; Noguchi, M. Using acoustic emission monitoring to detect termite activity in wood. *For. Prod. J.* 1990, 40, 34–36.
- [111] Le Conte, S.; Vaiedelich, S.; Thomas, J.H.; de Reyer, D.; Maurin, E. Acoustic emission to detect xylophagous insects in wooden musical instrument. *J. Cult. Herit.* 2015, 16, 338–343.
- [112] Potamitis, I.; Ganchev, T.; Kontodimas, D. On Automatic Bioacoustic Detection of Pests: The Cases of *Rhynchophorus ferrugineus* and *Sitophilus oryzae*. *J. Econ. Entomol.* 2009, 102, 1681–1690.
- [113] Detection of Movement of Termites in Wood by Acoustic Emission Techniques. U.S. Patent US 6883375. Available online: <https://patents.google.com/patent/US6883375> (accessed on 15 March 2019).
- [114] Eliopoulos, P.; Tatlas, N.-A.; Rigakis, I.; Potamitis, I. A “Smart” Trap Device for Detection of Crawling Insects and Other Arthropods in Urban Environments. *Electronics* 2018, 7, 161.
- [115] Moraes, F.S.; Nava, D.E.; Rosa, V.S.D. Optoacoustic intelligent sensor for real-time detection of fruit flies in McPhail traps. In Proceedings of the 2018 3rd International Symposium on Instrumentation Systems, Circuits and Transducers (INSCIT), Bento Goncalves, Brazil, 27–31 August 2018; pp. 1–6
- [116] Gedeon, C.I.; Flórián, N.; Liszli, P.; Hambek-Oláh, B.; Bánszegi, O.; Schellenberger, J.; Dombos, M. An Opto-Electronic Sensor for Detecting Soil Microarthropods and Estimating Their Size in Field Conditions. *Sensors* 2017, 17, 1757.
- [117] Sutin, A.; Flynn, T.; Salloum, H.; Sedunov, N.; Sinelnikov, Y.; Hull-Sanders, H. Vibro-acoustic methods of insect detection in agricultural shipments and wood packing materials. In Proceedings of the 2017 IEEE International Symposium on Technologies for Homeland Security (HST), Waltham, MA, USA, 25–26 April 2017; pp. 1–6.
- [118] Cocquempot, C.; Lindelöw, Å. Alien Terrestrial Arthropods of Europe. *BioRisk* 2010, 4, 193–218. doi: 10.3897/biorisk.4.56
- [119] Lanfranco, D.; Dungey, H. Insect damage in Eucalyptus: A review of plantations in Chile. *Austral Ecol.* 2001, 26, 477–481.

- [120] Ashry, I., Mao, Y., Al-Fehaid, Y., Al-Shawaf, A., Al-Bagshi, M., Al-Brahim, S., Ng, T.K. & Ooi, B.S. Early detection of red palm weevil using distributed optical sensor. *Scientific Reports* 10, 3155 (2020).
- [121] Zorović, M., Čokl, A. Laser vibrometry as a diagnostic tool for detecting wood-boring beetle larvae. *J Pest Sci* 88, 107–112 (2015). <https://doi.org/10.1007/s10340-014-0567-5>
- [122] Francis Juanes, Visual and acoustic sensors for early detection of biological invasions: Current uses and future potential, *Journal for Nature Conservation*, Volume 42, Pages 7-11, 2018.
- [123] Liu H, Lee SH, Chahle JS. A review of recent sensing technologies to detect invertebrates on crops. *Precision. Agriculture*. 2017; 18:635-666.
- [124] K Sindhura Bhairavi, Badal Bhattacharyya, Nang Sena Manpoong, Partha Pratim Gyanudoy Das, Elangbam Bidyarani Devi and Sudhansu Bhagawati, Recent advances in exploration of acoustic pest management: A review, *Journal of Entomology and Zoology Studies* 2020; 8(3): 2056-206.
- [125] Koubaa, A.; Aldawood, A.; Saeed, B.; Hadid, A.; Ahmed, M.; Saad, A.; Alkhoulja, H.; Ammar, A.; Alkanhal, M. Smart Palm: An IoT Framework for Red Palm Weevil Early Detection. *Agronomy* 2020, 10, 987.
- [126] Alexander Sutin, Alexander Yakubovskiy, Hady R. Salloum, Timothy J. Flynn, Nikolay Sedunov, and Hannah Nadel, Towards an Automated Acoustic Detection Algorithm for Wood-Boring Beetle Larvae (Coleoptera: Cerambycidae and Buprestidae), *Journal of Economic Entomology*, 112(3), 2019, 1327–1336
- [127] Mankin RW, Osbrink WL, Oi FM, Anderson JB. Acoustic detection of termite infestations in urban trees. *Journal of Economic Entomology*. 2002; 95(5):981-988.
- [128] Mankin RW, Weaver DK, Grieshop M, Larson B, Morrill W. Acoustic system for insect detection in plant stems: comparisons of *Cephus cinctus* in wheat and *Metamasius callizona* in bromeliads. *Journal of Agricultural and Urban Entomology*. 2004; 21(4):239-248.
- [129] Mankin RW, Samson PR, Chandler KJ. Acoustic detection of Melolonthine larvae in Australian sugarcane. *Journal of Economic Entomology*. 2009; 102(4):1523-1535.
- [130] Mankin RW, Moore A. Acoustic detection of *Oryctes rhinoceros* (Coleoptera: Scarabaeidae: Dynastinae) and *Nasutitermes luzonicus* (Isoptera: Termitidae) in palm trees in urban Guam. *Journal of Economic Entomology*. 2010; 103:1135-1143
- [131] Potamitis, I.; Rigakis, I.; Tatlas, N.-A.; Potirakis, S. In-Vivo Vibroacoustic Surveillance of Trees in the Context of the IoT. *Sensors*, 2019, 19, 1366.
- [132] Pinhas J, Soroker V, Hetzroni A, Mizrach A, Teicher M, Goldberger J. Automatic acoustic detection of the red palm weevil. *Computer and Electronics in Agriculture*. 63(2):131-139, 2008.

- [133] Siriwardena KAP, Fernando LCP, Nanayakkara N, Perera KFG, Kumara ADNT, Nanayakkara T. Portable acoustic device for detection of coconut palms infested by *Rynchophorus ferrugineus* (Coleoptera: Curculionidae). *Crop Protection*. 2010; 29(1):25-29.
- [134] Lampson BD, Han YJ, Khalilian A, Greene J, Mankin RW, Foreman EG. Automatic detection and identification of brown stink bug, *Euschistus servus* and southern green stink bug, *Nezara viridula*, using intraspecific substrateborne vibrational signals. *Computer and Electron., in Agriculture*. 2013; 91:154-159.
- [135] Mankin RW, Al-Ayedh HY, Aldryhim Y, Rohde B. Acoustic Detection of *Rynchophorus ferrugineus* (Coleoptera: Dryophthoridae) and *Oryctes elegans* (Coleoptera: Scarabaeidae) in *Phoenix dactylifera* (Arecales: Arecaceae) Trees and Offshoots in Saudi Arabian Orchards. *Journal of Economic Entomology*. 2016; 109(2):622-628
- [136] LeCun, Y., Bengio, Y. & Hinton, G. Deep learning. *Nature*, 521,436–444 (2015).
- [137] Olga Russakovsky, Jia Deng, Hao Su, Jonathan Krause, Sanjeev Satheesh, Sean Ma, Zhiheng Huang, Andrej Karpathy, Aditya Khosla, Michael Bernstein, Alexander C. Berg and Li Fei-Fei. ImageNet Large Scale Visual Recognition Challenge. *Intern. Journal of Computer Vision*, 2015
- [138] François Chollet, *Deep Learning with Python*, Second Edition, 2021, Manning Publications.
- [139] Abdul-Rassoul M. S. 2014. A new host record for tomato leaf miner *Tuta absoluta* (Meyrick, 1917) in Baghdad province, Iraq. *Bulletin of the Iraq Natural History Museum*, 2014, 13(1): 15-18.
- [140] Bahadur Khrisna, Dias G.M., Veeramani A., Swanton C.J., Fraser D., and D. Steinke D, et al. 2018. When too much isn't enough: Does current food production meet global nutritional needs? *PLoS ONE* 13(10): e0205683. <https://doi.org/10.1371/journal.pone.0205683>.
- [141] Bale J.S., Masters G.J., Hodkinson I.D., Awmack C., Bezemer T.M., Brown V.K., Butterfield J., Buse A., Coulson J.C., Farrar J., Good J.E.G., Harrington R., Hartley S., Jones T.H., Lindroth R.L., Press M.C., Symrnioudis I., Watt A.D., and J.B. Whittaker. 2002. Herbivory in global climate change research: Direct effects of rising temperature on insect herbivores. *Glob Change Biol*. 8:1–16
- [142] Cooke, B.M. 2006. Disease assessment and yield loss. In: Cooke BM, Jones DG, Kaye B, editors. *The Epidemiology of Plant Diseases*: Springer Netherlands. p. 43–80
- [143] Daniel T. I., and B. S. Bajarang, 2017. Control and management of *Tuta absoluta* (Meyrick) (Lepidoptera: Gelechiidae). *A review. J. Appl. Chem.* 10: 14-22.
- [144] Ding, W., and G Taylor. 2016. G. Automatic moth detection from trap images for pest management. *Comput. Electron. Agric.* 123: 17–28.

- [145] Dombos, M., Kosztolányi, A., Szlávecz, K., Gedeon, C., Flórián, N., Groó, Z., Dudás, P., and O. Bánszegi. 2017. EDAPHOLOG monitoring system: Automatic, real-time detection of soil microarthropods. *Methods Ecol. Evol.* 8 (3): 313–321.
- [146] Flórián, N., Gránicz, L., Gergócs, V., Tóth, F., and M. Dombos. 2020. M. Detecting Soil Microarthropods with a Camera-Supported Trap. *Insects.* 11:244.
- [147] Foley, J.A., DeFries, R., Asner, G.P., Barford, C., Bonan, G., Carpenter, S.R., Chapin, F.S., Coe M.T., Daily, G.C., Gibbs, H.K., Helkowski, J.H., Holloway, T., Howard, E.A., Kucharik, C.J., Monfreda, C., Patz, J.A., Prentice, I.C., Ramankutty, N., Snyder, P.K. 2005. Global consequences of land use. *Science* 309:570–574
- [148] Gutierrez, A., Ansuategi, A., Susperregi, L., Tubío, C., Rankić, I., and L. Lenža. 2019. Benchmarking of Learning Strategies for Pest Detection and Identification on Tomato Plants for Autonomous Scouting Robots Using Internal Databases. *J. Sens.* 1–15. doi.org/10.1155/2019/5219471
- [149] Hendricks, D.E. 1985. Portable electronic detector system used with inverted-cone sex pheromone traps to determine periodicity and moth captures. *Environ. Entomol.* 14: 199–204.
- [150] Hendricks, D.E. 1989. Development of an electronic system for detecting *Heliothis* spp. moths (Lepidoptera: Noctuidae) and transferring incident information from the field to a computer. *J. Econ. Entomol.* 82: 675–684.
- [151] Hufnagel, L., and M. Kocsis. 2011. Impacts of climate change on Lepidoptera species and communities. *Appl. Ecol. Env. Res.* 9(1): 43-72.
- [152] Karsholt, O., and J. Razowski. 1996. The Lepidoptera of Europe. – A distributional checklist. Apollo Books, Stenstrup.
- [153] Khoo, T., Muralindran M., Rosalyn R. P., and W. W. Kitt. 2020. Capacitive Mosquito Wing-beat Sensor: A Novel Sensor for Intelligent Traps. *Int. J. Eng. Res. Appl.* 10 (7) (Series-VII): 18-27.
- [154] Klem, C., and J. Zaspel. 2019. Pest Injury Guilds, Lepidoptera, and Placing Fruit-Piercing Moths in Context: A Review *Crystal, Ann. Entomol. Soc. Am.* 112(5): 421–432.
- [155] Liu, L., Wang, R., Xie, C., Yang, P., Wang, F., Sudirman, S., and W. Liu. 2019. PestNet: An End-to-End Deep Learning Approach for Large-Scale Multi-Class Pest Detection and Classification. *IEEE Access* 7: 45301–45312.
- [156] Liu, Z., Gao, J., Yang, G., Zhang, H., and Y. He. 2016. Localization and Classification of Paddy Field Pests using a Saliency Map and Deep Convolutional Neural Network. *Sci. Rep.* 6: 20410.
- [157] Mankin R., E., Jetter, B. Rohde, and M. Yasir. 2020. Performance of a Low-Cost Acoustic Insect Detector System with *Sitophilus oryzae* (Coleoptera: Curculionidae) in Stored Grain and *Tribolium castaneum* (Coleoptera: Tenebrionidae) in Flour. *Econ. Entomol.* <https://doi.org/10.1093/jee/toaa203>

- [158] Musa, R. M., Hassan, A. E., and A. A. Eisa. 2020. Flight Behaviour and Activity Time of *Tuta absoluta* (Meyrick) Males Trapped on Tomato and Miscellaneous Crops, Gezira State, Sudan. In *Sustainable Management of Invasive Pests in Africa* (pp. 293-303). Springer, Cham.
- [159] Nam, N.T., and P.D. Hung. 2018. Pest Detection on Traps Using Deep Convolutional Neural Networks. In *Proceedings, International Conference on Control and Computer Vision (ICCCV '18)*, Singapore, 18–21 November 2018, pp. 33–38.
- [160] Oerke, E.C. 2006. Crop losses to pests. *Journal of Agricultural Science. Agric. Sci.* 44:31–43.
- [161] Okuyama, T., Yang, E., Chen, C., Lin, T., Chuang, C., and J. Jiang. 2011. Using automated monitoring systems to uncover pest population dynamics in agricultural fields. *Agric. Syst.* 104: 666–670.
- [162] Preti, M., Verheggen, F. and Angeli, S. 2020. Insect pest monitoring with camera-equipped traps: strengths and limitations. *J Pest Sci.* <https://doi.org/10.1007/s10340-020-01309-4>
- [163] Qing, Y.A.O., Jun, L.V., Liu, Q.J., Diao, G.Q., Yang, B.J., Chen, H.M., and T.A.N.G. Jian. 2012. An Insect Imaging System to Automate Rice Light-Trap Pest Identification. *J. Integr. Agric.* 11: 978–985.
- [164] Ramalingam, B., Mohan, R.E., Pookkuttath, S., Gómez, B.F., Sairam Borusu, C.S.C., Wee Teng, T., and, Y.K. Tamilselvam. 2020. Remote Insects Trap Monitoring System Using Deep Learning Framework and IoT. *J. Sens.* 20: 5280.
- [165] Rechcigl, J. E., and N. A. Rechcigl. 2016. *Insect Pest Management*. CRC Press.
- [166] Rustia, D.J., and T.T. Lin. 2017. An IoT-based Wireless Imaging and Sensor Node System for Remote Greenhouse Pest Monitoring. *Chem. Eng. Trans.* 58: 601-606.
- [167] SAS Institute, 2013. *SAS/STAT guide for personal computers*, version 11.0.0 Ed. SAS Institute, Cary.
- [168] Simoglou, K. B., Karataraki, A., Roditakis, N. E., and E. Roditakis, E. 2012. *Euzophera bigella* (Zeller) (Lepidoptera: Pyralidae) and *Dasineura oleae* (F. Low) (Diptera: Cecidomyiidae): Emerging olive crop pests in the Mediterranean? *J. Pest Sci.* 85(2): 169-177.
- [169] Tóth, Z., Tóth, M., Jósvali, J.K., Tóth, F., Flórián, N., Gergócs, V., and M. Dombos. 2020. Automatic Field Detection of Western Corn Rootworm (*Diabrotica virgifera virgifera*; Coleoptera: Chrysomelidae) with a New Probe. *Insects* 11: 486.
- [170] Weber M., M. Geier, I. Potamitis, C. Pruszyński, M. Doyle, A. Rose, M. Geismar, and J. Encarnacao. 2017. The BG-Counter, the first operative automatic mosquito counting device for online mosquito monitoring: field tests and technical outlook. *AMCA 2017 83rd Annual Meeting*, 2017, pp 57.

- [171] Wen, C., and D. Guyer. 2012. D. Image-based orchard insect automated identification and classification method. *Comput. Electron. Agric.* 89: 110–115.
- [172] Xia, D., Chen, P., Wang, B., Zhang, J., and C. Xie, 2018. Insect Detection and Classification Based on an Improved Convolutional Neural Network. *J. Sens.* 18: 4169.
- [173] Xie, C., Zhang, J., Li, R., Li, J., Hong, P., Xia, J., and P. Chen. 2015. Automatic classification for field crop insects via multiple-task sparse representation and multiple-kernel learning. *Comput. Electron. Agric.* 119: 123–132.

9. APPENDIX

9.1 On Fresnel-Based Sensors for Insects Wingbeat Recording Schematics

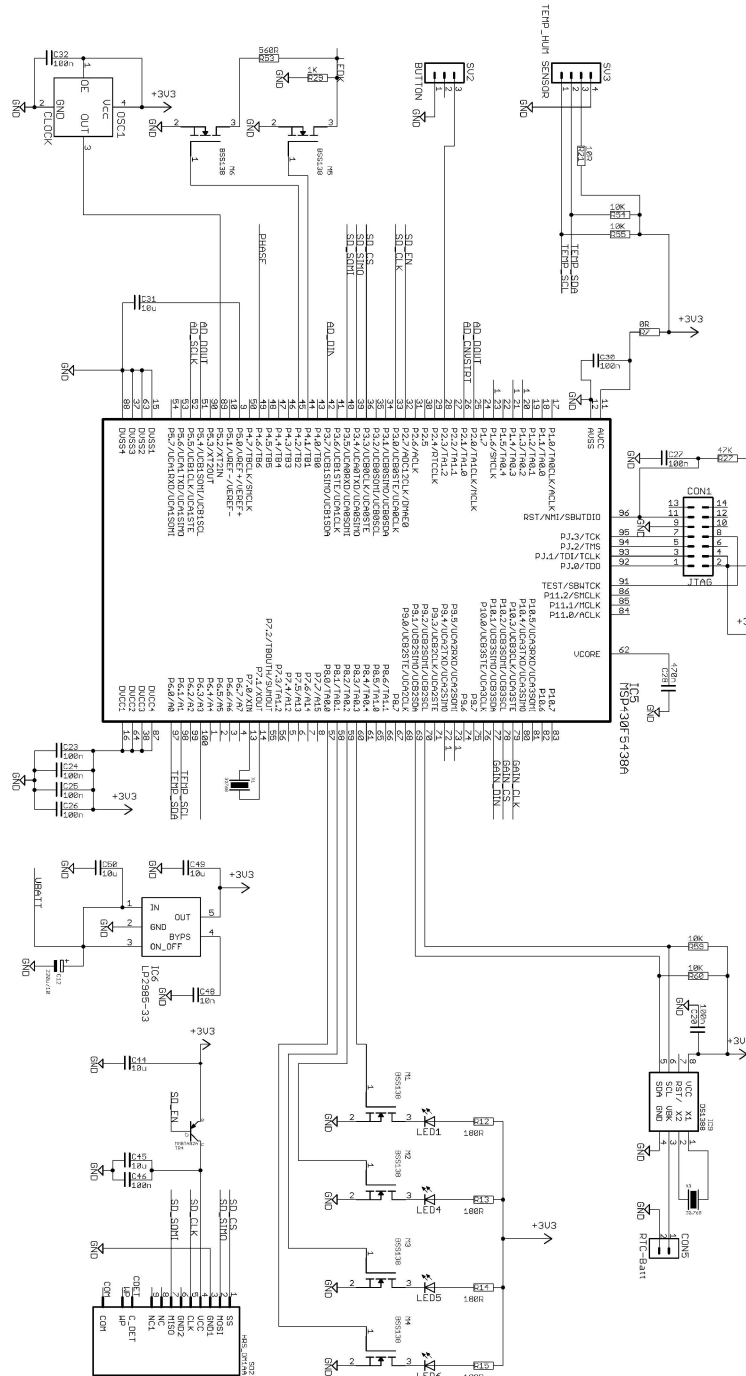


Figure 9-1. Main CPU of recorder.

The system is based on MSP430F5438A, a 16-BIT low power microcontroller. The 3.3V power supply is delivered from IC6 – LP2985-33, a low noise low power voltage regulator. The system time is provided from IC9-DS1388 RTC.

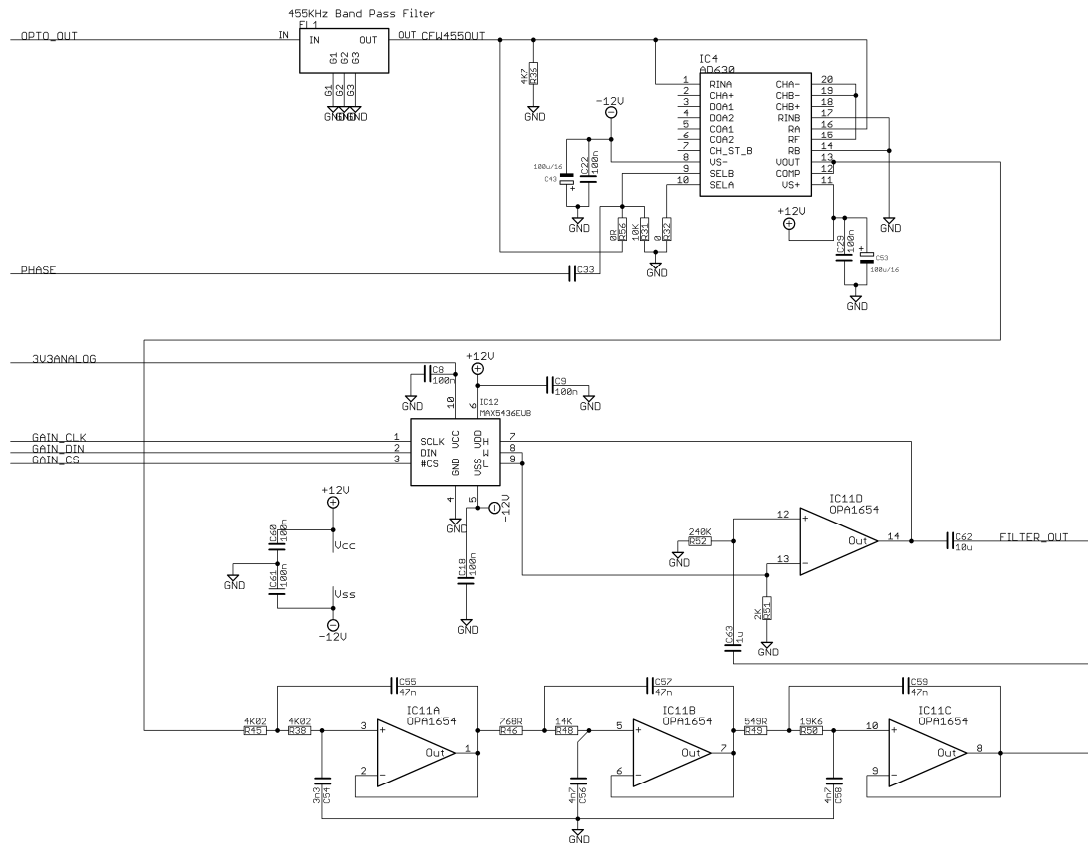
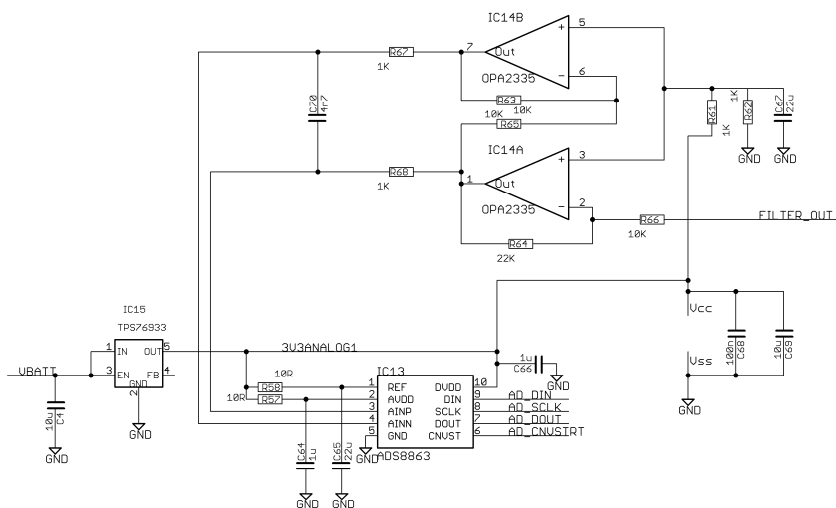


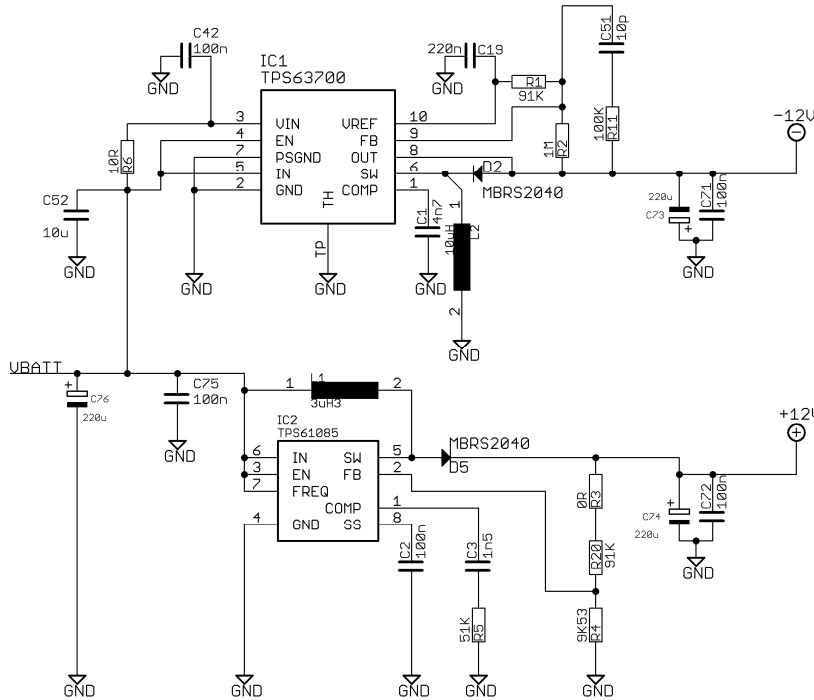
Figure 9-2. Demodulator, filter and gain control.

The signal from photodiode amplifier is filtered with FL1 a ceramic band pass filter in order to remove the low frequency noise from ambient light. The filtered signal drives the IC4-AD630 a Lock-in amplifier. The output of IC4 is the audio signal. The IC11A, IC11B and IC11C is a 4KHz low pass antialiasing filter. The digital potentiometer IC12 and OPAMP IC11D is the gain control.



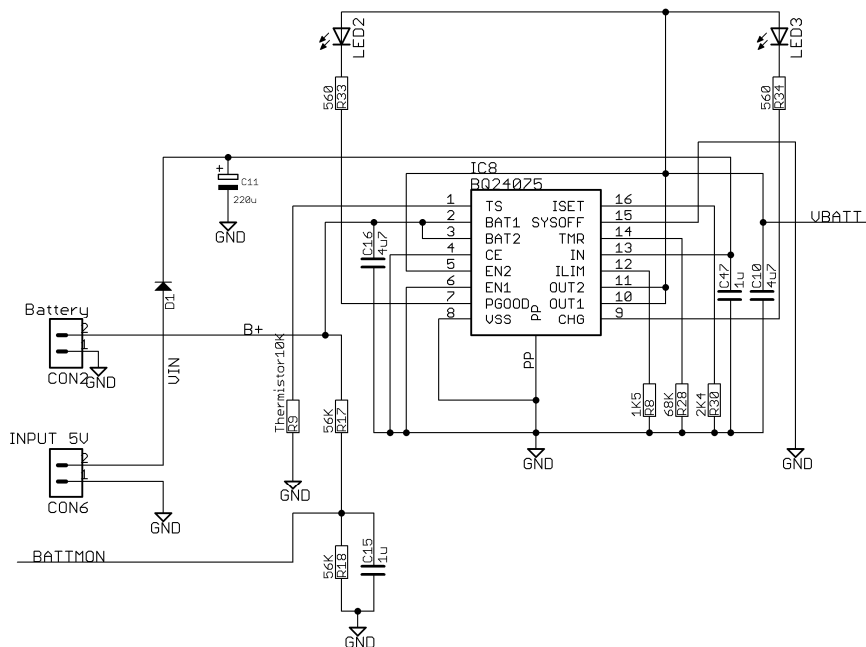
The ADC is based on ADS8863 ADC IC. A 16-BIT low power analog to digital converter IC. The input of ADC is differential and is coming from OPAMPs IC14A & IC14B connected as single ended to differential amplifier.

Figure 9-3. Analog to digital converter.



The main power source is a 3.7V lithium battery. The IC1 is a voltage inverting circuit from +3.7V to -12V and the IC2 is a step-up converter from +3.7V to +12V

Figure 9-4. ±12V power supply.



The IC8-BQ24075 is a lithium battery charger IC and charge the battery from 5V external power supply. The output of IC8 drives the ±12V power supply and the low voltage LDOs.

Figure 9-5. Battery charger.

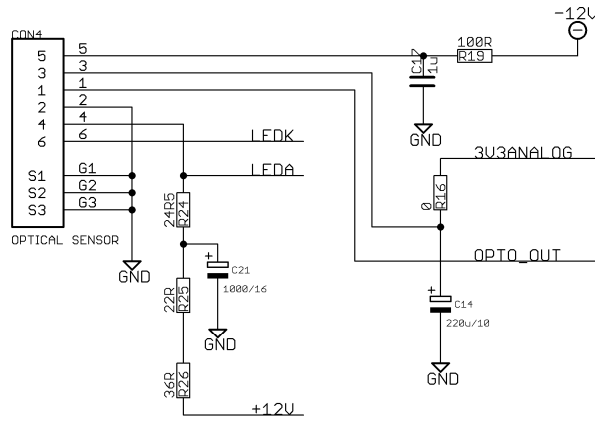


Figure 9-6. Optical sensor connector

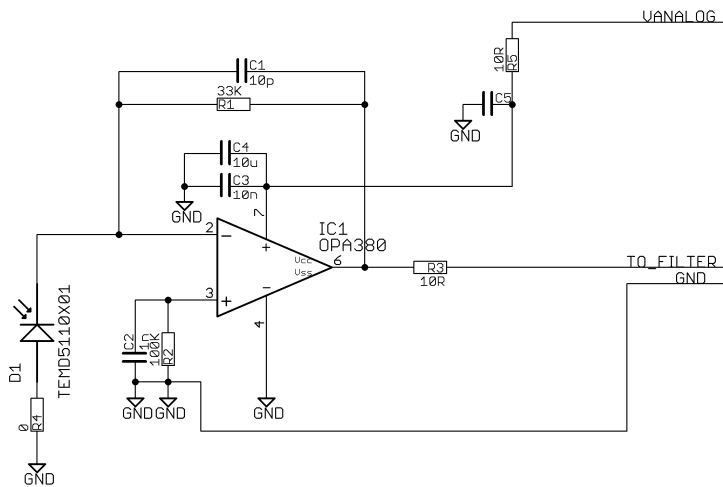


Figure 9-7. Photodiode transimpedance amplifier

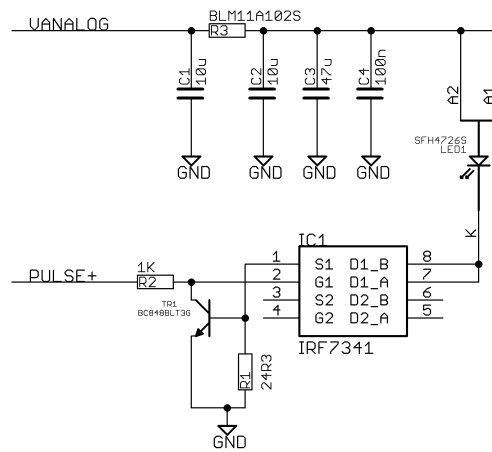


Figure 9-8. LED driver

9.2 Novel Noise-Robust Optoacoustic Sensors to Identify Insects through Wingbeats Parts List

Table 7. The recorder parts list

Power Supply Circuit		
Name	Description	Type
IC6	Power Supply IC	TPS63700
IC10	Power Supply IC	TPS61085
IC7	Power Supply IC	TPS71533
D3,D4	Schottky Diode	MBRS2040
R44	Resistor 0805	10R
R39	Resistor 0805	91K
R40	Resistor 0805	470K
R47	Resistor 0805	100K
R10,R43	Resistor 0805	51K
R41	Resistor 0805	10K
R42	Resistor 0805	15K
C41	Capacitor	10 μ F
C11,C12,C34,C35,C39,C44,C45,C46,C52	Capacitor	100nF
C33	Capacitor	4.7nF
C38	Capacitor	220nF
C40	Capacitor	10pF
C13,C37,C42,C43	Capacitor	220 μ F/16V
C36	Capacitor	1.5nF
C14	Capacitor	22 μ F
L3	Inductor	3.3uH
L6	Inductor	10uH
Photodiodes Receiver Circuit		
Name	Description	Type
D1 to D10	Photodiodes	TEMD5080X01
IC1	Operational Amplifier	AD8067
R2,R3	Resistor 0805	49K9
R1,R4	Resistor 0805	1K
C1,C2	Capacitor 0805	22 μ F
C3,C4	Capacitor 0805	220nF
C5,C6	Capacitor 0805	10pF
C7	Capacitor 0805	1 μ F
Clocks & Emitter Circuit		
Name	Description	Type
IC3	Microcontroller	MSP430F2132
TR1,TR3	MOSFET	BSS138
R5	Resistor 0805	2R2
R6	Resistor 0805	100R
R4	Resistor 0805	47K
Q1	Crystal	12MHz
C6	Capacitor 0805	100nF
C7	Capacitor 0805	3.3nF
C8	Capacitor 0805	2.2 μ F
C9,C10	Capacitor 0805	33pF
CON3	Infrared LED	TCRT5000
CON2	Laser Module	5mW focused laser diode
Filters & Demodulator Circuit		
Name	Description	Type
IC1	Switched Capacitor Filter	LTC1064CSW
IC4	Switched Capacitor Filter	LTC1064-2CN
IC2,IC5	Operational Amplifier	OP27Z
D2	Diode	LL103
C5,C19,C20,C21,C25,C26,C27,C28,C29	Capacitor 0805	1 μ F
C2,C4	Capacitor 0805	10 μ F
C1,C3,C17,C18	Capacitor 0805	100nF
C16	Capacitor 0805	470nF
C22	Capacitor 0805	220pF
C24	Capacitor 0805	10nF
R2,R11,R14	Resistor 0805	10K

R1	Resistor 0805	1K
R3	Resistor 0805	81K5
R7	Resistor 0805	14K72
R8	Resistor 0805	11K81
R9	Resistor 0805	38K25
R12	Resistor 0805	16K3
R13	Resistor 0805	70K3
R15	Resistor 0805	10K5
R16	Resistor 0805	39K42
R17	Resistor 0805	13K19
R18	Resistor 0805	6K9
R19	Resistor 0805	27K46
R20	Resistor 0805	69K7
R21	Resistor 0805	93K93
R22	Resistor 0805	5K6
R23	Resistor 0805	17K9
R28, R29	Resistor 0805	130K
R30	Resistor 0805	1K3
R31	Resistor 0805	3K9
R33	Resistor 0805	820R
R34	Resistor 0805	5K
R35	Resistor 0805	50R
R24	Potentiometer	10K

9.3 Multispectral Sensor Parts List & Schematics

Hereinafter, we present details schematics of the electronic device described in the text. Data supplemental to the main text is included in the directory of recordings.

Table 8. Cost break-down of the multispectral sensor and recorder (Euros).

Item	Manufacturer	Price
Photodiode 1X TEMD5080X01	Vishay Intertechnology, Malvern, USA	1.56E
LED GW CS8PM1.PM (8 pieces)	Osram, Munich, DE	10.48E
LED 810nm, SFH4780S (8 pieces)	Osram, Munich, DE	39.02E
LED 940nm, L110-094006000 (8 pieces)	LUMILEDS, San Jose, USA	23.68E
Fresnel lens, Part number: 3*	Fresnel Technologies Inc., USA	25E
CPU 1X STM32L4R7	Microelectronics. Geneva, Switzerland	12.67E
Four-channel ADC AD7768-4	Analog Devices	16.89E
ADC Drivers 3X THS4531	Texas Instruments	7.86E
Demultiplexer 1X OPA4376	Texas Instruments	3.27E
1X TS12A44514	Texas Instruments	1.35E
LED Drivers 3X ADA4805	Analog Devices	11.52E
1X TS12A44514	Texas Instruments	1.35E
2X IRF7341	Infineon	3.12E
Power Supplies 3X LP2985-33	Texas Instruments	1.48E
1X ADP7104	Analog Devices	3.58E
1X TPS76901	Texas Instruments	0.74E
1X TPS54302	Texas Instruments	1.65E

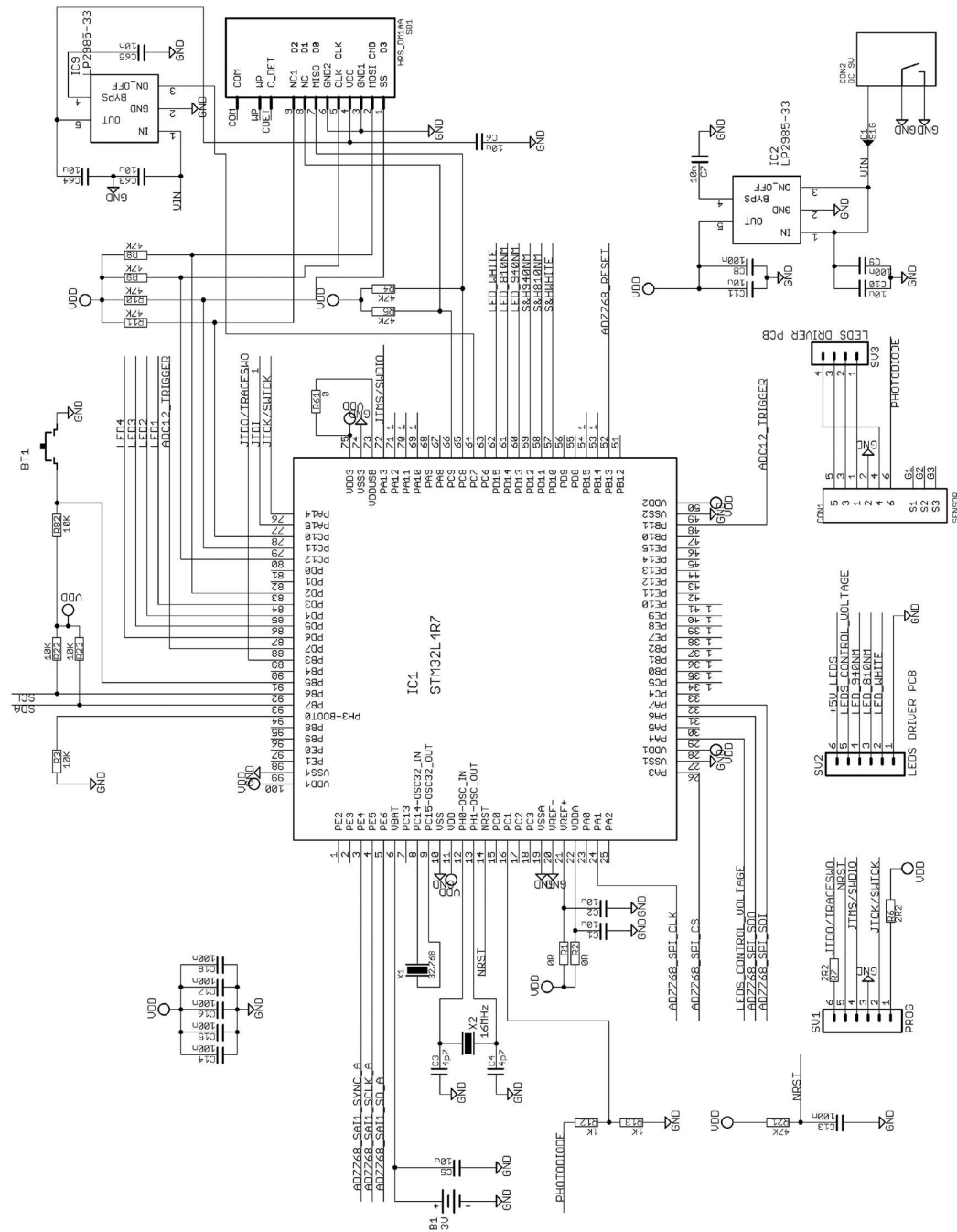


Figure 9-9. Multispectral Microprocessor unit. The microprocessor STM32L4R7 operates at 3.3 V and is synchronized by the 16 MHz clock provided by the oscillator X2. It controls all functions of the recorder: storing at the SD card, controlling the ADC, and production of the synchronization signals. The internal real time clock is powered from battery B1 and is clocked by X1 (32.768 kHz crystal) that time-stamps detection events. The CPU also drives the LEDs and the user interface through the function button and the status LEDs, named LED1 to LED4. The connector SV1 is used for programming the CPU, and the SV2 and SV3 is used for the connection of LEDs driver PCB to main PCB. The connector CON1 is used for the connection of the sensor with the device.

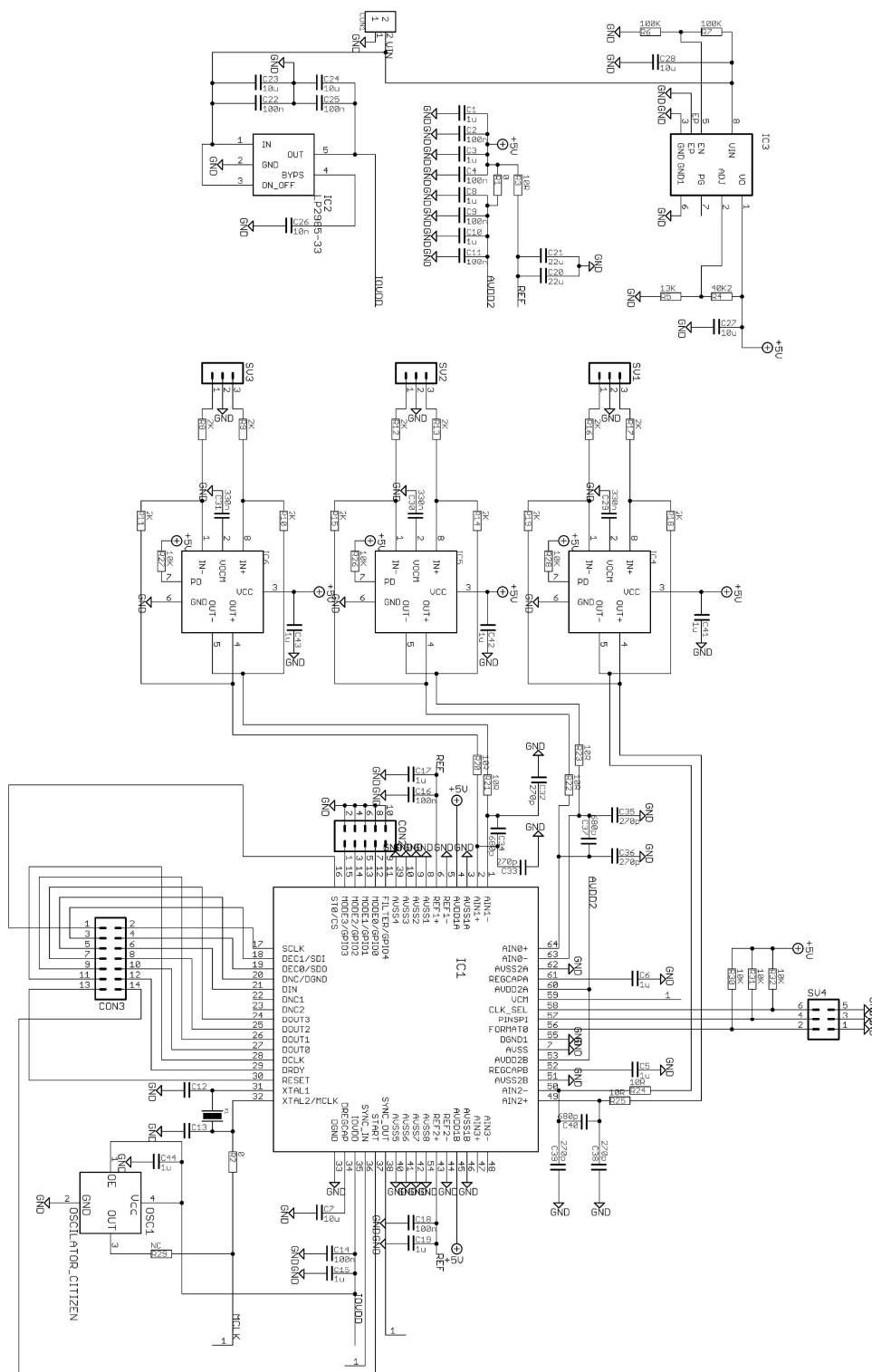
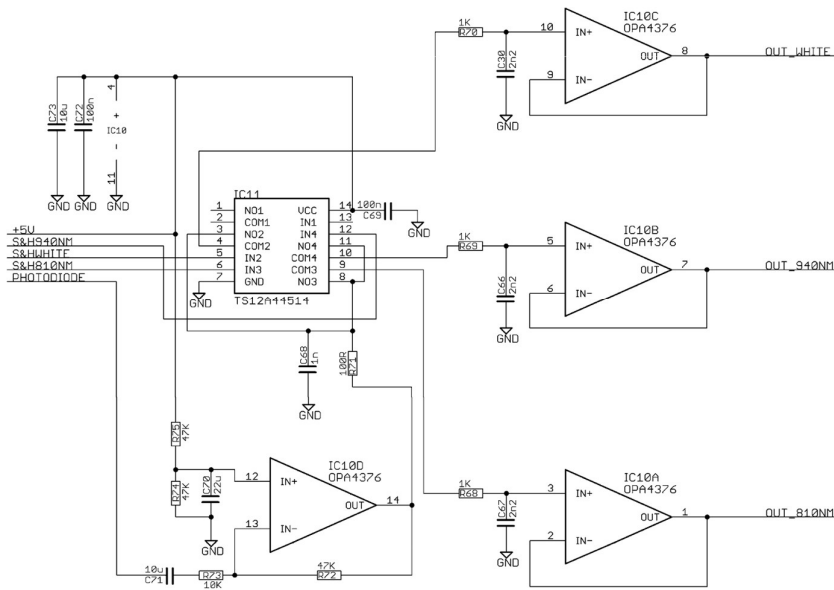


Figure 9-10. Three-channel ADC. The ADC is based on AD7768-4 (IC1) and converts the analogue audio signals to digital words. It is a four-channel 24-bit sigma delta ADC and we use the three of them. The three analog inputs of ADC are driven by three THS4531 differential amplifiers (ADC drivers). All functions of ADC (sampling rate, digital filtering, etc.) are controlled by the main CPU. The control interface is SPI and the digital audio data is transferred using the TDM protocol.



The demultiplexer receives the photodiode amplifier output and sends three dedicated analogue audio signals to the ADC

Figure 9-11. Demultiplexer.

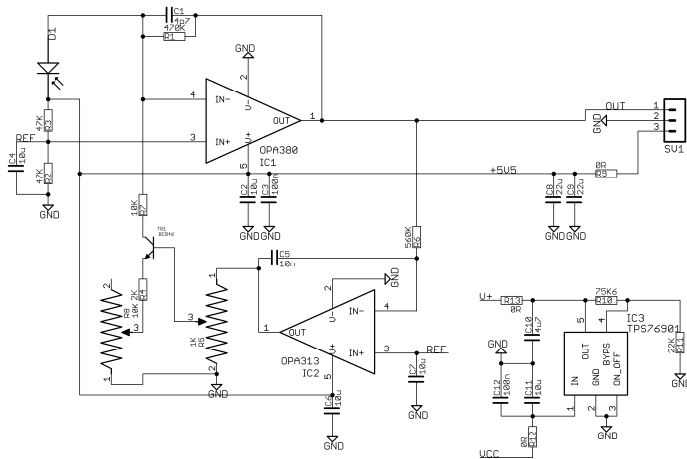


Figure 9-12. Photodiode receiver.

Photodiode receiver is based on the OPA380 transimpedance amplifier. The IC2 with the TR1 transistor functions as a feedback amplifier. Only the DC component of the IC1 output passes through IC2. The output of IC2 controls the conductivity of TR1, which in turn, subtracts the photodiode's DC current. Therefore, the input of IC1 is contains only the AC component of the current. This way, the sensor can function in the presence of sunlight. Without the feedback loop, it would not be possible to function properly due to the high amplification of the OPA380 (470K feedback resistor).

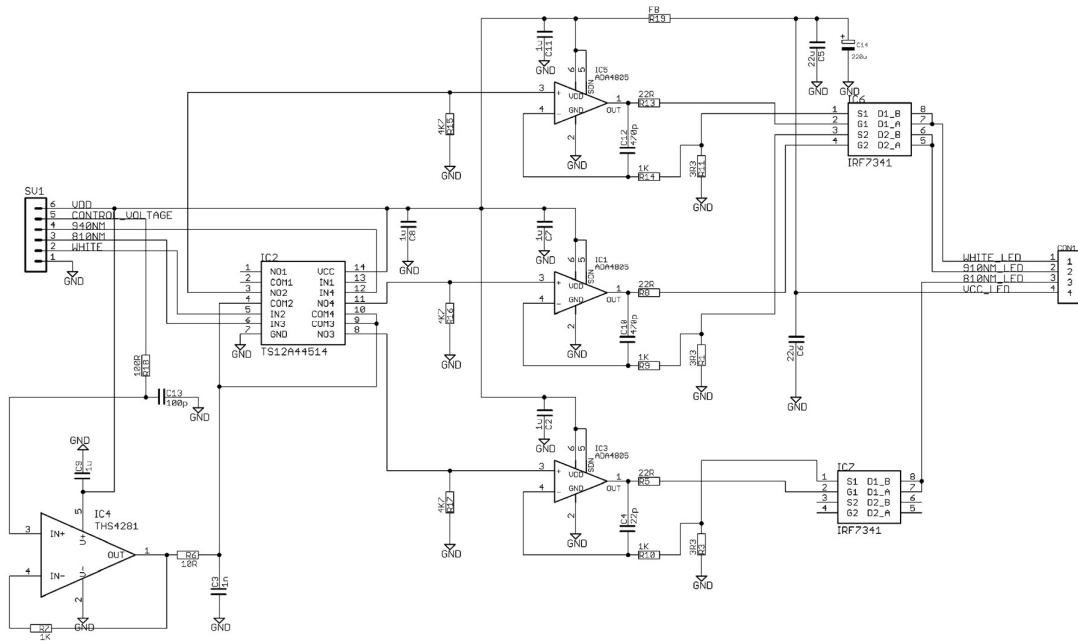


Figure 9-13. Three-channel LED driver.

The led driver is based on IC1, IC3, IC5, IC6, and IC7. The voltage in the input of each ADA4805 controls the current of each LED array. This circuit is controlled by the CPU that is connected to SV1. The control voltage of the drivers is different for each spectral band to account for the different sensitivity of the photodiode responding to different spectral bands and is produced by the DAC of the main processor. Therefore, with the help of the analogue switch IC2 and the timing signals for the 940nm, 810nm, and white LEDs, the different voltages, in turn, give input to the ADA4805.

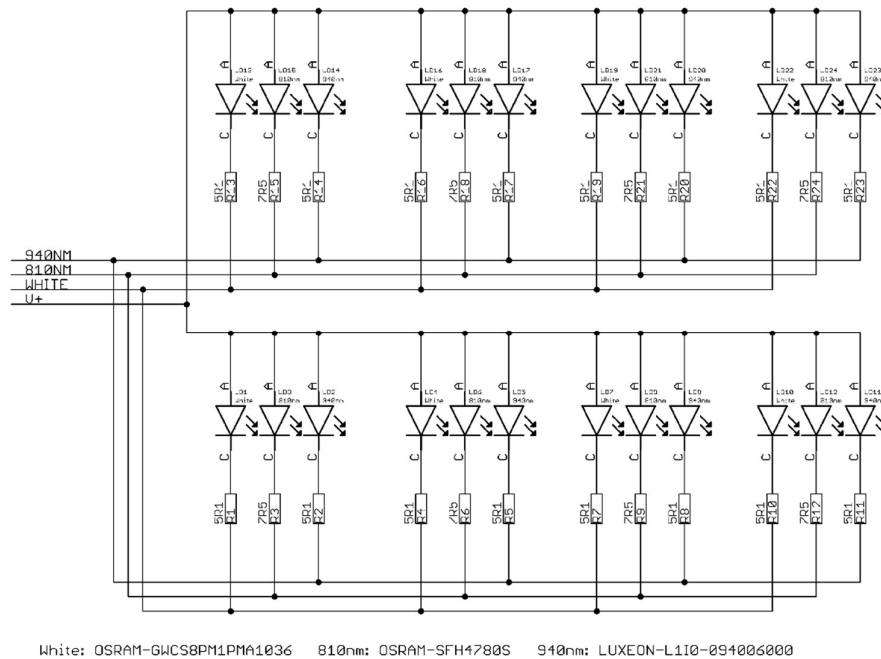


Figure 9-14. LEDs array. Three LEDs per spectral band.

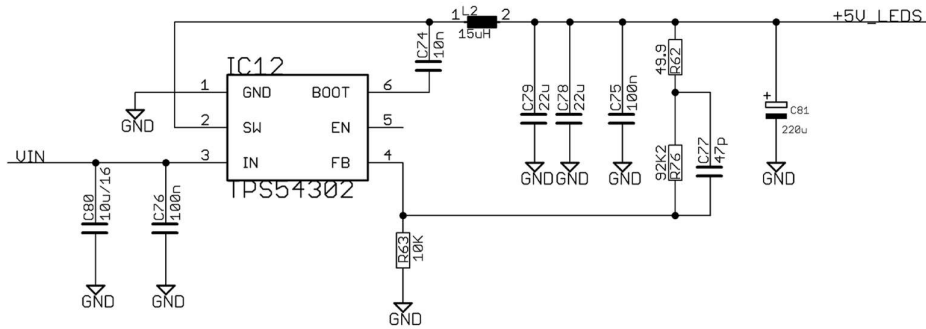


Figure 9-15. Sensor LEDs' power supply.

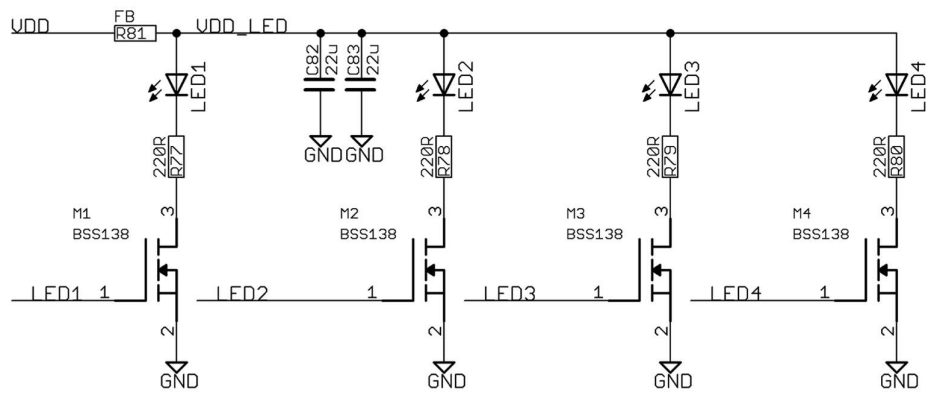


Figure 9-16. Indicator LEDs.

The LED arrays are powered with 5 V. The SMPS TPS54302 (IC12) produces this voltage. The indicator LEDs are controlled by the CPU through the MOSFETs M1, M2, M3, and M4.

9.4 Bees Electronic Gate Pictures

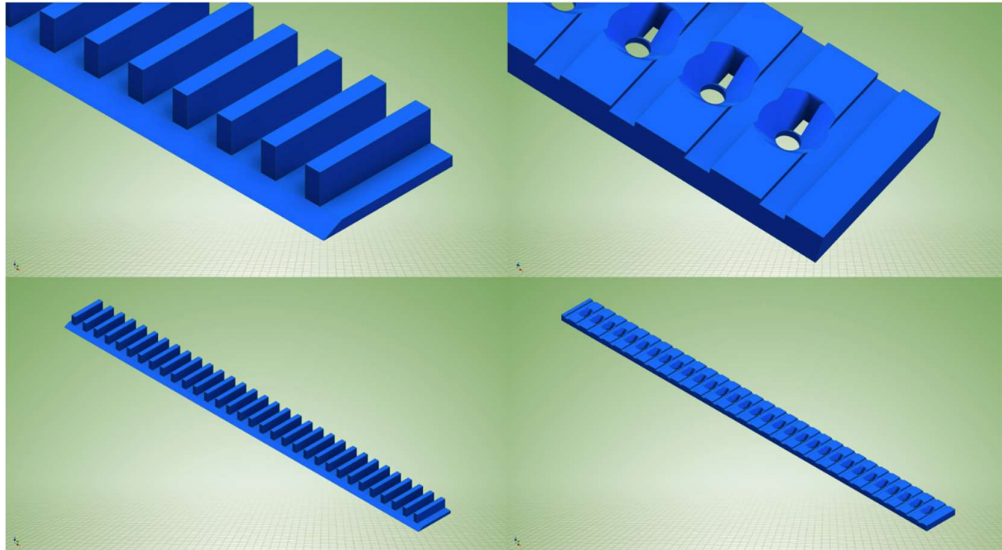


Figure 9-17. 3D Plastic design of the bee tunnels



Figure 9-18. Counter's placement in the beehive



Figure 9-19. Close up view of bee tunnels

9.5 TreeVibes Users Guide

9.5.1 Introduction

The purpose of this document is to present the operating procedures of the device and to communicate information on safety, use and performance. The intended use of the device is the long term systematic monitoring of trees and wooden structures against borers. A piezoelectric probe with an uncoated waveguide is inserted in the tree trunk to detect and record locomotion or feeding sounds of borers. The user can either use the supplied headphones and listen to the vibrations in-situ (i.e. to operate it manually) or install the device on the tree trunk and use the function that records and wirelessly transmits on a scheduled basis short recordings of the internal vibrations of a tree to the system server. In the latter mode of operation, the device is sleeping and wakes up, takes a recording and sleeps again. At some point it wakes up transmits the recordings to the server and goes back to sleep. The parameters of the recording and reporting sessions are handled by the system server, which also holds the transmitted recordings. The access and use of our server is free for our clients. The user can listen to the recording remotely and process it automatically to infer the infestation state of the tree with wood-boring insects that feed or move inside the tree. It has been extensively in field trials of the pests *Xylotrechus chinensis* and *Rhynchophorus ferrugineus*. The same approach can be applied to different trees and borers around the world by adjusting the length of the waveguide to the targeted trunk e.g., the mountain bark beetle, various longhorn beetles, *Rhynchophorus palmarum* and the *Anoplophora chinensis*.

This document supersedes any previous versions. The instructions manual is written in terms readily understood by the intended user and, where appropriate, supplemented with drawings and diagrams. Some pictures may include separate information for the professional user and the layperson.

9.5.2 Assembling Instructions

When you open the packaging cardboard, you will find the following parts inside. There may be small differences in the power supply unit provided or the colour of the cables/unit.

- USB Power cable (maybe different). You can use a USB Universal Mobile/Tablet charger
- SD card (embedded)
- Antenna
- Waveguides (2 pieces, 6mm x 16cm, 6mm x 30.5 cm. You need to open a hole with the d6.5mm drill bit and then insert them)

- Drill bits (2 pieces, d6mm x 24cm, and d2mm x 8.5cm)
- Waveguide adapter (2 pieces for fastening the d2mm and d6mm drill bit to the recorder)
- Recorder
- Headset

Assemble the device according to the following picture (see Figure 9-20). Note that the drill bits have different connectors and, therefore, it is not possible to mix them up with one another. The SD card comes embedded and fastened to the device. In any mode of operation, one needs to wait for approximately 6 seconds after switching on before the device becomes operational.



Figure 9-20. Complete tree vibes system
(Left) The main black box (10.8cm X 6.8cm X 6.8cm) contains the electronics and the SD card. A communication antenna, a waveguide and an adapter can be seen. The device has an embedded solar panel connected to its battery.
(Right) The assembled device.

9.5.3 Applications

Here are some possible applications of the device:

- Detection of wood-boring insects in forests, urban trees and trees of special/historic interest
- Inspection of wooden pallets for transportation of goods
- Detection of illegal chopping of trees or unauthorized removal of logs
- Inspection of quarantine trees transported for plantation in harbors
- Insertion of probe to the ground to detect larvae feeding on the root system of plants
- Smart home monitoring of wooden houses and structures for termites
- Detection of stored product pests in silos

9.5.4 Waveguides and drill bits

The waveguide is a solid, stainless-steel bar, but large nails, bolts and drill bits can serve the same function, that is to act as a sound coupler between the wood and the piezoelectric crystal (see Table 9). A picture of the waveguides offered along with the purchased device is shown in Figure 9-21. The adapter provided can be adjusted to other drill bits the user chooses as well. The drill bit itself can be used as a waveguide for a quicker installation but for optimal performance one should first drill a hole in the tree trunk using a drill bit and then fasten the associated waveguide. The small drill bits are used for wooden columns, decks, porch tongues, ceilings, furniture.

The sampling rate of the device is 8kHz in any mode of its operation. According to the Nyquist criterion, the spectral range of the recordings are half of the sampling rate. This is more than enough to identify the sound of wood-boring insects, which is of low pass nature.

Table 9. Dimensions of provided waveguides

	Length (cm)	Diameter (mm)	Usage
1	30.5	6	Large trees (e.g. palms, pines), roots of trees
2	16	6	Medium to small trees, roots of plants
3	24	6	Medium to small trees, roots of plants
4	8.4	2	Wooden structures, decks, ceilings, wooden pallets

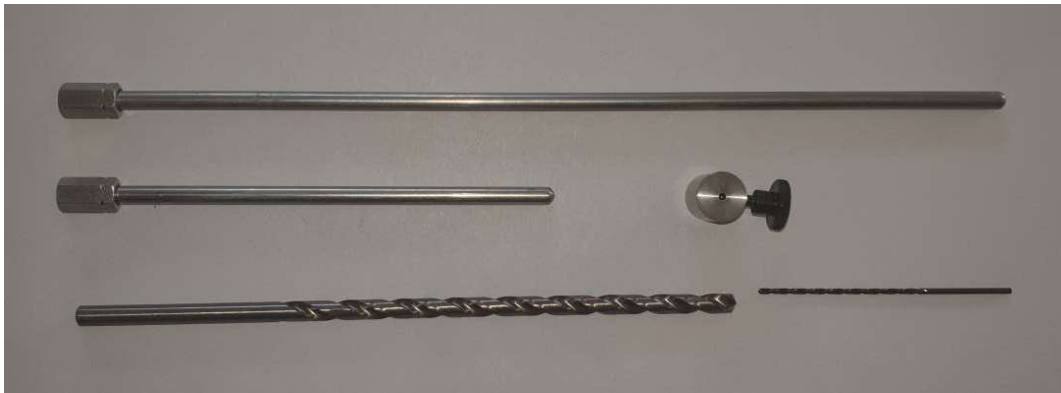


Figure 9-21. Waveguides that can be inserted in the tree trunks or wooden surfaces.

The drill-bit can serve as a waveguide when fastened to the adapter (included).

9.5.5 Remote vs Manual Operation

A close-up of the cables' connectivity and switches can be seen in Figure 9-22. The side lid is gradually removed when unfastening the large screw. Here we explain the connectivity of the cables from left to right. The first cable connects to the charger. While charging a red LED is on. Once the device is fully charged, the LED switches off. The second item is a three-positional switch. In the central position of the switch, the device is off. In the right position of the switch (R), the device outputs continuously to the earphones and does not store, neither transmits the recording. A green light is on during operating in the Right position. We include an earphone pair but any earphone/headphone is suitable. In the left position (L), it follows the recording schedule and writes to the SD card. The audio recording will be compressed and uploaded to the server. The circular socket is where the earphones must be plugged in.



Figure 9-22. The back of the device.

Connectivity from left to right: The charger connects to the first input from the left (Charge). The second is a three-positional switch (Left-Middle-Right). The circular socket is where the earphones are plugged-in (E). The first slot on the right is the SD slot. The supplied SD card must be always fastened before powering-on.

The device contains batteries that must be charged before outdoors use. For indoor use, we suggest the mains supply in collaboration with our USB cable. For outdoor operation, the device has a solar panel on its back (see Figure 9-23). The amount of power that can provide depends on the weather conditions and the shadow the tree provides but for many recording scenarios is sufficient to function indefinitely.



Figure 9-23. For outdoor operation, the device has a solar panel on its back.

Do not cover the solar panel. The device is waterproof against rain. The antenna must always be pointing towards the sky when transmitting.

9.5.6 The communication Modem

The device bears a 4G-communication modem and uses an EMNIFY SIM-card to offer global coverage (see <https://www.emnify.com/>). The product comes with 1 GB free data pack but the user is responsible to renew the data bundle in the same way as ones mobile phone. The user can see the progressive consumption of his/her own device MBs through the system server.

9.5.7 The Use of SD Card

The simpler and preferred way to access the recordings is through the system server from where they can be downloaded by the user. This is a powerful feature of this device as it allows retrieving data from remote trees the moment they are created. If there is no access because of bad mobile connection the recordings will be uploaded once the connection has been restored. The access to the sytem server comes with a password that is delivered with the device.

IMPORTANT: The SD card must be inserted in the device BEFORE powered on as seen in the picture below. When you insert the SD you will hear a click that tells you it is fastened OK. The SD card will contain the time-stamped recording in compressed format.

9.5.8 Deployment on Trees

Quick start of using the device on trees. See examples of its use in Figure 9-25 & Figure 9-26

- Make a hole in the tree trunk using the d6.5mm drill (provided). The waveguide will not fasten correctly into a hole made with a drill of a different diameter.
- Insert the FULL LENGTH of the steel waveguide in the hole (see Figure 9-25 (right), Figure 9-26). Alternatively, use the provided adapter to match the d6mm drill bit as a waveguide.
- Fasten the device on the waveguide. NEVER hit the device or the waveguide with a hummer to fasten it.
- The antenna must be facing UP towards the sky (not down).
- Switch the 3-positional switch to the left and see the blue LED blinking.
- Close the slit leading to the switches/SD with the plastic cover. The switches and sockets must not be visible. Fasten the plastic screw by hand.



Figure 9-24. A *X. chinensis* positive case in a mulberry trunk.

(Left) The sensor mounted horizontally in a suspicious trunk in the laboratory (left). Two alive larvae have been found after cutting the suspicious trunk in slices (middle and right). The larvae tunnels can be seen in the picture on the right.



Figure 9-25. Operating in continuous output mode. The user examines the internal activity in the trunk through the headphones, (Left) Manual inspection of slices of a trunk. (Right) Remote examination of tree in the field.



Figure 9-26. Operating in transmission mode. The device attached to a palm tree listening for *R. ferrugineus*. The white rectangle is located around the device. The recordings bearing a time-stamp are uploaded to system server where the user can examine them and download them.

9.5.9 Time-Scheduling of the Device's Operation

The device is pre-configured to record at any time of the day. However, the user may want to record e.g. every hour except at nights or to shut down the device for a week. In such a case, use your password to access your device through the system portal (<https://www.insectronics.net/login>). Once you enter the portal, click on the icon of your device and you will see a pop-up window like in Figure 9-27. You need to schedule your device by clicking on the tab 'schedule' of the corresponding device. Define the time span within which you want the device to operate (see Figure 9-29). The time-scheduler is preconfigured to operate at a 24/7 basis. You can click on the blocks to exclude hours/days that you want them to be excluded.

The device will function within the time span the user selects. The device will be updated on the user's preferences the next time it is connected to the server to upload recordings (i.e. the effect of changing these settings is not immediately valid). The exact time of the next update can be seen on the screen (see in Figure 7 Next-update column below Time zone).

CAUTION: If you do not have a specific reason to change the scheduler, consider leaving it in the pre-configured mode. If you exclude certain days and hours by mistake and then you forget that you have done so, you will not be receiving the recordings you expect. If that happens, see again the Time-Scheduling and correct the timetable according to your needs.

9.5.9.1 Explaining the System Server

After changing the location of the device, in case you do not see the correct GPS coordinates on the map you need to logout and then login again so that it is updated. Make sure that the antenna is facing towards the sky.

Next Update: The time new data and possibly setting will be uploaded to the server.

Battery Life: Power sufficiency (%)

Signal Level: Quality of wireless communication

Data consumption: The MB you have used so far. You have available 1GB. When you consume this amount, the device will stop reporting to the server and will resume after the communication fee is paid. However, the line-out operation through the earphones is not affected.

Action: Center map/Notes/Schedule/Edit. Center Map centers the map on the device, Notes allows you to keep some notes in case you are in the field inspecting a tree. You can write

down in the text box and/or upload a picture of the tree surroundings. Schedule allows you to set the recorder to follow a timetable in case e.g. you want to shut down the recording sessions for a week because of bad weather, or record only at daylight or only at nights etc. Edit allows you to set the duration and frequency of the recordings. It also allows you to set the frequency with which you want these data to be delivered to the server through which they will be available to the observer.

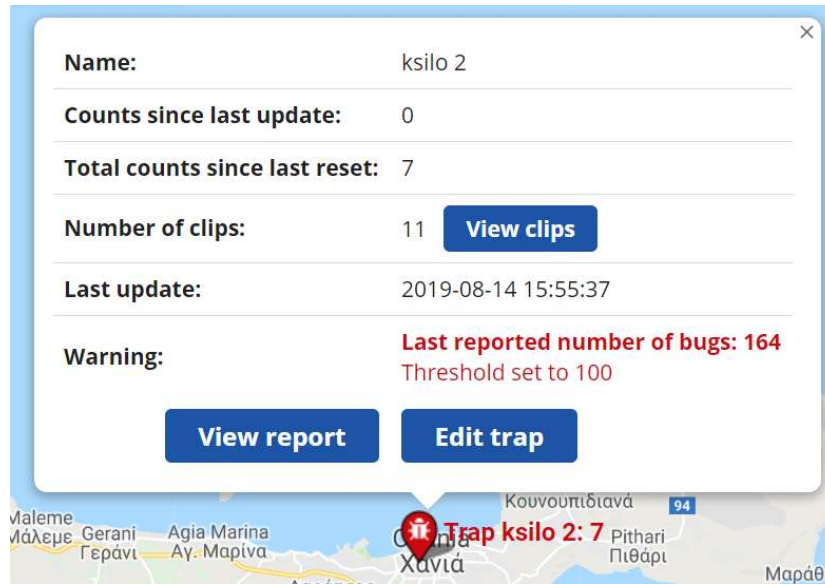







Figure 9-27. Pop-up window when someone clicks on device’s icon on the map in system server. View clips, leads to a window where one can listen and manipulate recordings (e.g. download them), View report, leads to a window where temperature and number of clips per day are plotted, Edit trap, leads to settings configuration (e.g. repetition, duration and uploading frequency).

 **Yellow**
Running out of battery

 **Red**
Insect count out of bounds

Traps: Timezone: Europe/Athens

Name	Number	Next update	Counts	Battery level	Signal level	Data consumption	Reset	Enabled	Actions
<input type="checkbox"/> flyMagnet	5	2018-07-22 10:44:58	0	91% (V)		N/A	0	1	Center map Notes Schedule Edit
<input type="checkbox"/> Ksilofagos	3	2019-06-19 13:58:13	0	56% (V)		N/A	0	1	Center map Notes Schedule Edit
<input type="checkbox"/> ksilo 2	42	2019-08-14 15:55:37	7	100% (V)		N/A	0	1	Center map Notes Schedule Edit

0 traps selected:

Figure 9-28. System server Schedule, leads to Figure 8 time-scheduler. Recordings will be made within the time span of the scheduler.

Duration and frequency of recordings have an effect on the power consumption only. The frequency of data transmission affects the amount of data you have prepaid as well as power consumption.

After one clicks the Schedule tab of the corresponding device, a clickable timetable appears as in Figure 9-29.

Unselect All							
	Monday	Tuesday	Wednesday	Thursday	Friday	Saturday	Sunday
00:00							
01:00							
02:00							
03:00							
04:00							
05:00							
06:00							
07:00							
08:00							
09:00							
10:00							
11:00							
12:00							
13:00							
14:00							
15:00							
16:00							
17:00							
18:00							
19:00							
20:00							
21:00							
22:00							
23:00							

Figure 9-29. System server time-table of a specific device.

The user may select the hours and days of device’s functioning. The device is pre-set to a 24/7 basis recording schedule.

9.5.9.2 How to Set the Recording and Reporting Update

Look at Figure 9-27 the ‘Edit trap’ tab. Click on the ‘Edit trap’ tab. You will see a picture like in Figure 9-30. You need to specify General Parameters in `recTime=5_repeatPeriod=60_Reg2=5678` and click on ‘Update trap’ in the same figure.

The repeatPeriod is in MINUTES

The recTime in SECONDS

recTime=5_repeatPeriod=60 means every 1 hour the device will record vibration activity for 5 secs and will store the recording to the SD card.

In the following picture, on the left column one can see the ‘Trap updates’ in minutes. This is how often one needs to upload the recordings to the server. Though the device records every 1 hour the user may want to examine the recordings collectively once every half-day. If so, the ‘Trap update’ needs to be set to $60 \times 12 = 720$

9.5.9.3 Where Are My Uploaded Recordings?

- Click on the corresponding balloon of the device you want on the map.
- Click ‘View clips’
- Click inside the ‘Date from’ and ‘Date to’ tabs to select the days you want from the pop-up calendar
- Click ‘Refresh’
- Select the recordings you want by either clicking few in the tic-box of each recording or ‘Select All’.
- Click on ‘Download’
- You need to wait a little depending on the number of the recordings selected. On the down-left corner, you will see zip file downloading in your computer. Inside the zip are the requested files.

IMPORTANT NOTICE

To avoid users the settings are constrained in between reasonable limits. If the user by mistake violates the range of a parameter e.g. set 0 as duration of recordings, the device ignores the settings of frequency of recordings, duration and reporting and defaults to the values record time=10, repeat period=60 and trap update 720. Of course, the user can change any parameter as long as it is correct. These are the hard limits applied by the manufacturer to ensure reasonable functioning.

recTime: minimum 1 sec, maximum 20 minutes

repeatPeriod: minimum every 5 minutes, maximum every 1 week

Device update: minimum every 5 minutes, maximum every 2 weeks

Figure 9-30. Trap update controls how often one needs to see the recordings (e.g once per day). General Parameters control how often one needs recordings to be taken (e.g. 20 seconds recording's duration every 1 hour).

9.5.10 Frequently Asked Questions

- **Where are my recordings? I do not see them in the 'View clips' tab**

ANSWER: Ensure you have fastened the antenna on the device. The antenna is mandatory when you transmit recordings and is not needed in a continuous manual mode (i.e. when you hear through headphones). Check that you have switched to the Left and not to the Right. Ensure the device is charged. Ensure that there is a mobile signal in the area. If there is no mobile signal, the recordings will be stored in the SD card and will be uploaded once connection is re-established. Ensure that you have not accidentally unselected all days and all hours in the time-scheduler.

- **My device is not in its correct location on the map. Why?**

ANSWER: Ensure you have fastened the antenna on the device and the antenna looks towards the sky. If you are inside a building, you cannot get the coordinates and what you see on the map are the coordinates of the previous connection. The location will be updated in the next transmission of recordings (see next update in the main menu). You can speed up this process by switching off the device and then on again while you are outside the building. Try logging out and the logging in again.

- **It is raining. Should I leave it on the tree? Will it malfunction later on?**

ANSWER: Ensure you have fastened the side lid and the antenna is pointing towards the sky. The device has been design for outdoor operation so yes leave it. Do not submerge the device into water.

- **The waveguide does not fit in the whole I have drilled. What can I do?**

ANSWER: You have two options: a) use the drill bit as a waveguide by fastening the adapter on the free side of the bit. Then fasten the device on the adapter or, b) reverse the rotation in your electric drill and move the drill bit during rotation inside out the hole many times so that you remove any debris. The waveguide will then fit in the drilled whole. Do not hit the waveguide with the device as you will harm the device.

- **Are my recordings stored in the SD card permanently?**

ANSWER: It is pre-configured that the transmitted recordings are also kept in the SD card. You can alter this option in the setting menu. Once the SD card is full it will start erasing old files so you have better keep an eye on the process.

- **Can I use the device in a location without mobile connection?**

ANSWER: Yes. If there is no connection the recordings will be stored in the SD card and will be uploaded once the connection is re-established. Moreover, they can always be retrieved manually from the SD card (the recordings bear a creation time-stamp on their filename).

9.5.11 Power Sufficiency & Data Consumption

When users install the device on a tree they want to know, how long it will operate without having to recharge it. The device has a solar panel in its back; therefore, there is trade-off between incoming energy and consumed energy to satisfy a recording/reporting schedule. The amount of harvested solar power depends on the illumination condition of the location and the season. We offer some approximate calculations in Table 10 based on the assumption that the user has fully charged the device before installing it.

Table 10. Time schedule and reporting to the server vs. Power sufficiency and data consumption.

Interval between recs	Duration (seconds)	Reporting	Power Sufficiency	Data consumption
Every 1 hour	20	1 per day	Indefinitely	1.15 MB/day 34.56MB/month
Every 1 hour	20	2 per day	Indefinitely	1.15 MB/day 34.56MB/month
Every 1 hour	20	12 per day	Indefinitely	1.15MB/day 34.56MB/month
Every 1 hour	60 (1 min)	4 per day	Probably Indef.	3.4 MB/day 102.24MB/month
Every 1 hour	600 (10 min)	4 per day	1-3 days	34.08 MB/day 1GB/month
Every 2 hours	10	1 per day	Indefinitely	288 KB/day 8.64MB/month
Every 3 hours	20	1 per day	Indefinitely	384 KB/day 11.52MB/month
Every 3 hours	60 (1 min)	1 per day	Probably Indef.	1.13 MB/day 34MB/month
Every 3 hours	600 (10 min)	1 per day	10days-1 month	11.36 MB/day 341MB/month

In bold, the suggested and pre-configured schedule. Proposed schedules in bold. The device comes with a 1GB data bundle.

9.5.12 Format of the Files

An example of the filename if the stored snippets is as follows:

F_20190812193118_1.wav

The file name “keeps” the time of an event and registers the environmental parameters if the temperature-humidity-illumination sensor is attached.

F stands for File

2019 stands for the year (e.g. 2019)

08 for the month (August)

12 for the day of the month

19 for the hour of the day

31 for the minute of the hour

18 for the second of the minute (therefore the time stamp is 30/04/2019 00:15:23)

_1 is a serial number of the recording that allows it to be better eye-tracked in the folder

Temperature is transmitted to the server but is mainly used for telemetry. It can be accessed by the ‘View report’ tab and looking at the temperature chart.

9.5.13 Setting The Time Correctly To Different Time-Zones

A real-time clock is embedded in the device. The device will be delivered tuned to the local time of the client. However, the real-time clock can be altered to any local time as follows:

- Insert the SD card of the device to a personal computer/laptop
- Create a new file in the SD card with name time.txt (use a simple editor)
- Write with a text editor (e.g. notepad) according to the following example:
- 29/04/19 23:38:51
- Remove the SD card from the computer
- With the recorder switched off, insert the SD card to the recorder
- Turn ON the recorder. The data will be passed to the device and the time.txt will be deleted

9.5.14 Examples of Recordings

In Figure 9-31 there some examples of the recordings that can be obtained. The recordings can be read and processed with typical languages as Python and Matlab as well as with commercial sound processing such as Adobe Audition. The Figure 9-31 has been obtained via Matlab 2018b using the following commands:

```
[x,fs] = audioread([File.folder '\ File.name]);
x2=x(50*fs:50*fs+2*44100);
subplot(2,1,1); t=0:1/fs:(length(x)-1)/fs;
plot(t,x);grid on;axis('tight');xlabel('Time (s)');
subplot(2,1,2); t2=50+0:1/fs:50+(length(x2)-1)/fs;
plot(t2,x2);grid on;axis('tight');xlabel('Time (s)');
```

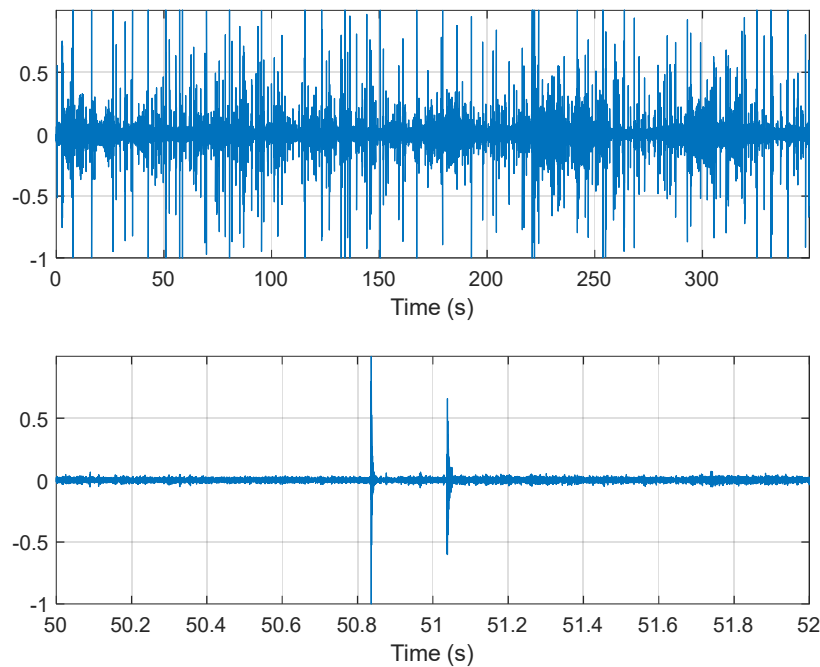


Figure 9-31. Mulberry examined in the field was found positive for *X. chinensis*.

(Top) time domain recording of the vibrations inside a tree trunk acquired using the device, (bottom) zoom-in detail of the same recording between the 50-52 sec. One can clearly see and hear the pulses standing out from the background noise.

9.5.14.1 Caution

Please read the following carefully to avoid problems with the use of the device.

- If you want to experiment to be acquainted with the device, turn the 3-positional switch to the right. You will be able to record continuously and to listen through the headphones.

This action does not involve the communication modem and does not consume your pre-bought communication time that comes along with the buying of this device.

- Once you turn the 3-positional switch to the left, you decide to transmit data. This action costs as if you would use your mobile phone in a foreign country. Therefore, one needs to be careful not to consume the available prepaid GB data-pack that comes along with your order. The device is preconfigured to get 10 sec recordings every 1 hour and transmit them every 4 hours. Read carefully 9.5.11, Table 10.
- Your device has been tested extensively prior to shipping in environments exceeding 35 oC and high humidity working on a 24/7 basis for at least 10 days without observing malfunctioning.
- Avoid using it in environments with extreme intensity of electric light and electromagnetic radiation. Avoid holding an activated mobile phone/tablet near the device (<1m) while operating the insect recorder. It will not cause a permanent malfunction but may cause interference in some recordings.

9.5.15 TreeVibes Designed Parts

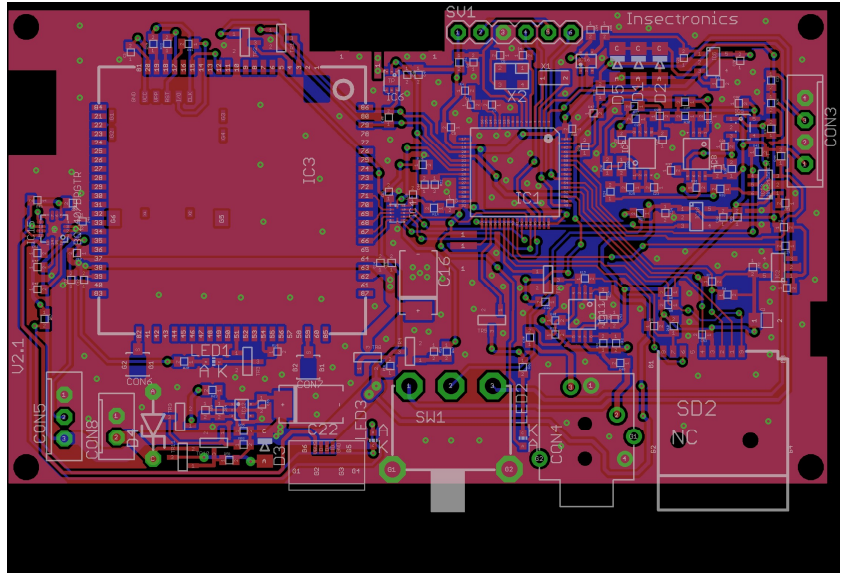


Figure 9-32. The designed printed circuit board of TreeVibe

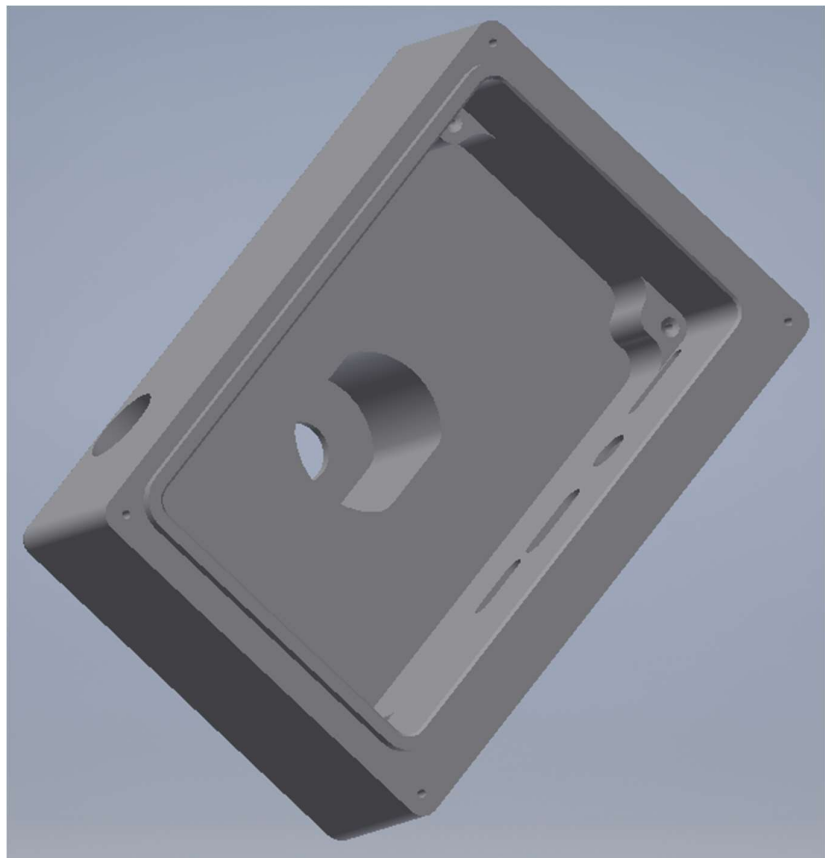


Figure 9-33. The designed main plastic enclosure internal view

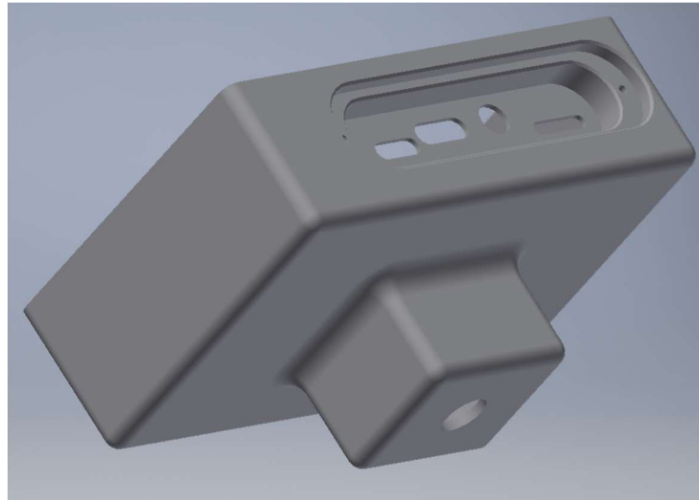


Figure 9-34. The external view of TreeVibe main plastic enclosure

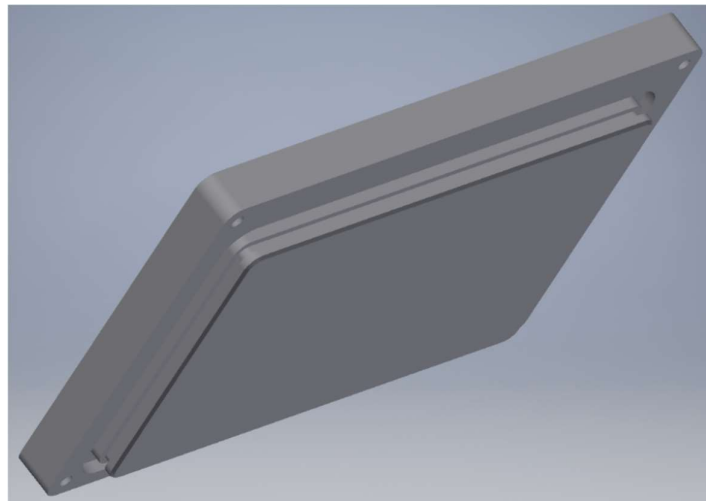


Figure 9-35. The Top plastic of enclosure (internal view)

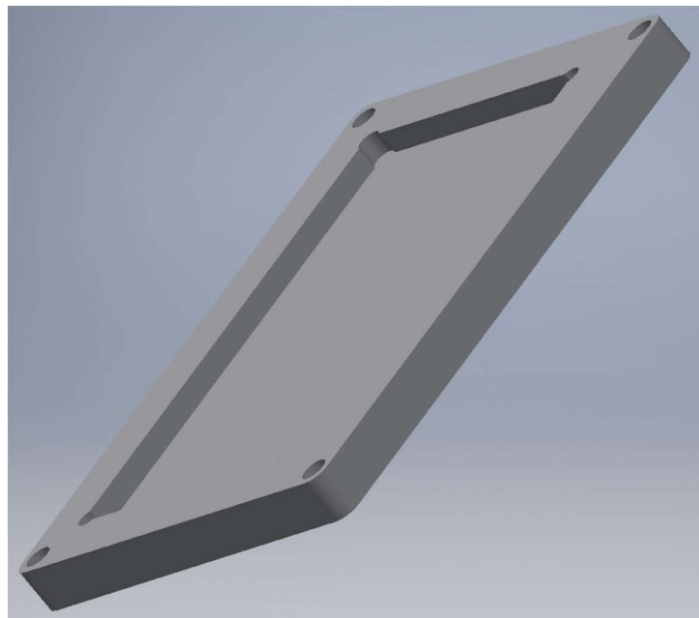


Figure 9-36. Top plastic of enclosure(external view)

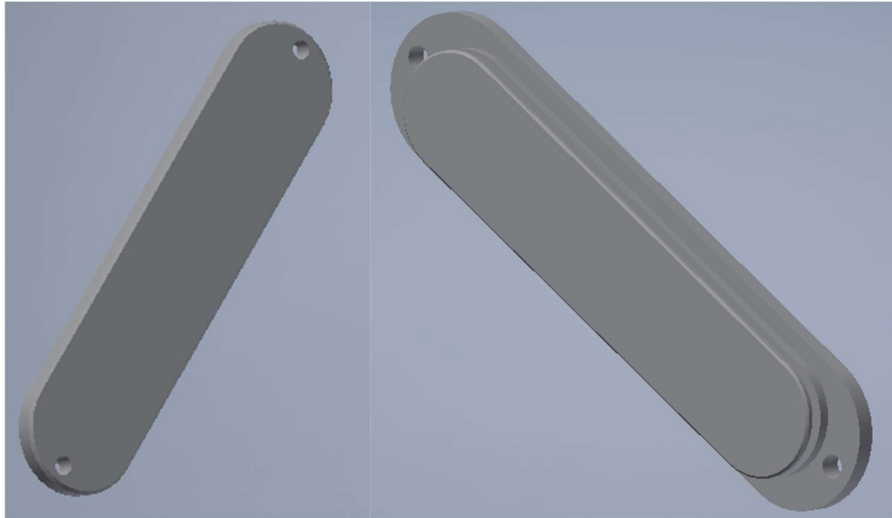


Figure 9-37. The plastic protector of TreeVibe interface

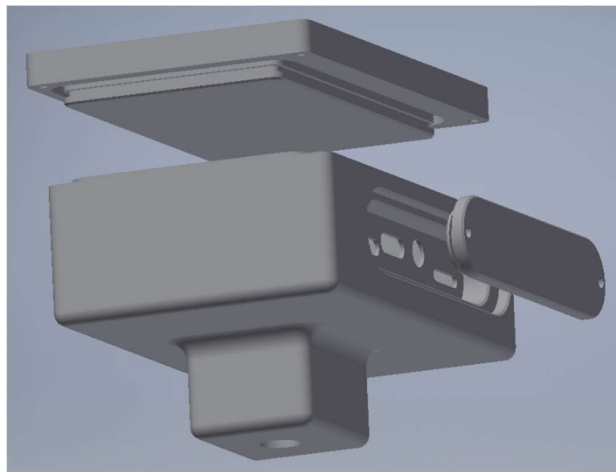


Figure 9-38. TreeVibe plastic enclosure parts



Figure 9-39. Assembled PCB (SMT components only)



Figure 9-40. Assembled PCB (all components placed)



Figure 9-41. Assembled Device

9.6 e-Funnel Users Guide

9.6.1 Introduction

The purpose of this document is to present the operating procedures of the device and to communicate information on safety, use and performance. The intended use of the device is remote monitoring of agricultural pests. It is a funnel trap that counts and transmits the number of captured insects. The e-funnel does not recognize what it counts, therefore, the selectivity of the trap must be ensured through species-specific pheromones. Pests fly around the pheromone dispenser until they are exhausted. Once they fall through the funnel, they interrupt the flow of infrared light (not visible to humans and insects) from emitter to receiver and thus are counted (Figure 9-42). Subsequently, the insects end up into the soapy water. The user has the possibility to set the size of the targeted insect remotely through his/her account in the system server. The e-trap wirelessly transmits on a scheduled basis: a) insect counts, b) time-stamps of all capturing events, c) GPS coordinates and d) temperature recordings to the system server. The access and use of our server is free for our clients. The user can see charts of counts and temperature with respect to time that are correlated with insect counts. All measurements can be downloaded from the server in Excel format. It has been used extensively in field trials of many Lepidoptera in cotton, vineyards, olives, tomato, and peaches: *Lobesia botrana*, *Tuta absoluta*, *Prays oleae*, *Helicoverpa armigera*, *Pectinophora gossypiella*, *Grapholita molesta*, *Adoxophyes orana*. The device can operate for months without re-charging and the user needs only to replace the pheromones once they expire.

9.6.2 Assembling Instructions

When you open the packaging cardboard, you will find the following parts inside. There may be small differences in the power supply unit provided or the colour of the cables/unit.

- USB Power cable (may be different)
- A set of typical funnel traps (see Figure 9-42)
- An optical counter, one for each funnel trap
- A gateway that concentrates data from all traps and uploads them to the server (in case the customer chose the LoRa network instead of standalone independent e-traps)

Assemble/disassemble the device according to the following pictures (see Figure 9-42 &

Figure 9-43)



Figure 9-42. (Left) A typical funnel trap. (Right) The optical counter attached to the funnel trap.

The e-funnel trap comes with its default protection cap. In case of a strong rain, the default cap will not prevent the optical counter from registering false counts due to rain drops. In such case, the device should be remotely de-activated through the scheduler (see section 9.6.3.5).

9.6.3 Connectivity and Insect Counting

The e-funnels are offered as single independent devices or as a LoRa network. E-funnels (see Figure 9-44) are offered in packs of 10 and they form a wireless network of their own using the LoRa wireless protocol. The network can have hundreds of e-funnels. Once the network has been activated the devices will try to establish connectivity with the gateway and with the satellites through their embedded GPS. The gateway will also establish contact with the cloud services (i.e. the system server). After that, the network is ready to count and report collectively through the gateway (see Figure 9-44-right). The only connectivity through cable is the USB charger. The pheromone is placed in the basket in the centre of the protective green cup.

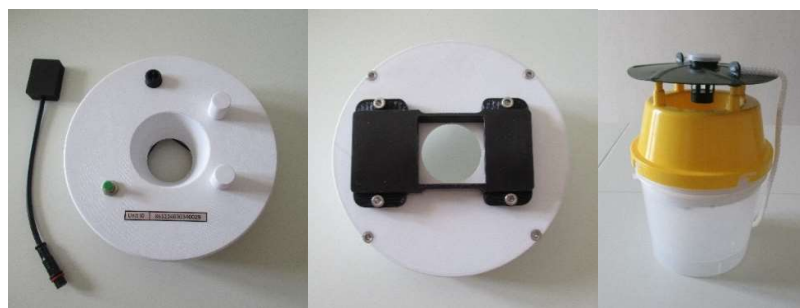


Figure 9-43. The torus in the picture is the optical counter.

The small black element is the power socket that connects to the USB power-charging cable and the green is the power up/down push button. The two white blobs are the GSM and the LoRa antennas. (Middle) When the insect falls through the hole, it interrupts the flow of light from emitter to receiver. The light fluctuation is turned to a voltage variation that is finally turned to an insect count. (Right) The complete e-funnel trap.



Figure 9-44. e-Funnel & LoRa Gateway on trees.

(Left-first two) The e-funnel on a tree. (Right-last two) The gateway (dim 12x12x11 cm) collects data from all e-funnels (through a LoRa network) and uploads it to the server through the mobile network (3G).

9.6.3.1 The Communication Modem

The device bears a 4G-communication modem and uses an EMNIFY SIM-card to offer global coverage (see <https://www.emnify.com/>). The product comes with one-year free data pack but the user is responsible to renew the data bundle in the same way as in a mobile phone. The user can see the progressive consumption of his/her own device MBs through the system server.

Note that the traps form a local network based on the LoRa protocol and, therefore, they do not consume the data bundle. Only the gateway transmits collectively the measurements to the server using the mobile network (see Figure 9-44).

9.6.3.2 The Activation of the Network and the Role of the Buzzer

One should pay attention on the following order of events to activate the network.

First, we activate the gateway of the network (see Figure 9-44-right) and place it on a tree.

- Subsequently, we press the green button of an e-funnel trap and we hear a short beep. After 2 seconds, the e-funnel will try to access the embedded SD card. The SD holds recordings of all events and its use is optional and only for research. If there is an SD card, one will hear a long beep, otherwise, 4 short beeps. The process continues with the e-funnel trying to retrieve the GPS coordinates. The latter step lasts 30 seconds and if successfully executed one will hear

two short beeps. If the GPS does not receive the signal from the satellites one hears a short beep.

- Subsequently, the e-funnel tries to connect with the gateway to declare its presence and submit its parameters to the gateway. Depending on the number of nodes, this procedure takes a few seconds to a couple of minutes. Once an e-funnel has been registered successfully, one can hear a prolonged beep. Do not power-on many e-funnels simultaneously. Repeat steps A-B for all traps in turn, so that each trap registers itself to the gate.

At this point, the network is ready to detect insects and the e-traps appear on the map of the server (see Figure 9-45). In case something interrupts the flow of light, the optical buzzer is activated. If it detects an incoming insect that lies between the detection thresholds as defined in the trap parameters one will hear a beep and a blue light (see in Figure 9-45 the Edit functionality on each trap in the main menu).

A sharp beep and a white light indicate that something has interrupted the flow of light but is not a valid count. This may happen because the fluctuation is too small (e.g. a midge) or too big (e.g. a moth) to originate from a targeted insect (i.e. the device examines the size of the insect). In such a case, the internal counter of the insects is not increased (the measurement is rejected and will not be time-stamped nor transmitted). The buzzer is mainly for in-lab experiments and as a field-test for registration procedures. It has no meaning for long-term measurements in the field and we recommend that is de-activated. If in the parameters of the LoRa gateway one deletes the `useBuzzer_ flag`, then there is no buzz sound.

Once an insect is counted, there is a delay for the next valid count because sometimes insects fly for a while before they reach the surface of the liquid. We do not suggest the use of water or anti-freezer to terminate the insects because they may attract non-targeted insects. A vapona and the sun will terminate the insects. The device will not double count captured insects.

The device can be deactivated by pressing the green button. In this case, the buzzer will beep sharply, for three consecutive times.

9.6.3.3 Power Sufficiency

The gateway (i.e. the device that collects data from all e-funnels) is low power and has a solar panel. Therefore, it is power sufficient. Each optical counter has a battery that is sufficient to power it for about 20-30 weeks given that it reports once or twice per day.

9.6.3.4 Quick Start

To start a counting session follow the steps:

- Insert a vapona in the bucket. You do not need liquid to reduce the chance for a double count.
- Fasten the torus on the top of the bucket.
- Press the green button of the optical counter.
- Follow Section 9.6.3.2 for each trap of the network.
- Insert the pheromone in the basket.
- Place the pheromone basket in the center of the green protective cup.
- Fasten the upper yellow part of the trap to the semi-transparent bucket bearing the optical counter.
- Hung the trap from a branch or a pole stick. The trap may swing freely.

To end a counting session follow the steps:

- Unfasten the upper yellow part of the trap to the semi-transparent bucket bearing the optical counter.
- Press the green button of the optical counter. You must hear three consecutive beeps.
- Remove gently the optical counter.
- Count the insects/replace the pheromone/refill the liquid if needed.

9.6.3.5 Time-Scheduling of the Device's Operation

The device is pre-configured to record on a 24/7 basis. However, the user may want to record e.g. during day-time or to shut down the device for a week due to extreme weather conditions. In such a case, use your password to access your network through the system portal (<https://www.insectronics.net/login>). You will see a window like in Figure 9-45. You need to schedule your device by clicking on the tab 'Schedule' of the corresponding device under the column 'Actions'. Define the time span within which you want the device to operate (see Figure 9-45). You can click on the blocks to exclude hours/days that you want excluded.

The device will function within the time span the user selects. The device will be updated on the user's preferences the next time it is connected to the server to upload recordings (i.e. the effect of changing these settings is not immediately valid). The exact time of the next update can be seen on the screen (see in Figure 9-45-Next-update column below Time-zone).

NOTE: The e-funnel will not register false alarms during a light rain. During a heavy rain, one needs to de-activate the device through the scheduler (see Section 9.6.3.5), otherwise the device will report false alarms due to rain-drops.

9.6.3.6 Explaining System Server Functionality

Next Update: The time new data and - possibly- new setting will be uploaded to the server.

Battery Life: Power sufficiency (%)

Signal Level: Quality of wireless communication

Data consumption: How many MB you have used. 1000 MB are available. When you consume this amount, the device will stop reporting to the server and will resume after the communication fee is paid.

Action: Centre map/Notes/Schedule/Edit. Center Map centres the map on the device, Notes allows you to keep some notes in case you are in the field inspecting a tree. You can write down in the text box and/or upload a picture of the tree surroundings. Schedule allows you to set the device to follow a timetable in case e.g. you want to shut down the operation for a week because of bad weather, or record only at daylight or only at nights etc. Edit (see Figure 9-46 as well) allows you to set alert points and interact with the trap by changing its parameters. It also allows you to set the frequency with which you want these data to be delivered to the gateway. Edit the Lora Gateway settings to set how often you want data from all traps to be delivered. Transmission of measurements from the –funnels to the gateway affects only the power consumption. The frequency of collective data uploading from the gateway to the server affects the amount of data you have prepaid (because it uploads through the mobile network) as well as the power consumption. Since the gateway has a solar panel, its power consumption is insignificant and in our experiments is always close to being fully charged.

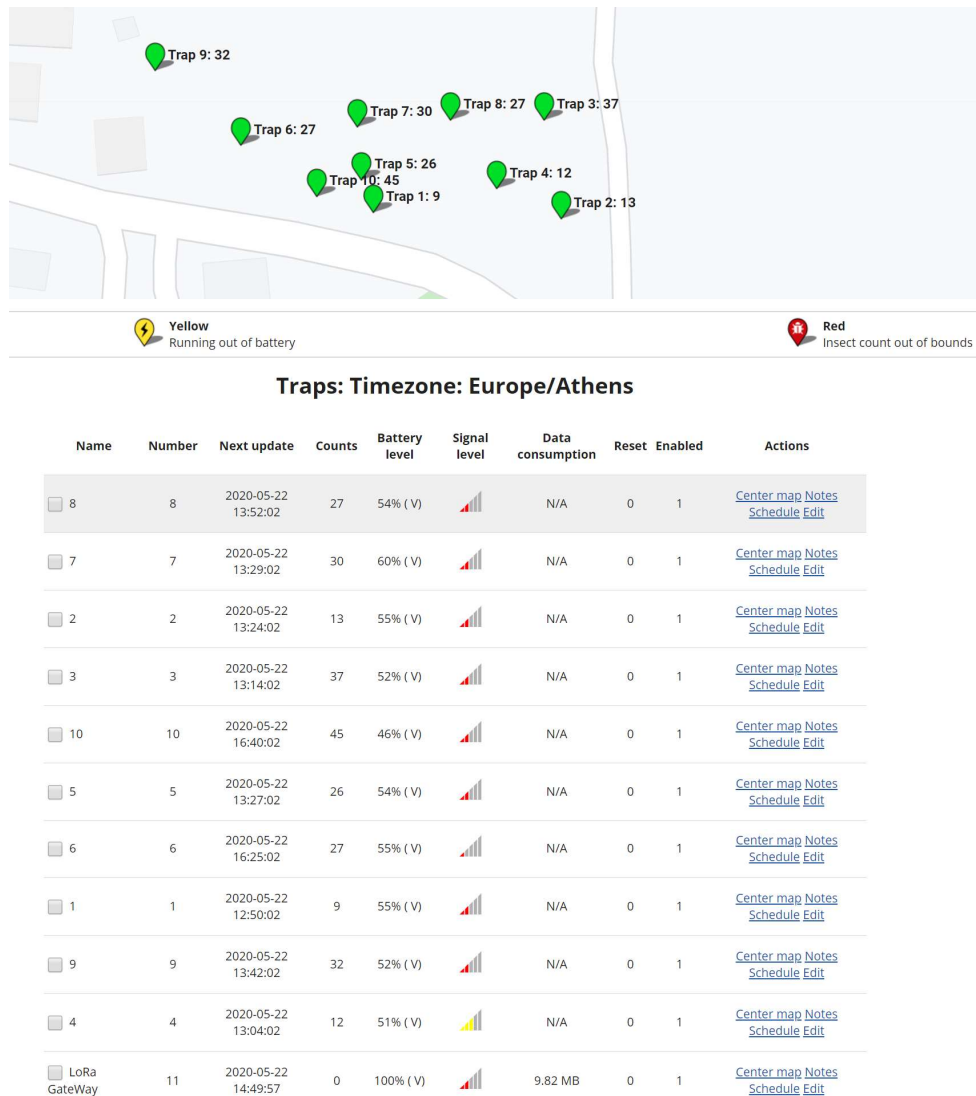


Figure 9-45. A network of 10 e-funnel traps on the map.

The traps and the Time zone appear automatically on the map based on the GPS of each e-funnel. Regarding the columns: Name of the trap e.g. ‘Jimmy’s’, Number is an integer associated to the trap. Put the same number on a sticker onto the corresponding trap so that you easier cross-check manual observations to automatic counts. Next Update of the e-funnels corresponds to the time the next measurements will be delivered to the gateway, whereas the Next Update of the Lora Gateway corresponds to the time the measurements will be uploaded to the server and on the map. Counts denote the insects counted. Battery level corresponds to the available power. Signal level denotes the quality of the signal strength. Data consumption denotes the amount of prepaid data bundle that has been consumed so far due to the uploading of data to the server. Reset, is a binary flag. Once set to 1 the counter will be reset to zero. Enabled, is a binary flag that shows if a device is active. The list of actions are explained in Paragraph 5.1.

Edit device settings

IMEI: **
865234031025595

Name: *
Cotton

Minutes interval until the next update:*
180

Alarm email:
Email address for alarms

Threshold for alarm email:
300

Threshold (%) for low battery alarm:
10

Description:
Test

Number:
7

Latitude:
39.4692040
[Pick latitude from current centre of map](#)

Longitude:
22.7753340
[Pick longitude from current centre of map](#)

General Parameters:
TH=10_LT=7500_HT=65535_PT=1_SR=2000_NS=2048_

Device Parameters:
DC=1800_GF=1_useGPS=1_useGSM_algTrack_useBuzzer_

Device enabled
 Check to reset count in next update

Update device Cancel

Figure 9-46. IMEI is a unique number related to the hardware of the e–funnel.

IMEI comes from the manufacturer. Trap update in minutes controls how often one needs to see the new insect-counts (e.g once per day). The Alarm email is the e-mail in which an alert message is sent after the number of counts exceeds in a week the number as defined in the Threshold for alarm email. The threshold for low battery defines the threshold under which a yellow icon related to power supply appears in the main window under the map. The Latitude-Longitude entries are automatically updated from the received GPS measurements. In the general parameters cell LT, HT define the lower and upper thresholds for insect detection based on size.

9.6.3.7 How to Set the Recording and Reporting Update

After one clicks the Schedule tab of the corresponding device, a clickable timetable appears as in Figure 9-47. The schedule is pre-configured to a 24/7 recording schedule. By clicking, de-clicking a cell and selecting the ‘Update trap schedule’ one can exclude/include an hour respectively. Be careful not to deactivate all cells as then the network will not be able to send its data to the server.

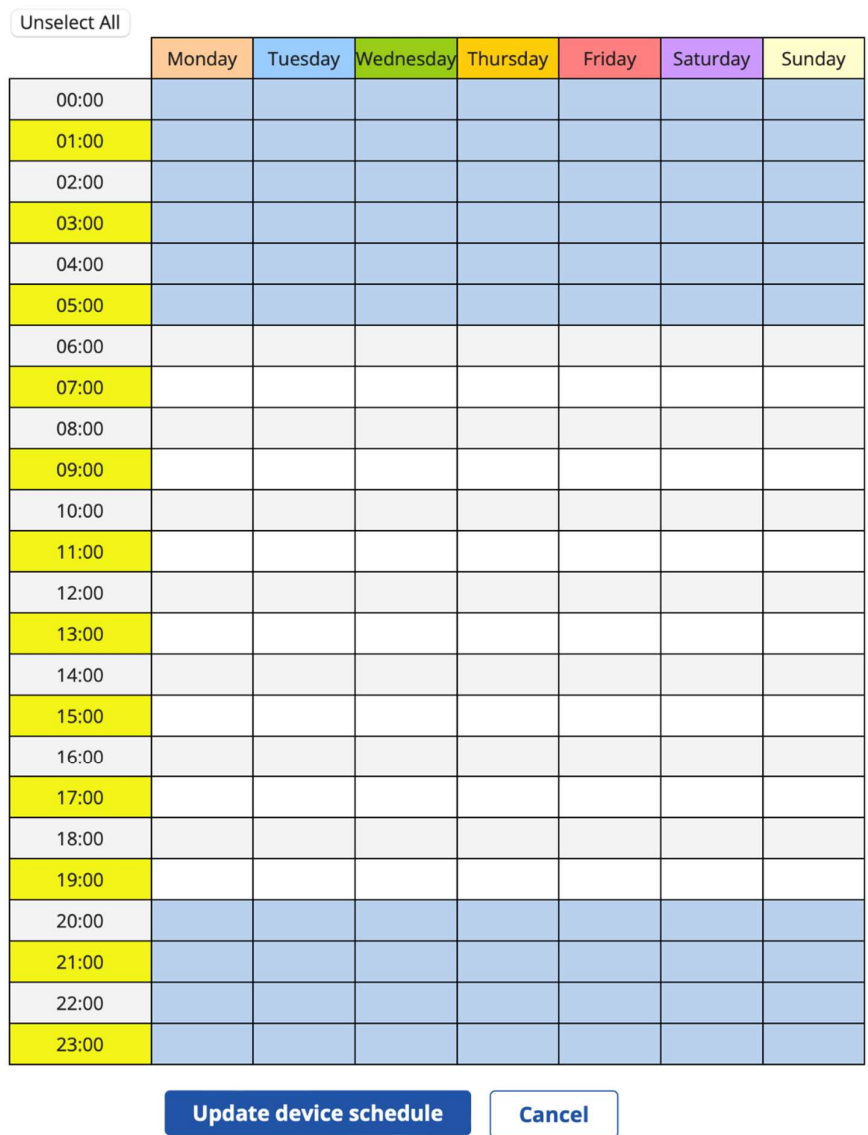


Figure 9-47. System server timetable of a specific device.

The user may select the hours and days of the device’s functioning. The device is pre-set to a 24/7 basis recording schedule.

If one clicks on the balloon icon of a trap on the map the a window will pop-up. By selecting ‘View report’ a figure like one in Figure 9-48 will appear where one can select to see the distribution of counts w.r.t. temperature over specific dates. All data (including time-stamps of captured insects) can be exported to an excel file for further processing by clicking on Export data in Excel Format.



Figure 9-48. A Pop-up window will appear when someone clicks on device’s icon. On the map in system server. View report leads to a window where temperature and a number of clips per day are plotted. The user sees a time-series of counts, collective counts and associated temperature recordings. All information can be downloaded by clicking the ‘Export data in Excel format’ tab.

9.6.3.8 How to Set the Detectable Size Limits of Insects

One can choose the size of the detectable target-insect by setting the corresponding parameter in the General parameters (see Figure 9-46). One can also set an absolute threshold between 3000 (size of a midge) and 65535 (**TH=10_LT=7500_HT=65535_PT=1_SR=2000_NS=2048**). The best way to set thresholds is to devote some days to manual monitor captures in the field. Ideally, the threshold must be low enough so that one does not miss the targeted signal and high enough so that it does not capture false alarms (usually small midges).

9.6.3.9 Power Sufficiency and Data Consumption

When users install the e-funnel they want to know for how long it will operate without having to recharge it.

Table 11. Time schedule and reporting to the server with respect to power sufficiency and data consumption.

Update Time	Funnel	
	With GPS	W/O GPS
1	94	125
2	120	143
4	140	154

We offer some calculations in Table 11 based on the assumption that the user has fully charged the device before installing it. Exact values depend on the signal strength of the gateway and on the good **connection** of the nodes with the gateway. The LoRa gateway has a small solar panel that covers its power needs.

9.6.3.10 Setting the Time Correctly to Different Time-Zones

The device carries a GPS and infers the local time of the client from the location. Therefore, in order to set the correct time the e-funnel must be activated in the field as the GPS requires a direct link to the sky.

9.6.4 Frequently Asked questions

- **I find few trapped insects but the site reports many. Why?**

False alarms can be created for two reasons: a) electronic interference. Turn your mobile phone to airplane mode when you inspect an activated device. Wi-fi and phone signals can create interferences that trigger the device, b) heavy rain. One needs to de-activate the device through the scheduler as raindrops that slip into the e-trap can be registered. Alteration of the trap may affect its attractiveness towards insects and therefore, we do not use larger caps.

- **I find many trapped insects but the site reports few. Why?**

In short, the optical detector cannot miss a dropping insect. The device may fail to register a count for two reasons: a) during transmission, the device does not count insects for about 1 min and 30 secs. During that time, if an insect falls inside it will not be counted (i.e. a miss), b) it may happen that two insects fall simultaneously. In such a case only one count will be registered.

- **Can an insect fly inside the bucket and therefore create false counts?**

In short, no. The optical sensor has a double-layer. An insect moving from outside into the bucket can be counted but not vice-versa. You can check that in the lab by dropping an insect from top to bottom and from bottom to top by reversing the optical-counter. Notice the difference in the sound.

- **Should I put water or detergent in the bucket?**

Insects are usually terminated naturally by dehydration. One can optionally use a vapon type insecticide. Alternatively, a small quantity of water can be used in the bucket (about 15% of

the volume of the bucket). The latter is not suggested because it may attract non-targeted insects.

- **The name of the trap turned red in the server. Why?**

This means that it did not report data in the next update that was scheduled. This may have happened for one of the following reasons a) you forgot to activate the device. Press the button on top once, b) The communication signal was weak and the modem could not deliver data. It will try again in 30 minutes. If again it does not establish contact it will try in the next update, c) your data bundle has been exhausted and you need to buy more data after 1 year.

9.6.5 e-Funnel Design Files

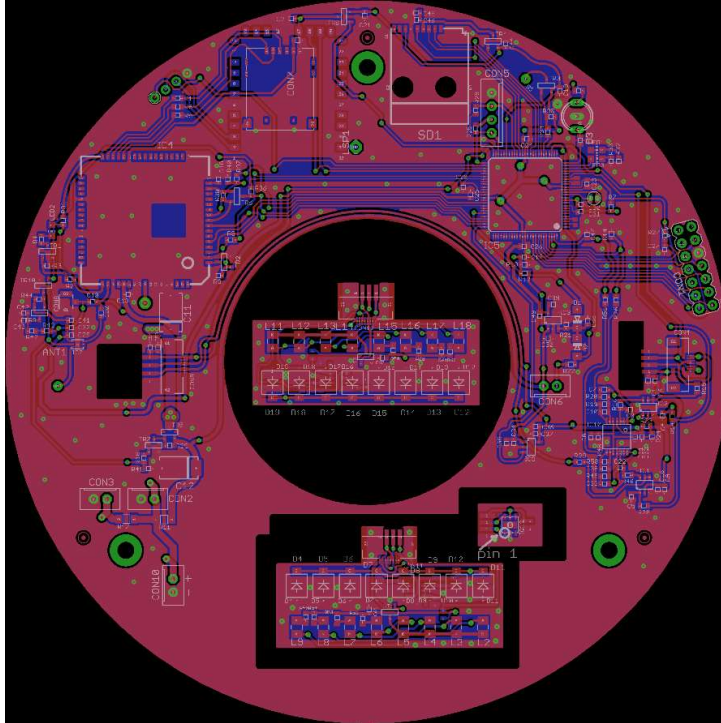


Figure 9-49. The designed Printed circuit board of Funnel (panel)

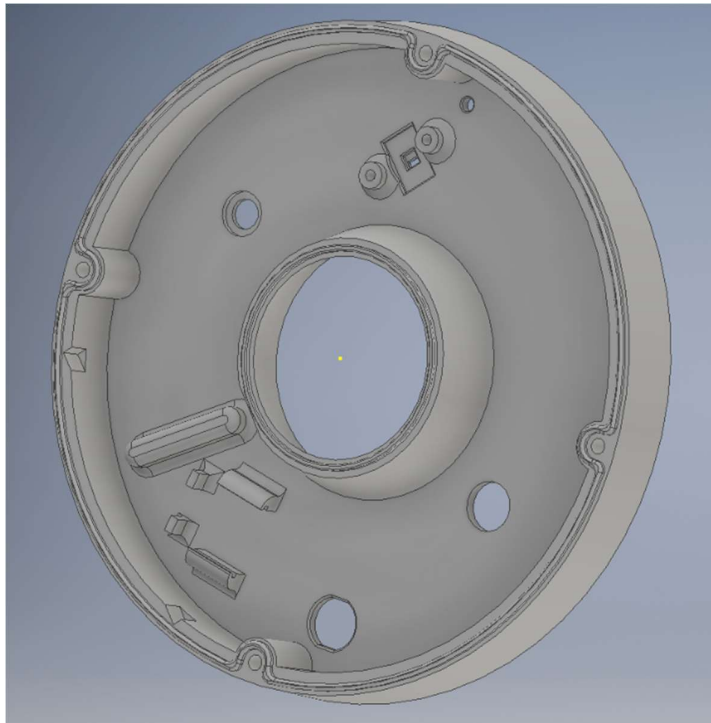


Figure 9-50. e-Funnel plastic enclosure Top Internal View

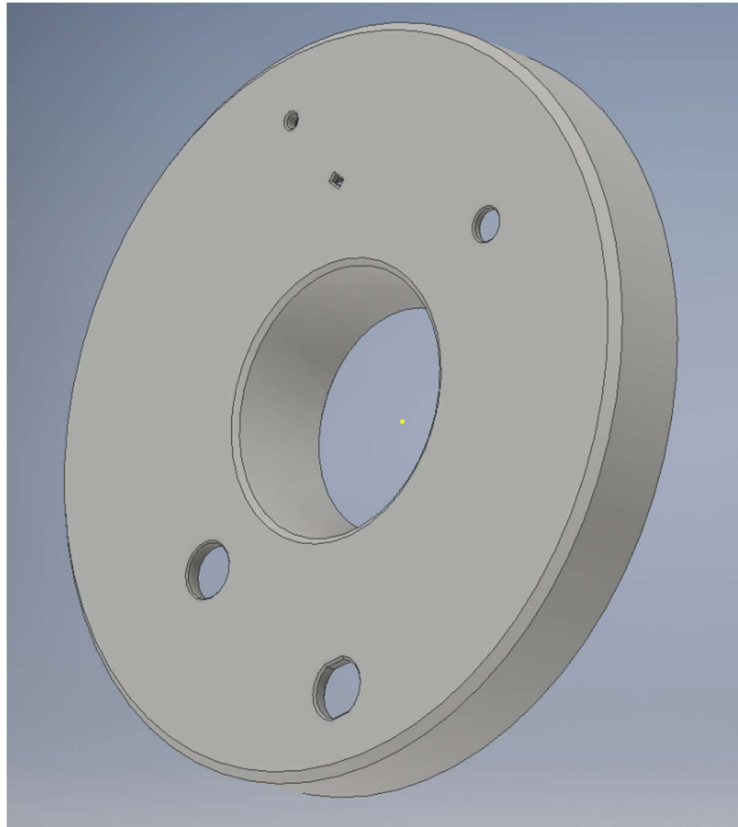


Figure 9-51. e-Funnel plastic enclosure Top external View

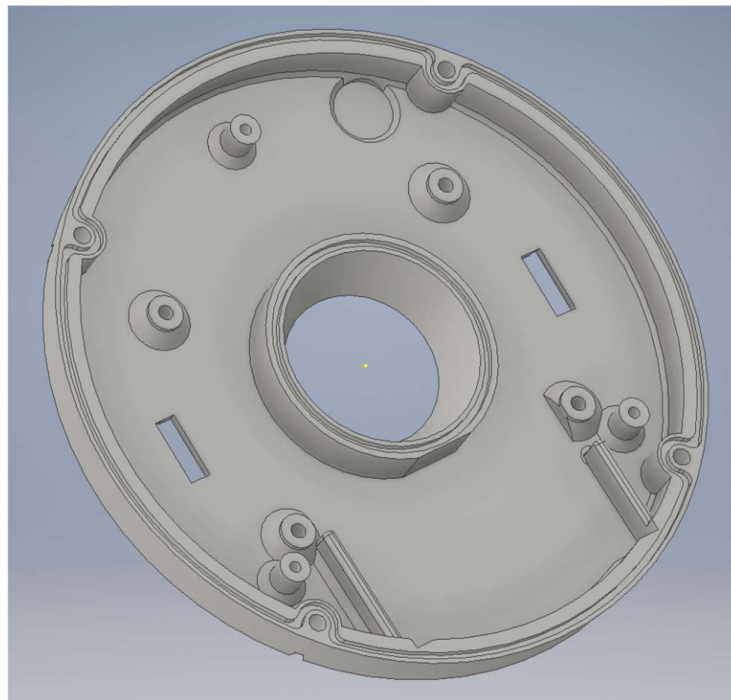


Figure 9-52. e-Funnel plastic enclosure Bottom Internal View

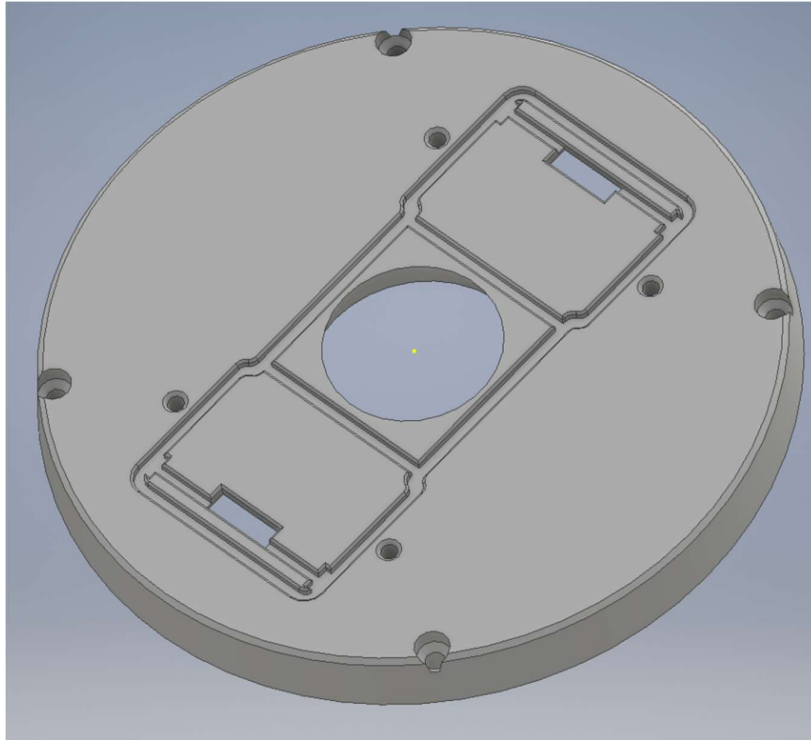


Figure 9-53. e-Funnel plastic enclosure Bottom External View

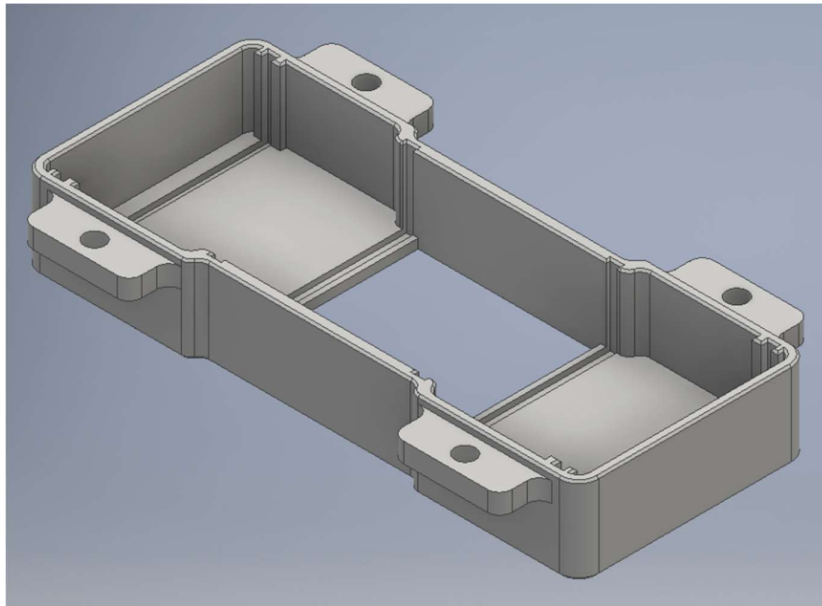


Figure 9-54. e-Funnel Optical parts plastic enclosure internal view

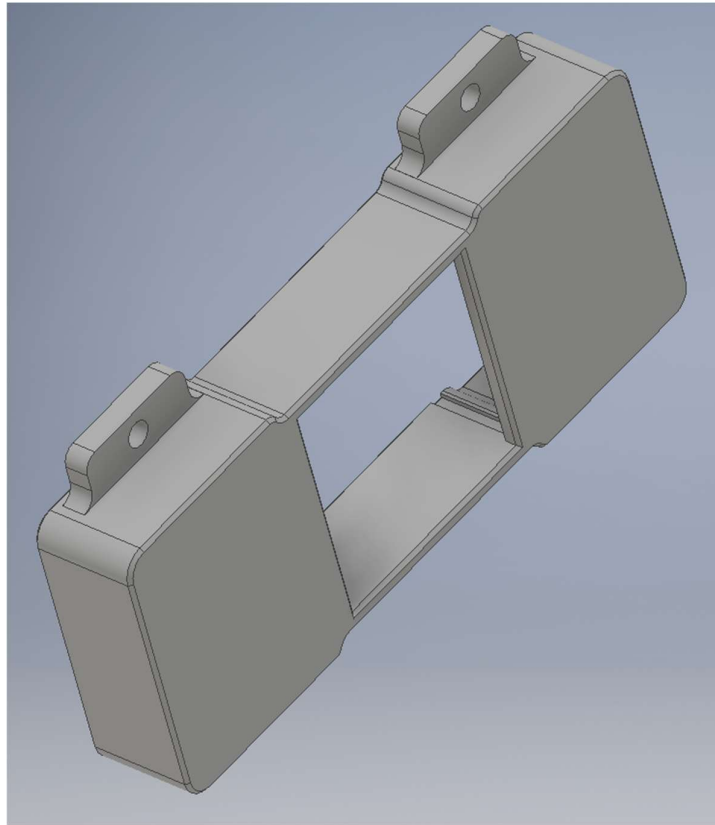


Figure 9-55. e-Funnel Optical parts plastic enclosure external view

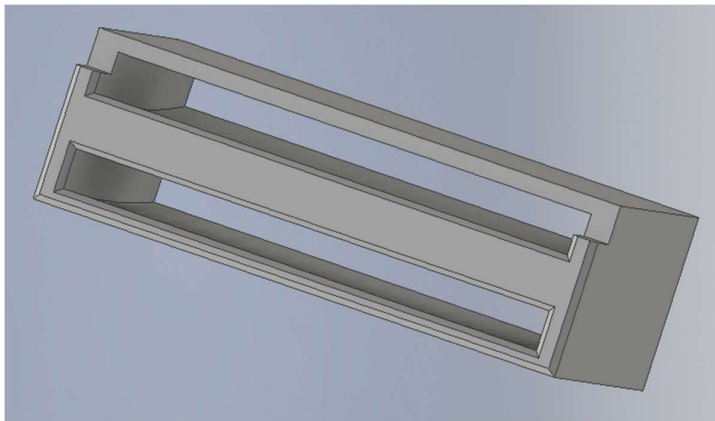


Figure 9-56. Sunlight Blocker



Figure 9-57. Prototype e-Funnel Top View

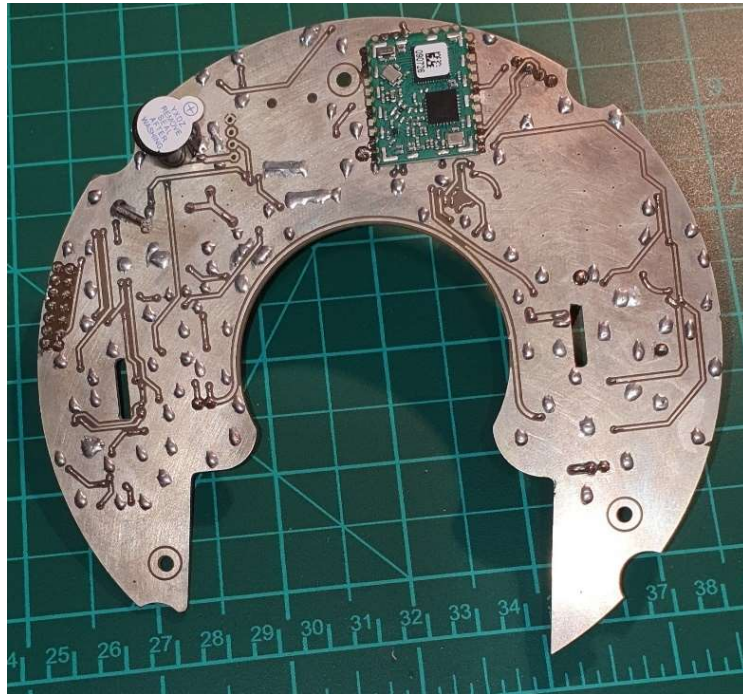


Figure 9-58. Prototype e-Funnel Bottom View

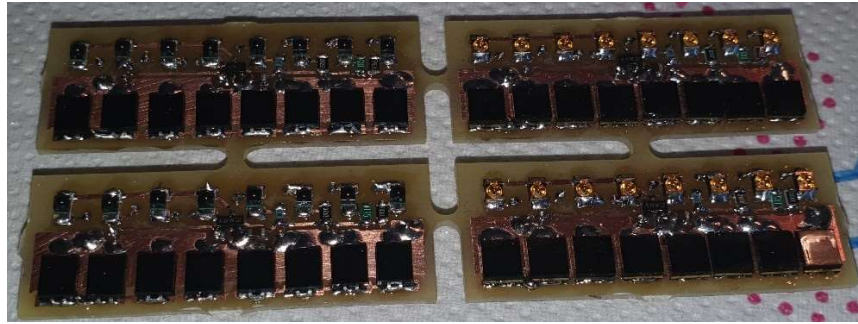


Figure 9-59. Prototype of optical parts



Figure 9-60. Assembled PCBs



Figure 9-61. The production for real experiments